NOTICE

The quality of this microform is heavily dependent upon the quality of the original thesis submitted for microfilming. Every effort has been made to ensure the highest quality of reproduction possible.

If pages are missing, contact the university which granted the degree.

Some pages may have indistinct print especially if the original pages were typed with a poor typewriter ribbon or if the university sent us an inferior photocopy.

Reproduction in full or in part of this microform is governed by the Canadian Copyright Act, R.S.C. 1970, c. C-30, and subsequent amendments.

AVIS

La qualité de cette microforme dépend grandement de la qualité de la thèse soumise au microfilmage. Nous avons tout fait pour assurer une qualité supérieure de reproduction.

S'il manque des pages, veuillez communiquer avec l'université qui a conféré le grade.

La qualité d'impression de certaines pages peut laisser à désirer, surtout si les pages originales ont été dactylographiées à l'aide d'un ruban usé ou si l'université nous a fait parvenir une photocopie de qualité inférieure.

La reproduction, même partielle, de cette microforme est soumise à la Loi canadienne sur le droit d'auteur, SRC 1970, c. C-30, et ses amendements subséquents.

Computerized Analysis and Design of Vehicle Multi-Body Systems

James Alanoly

A Thesis

in

The Department

of

Mechanical Engineering

Presented in Partial Fulfillment of the Requirements
of the Degree of Doctor of Philosophy at
Concordia University,
Montréal, Québec,
Canada

September 1989

ISBN 0-315-51327-6

CONCORDIA UNIVERSITY
Division of Graduate Studies

This is to certify that the thesis prepared

By: James Alanoly

Entitled: Computerized Analysis and Design of Vehicle Multi-Body Systems

and submitted in partial fulfillment of the requirements for the degree of Doctor of Philosophy

complies with the regulations of the University and meets the accepted standards with respect to originality and quality.

Signed by the final examining committee:

M.E. Szabo — Chair
Dr. M.E. Szabo

V. Ramamurti — External Examiner
Dr. V. Ramamurti

R.V. Patel — External to Program
Dr. R. Patel

S Rakheja — Examiner
Dr. S. Rakheja

A.K.W. Ahmad — Examiner
Dr. A.K.W. Ahmad

S. Sankar — Thesis Supervisor
Dr. S. Sankar

Approved by Ramakrishna
Chair of Department or Graduate Program Director

Oct 18 1989

Dean of Faculty

ABSTRACT

COMPUTERIZED ANALYSIS AND DESIGN OF VEHICLE MULTI-BODY SYSTEMS

James Alanoly, Ph.D.
Concordia University, 1989

This thesis deals with computer-aided modelling analysis and design of vehicle systems for ride and handling studies. Characteristics of vehicle multi-body models are identified and formalisms are developed for automatic computerized equation generation and solution. These are implemented using interactive graphics and applied to several vehicle dynamics studies.

The method of velocity coefficients is proposed as a versatile tool to model and analyze suspension linkages for ride and handling. The velocity coefficients can be evaluated from a kinematic analysis and then used to characterize a linkage suspension as a linkage-free suspension of equivalent isolation and handling properties. Dynamic analysis can then be carried out without solving for the kinematics at each integration step, leading to efficient solution.

When the suspensions are represented as force-generating elements, most vehicle models can be represented by free-multi-body systems or multi-body systems in tree configuration. For these systems, a computer-based modelling strategy is formulated which parallels the intuitive and customary techniques used by vehicle system dynamicists. In this scheme, each rigid body may have any number of degrees of freedom between 1 and 6. The implicit constraints are automatically taken care of in the formulation so that a minimal set of differential

equations are generated.

General purpose formulations are presented for the velocity coefficient and design sensitivity analysis of suspensions. A general analytical method has been derived to determine the vehicle roll stiffness and roll centre location, which has hitherto been done graphically. Some prevalent misconceptions regarding roll centre arising from the graphical construction, and compounded by an official SAE definition, have been clarified.

Implementation of the formalisms developed is presented in the form of two pieces of software - GENKAD and CAMSYD. GENKAD is a comprehensive set of programs for the kinematic analysis and design of planar mechanisms, featuring automatic symbolic equation derivation. GENKAD can compute positions and velocity coefficients and determine their sensitivities to any of the system parameters, to be used for optimal design. CAMSYD is used for modelling and dynamic analysis of planar, lumped parameter mechanical systems. The system equations are generated symbolically and can be solved for a variety of analysis options. CAMSYD has interface to GENKAD to represent linkage suspensions.

The theory as well as the software have been verified and validated through comparison with results from published literature. The software was also used for the modelling and dynamic analysis of a snowmobile. Displacement and acceleration time histories of the vehicle going over a bump obtained from simulation are compared with measurements made on an instrumented snowmobile.

ACKNOWLEDGEMENTS

I wish to express my deep appreciation and gratitude to my thesis supervisor, Dr. S. Sankar, for his years of guidance, support and friendship, dating from my undergraduate days.

I also thank other faculty members, graduate students, and staff of CONCAVE Research Centre and the Department of Mechanical Engineering at Concordia University, for their help and encouragement. Special thanks are due to Messrs. Fred Labelle and Moses Levy.

I also gratefully acknowledge the support and collaboration from Messrs. Geoff Burgess, Denis Germain, and Daniel Boulanger of Bombardier Inc., Valcourt, Quebec.

Financial support provided through Natural Sciences and Engineering Research Council of Canada and MESS of the Government of Quebec are gratefully acknowledged.

Last, but not least, I thank my wife, Lucy, for her love, encouragement, patience and many sacrifices, which made this work possible. I dedicate this thesis to her and to our daughters, Beth, Mary Anne, and Susanna.

TABLE OF CONTENTS

	Page
LIST OF FIGURES	xi
LIST OF TABLES	xvi
NOMENCLATURE	xvii

Chapter 1

INTRODUCTION AND LITERATURE REVIEW

1.1 GENERAL INTRODUCTION	1
1.2 STATE OF THE ART AND LITERATURE REVIEW	3
1.2.1 Analytical Methods and Computer Programs	6
1.2.2 Vehicle System Dynamics	13
1.3 SCOPE OF THE PRESENT STUDY	21
1.3.1 Objectives	21
1.3.2 Organization of the Thesis	26

Chapter 2

A GENERAL PURPOSE FORMALISM FOR LUMPED PARAMETER VIBRATORY SYSTEMS WITH APPLICATION TO VEHICLE DYNAMICS

2.1 INTRODUCTION	29
2.2 EQUATIONS OF MOTION FOR MULTI-BODY SYSTEMS : BACKGROUND	34
2.3 A NEW FORMALISM FOR A CLASS OF MULTI-BODY SYSTEMS	38
2.3.1 Characteristics of a Class of System Models	38
2.3.2 Modelling Techniques and Reference Frames	40
2.3.3 Free Bodies	42

2.3.3.1 Kinematics of Free Bodies 42

2.3.3.2 Dynamics of Free Bodies 43

2.3.4 Constrained Multi-body Systems 44

2.3.4.1 Description of Interconnection Structure 44

2.3.4.2 Kinematics of Constrained MBS 47

2.3.4.3 Dynamics of Constrained MBS 49

2.3.5 Applied Forces 52

2.4 SUMMARY 53

Chapter 3

CAMSYD: AN INTERACTIVE GRAPHICS BASED SOFTWARE FOR PLANAR MULTI-BODY SYSTEM DYNAMICS

3.1 INTRODUCTION 54

3.2 SCOPE OF THE NEW SOFTWARE, CAMSYD 58

3.3 USAGE OF CAMSYD 60

3.4 IMPLEMENTATION 65

3.5 APPLICATION TO VEHICLE RIDE ANALYSIS 67

3.5.1 Automobile Ride Analysis 69

3.5.2 Tractor Semitrailer Ride Analysis 77

3.6 SUMMARY 86

Chapter 4

ANALYSIS OF SUSPENSION SYSTEMS USING THE METHOD OF VELOCITY COEFFICIENTS

4.1 INTRODUCTION 87

4.2 THE DERIVATION OF VELOCITY COEFFICIENTS 90

4.3 DESIGN SENSITIVITY ANALYSIS 99

4.3.1 Sensitivity of ϕ with respect to b 101

4.3.2 Sensitivity of K with respect to b 102

4.3.3 Derivative of K with respect to q 104

4.4 APPLICATION TO VEHICLE RIDE AND HANDLING ANALYSIS 104

4.4.1 Suspension Forces Using Velocity Coefficients 110

4.4.1.1 Special Cases 113

4.4.2 Vehicle Handling Analysis 114

4.4.3 Kinetostatic Analysis 115

4.5 ROLL CENTRE LOCATION AND ROLL STIFFNESS 118

4.5.1 Definition of Roll Centre 120

4.5.2 Determination of Roll Centre 125

4.5.2.1 Bodies with 3 Degrees of Freedom 130

4.5.2.2 Bodies with 2 Degrees of Freedom 133

4.5.2.3 Bodies with 1 Degree of Freedom 134

4.5.3 Roll Stiffness 135

4.6 SUMMARY 138

Chapter 5

APPLICATION OF VELOCITY COEFFICIENT METHOD IN THE ANALYSIS OF SUSPENSION SYSTEMS

5.1 INTRODUCTION 140

5.2 A New SOFTWARE IMPLEMENTATION, GENKAD 142

5.2.1 Scope of the Software 142

5.2.2 Usage of GENKAD Package 144

5.2.2.1 Modelling of Mechanisms 146

5.2.2.2 Equation Derivation 148

5.2.2.3 Analysis Options149

5.2.2.4 Post-Processing 153

5.3 APPLICATION TO VEHICLE SUSPENSIONS 154

5.3.1 Suspension Force Analysis 155

5.3.1.1 Racing Car Independent Suspension 156

5.3.1.2 Snowmobile Rear Suspension 164

5.3.2 Kineto-static Analysis and Roll Centres 172

5.3.2.1 Racing Car Beam-Axle Suspensions 174

5.3.2.2 Analysis Results and Comparison 178

5.4 SUMMARY 196

Chapter 6

COMPUTER SIMULATION AND TESTING OF
SNOWMOBILE RIDE DYNAMICS

6.1 INTRODUCTION 198

6.2 DESCRIPTION OF THE SNOWMOBILE 202

6.3 MATHEMATICAL MODELLING AND COMPUTER SIMULATION 204

6.3.1 Subsystem Models 207

6.3.1.1 Shock-Absorbers and Springs 208

6.3.1.2 Suspension Linkages 208

6.3.1.3 Chassis and Driver Model 214

6.3.2 Snowmobile Ride Dynamic Model 214

6.3.2.1 Equations of Motion 215

6.3.2.2 Terrain Pre-Processor 217

6.3.3 Dynamic Analysis 218

6.4 FIELD TESTING AND VALIDATION OF SIMULATION RESULTS 224

6.4.1 Description of Test Setup and Procedure 224

6.4.2 Signal Processing 229

6.4.3 Comparison of Simulation and Test Data 237

6.4.3.1 Some Additional Notes on Computer Simulation 239

6.4.3.2 Vehicle Speed of 10 km/hr 241

6.4.3.3 Vehicle Speed of 20 km/hr 249

6.4.3.4 Vehicle Speed of 30 km/hr 263

6.5 SUMMARY

Chapter 7

CONCLUSIONS AND RECOMMENDATIONS FOR FUTURE WORK

7.1 HIGHLIGHTS OF THE PRESENT WORK 266

7.2 GENERAL CONCLUSIONS 269

7.3 RECOMMENDATIONS FOR FUTURE WORK 270

REFERENCES 275

APPENDIX A 286

LIST OF FIGURES

		Page
Fig. 1.1:	Examples of multi-body systems.	4
Fig. 1.2:	Vehicle system models used in ride comfort studies	8
Fig. 1.3:	Examples of vehicle suspension linkage arrangements	16
Fig. 1.4:	Lumped parameter model of a automobile with a driver (a) conventional schematic, (b) mechanism model	23
Fig. 2.1:	A double lever cam mechanism: (a) physical system (b) initial model, (c) final model	30
Fig. 2.2:	Typical gear dynamic models	31
Fig. 2.3:	Roll-plane model of a railroad flatcar	32
Fig. 2.4:	Ride dynamic model of a tractor semitrailer	33
Fig. 2.5:	A particle constrained to move on a line	36
Fig. 2.6:	A generic planar multi-body system: (a) system model and coordinate frames, (b) system graph (c) directed graph	41
Fig. 3.1:	Contrast between conventional and computerized approaches	55
Fig. 3.2:	Schematic of the usage of CAMSYD	61
Fig. 3.3:	Organization of CAMSYD	62
Fig. 3.4:	Components in CAMSYD library	63
Fig. 3.5:	Schematic of two degree of freedom automobile model	70
Fig. 3.6:	Two DOF automobile model generated using CAMSYD	71
Fig. 3.7:	Transient response of system shown in Fig. 3.6	73
Fig. 3.8:	Model of automobile with vibration absorber	74
Fig. 3.9:	Model of Fig. 3.8 generated using CAMSYD	75
Fig. 3.10:	Frequency response of vehicle body acceleration	76
Fig. 3.11:	Six degree of freedom tractor-semitrailer model	78
Fig. 3.12:	Tractor-semitrailer model generated using CAMSYD	79

Fig. 3.13: First mode of vibration for 3 different positions of fifth-wheel. (a) 0.5m forward, (b) nominal location (c) 0.5m rearward. 82

Fig. 3.14: Second mode of vibration for 3 different positions of fifth-wheel. (a) 0.5m forward, (b) nominal location (c) 0.5m rearward. 83

Fig. 3.15: Frequency response of tractor CG bounce acceleration 84

Fig. 3.16: Frequency response of tractor CG pitch acceleration 85

Fig. 4.1: A generic linkage suspension system 91

Fig. 4.2: Kinematic model of a shock-absorber (a) conventional model. (b) 'rubber band' link model 92

Fig. 4.3: A double wishbone system with conventional outboard shock-absorber and coil-spring 95

Fig. 4.4: Kinematic model of the conventional double wishbone system shown in Fig. 4.3 96

Fig. 4.5: MacPherson strut type front suspension 106

Fig. 4.6: Variations of double wishbone suspension system in racing cars 107

Fig. 4.7: Variations of swing-arm rear suspension system in off-road motorcycles 108

Fig. 4.8: Flowchart of kineto-static analysis procedure 119

Fig. 4.9: Instantaneous centre location for a 2 DOF body acted upon by a vertical load 124

Fig. 4.10: Suspension system model with 5 degrees of freedom 126

Fig. 4.11: Suspension system models with 3 degrees of freedom 127

Fig. 4.12: Suspension system model with 2 degrees of freedom 128

Fig. 4.13: Suspension system model with 1 degree of freedom 129

Fig. 4.14: General notation for determination of roll centre location 131

Fig. 5.1: Schematic of the overall structure of GENKAD 145

Fig. 5.2: Some frames from the animation of inboard rocker configuration. 158

Fig. 5.3: Deflection of spring/shock-absorber vs wheel vertical motion 159

Fig. 5.4: Leverage Ratio vs wheel displacement for four configurations of double wishbone suspension 160

Fig. 5.5: Non-dimensional effective wheel rate for four configurations of double wishbone suspension 163

Fig. 5.6: Non-dimensional effective damping force for four configurations of double wishbone suspension 165

Fig. 5.7: View of a snowmobile rear suspension system 166

Fig. 5.8: Schematic of snowmobile rear suspension system linkages 167

Fig. 5.9: Frames from the animation of rear suspension with track moving up 169

Fig. 5.10: Deflection of springs vs track vertical motion 170

Fig. 5.11: Velocity coefficients of shock-absorbers/spring motion vs track vertical motion 171

Fig. 5.12: Three types of beam axle suspensions - (a) Panhard bar, (b) Watt linkage, and (c) Roberts linkage 175

Fig. 5.13: Kinematic model of Panhard bar beam axle suspension 177

Fig. 5.14: Animation of Panhard bar suspension vertical motion. 179

Fig. 5.15: Animation of Watt linkage suspension vertical motion. 180

Fig. 5.16: Animation of Roberts linkage suspension vertical motion. 181

Fig. 5.17: Roll centre x coordinate of Panhard bar suspension 186

Fig. 5.18: Roll centre y coordinate of Panhard bar suspension 187

Fig. 5.19: Roll stiffness of Panhard bar suspension 188

Fig. 5.20: Roll centre x coordinate of Watt linkage suspension 190

Fig. 5.21: Roll centre y coordinate of Watt linkage suspension 191

Fig. 5.22: Roll stiffness of Watt linkage suspension 192

Fig. 5.23: Roll centre x coordinate of Roberts linkage suspension 193

Fig. 5.24: Roll centre y coordinate of Roberts linkage suspension 194

Fig. 5.25: Roll stiffness of Roberts linkage suspension 195

Fig. 6.1:	Schematic of analysis methodology	201
Fig. 6.2:	Ski-Doo FORMULA MACH I snowmobile	203
Fig. 6.3:	A View of the front suspension system	205
Fig. 6.4:	Schematic of front suspension linkage	206
Fig. 6.5:	Deflections and forces at the base of suspensions	210
Fig. 6.6:	Shock-absorber deflection vs ski vertical deflection	212
Fig. 6.7:	Leverage ratio of shock-absorber deflection vs ski vertical deflection	213
Fig. 6.8:	Dynamic model of snowmobile	216
Fig. 6.9:	Menu of profiles from terrain pre- processor	219
Fig. 6.10:	Ski at various positions as it goes over a half-sine profile	220
Fig. 6.11:	Positions of the ski pivot for the motion shown in Fig. 6.10	221
Fig. 6.12:	Profile of 'bump'	223
Fig. 6.13:	Locations of measuring instruments	225
Fig. 6.14:	A sample of vehicle speed	227
Fig. 6.15:	Displacement measurement, C1, at 10 km/hr	228
Fig. 6.16:	Acceleration signal, A7, measured at 10 km/hr	230
Fig. 6.17:	Filtered displacement signal, C1, for three test runs	232
Fig. 6.18:	Filtered acceleration signal, A7, for three test runs	234
Fig. 6.19:	Zero-shifted acceleration signal, A7, for three test runs	235
Fig. 6.20:	Zero-shifted acceleration signal, A8, for three test runs	236
Fig. 6.21:	Actual vehicle speed at 10 km/hr	242
Fig. 6.22:	Ski shock-absorber deflection, C3, at 10 km/hr	243
Fig. 6.23:	Rail relative deflection, C1, at 10 km/hr	244
Fig. 6.24:	Rail Relative deflection, C2, at 10 km/hr	246

Fig. 6.25: Acceleration signal, A7, at 10 km/hr 247

Fig. 6.26: Acceleration signal, A8, at 10 km/hr 258

Fig. 6.27: Actual vehicle speed at 20 km/hr 250

Fig. 6.28: Ski shock-absorber deflection, C3, at 20 km/hr 251

Fig. 6.29: Rail relative deflection, C1, at 20 km/hr 252

Fig. 6.30: Rail Relative deflection, C2, at 20 km/hr 253

Fig. 6.31: Acceleration signal, A7, at 20 km/hr 254

Fig. 6.32: Acceleration signal, A8, at 20 km/hr 255

Fig. 6.33: Actual vehicle speed at 30 km/hr 257

Fig. 6.34: Ski shock-absorber deflection, C3, at 30 km/hr 258

Fig. 6.35: Rail relative deflection, C1, at 30 km/hr 259

Fig. 6.36: Rail Relative deflection, C2, at 30 km/hr 260

Fig. 6.37: Acceleration signal, A7, at 30 km/hr 261

Fig. 6.38: Acceleration signal, A8, at 30 km/hr 262

LIST OF TABLES

		Page
Table 3.1:	Implementation of CAMSYD	68
Table 3.2:	Parameter values for models shown in Fig. 3.5 and 3.8	68
Table 3.3:	Parameter values for tractor semitrailer model	81
Table 5.1:	Results for Panhard bar, and comparison with [67]	182
Table 5.2:	Panhard bar roll centre results for incremental vertical load	183

NOMENCLATURE

a	A constant
A	Jacobian matrix of kinematic constraint equations
b, b_i	A constant or a design variable
B	A matrix
c, c_i	Damping coefficient or a numerical constant
c_i^a	Constant part of α_i
c_i^r	Constant part of r_i
$\mathcal{C}$	Damping matrix
d_i	A constant, usually representing distance
D	Distance matrix
f	Number of degrees of freedom
$f()$	A function
F, F_i	Force or a force component
I	Moment of inertia
I_i, J_i	Moment of inertia of body i
$\mathcal{I}$	A diagonal matrix of moment of inertias
k, k_i	Stiffness coefficient
K	Velocity coefficient matrix
$\mathcal{K}$	Stiffness matrix
$\mathcal{K}_r$	Roll stiffness
l	Number of independent kinematic variables
L	"Lagrangian"
m, m_i	Mass
m	Number of kinematic constraint equations

m_{tot}	Total mass of a system of kinematically coupled bodies
M_i	Sum of all moments acting on body i
M_r	Roll moment
M	A diagonal matrix of masses
n	A counter or number of Lagrangian coordinates
p	Number of bodies in a multi-body system
q, q_i	A generalized coordinate
Q, Q_i	A generalized force
r	A constant
r_i	Length of link. May consist of a variable part and a constant part
S	Incidence matrix
t	Time
T	Path-to-datum matrix
v_i^a	Variable part of α_i
v_i^r	Variable part of r_i
W	Total amount of work done
x, x_i	A measurement coordinate
x_p	Inertial X coordinate of roll centre
x_{cg}	X coordinate of roll centre in the body-fixed frame
X_j^c	Constraint force in hinge j
XY	An inertial reference frame
XY^G	An inertial reference frame fixed to the ground
XY_i^B	A body-fixed reference frame at the CG of body i
XY_i^N	An inertial reference frame coincident with XY_i^B in the nominal position
y, y_i	A measurement coordinate

y_p	Inertial Y coordinate of roll centre
y_{cg}	Y coordinate of roll centre in the body-fixed frame
Y_j	Moment acting through hinge j
z, z_i	A measurement coordinate
α	Distance between body CG and roll centre along inertial frame X coordinate
α_i	Angle between a link and the inertial X axis. May consist of a variable part and a constant part
β	Distance between body CG and roll centre along inertial frame Y coordinate
Δ	Determinant of a matrix
ϕ, ϕ_i	A variable, usually a dependent kinematic variable
ψ_i	A kinematic variable. Dependent or independent
Ψ_j	Objective or constraint functions for optimization
λ	A Lagrange multiplier
λ_i	An eigenvalue
θ	An angle, or body roll angle

Chapter 1

INTRODUCTION AND LITERATURE REVIEW

1.1 GENERAL INTRODUCTION

Simulation plays a major role in almost all fields of science and engineering. Simulation can be defined as "experimentation with models" [1]. In computer simulation, the emphasis can be either on *experimentation* or *models*. Traditionally, the emphasis has been on experimentation where the same model is used repeatedly to generate trajectories of certain descriptive variables. This is mainly because modelling is a very costly and error-prone task.

Computer simulation involves modelling, derivation of equations and solution on computer. Modelling is a creative and intuitive process. Since we cannot model the world, we must isolate and idealize various components to build our system. Model building is an incremental, evolutionary process. A modeller often starts with a simple model which grows in complexity as he studies its behaviour, or components of the model are built and tested separately before being put together. In any case, manually deriving the system equations and coding them for computer solution makes modelling an expensive process. Therefore there has been considerable interest in the computerization of equation generation and solution processes.

This is the aim of so-called *self-formulating* programs. For

dynamic analysis of mechanical systems, there are several such programs available, as listed in Ref. [2]. They include IMP, DADS, ADAMS, DRAM etc.. One important drawback of many of these is that the problem formulation can be very tedious and that the user is required to know specialized theory and syntax. The analytical methods used in these programs for modelling constrained mechanical systems give rise to a very large number of differential equations, leading to numerical difficulties in solving them.

The general objectives of the current research program are: (1) to create formulations that are suitable for computer implementation which allow the system (especially a vehicle system) description to be input in a schematic or graphical form, and automatically generate the governing equations; and (2) to develop and implement numerical algorithms that automatically solve the system equations for dynamic response of the system, and provide computer graphic output of the results to the designer or analyst. With these objectives achieved, the engineer is relieved of a lot of routine manual calculations and programming, and the power of the digital computer is exploited to the maximum.

In the following section we present a review of the theoretical background of multi-body dynamics, the different methods of formulation for computer implementation, and examine some of the commercially available general purpose software. We evaluate the suitability of these software for the analysis of vehicle system dynamics. It is found

that most of the theoretical and software development has been carried out for the kinematic and dynamic analysis of machine mechanisms and spacecraft structures. We note that in vehicle system dynamics, the topology of the models and their scale of motion differ significantly from the other applications mentioned earlier. We use this information in formulating generalized modelling, analysis and design synthesis strategies for vehicle dynamic applications.

1.2 STATE OF THE ART AND LITERATURE REVIEW

A system of interconnected bodies (rigid or flexible) that can move relative to one another is called a Multi-Body System (MBS). This term now enjoys widespread acceptance and it describes a large class of mechanical systems such as spacecraft, ground vehicles, manipulators, machine mechanisms etc.. The coupling between bodies may be through joints with certain kinematic properties, or springs, dampers and active force generators. The term, multi-body, dynamics is usually reserved for systems that undergo large motion and therefore can only be described by nonlinear (inertia variant) differential equations of motion.

Figure 1.1 shows examples of different multi-body systems. A multi-body system without any constraints (Fig. 1.1 (a)) is called a free multi-body system. Generation of equations of motion for this class of systems is relatively easy. Systems of constrained bodies may

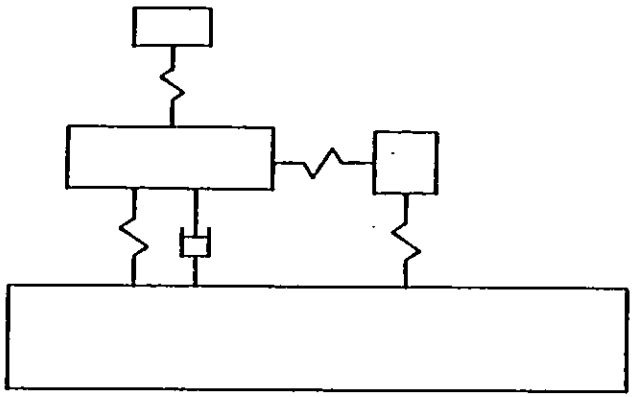

(a)

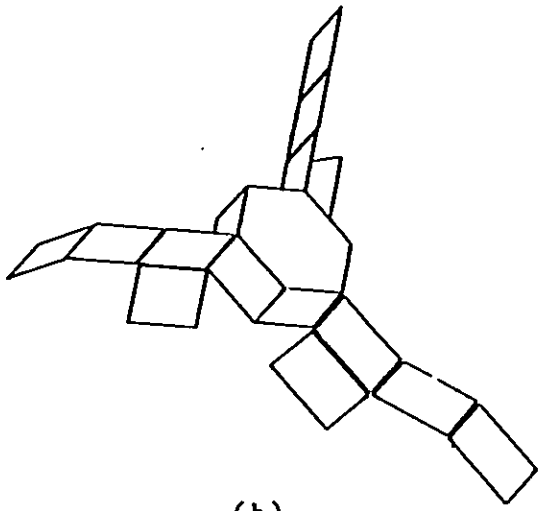

(b)

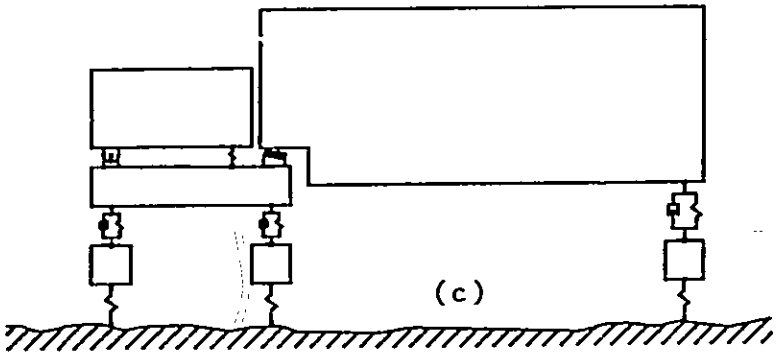

(c)

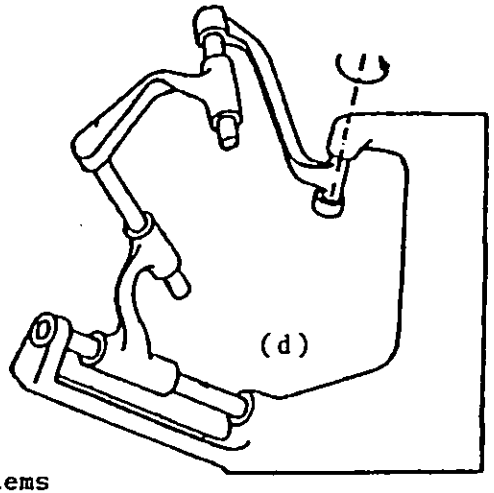

(d)

Fig. 1.1: Examples of multi-body systems

be ordinary multi-body systems (holonomic constraints and proportional-differential force elements), or general multi-body systems (nonholonomic constraints and proportional-integral force elements). We concentrate mainly on ordinary multi-body systems. In constrained MBS, the bodies may form open kinematic chains (Fig. 1.1 (b),(c)) or closed chains (Fig. 1.1 (d)). This distinction is important because the methodology for generating the equations of motion can be different for each.

Leading researchers in computer aided analysis of mechanical system dynamics are found in 6 groups, 3 in West Germany, and 3 in the United States. They are, in Germany, Schiehlen, et al. (University of Stuttgart), Kortüm, Wallrapp et al (DFVLR, the German Aerospace Research Establishment), Wittenberg, et al. (University of Karlsruhe); and in the US, Uicker and Seth (University of Wisconsin), Orlandea, Chace, et al. (Mechanical Dynamics Inc.), and Haug, Nikravesh, et al. (University of Iowa/Computer Aided Design Software Inc.). Other important names include Paul (University of Pennsylvania) and Andrews (University of Waterloo).

The NATO Advanced Study Institute on Computer Aided Analysis and Optimization of Mechanical System Dynamics (1983) brought together most of the leading researchers in this area and the lecture notes were published [3]. These notes provide a very comprehensive and almost up to-date information on the state-of-the-art. Other important conferences on this subject include the 1977 IUTAM symposium in Munich,

FRG [4], the 1985 IUTAM/IFToMM symposium in Udine, Italy [5], and the 1986 ICTS seminar in Amalfi, Italy [6]. Kortüm and Schiehlen [7] surveyed general purpose vehicle dynamics software. Wittenberg [8] has also provided an excellent bibliography on multi-body system dynamics. These and other publications (most of them by researchers mentioned above) provide the bulk of the information in this field.

The researchers who have tackled the multi-body dynamics problem come from two distinct backgrounds, namely, spacecraft dynamics and machinery dynamics. Spacecraft dynamicists considered mainly systems with open chain (tree) topology. These systems usually have a large number of degrees of freedom and some elegant multi-body formalisms are available for generation of equations of motion. However, the mechanism dynamicists have to deal with systems with closed chains. In most mechanism applications there are large number of bodies interconnected with so many constraints that the total degree of freedom is only one. Therefore the treatment of the problem differs significantly from that of open loop ones. We will review the analytical and computational techniques of mechanical system dynamics in the next section.

1.2.1 Analytical Methods and Computer Programs

There are several analytical methods in classical mechanics dealing with the dynamics of systems of rigid bodies. To be useful in a general purpose computer application, these methods should satisfy two important requirements which, in general, are not easily fulfilled simultaneously.

First, they should be general enough to describe the dynamic behaviour of a wide range of dynamic systems. Second, their application to any particular mechanical system should be possible with a minimum amount of preparatory work. For example, Lagrange's equations of the second kind,

$$\frac{d}{dt}\left(\frac{\partial L}{\partial \dot{q}_k}\right) - \frac{\partial L}{\partial q_k} = Q_k , \qquad k = 1, 2, \ldots . n \tag{1.1}$$

satisfy the first requirement, but not the second. Therefore, this formulation is avoided in most general purpose programs. The ones that have been commonly used are: Newton-Euler equations (vectorial mechanics), Lagrange's form of d'Alembert's principle, and the use of Lagrange Multipliers. Paul [9,10] and Wittenberg [11,12] give excellent reviews of the different analytical techniques.

GMR DYANA from General Motors Research Laboratories [13,14] seems to have been the first self-formulating program for mechanical system dynamics. However, it was restricted to one-dimensional (scalar) systems. For example, models shown in Figure 1.2(a). Scalar systems are free multi-body systems with each body's motion restricted along one direction and they have a simple, direct analogy with electrical networks. This recognition has led to other general purpose computer codes, such as the one by Ferrer [15], for linear, scalar mechanical systems. These programs are of limited use and have not been further developed.

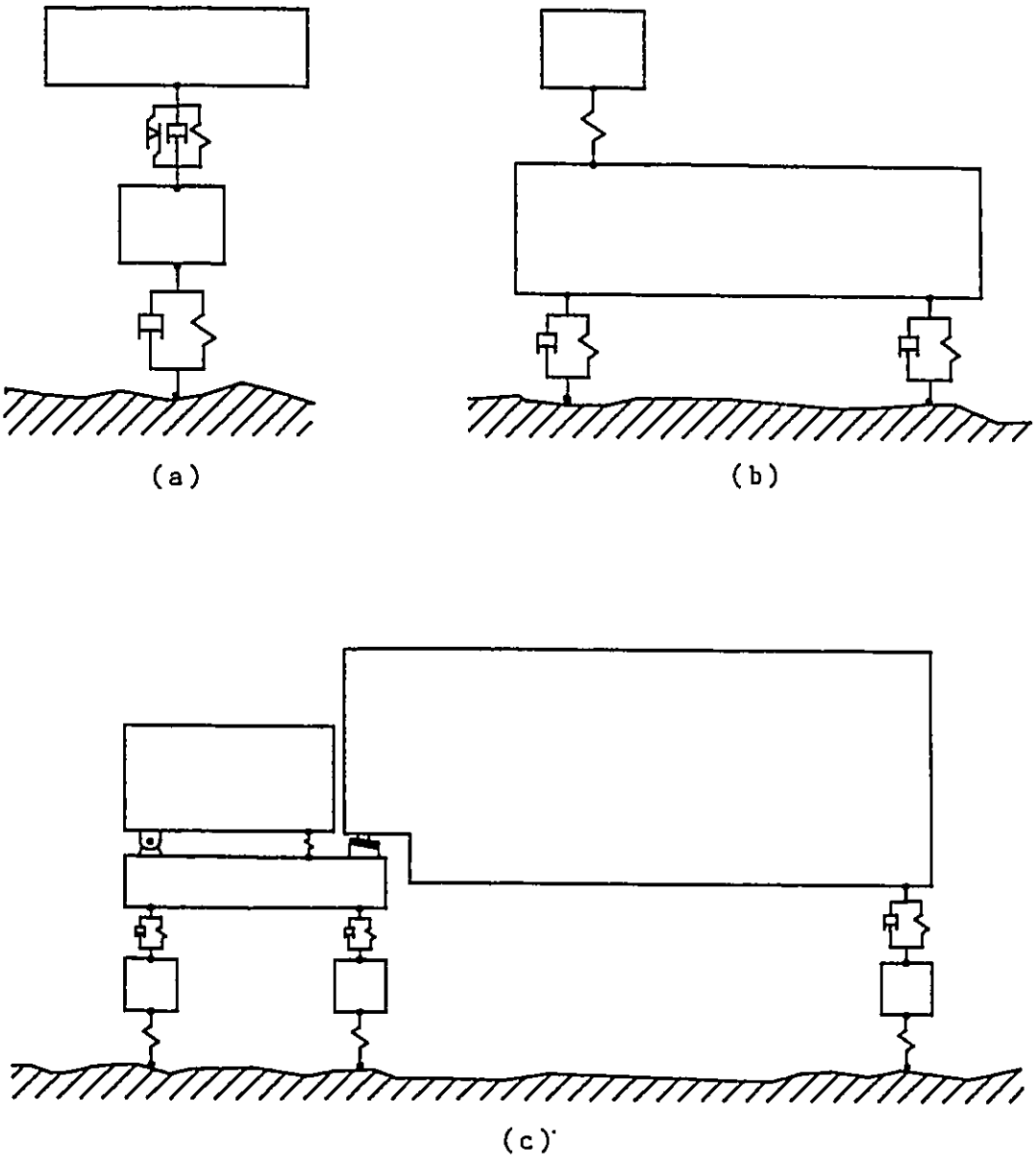

Fig. 1.2: Vehicle suspension models used in ride comfort studies

The equations of motion for free multi-body systems in space are derived most easily and directly using vectorial mechanics by applying Newton-Euler equations to each free body. No commercial software exists based on this principle because their application would be limited. For motion in 3D, there is no direct electrical analogy since the motions are coupled. However, Andrews and Kesavan combined the concepts of graphs theory and vector mechanics to formulate the *vector-network* method for 3-dimensional mechanical systems [16,17]. This gave rise to computer programs, such as VECNET and PLANET, developed as research tools. The original formulation was applicable only to free MBS, and also required the user to draw two separate networks - one for translation and the other for rotation. Recent developments have seen these barriers removed [18-24]. Two general purpose programs, ADVENT for 2D systems [20] and RESTRI for 3D systems [24] have also been presented. However these are still not fully developed programs since they require much preparatory work by the user, such as drawing vector-network diagrams.

All the other multi-body formalisms also make use of concepts of graph theory, but in a more limited form. The major problem in any MBS formalism is the need to handle the kinematic constraints in the joints. The constraints give rise to algebraic relations among the coordinates and velocities representing the relative motion between the constrained bodies. There are two basic strategies to handle constraints. In the first, a maximal set of equations of motion for the free body diagram of each body is established using the *Cartesian coordinates*. These are

augmented by the algebraic constraint equations. Then the combined set of differential and algebraic equations are solved using special algorithms [25,26]. In the second strategy, a minimal set of differential equations is generated by reducing the order through incorporation of the constraint equations. The number of equations that remain are equal to the degrees of freedom and these coordinates are called generalized coordinates. A combination of the these two strategies is also possible.

The popular modern constrained multi-body dynamics programs, ADAMS, and DADS, saw their inception in the work by Chace and Bayazitoglu [27]. This work led to the program DAMN [28,29], and its successor DRAM [30], both of which were for planar systems. The analytical basis of these programs is the Lagrange Multiplier method. In DRAM the angular orientation if links and the translation of slider joints were used as the set of Lagrangian coordinates. When there are closed loops the number in this set exceeds the degrees of freedom of the system, and therefore the ordinary form of Lagrange's equations (Equation 1.1) cannot be used. Instead a form involving Lagrange Multipliers is used together with a set of second order equations obtained by twice differentiating the algebraic constraint equations.

ADAMS [31,32] and DADS [33] are three dimensional cousins of DRAM. In ADAMS and DADS, each rigid body has 6 Lagrangian coordinates associated with them, say, for a total of N of them. In a free multi-body system, these coordinates correspond to the degrees of

freedom of the system. But in a constrained system with M holonomic constraints, there are algebraic compatibility equations at each joint which relate these coordinates to each other. The system has only $P = N-M$ degrees of freedom. But the N Lagrangian coordinates can be treated as independent, if we conceptually remove the explicit constraints but consider the reactions produced by the constraints as external forces. This leads to the equation of motion in the form of Lagrange's equations with multipliers. These are N differential equations with $N+M$ unknowns (N Lagrangian coordinates and M Lagrange multipliers). They are augmented with the M algebraic constraints and the resulting differential algebraic system of equations (DAE) are solved using special techniques [34-37].

Another popular general purpose program is IMP (Integrated Mechanism Program), developed by Uicker and Seth in 1971 [38]. It is in fact the first general purpose code for large displacement MBS in 3D. This program is available as part of the popular CAD system called I-DEAS [39]. The mechanism may be modelled and assembled using the solid modelling module, GEOMOD, of I-DEAS, and analyzed using IMP. It uses Lagrangian coordinates and loop-closure techniques to derive the equations in the form of Lagrange's equations of the second kind. This leads to a minimal set of equations, although in an extremely complex form, which can be integrated using standard techniques.

MEDYNA was developed with high speed transportation systems in mind. It has analysis options useful for vehicle ride and stability

analysis and special modules for vehicles on rails [40,41]. It allows for closed kinematic loops, but only small deflections for the bodies. MEDYNA generates a minimal set of equations by incorporating the constraint equations. Another significant way in which it differs from other MBS programs is that the equations can be generated with respect to a moving coordinate system instead of an inertially fixed system. An inertial frame is valid for mechanisms and robots but for vehicles, there could be numerical difficulties due to the combination of large position vectors and very small relative motions.

The programs mentioned above are the more common of several general purpose software currently in the market. Others include DYMAC, NEWEUL, MESA VERDE, SD-EXACT, SPACAR, NEUBEMM etc. [2,7].

Computer implementation of a particular formalism may either be numerical or symbolic. In a numerical formalism the equations of motion are generated numerically. They have the shortcoming of having to be generated for each set of parameters and at each time step in the integration procedure. In a symbolic formalism the equations of motion are generated symbolically, and usually written out in a high level programming language [42]. These equations are then compiled and used by an analysis program. This leads to fast execution as well as ease in parametric variation. The programs NEWEUL, MESA VERDE and SD-EXACT generate the equations of motion symbolically [7].

In most of the commercial programs the use of a maximal set of

equations to take care of the constraints greatly increases the number of equations to be solved. It is not unusual to have hundreds of differential equations to be solved even when the multi-body system has only one or two degrees of freedom. In some applications of these programs for vehicle dynamic simulation, one second of vehicle motion simulation has taken 1 hour of mainframe cpu time [43]. Because of this the general purpose programs are used only for *critical event simulation*. In fact, time simulation is the only dynamic analysis option available in most programs. Several users of these programs also complain about the inadequate and 'unfriendly' user interface.

General purpose programs can solve a very wide range of problems and can give accurate results. But their general use is limited by the drawbacks pointed out above. Another disadvantage of these programs is that the mechanical system has to be modelled as a spatial mechanism to be input to the program. This may not be the procedure all mechanical system analysts are used to. In vibration analysis, schematic models of mechanical systems are of the form shown in Figure 1.2. The analysis to be carried out may be transient response, eigenanalysis, transfer functions etc.. Using existing general purpose programs solution of these kinds of problems is either impossible or very cumbersome.

1.2.2 Vehicle System Dynamics

In ground vehicles, the vehicle dynamic analysis deals with three essential aspects: ride quality, handling, and load support. In this

research project we are primarily concerned with ride and handling. Although for a passenger, the quality of ride is determined by such factors as seat layout and noise, we use ride quality to mean the vibration level in the vehicle (experienced by passengers, cargo or vehicle components). There are three primary sources of vibration in vehicles, namely, engine and drive-train, aerodynamic loads, and vibration induced by the terrain and driver maneuvers. We concentrate on the last of these as it is the most dominant. Handling analysis is concerned with driver manoeuvres such as turning, braking and acceleration, and their influence on the response of the vehicle. In the present study we focus some aspects of roll dynamics due to steady-state turning.

There is a large body of research dealing with ride and vibration problems of road vehicles, off-road vehicles, rail-vehicles, and aircraft on runways [44-47]. Most of these studies deal with analytically predicting the dynamics of vehicles to different kinds of inputs, and the design and analysis of passive vehicle suspension systems to provide better isolation. In most vehicle systems, there are three stages of suspension units. With reference to an automobile these are (1) primary suspension (tires), (2) secondary suspension (assembly of spring-damper and linkages at the wheels) and (3) tertiary suspension (seat). The majority of ride comfort studies use the vehicle models such as those shown in Figure 1.2. Most of these studies are also based on linear analysis. When nonlinear effects are included, they are usually those due to dry friction and other non-viscous damping

phenomena.

Ride quality is achieved mainly by isolating shock and vibration from the ground. The main isolation units, usually consisting of springs and dampers, are connected between the wheels and the vehicle frame. Development of different types of suspension systems such as passive, active and semi-active systems to improve the ride quality is an important area of current research [48-50]. The application of the methodology and software packages that we develop in this research is envisaged mainly in this field.

The spring-damper isolator units usually appears as part of a linkage arrangement connecting the vehicle frame to the wheel or track. Figure 1.3 shows some examples of linkage geometries in vehicle suspensions. The linkage configuration in the suspension affect the vehicle ride comfort, often unintentionally. Therefore, a complete study of ride comfort must also include the effects of the linkage configuration in the suspension. This study can be divided into two areas:

1. Analysis, to investigate the effect of various linkage configurations on ride performance;
2. Design, involving the synthesis of a linkage geometry to achieve desired goals of ride performance as well as the requirements of proper support and handling.

These two aspects of the problem have gained little attention from

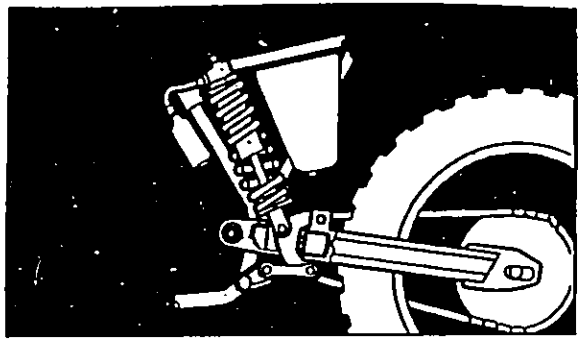

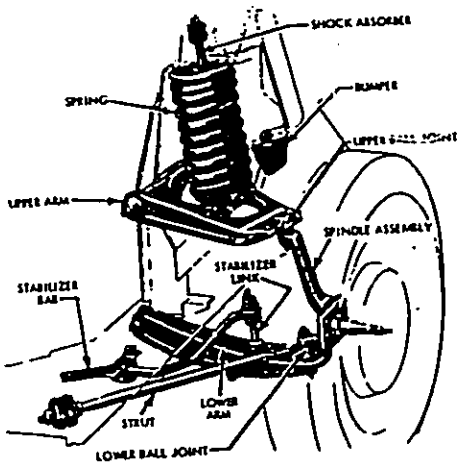

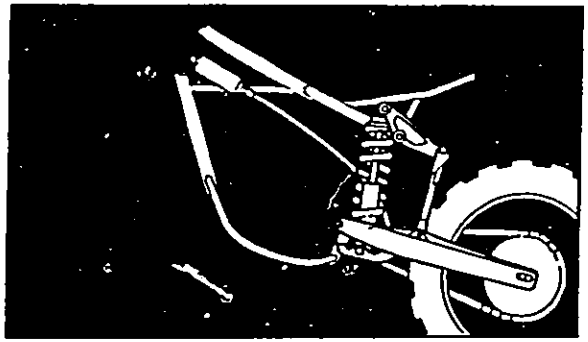

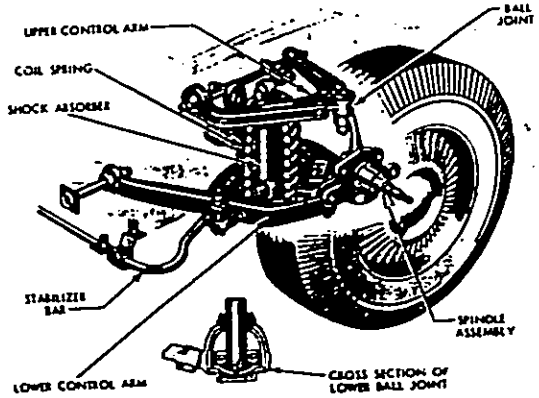

Fig. 1.3: Examples of vehicle suspension linkage arrangements

researchers so far. The linear analysis used in most ride comfort studies are in general valid only when the displacements are small. In the case of a linkage suspension, its change in geometry under large deflections often causes highly nonlinear effects. Although these aspects have not been examined from the point of view of ride comfort, studies are reported for handling behaviour and component stress analysis. In fact, it seems that suspension linkage geometry design is entirely determined by handling behaviour [51].

Vehicle handling and stability studies have considered suspension kinematics in detail [52]. Hales [53] proposed the *suspension derivatives* method for a planar suspension system to study the relationship between the roll and bounce movements of the vehicle body and the camber and scrub movements of the road-wheel. Butler and Ellis [54] later extended it for spatial kinematics and provided experimental validation. Cronin [55] has modelled the MacPherson strut suspension and studied the influence of wheel bounce on the changes in camber, toe, scrub, etc..

Several researchers have included the kinematics of suspension linkages in their study of vehicle dynamics. Dorgham and Ellis [56] used the suspension derivatives method in the modelling of a planar suspension for dynamic analysis. Majcher et al. [57] carried out large-deflection kinematic analysis of suspension linkages, using a linearized model for dynamic analysis. Morman [58] modelled the suspension system as an inertia-variant multi-body system and derived

dynamic equations using the Lagrange Multiplier method. Reddi et al [59] studied the dynamics of a helicopter with semi-levered landing gear traversing the runway. Nalecz [60] has presented a PC based program to evaluate the handling behaviour of a number of light vehicles. He has also considered suspension kinematics in the study of 4 wheel drive car handling maneuvers [61-62]. Many others have presented dynamic models of automobiles which include the kinematics of the suspension linkages [63,64].

An important aspect of vehicle handling is its turning behaviour. The distribution of lateral load-transfer due to centrifugal forces can cause understeer or oversteer effects [52]. A commonly employed method of characterizing the roll dynamics of different suspension systems is via its *roll centre* location and *roll stiffness* . These are determined by the kinematics of the suspension linkages, and therefore, several authors have presented methods of determining them [52,60-62,65-69]. Others [63-64] have either used or computed roll centres, without describing how they are computed. However, there has been some confusion as to what exactly is the roll centre, and how to determine its location etc. [69].

We now examine the use of some general purpose programs in vehicle system dynamic analysis. Some researchers have used finite element programs for ride comfort studies [70,71]. However, they are cumbersome to use and of limited application. Some researchers have also used the general purpose multi-body programs mentioned earlier for various

suspension studies. Giannopoulos and Rao [72] used IMP to carry out the dynamic simulation of an automobile wheel impacting a curb. The purpose of the study was to compare vehicle models of varying complexity for suspension load determination. Rai et al [73] used ADAMS to determine peak loads on suspension components during abuse events. Orlandea [74] and Orlandea and Chace [75] used ADAMS to compute suspension forces in a Chevorlet Malibu model. Chace [32], Antoun et al. [76] and Hackert et al. [77] carried out transient handling dynamic simulation of light trucks using detailed suspension models. Farm vehicle manufacturers also have been using the programs ADAMS and DRAM [78,79]. But their primary interests are the dynamics of different mechanisms (for planting, harvesting, etc.) attached to the farm vehicle, and not vehicle dynamics.

The program DADS has also been used for vehicle dynamic studies. Trom et al. [80,81] modelled a mid-size passenger car and simulated turning maneuvers, as well as, the dynamics of a simple load-levelling control algorithm. McCullough [82] studied tracked vehicle dynamics using super-element representation of suspensions and track.

Most applications of MEDYNA have been in the area of high speed rail transportation systems. Duffek and Kortüm [40] have presented simulation results for a magnetically levitated vehicle. Jaschinski and Kortüm [83] and Jaschinski [84] presented the theory of wheel-rail interaction structure, and simulated a 4-axle rail passenger car travelling at high speed. They also demonstrated the application of the

software in the analysis of low speed hunting behaviour of a freight car. Fuhrer has [85] detailed the many vehicle system dynamic analysis methods implemented in MEDYNA.

NEWEUL is a program that can generate symbolic linear or nonlinear equations of motion which may then be solved by other simulation programs. Schiehlen [86] has presented equations of a simple vehicle model for lateral dynamic analysis, and those of a complex automobile for vertical vibration. Both NEUBEMM and NEWEUL has been used by researches at BMW to study transient and steady-state analysis of a motorcycle and an automobile [87].

MEDYNA does not take into account large rigid body motions in suspensions. Two other programs, ADAMS and DADS, which do this, are based on formalisms that generate a maximal set of equations for the multi-body system. For example, even a simplified model of a MacPherson strut suspension unit gives rise to 35 second order differential equations together with 33 algebraic constraint equations [81]. Full vehicle models may have hundreds of equations and may take an hour or more of main frame CPU time for a single second of vehicle dynamic simulation. These programs also require large amounts of geometrical and physical data, and require a high level of modelling expertise and time. Furthermore, due to the complexity of the model, little physical insight can be gained about the effect of various components on the overall system performance.

1.3 SCOPE OF THE PRESENT STUDY

Vehicle system dynamicists do not usually make use of the general purpose mechanisms programs described earlier. Apart from the high cost of these software, there are other important reasons why this is the case. One reason is apparent when we look at the kind of mechanical system models that these dynamicists use, shown in Figure 1.2. These are most of the time inertia-invariant systems of free multi-bodies or articulated multi-bodies in tree configuration. It is cumbersome and sometimes meaningless to model these systems as spatial mechanisms as most of the general purpose programs require. The second reason is that the analysis options available in the general purpose programs are usually limited to time simulation. However, the vehicle system dynamicist must be able to carry out frequency and time domain analysis of vehicles traversing deterministic and stochastic terrains, as well as optimization studies. Another disadvantage of the general purpose mechanism programs is that they do not allow a *modular* approach to analysis and design. Since the vehicle-terrain system is modelled as one system, it is not easy to understand the effect of various subsystems on the overall performance. Therefore the use of these programs in design is very limited.

1.3.1 Objectives

In ground vehicle applications, the multi-body model of the vehicle

is characterized by bodies of relatively large masses interconnected by springs and dampers, or by kinematic joints in the case of articulated vehicles. The linkages making up the suspension assembly are of much smaller mass and often form closed kinematic chains. The large bodies representing the vehicle sprung masses go through only small rotation angles, at least in roll and pitch modes, whereas the links in the suspension assembly may experience large motions. These characteristics warrant a different approach to the modelling and analysis of vehicle systems.

In the current research program we seek: (1) to create an analytical formulation that is suitable for digital computer implementation which allows the engineer to input data that defines the mechanical system of interest (especially vehicle systems) and automatically generates the governing equations; (2) to develop and implement numerical algorithms that automatically solve the equations for dynamic response of the system, and provide computer graphic output of the results to the designer or analyst; (3) to develop new techniques for the analysis and design of suspension linkages; (4) to implement these in a general purpose program; and (5) to use these techniques and software for the analysis of suspension systems for a snowmobile.

As part of the first objective we seek to create a formulation whose modelling strategy parallels the intuitive and customary techniques used by mechanical system dynamicists. We explain what we mean by this with reference to an example. Figure. 1.4(a) shows a

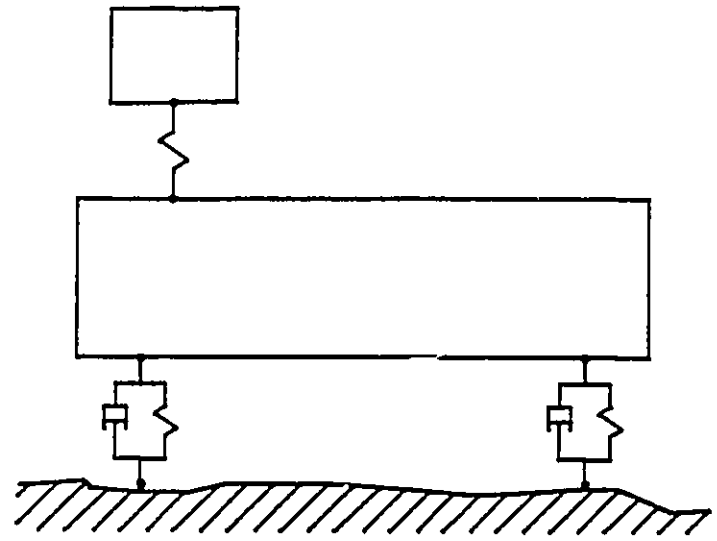

(a)

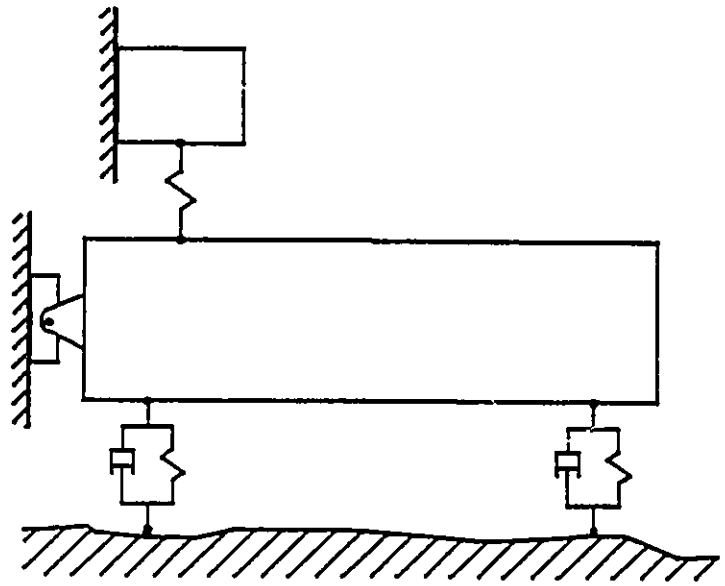

(b)

Fig. 1.4: Lumped parameter model of a automobile with a driver (a) conventional schematic, (b) mechanism model

typical model of an automobile with a driver. The driver is represented by a mass which may move vertically up and down (bounce). The vehicle may bounce and pitch. The suspensions are represented as two-port force generators. Totally there are 3 degrees of freedom and we can easily write down 3 second order differential equations of motion. We have intuitively regarded this as a free multi-body system and applied Newton-Euler equations for each body. In general, an unconstrained rigid body in a plane has three degrees of freedom. Therefore there are implicit constraints imposed on the driver and the vehicle so that the driver has only one, and the vehicle two degrees of freedom, as shown in Figure 1.4(b). We have written the equations for each degree of freedom by considering only the *relevant* forces and torques. If this system were to be analyzed using certain general purpose programs, it may have to be modelled as shown in Figure 1.4(b). We may typically expect 6 second order differential equations together with 3 algebraic constraint equations ! We consider this situation unacceptable as the computer has complicated the problem. In this research program we present a formulation which would closely follow the manual modelling techniques.

The second objective is the implementation of the new formulation as a general purpose program for mechanical systems dynamics. We seek an implementation which makes use of interactive graphics to full advantage. The model description to the program should be as easy as constructing the schematic drawing of the system by assembling its various components on a graphics screen. The program should be able to carry out a wide range of analyses for stochastic, harmonic and

transient inputs. The software should also be able to generate the system equations symbolically in a high level language, so that the analyst may use it in his own special analysis programs. Most of these are features nonexistent in the current programs.

Vehicle suspensions are not made solely of a spring and damper attached to the wheel and the body. They often appear as parts of a linkage assembly. But in the models shown above they have been idealized and represented by an equivalent isolator. Since the suspension linkages go through large deflections, they introduce geometric nonlinearities on the force generation of the suspension system. As seen from the literature review, previous researchers have taken two approaches to this problem. The common solution is to linearize the model about the operating point. The other is to include the nonlinear suspension kinematic model and solve it in each step of numerical integration of a transient analysis. We develop a new methodology for the analysis of linkage suspensions, called the *method of velocity coefficients.* In this modelling scheme, the linkage suspension is replaced by a linkage-free *equivalent force-generator model* of identical isolation characteristics. A kinematic analysis is performed *a priori*, to extract precisely and completely, the information required for a separate dynamic analysis. This is Objective (3) and it complements Objective (1) mentioned above, and leads to a certain modularity in the analysis and design stages. Another aspect of the third objective is to take a fresh look at the concept of roll centres, and to clarify some disputed points. We show that the method of

velocity coefficients provides an analytical method of computing roll centres and roll stiffness, in contrast to the existing graphical methods.

The fifth objective is to apply the techniques and software developed as part of the first three objectives, to the kinematic and dynamic analysis of suspension systems for a snowmobile. The suspension model under study has a very complex linkage arrangement and it has been shown that their kinematics have significant effects on the ride comfort.

The present research project has been conducted over the past three years and has resulted in several publications given in Ref. [88-93].

1.3.2 Organization of the Thesis

In Chapter 2, we present a mathematical formalism for modelling vehicle system dynamics. This methodology parallels the intuitive and customary techniques used in manual modelling and leads to symbolic derivation of system dynamic equations. In Chapter 3, we present a software called CAMSYD (Computerized Analysis of Mechanical System Dynamics) which has been developed based on this work. This is a general purpose, modelling and analysis program for two-dimensional multi-body systems. The program features interactive graphic input and output, automatic symbolic equation generation, and a wide variety of

analysis options for vehicle dynamic analysis. Its usage is illustrated through several typical examples.

In the modelling technique used in Chapter 2, the vehicle suspension systems are represented as 'black box' force generators. In reality, a suspension system consists of several linkages with springs and dampers forming a part of it. In Chapter 4 we present new techniques for the modelling and analysis of linkage suspensions. Using this method, large deflection force deflection characteristics of the suspension system can be evaluated from a kinematic analysis separate from the total system's dynamic analysis. We also present new methods of determining roll centre locations and roll stiffnesses of linkage suspensions.

In Chapter 5 we present a software package called GENKAD (General Purpose Kinematic Analysis and Design) for kinematic and kineto-static analysis of linkages. It features interactive graphic data input and output, animation, and design sensitivity analysis. Several vehicle suspension systems are modelled and analyzed.

In Chapter 6 we present modelling and analysis of a snowmobile for ride comfort. GENKAD is used for kinematic analysis to determine the equivalent force-generator models of the suspensions and CAMSYD is used for dynamic modelling and analysis. Analysis results are compared with results from field tests on an instrumented snowmobile. Finally, Chapter 7 presents general conclusions and some recommendations for

future research.

Chapter 2

A GENERAL PURPOSE FORMALISM FOR LUMPED PARAMETER VIBRATORY SYSTEMS WITH APPLICATION TO VEHICLE DYNAMICS

2.1 INTRODUCTION

In very many applications in mechanical system dynamics, we encounter models of the sort shown in Figures 2.1 through 2.4. These include a dynamic model of a cam mechanism (Fig. 2.1) [94], gear dynamic models (Fig. 2.2) [95], roll-plane model of a railroad car (Fig. 2.3) [96], and ride dynamic model of a tractor semitrailer (Fig. 2.4) [97]. We have cited a few examples, but is clear that this type of lumped parameter models are commonplace in engineering analysis. In this chapter we present a general purpose formalism suitable for computerized derivation of equation of motion for this class of systems.

Models shown above may lack a certain realism, compared to 'mechanism' models. But their widespread use indicates that they are valuable in both analysis and design of mechanical system dynamics. Furthermore, they are in keeping with the paradigm that models should be "no more complicated than absolutely necessary to provide the necessary information with the desired accuracy and timeliness, while minimizing the use of resources" [98].

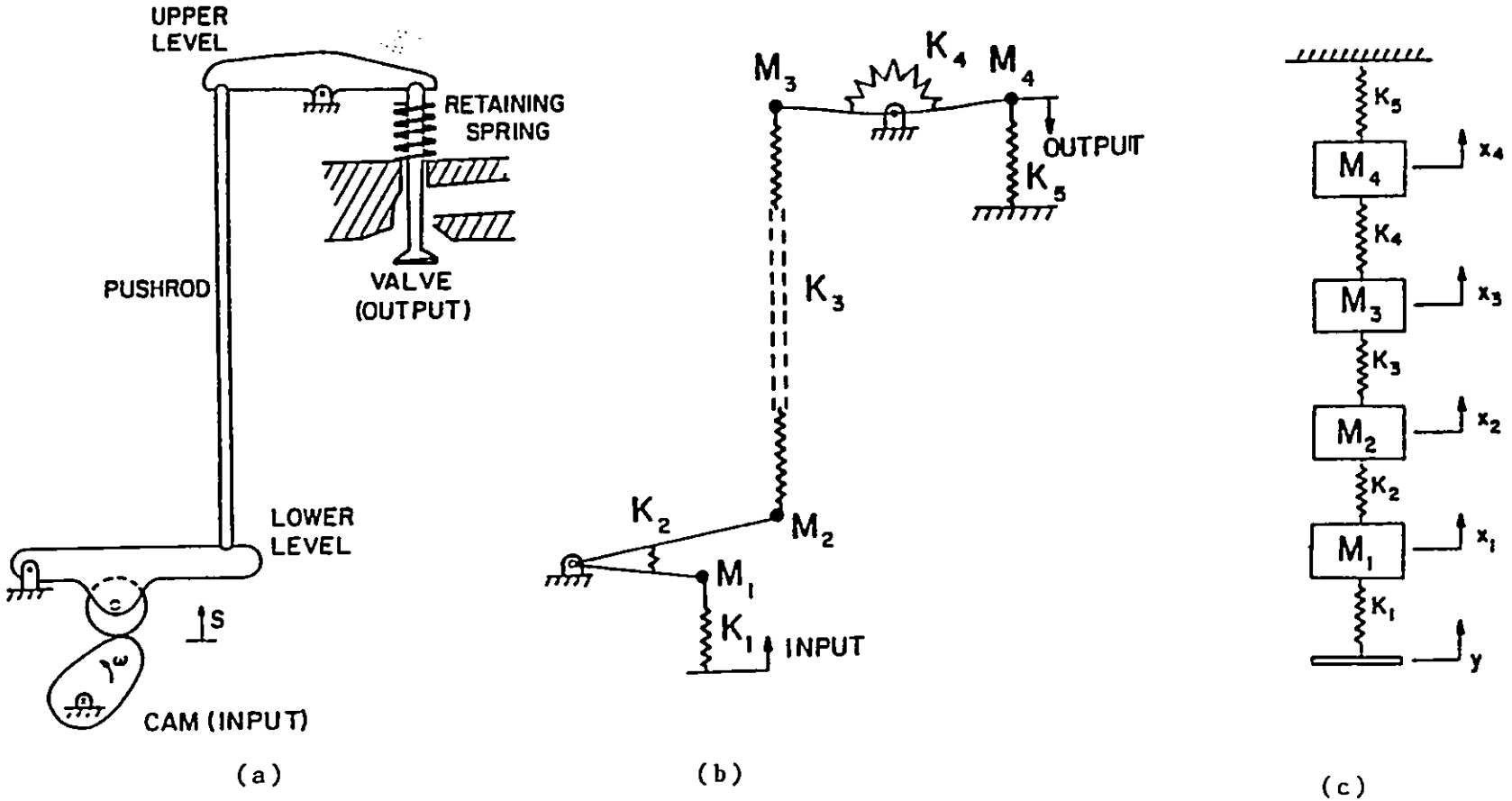

Fig. 2.1: A double lever cam mechanism: (a) physical system (b) initial model, (c) final model

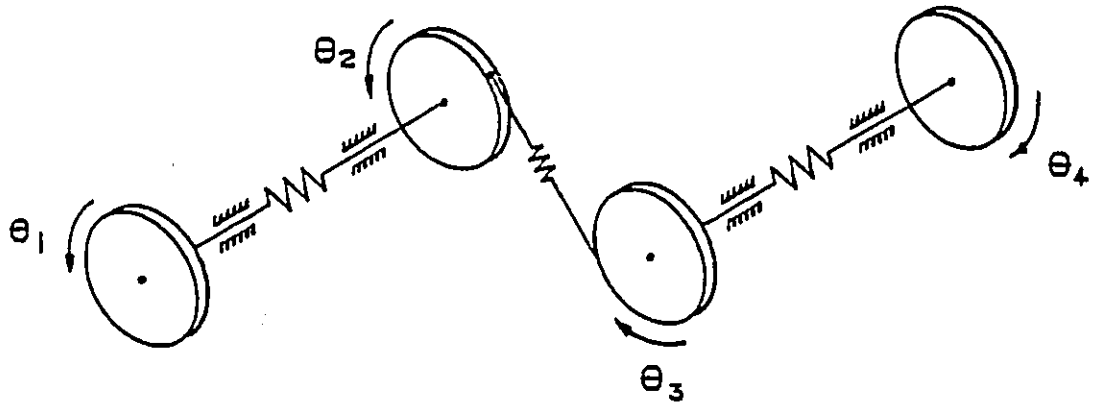

(a)

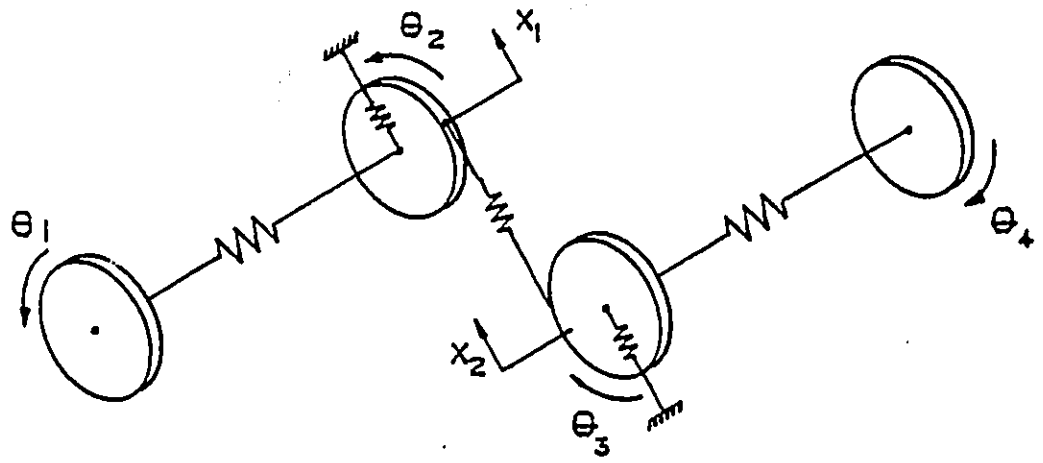

(b)

Fig. 2.2: Typical gear dynamic models

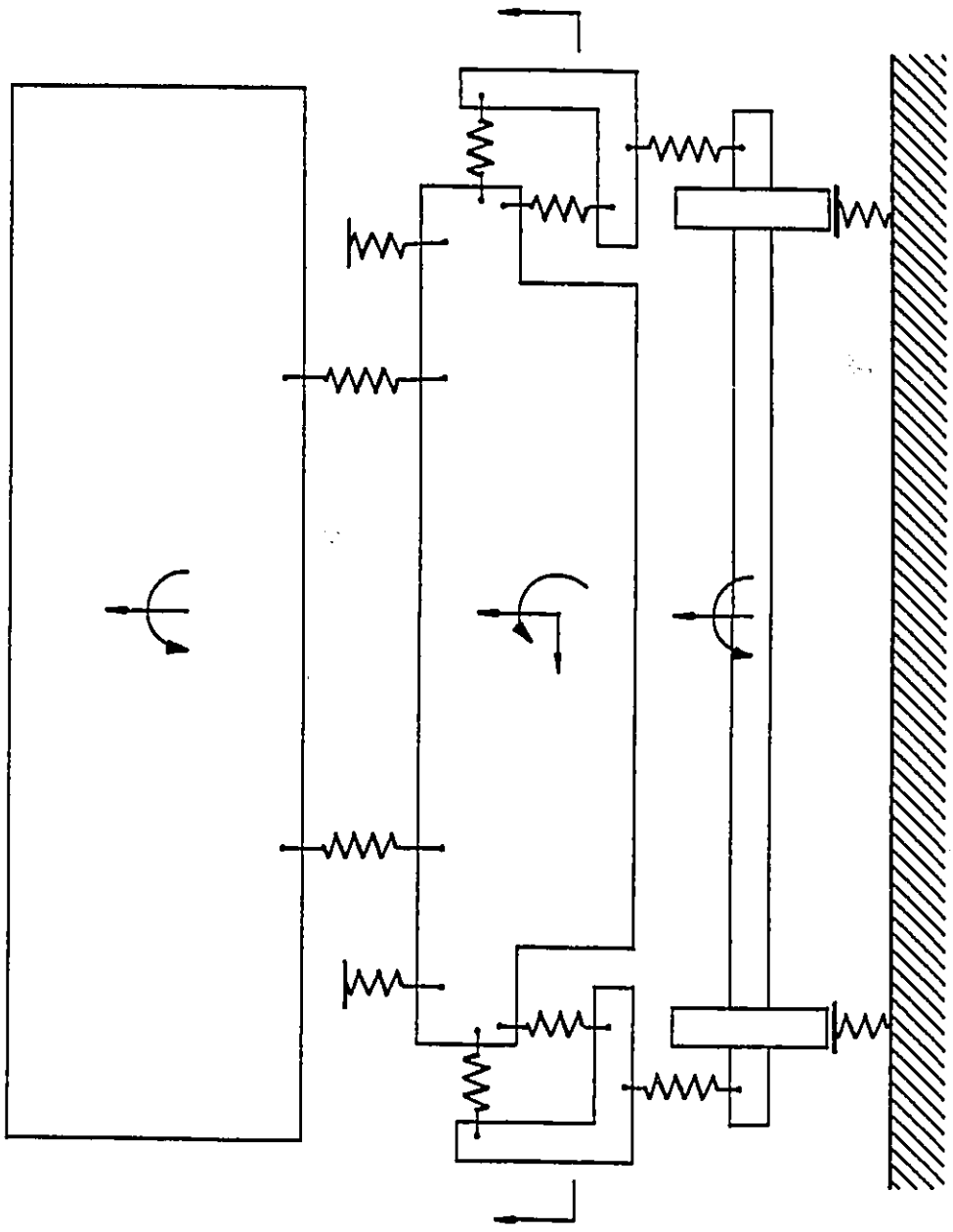

Fig. 2.3: Roll-plane model of a railroad flatcar

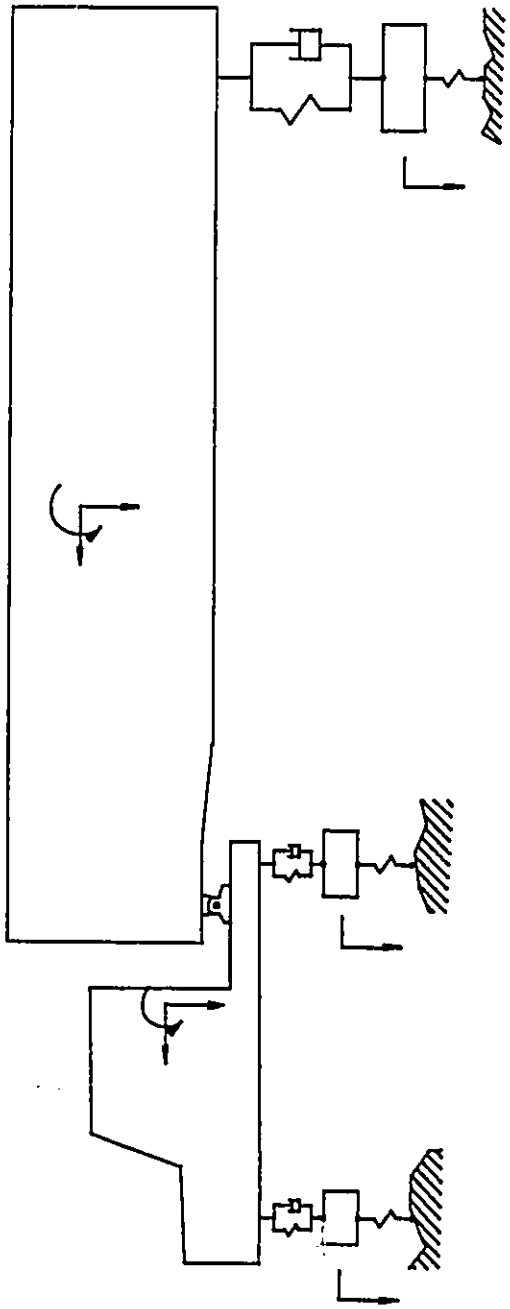

Fig. 2.4: Ride dynamic model of a tractor semitraller

2.2 EQUATIONS OF MOTION FOR MULTI-BODY SYSTEMS : BACKGROUND

Multi-body systems are characterized by rigid bodies with inertia; and springs, dampers, and other force-generators without inertia; and kinematic joints without friction. Multi-body systems may be free, holonomic, or non-holonomic, depending on the bearings and supports which constrain the motion. Free multi-body systems have no kinematic constraints. Such a system of p bodies in 3-dimensional inertial frame is represented by $n = 6p$ generalized coordinates. A holonomic system of p bodies and m holonomic, rheonomic constraints has $f = 6p-m$ degrees of freedom.

There are several analytical methods in classical mechanics dealing with the dynamics of constrained rigid body systems. The preferred approach used in many current general purpose programs is the *Lagrange Multiplier Method.* Using this scheme each rigid body is modelled with 6 Lagrangian coordinates associated with them, say, for a total of n of them. In a free multi-body system, these coordinates correspond to the degrees of freedom of the system (i.e., they are the generalized coordinates). But in a constrained system with m holonomic constraints, there are algebraic compatibility equations at each joint which relate these coordinates to each other. The system has only $f = n-m$ degrees of freedom. But the n Lagrangian coordinates can be treated as independent, if we conceptually remove the explicit constraints but consider the reactions produced by the constraints as external forces. This leads to the equation of motion in the form of Lagrange's Equations with Multipliers. These are n differential equations with $n+m$ unknowns

(n Lagrangian coordinates and m Lagrange multipliers). They are augmented with the m algebraic equations of constraints and the resulting system of differential - algebraic equations (DAE) are solved using special techniques [34-37].

As a simple example, consider a particle of mass m in 2-dimensional space. If there are no constraints on the mass, it is allowed to move in x_1 and x_2 directions, which are the degrees of freedom of the system. Consider forces F_1 and F_2 acting along the same directions. Then the equations of motion follow directly from Newton's Second Law as:

$$\left.\begin{aligned} m\ddot{x}_1 &= F_1 \\ m\ddot{x}_2 &= F_2 \end{aligned}\right\} \tag{2.1}$$

These equations are independent and can be solved without difficulty. Consider, now, that this particle is constrained to move along the line:

$$a\, x_1 + b\, x_2 + c = 0 \tag{2.2}$$

The situation is shown in Figure 2.5. We cannot treat x_1 and x_2 as independent unless we include the reaction forces due to the constraint. Using the Lagrange Multiplier method we can write,

$$\left.\begin{aligned} m\,\ddot{x}_1 &= F_1 + a\,\lambda \\ m\,\ddot{x}_2 &= F_2 + b\,\lambda \\ a\, x_1 + b\, x_2 + c &= 0 \end{aligned}\right\} \tag{2.3}$$

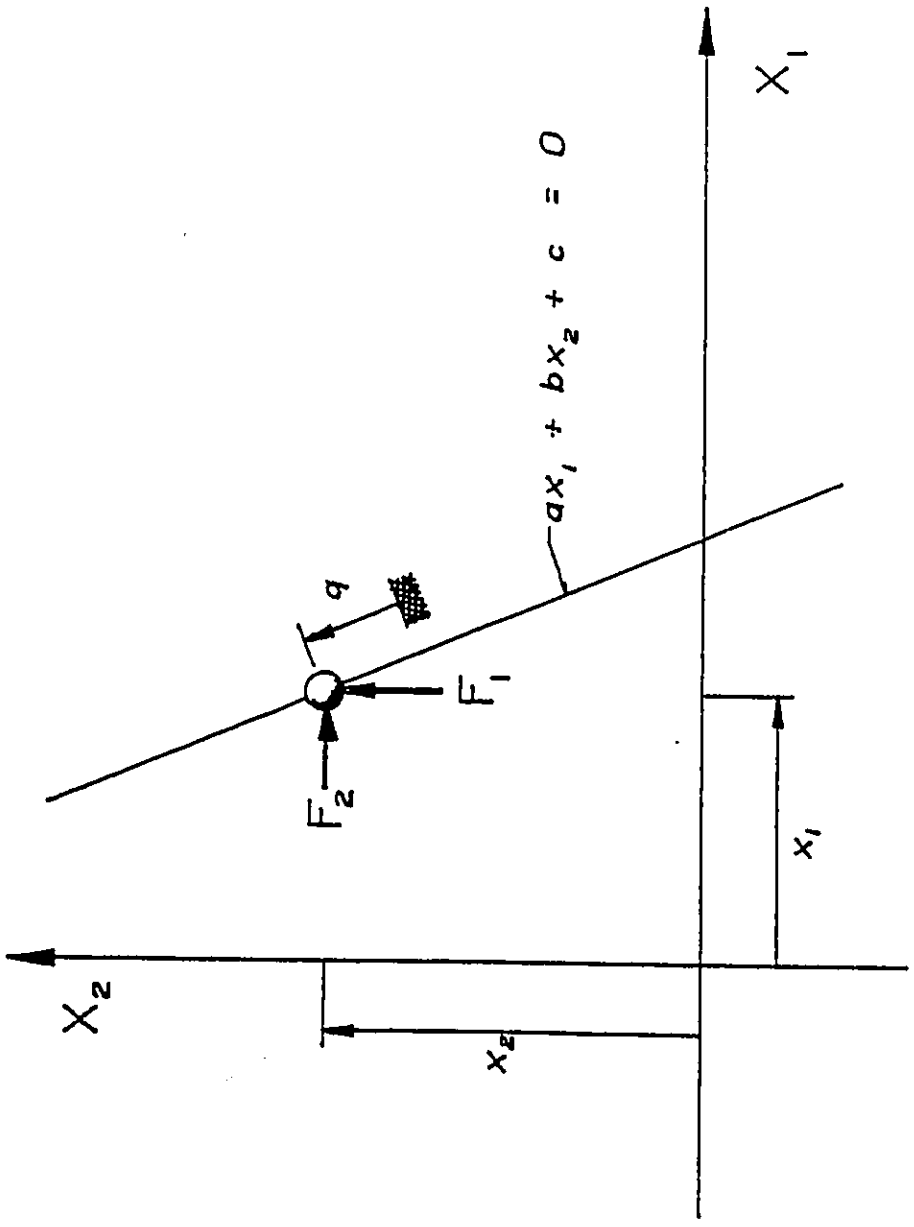

Fig. 2.5: A particle constrained to move on a line

Now we have 3 unknowns, x_1, x_2 and λ, and 3 equations which can be solved. Note that this procedure generates 3 equations although the system actually has only 1 degree of freedom.

If we choose the variable q as shown in Figure 2.5 as the generalized coordinate, we will get the equation:

$$m\,\ddot{q} = -\,(b/r)\,F_1 + (a/r)\,F_2 \qquad (2.4)$$

where $r = \sqrt{a^2 + b^2}$.

The quantities $-(b/r)$ and (a/r) are the direction cosines of q. Therefore, the expression on the right-hand side of Equation (2.4) is simply the sum of the components of the external forces in the direction of q. In this formulation, we get exactly one equation for the one degree of freedom. For this simple example, where the constraint was between the particle and the inertial frame, it was possible to find a Lagrangian coordinate which greatly reduced the complexity of the equation. But it may not generally be the case. Nevertheless the above example serves to illustrate the contrast between computer aided formalisms based on a 'general' approach, and a more traditional approach whereby one makes use of the special characteristics of a given problem.

2.3 A NEW FORMALISM FOR A CLASS OF MULTI-BODY SYSTEMS

2.3.1 Characteristics of a Class of System Models

Models of the sort shown in Figure 2.1 through 2.4, which represent the majority of models used in mechanical systems dynamics, are of the inertia-invariant type. This characteristic is a result of deliberate modelling decisions based on an understanding of the system that is being studied. For example, models used in vehicle dynamics are characterized by bodies of relatively large masses interconnected by springs and dampers, or by kinematic joints in the case of articulated vehicles. The linkages making up the suspension assembly are of much smaller mass and often form closed kinematic chains. The large bodies representing the vehicle sprung masses go through only small rotation angles, at least in roll and pitch modes, whereas the links in the suspension assembly may experience large motions. Therefore, if suspensions are represented as spring-damper elements, the resulting system is of inertia-invariant type.

Before presenting our modelling formalism, we would point out some additional features of the models referred to earlier. Figure 2.1 shows the modelling steps involved in studying the dynamics of cam mechanism [94]. The modeller's knowledge of the behaviour of such a system leads to an abstract representation of the model as shown in Figure 2.1(c). The flexibilities and inertias of various links are lumped at discrete points. Each of the masses has a single degree of freedom and is assumed to move vertically up and down. Figure 2.2 shows some models

used in gear dynamics [95]. In some models the gears have a single rotational degree of freedom. The shafts have rotational stiffness and the gear meshing is represented by the linear stiffness of the contacting teeth. In some other models, some of the gears have a single rotational degree of freedom, while others possess an additional linear degree of freedom. Figure 2.3 shows the roll plane model of a railroad flatcar [96]. Once again we observe that different bodies are modelled with different numbers of degrees of freedom. In the tractor semitrailer model [97] shown in Figure 2.4, each of the wheel axle assemblies are modelled as a point mass restricted to move in the vertical direction. The tractor and the semitrailer are modelled with 3 degrees of freedom. The *fifth-wheel* coupling is modelled as a hinge.

So, we note that in traditional modelling it is customary to model different bodies with different numbers of degrees of freedom. This decision is made by the modeller based on his experience and his understanding of the particular problem. When he manually derives the differential equations of motion for these systems, he does not explicitly write six equations for six of the possible degrees of freedom and then write additional constraint equations to represent the gearing, bearings etc.. These constraints are automatically taken care of when the actual degrees of freedom are identified in the modelling stage and equations are written only for those degrees of freedom. In this chapter, we formalize this customary equation derivation strategy. The methodology leads to a straightforward algorithm for computerization of equation generation.

In vehicle systems, the suspensions are not made solely of a spring and damper attached to the wheel and the body. They often appear as parts of a linkage assembly. But in the models shown above they have been idealized and represented by an equivalent isolator. Since the suspension linkages go through large deflections, they introduce geometric nonlinearities on the force generation of the suspension system. In Chapter 5, we present a methodology whereby the linkage suspension can be replaced by a linkage-free *equivalent force-generator* model. Once the large deflections in the suspension linkage are taken care of in this manner, there is no real need to model the entire vehicle as a mechanism to use general purpose programs.

2.3.2 Modelling Techniques and Reference Frames

The formalism accounts for all of the models shown in Figures 2.1 through 2.4. A generic system is shown in Figure 2.6(a), along with appropriate reference frames. In deriving equations of motion we recognize two types of bodies - free bodies without any kinematic connection to other bodies, and those with kinematic constraints. A single system model may consist of groups of articulated bodies as well as kinematically isolated bodies, connected together via springs and dampers. This is typical of vehicle system applications. The formalism treats free bodies individually and each set of articulated bodies as a group. Only planar cases are considered with revolute joints being the only joint type. The methodology can, however, be extended to spatial systems as well.

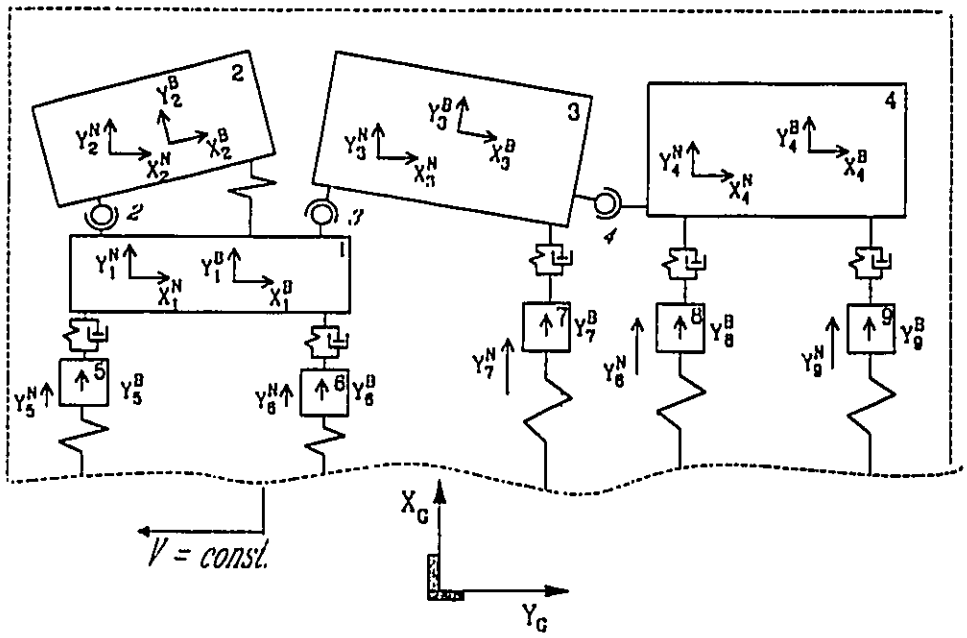

(a)

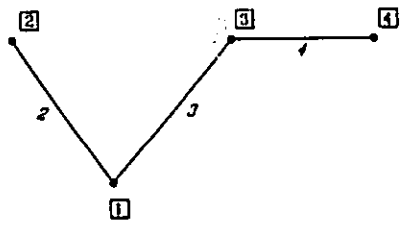

(b)

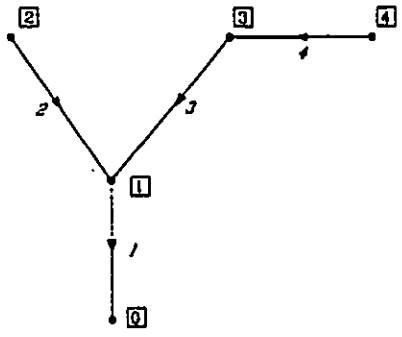

(c)

Fig. 2.6: A generic planar multi-body system: (a) system model and coordinate frames, (b) system graph (c) directed graph

The system is represented in an inertial reference frame XY as shown in Figure 2.6. This frame may have a constant velocity motion with respect to a ground-fixed frame XY^G. Each body, i, has a body fixed frame XY_i^B at its CG. In the system nominal position, each of these frames coincide with frames, XY_i^N, which have constant positions and orientations with respect to the inertial frame. Each of the bodies may undergo large translational motions and/or small rotational motions with respect to their nominal positions.

2.3.3 Free Bodies

Free bodies have no explicit kinematic constraints relating their motion to other bodies. The study of these bodies is therefore quite straightforward.

2.3.3.1 Kinematics of Free Bodies

As discussed in Section 2.3.1, the bodies may have *implicit* scleronomic constraints so that certain of their degrees of freedom are restricted with respect to the inertial frame. Thus, we have 1-degree-of-freedom bodies, which may have either translational motion along a line or rotational motion. 2-DOF bodies may have either two translational degrees of freedom, or one rotational degree of freedom and one translational degree of freedom. A 3-DOF body is a truly free body in the conventional sense.

Kinematics is the description of absolute motion. For a free body

this is given by the generalized coordinates representing each of its degrees of freedom. The nominal body reference frame, XY_i^N, is defined so that it aligns with the possible degrees of freedom of each body. Therefore, the body position is given by an appropriate combination of X_i^N, Y_i^N, and θ_i^N in this reference frame.

2.3.3.2 Dynamics of Free Bodies

For each free body dynamic equations can be written independently of other bodies, once applied forces are known. The dynamic equations are written in the body's nominal reference frame, corresponding to each of its degrees of freedom. The total applied force on the body, F_i, is given in inertial frame. Its components along X_i^N and Y_i^N are determined as F_i^x and F_i^y . Then the equations of motion are:

$$m_i \ddot{x}_i = F_i^x \qquad (2.5a)$$

$$m_i \ddot{y}_i = F_i^y \qquad (2.5b)$$

$$J_i \ddot{\theta}_i = M_i \qquad (2.5c)$$

where θ_i is the rotation of body i, if it is allowed, and M_i is the sum of all the moments acting on it. A combination of Equation (a), (b), or (c) apply depending on whether the corresponding degree of freedom exists. For each body there are only as many equations as there are degrees of freedom.

2.3.4 Constrained Multi-body Systems

The analytical development in this section closely follows that given by Wittenberg [11] with some modifications. Wittenberg ([11], Chapter 5) has derived equations for large displacement dynamics of systems of rigid bodies in tree configuration. All kinematic joints are assumed to be ball and socket joints. Two special cases are considered: (1) a system with one body coupled to an external body whose motion is specified; and (2) a system without any coupling to an external body. Case 1 refers to systems such as robot manipulators, human body in locomotion, etc.. Case 2 refers to spacecraft in orbit, vehicle systems etc.. For systems of Case 2, Wittenberg derived equations of motion with the set of coordinates of the composite system centre of gravity as one of the vector variables. This is appropriate for spacecraft, but in many applications including for vehicle dynamics, it is more sensible to treat one of the bodies as the main body and derive equations in terms of that body's coordinates. This is the approach we follow here. For the sake of clarity we present the derivation for a system of articulated 2 degree-of-freedom bodies in a plane (each with bounce and pitch degrees of freedom). The method can be extended as in Ref. [11] to 3-D systems and other types of joints.

2.3.4.1 Description of Interconnection Structure

Ideal springs, dampers etc. do not constrain the motion of bodies to which they are attached, but kinematic joints do. In Figure 2.6(a) bodies 5, 6 and 7 are free bodies as dealt with in Section 2.3.2.

Bodies 1, 2, 3, and 4 form a system of constrained bodies. A very convenient way to describe the interconnection structure is by using a system graph. A *graph* consists of two finite sets: a set of elements called *vertices* and a set of elements called *edges* [99]. The vertices in this graph represent bodies and edges represent hinges. The graph has a tree structure if there is a unique path between two vertices. Figure 2.6 shows a typical example of the system under study (a), and its associated system graph (b).

Each hinge appears between two bodies, and we associate an arbitrary direction with it. Each hinge has a direction which points away from one body and points toward the other. When there are n bodies interconnected in the form of a tree, there are $n-1$ hinges. We designate any one of the bodies as the 'main body', and it is numbered as body 1. We assume a fictitious hinge, numbered as hinge 1, between body 1 and the inertial frame. Now there are n bodies and n hinges. Figure 2.6(c) shows this structure along with directions assigned to each hinge.

The interconnection structure can also be described using an *incidence* matrix, S. This is a square matrix. Its rows correspond to bodies and columns to hinges. The elements of this matrix are defined as:

$$S_{ij} = \begin{cases} +1 , & \text{if hinge } i \text{ is pointing away from body } j \\ -1 , & \text{if hinge } i \text{ is pointing toward body } j \\ 0 , & \text{otherwise} \end{cases}$$

For the systems shown in Figure 2.6, the incidence matrix is:

$$S = \begin{bmatrix} +1 & -1 & -1 & 0 \\ 0 & +1 & 0 & 0 \\ 0 & 0 & +1 & -1 \\ 0 & 0 & 0 & +1 \end{bmatrix}$$

Another matrix is also constructed to describe the interconnection structure. It is called the *path-to-datum* matrix, T. Its rows correspond to hinges and columns to bodies. Its entries are also 0, +1 or -1. If a hinge, i, belongs to the path from body j to the datum (inertial frame), and is directed toward it, then T_{ij} is +1. If it is directed away then T_{ij} is -1, otherwise it is 0. It can be shown that that matrix T is the inverse of S, and this inverse always exists for a tree. For the systems shown in Figure 2.6, the path-to-datum matrix is:

$$T = \begin{bmatrix} +1 & +1 & +1 & +1 \\ 0 & +1 & 0 & 0 \\ 0 & 0 & +1 & +1 \\ 0 & 0 & 0 & +1 \end{bmatrix}$$

We note in passing that this matrix has a special structure. It is an upper diagonal matrix, with all non-zero elements and all diagonal elements equal to +1. This is a result of the particular way in which the bodies and hinges were labelled. There are three conditions to be satisfied - (1) all edges in the directed graph are pointing towards the ground; (2) for each body the number for the inboard-pointing hinge is

the same as the body number; and (3) body numbering is such that they monotonically increase radially. The theory that follows is equally valid no matter what the manner of labelling. But obviously the structure of the matrix has a bearing on the form of the equations, the complexity of matrix operations, as well as, storage requirements in a computer implementation.

2.3.4.2 Kinematics of Constrained MBS

Kinematics describes absolute motion of the system, i.e., position, velocity, and acceleration. For free MBS, position coordinates of each body are also generalized coordinates. However, for constrained systems, they are not all independent. For the case of a system of 2-DOF bodies in tree configuration, the kinematics is described in the nominal reference frame of the main body (body 1). The generalized coordinates are selected as the set consisting of: 2 main body coordinates (y_1, θ_1) and rotation angles of each of the other bodies (θ_i, $i = 2 \ldots n$). The rotations are considered to be small. The (n+1)-vector, $\underline{q}$, of generalized coordinates is,

$$\underline{q}^T = (y_1, \underline{\theta}^T)^T \tag{2.6}$$

Position kinematics is solved when each of the dependent coordinates ($y_2 \ldots y_n$) are expressed in terms of $\underline{q}$. In order to achieve this, we describe another matrix. This is a matrix, c, whose elements, c_{ij} correspond to the X_i^B distance from the centre of gravity of body i to hinge j incident on it. From this we construct the matrix C, whose

elements are the products of the corresponding elements in S and c. Since hinge 1 is fictitious, c_{11} has no significance and is set to zero. Using matrices C and T we define the *distance* matrix, D, as:

$$D = -(CT)^T \tag{2.7}$$

The structure of C and T is such tnat the top row of D is all zeros.

Now we can write each of the bounce coordinates as:

$$y_i = y_1 + \sum_{j=1}^{n} D_{ij}\,\theta_j \qquad i = 1 \ldots n \tag{2.8}$$

or, in matrix form as :

$$\underline{y} = \underline{1}_n y_1 + D\underline{\theta} \tag{2.9}$$

where $\underline{1}_n$ is a n-vector with each entry equal to 1. This establishes position kinematic relations for small rotations. Velocities and accelerations are obtained by differentiating 2.9 with respect to time as:

$$\dot{\underline{y}} = \underline{1}_n \dot{y}_1 + D\dot{\underline{\theta}} \tag{2.10}$$

$$\ddot{\underline{y}} = \underline{1}_n \ddot{y}_1 + D\ddot{\underline{\theta}} \tag{2.11}$$

For the sample system shown in Figure 2.6, application of Equation 2.9 gives,

$$y_1 = y_1$$

$$y_2 = y_1 + c_{12}\theta_1 - c_{22}\theta_2$$

$$y_3 = y_1 + c_{13}\theta_1 - c_{33}\theta_3$$

$$y_4 = y_1 + c_{13}\theta_1 - (c_{33} - c_{34})\theta_3 - c_{44}\theta_4$$

These can be verified by inspection from the figure.

2.3.4.3 Dynamics of Constrained MBS

Equations of motion are derived by applying Newton's Second Law to the total system and the law of moment of momentum to each individual body. Each body, i, has a mass m_i, and moment of inertia I_i. Setting effective forces equal to applied forces, for the overall system, we have,

$$\sum_{i=1}^{n} m_i \ddot{y}_i = \sum_{i=1}^{n} F_i \qquad (2.12)$$

i.e.,

$$\underline{m}^T \ddot{\underline{y}} = \sum_{i=1}^{n} F_i \qquad (2.13)$$

Substituting for $\ddot{\underline{y}}$ from Equation 2.11,

$$\underline{m}^T \left(\underline{1}_n \ddot{y}_1 + D\ddot{\underline{\theta}} \right) = \sum_{i=1}^{n} F_i \qquad (2.14)$$

or,

$$m_{tot} \ddot{y}_1 + \underline{m}^T D\ddot{\underline{\theta}} = \sum_{i=1}^{n} F_i \qquad (2.15)$$

where $m_{tot} = \sum_{i=1}^{n} m_i$, is the total mass of the system. Equation 2.15 is one of the $n+1$ equations representing the system dynamics in $n+1$ variables. The other n are obtained by applying the law of moment of momentum to each body separately. For this purpose we cut each of the hinges and consider the free-body diagrams of each body. Now the internal forces in hinges appear as applied forces and torques along with external forces and torques.

$$I_i \ddot{\theta}_i = M_i + \sum_{j=1}^{n} (S_{ij} Y_j + C_{ij} X_j^c) \qquad (2.16)$$

or in matrix form as

$$\mathcal{I}\ddot{\underline{\theta}} = \underline{M} + S\underline{Y} + C\underline{X}^c \qquad (2.17)$$

where Y_j is the torque generated due to friction or rotational stiffness, and X_j^c is the constraint force in hinge j. X_j^c can be determined as follows.

Applying Newton's Law to each free-body, we have,

$$M\ddot{\underline{y}} = \underline{F} + SX_j^c \qquad (2.18)$$

$$\Rightarrow \quad X_j^c = S^{-1}(M\ddot{\underline{y}} - \underline{F})$$

$$= T [M(\underline{1}_n \ddot{y}_1 + D\ddot{\underline{\theta}}) - \underline{F}]$$

$$= \ddot{y}_1 T\underline{m} + TMD\ddot{\underline{\theta}} - T\underline{F} \tag{2.19}$$

Substituting this in Equation (2.17), we get,

$$D^T\underline{m}\ddot{y}_1 + (\mathcal{I}+D^TMD)\ddot{\underline{\theta}} = \underline{M} + S\underline{Y} + D^T\underline{F} \tag{2.20}$$

All the vectors above are *n*-vectors, and the matrices are *nxn*.

Equations 2.15 and 2.20 can be combined in matrix form to obtain the final equations of motion as:

$$A\ddot{\underline{q}} = B(\dot{\underline{q}}, \underline{q}, t) \tag{2.21}$$

where,

$$A = \begin{bmatrix} m_{tot} & \underline{m}^T D \\ D^T\underline{m} & \mathcal{I}+D^TMD \end{bmatrix} \tag{2.22}$$

and

$$B(\dot{\underline{q}}, \underline{q}, t) = \begin{bmatrix} \sum F_1 \\ \underline{M}+S\underline{Y}+D^T\underline{F} \end{bmatrix} \tag{2.23}$$

A is the generalized mass matrix of the system and it is constant and symmetric. This can be evaluated once and inverted, to write the system equations in state-space form as:

$$\dot{\underline{x}} = \underline{f}(\underline{x}, t) \tag{2.24}$$

where $\underline{x}^T = [\ \underline{q}^T,\ \dot{\underline{q}}^T\ ]$ is the state-vector.

These equations are in a form easily implemented in a computer algorithm. This has, in fact, been carried out in the general purpose program, CAMSYD, to be described in Chapter 3.

2.3.5 Applied Forces

In the forgoing discussions it was assumed that the applied forces and moments acting on each body are known. This Section shows how these can be computed. All forces acting on a body except those due to kinematic constraint forces are called applied forces. These include gravity loads, external loads, and those imposed by springs, dampers, etc.. They can be proportional or proportional-differential forces. Proportional forces depend on the systems position, defined by the set of generalized coordinates, $\underline{q}$. Proportional-differential forces depend on position and velocity. Thus, if we know the state of the system defined by the state-vector $\underline{x} = [\underline{q},\ \dot{\underline{q}}]^T$, we can determine all the proportional and proportional-differential forces. Forces in passive springs and dampers depend only on the relative motion across their terminals. When a terminal point is connected to a rigid body, the motion of this point can be computed from the state-vector using a constant transformation matrix. Once all the forces are computed in the inertial frame, they can be summed for each body and expressed in its own reference frame. After this the derivation of equations of motion follows as described in the previous sections.

2.4. SUMMARY

A large class of mechanical systems can be modelled as lumped parameter systems undergoing small rotations, and interconnected by springs, dampers and hinges. Conventionally each body is modelled with an limited number of degrees of freedom, so that the modeller can study a particular behaviour without building a full mechanism type model. For this class of systems, we have presented a formalism which leads to straightforward computerization of the equation derivation process.

Rigid bodies may appear as free-bodies or groups of constrained bodies in tree configuration. For free-bodies, the Newton-Euler equations are applied directly to each free body. Groups of articulated bodies can be treated separately and the equations derived for each group. In this manner we avoid having to construct a large mass matrix for the entire system. There are smaller mass matrices for each set of hinged bodies. The applied forces can be proportional or proportional-differential type. A general purpose computer code based on the above formalism is presented in next Chapter.

Chapter 3

CAMSYD: AN INTERACTIVE GRAPHICS BASED SOFTWARE FOR PLANAR MULTI-BODY SYSTEM DYNAMICS

3.1 INTRODUCTION

The terms *computer-aided* analysis, design etc. have become commonplace in modern engineering practice. However, in most instances they only mean that the computer is used sometime, somewhere in the analysis/design process. Most of the time it is used only as a dumb, albeit powerful, calculator. The engineer performs such tasks as problem formulation, equation derivation, deciding on a solution procedure, coding these in a computer language, debugging, plotting the results, etc.. In a truly intelligent computer-aided engineering environment, most of these tasks would be relegated to the computer. The program CAMSYD, which we present in this chapter, is an attempt at achieving this computerization. The contrast between the conventional, manual or computer-aided approach, and the computerized approach is illustrated in Figure 3.1. We use the term '*computerized*' as opposed to 'computer *aided*' to signify this contrast.

The many self-formulating programs reviewed in Chapter 1 have greatly contributed to this computerization by automatic generation of equations. However, the use of these programs require a fair amount of work on the part of the user in problem formulation, data preparation

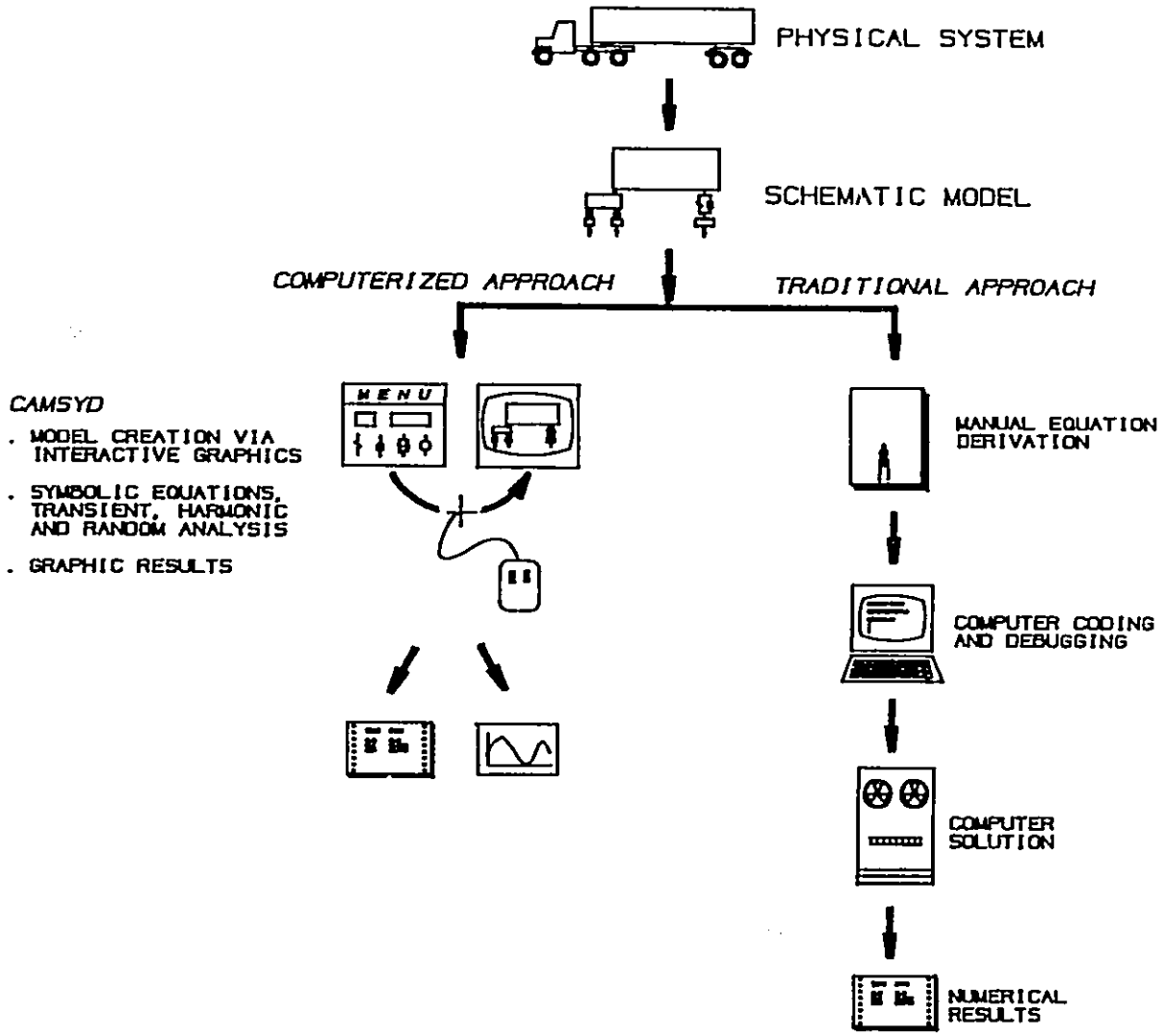

Fig. 3.1: Contrast between conventional and computerized approaches

and entry, and selection of numerical solution methods. Because of this many a user has commented about poor user-program interfaces.

The general purpose programs have user interfaces of varying degrees of sophistication. The earlier programs (e.g. GMR DYANA [13]) were executed in batch mode. ADAMS, DADS, and DRAM allow interactive data entry using a command language. For example, Reference [30] gives a brief description of the syntax of the DRAM command language and application to an automobile hood linkage. MEDYNA has interactive data entry using menus and queries. The programs provide some error checking and feedback to the user, as well as detailed on-line help. However, data entry is entirely in textual form. In IMP, the pre-processor displays links as lines on a graphics screen. Post-processing modules of IMP, DRAM, ADAMS, and DADS feature graphics for generating plots and animation. Reference [32,78] shows animation outputs from DRAM and ADAMS. Reference [100] shows some examples of DADS animation capability.

Multi-body dynamics programs designed with integrated graphics features include DAVIS [101] and a new program described in Ref. [102]. The former is for scalar (one-dimensional) spring-mass-damper vibratory systems and was developed on now obsolete equipment. The latter, presented in 1988, is for planar systems and has features very similar to CAMSYD. It has a library of elements and the system model is assembled on a graphics screen using a mouse. The elements include particle mass, rigid body, as well as linear and nonlinear springs and dampers. The rigid bodies may be interconnected in tree configuration

using hinges. However, the program only generates the equations of motion in symbolic form, and does not solve them.

Several commercial CAD systems feature 'mechanism' modules integrated with the rest of CAD operation. This allows for geometrical models to be built using the interactive graphics features of the CAD system, and in some cases provides animation of system motion. In most CAD systems the only analysis possible is kinematic analysis of planar mechanisms. The 3-D mechanism code IMP is used in I-DEAS software from SDRC [39]. I-DEAS solid modeller can be used to generate realistic 3-D component link models, or links can be represented as lines in the mechanism module. Outputs can be viewed in X-Y plots or animated graphics. I-DEAS can also be used as a graphic pre-processor to ADAMS. This is an external interface, meaning that I-DEAS simply translates its database of the model into an ASCII input file formatted for ADAMS. Some other CAD systems such as COMPUTERVISION also has interfaces to ADAMS, while yet others (MEDUSA, INTERGRAPH, etc.) are either creating interfaces for ADAMS or completely integrating it.

It is clear that interactive graphics is the preferred medium for creating mechanical system models. The proliferation of inexpensive, yet powerful engineering workstations has made it almost an imperative. The main advantage of graphics is that it gives the analyst a clear understanding of what his system looks like, and allows efficient visual error checking. However, using CAD systems to generate mechanism models has some disadvantages as well. First of all, a CAD model often requires far more dimensional data than what is actually used by the

analysis program. This means that even when one wants to perform exploratory, preliminary analysis, a large investment in time is necessary for data entry. A more important drawback of CAD systems, especially the wireframe variety, is that the CAD system has no understanding of the physical object created by the user other than its graphical manifestation on the screen. Therefore, the system is unable to use any of the properties of the underlying physical objects to help and guide the user through the modelling stage. This also means that even minor changes, such as changing the length of a link in an existing assembly, may necessitate having to redraw many different components to which that link is connected.

3.2 SCOPE OF THE NEW SOFTWARE, CAMSYD

CAMSYD (*C*omputerized *A*nalysis of *M*ulti-body *Sy*stem *D*ynamics) is primarily an interactive graphics based software. While the graphic pre-processors reviewed above can be classified as a 'drafting board' variety, CAMSYD uses a 'sketch-pad' type of model description. Engineers use sketches to symbolically represent physical objects and their configuration in space. These sketches are often not drawn to scale. Rather the relevant dimensions are simply marked on them. Using CAMSYD, the analyst can input his model in this symbolic fashion. The graphic pre-processor has a 'knowledge' about the underlying physical model, so that it can guide him through the modelling phase.

The class of problems we attempt to solve is somewhat different

from those to which the general purpose programs mentioned above are applied. However the above review and discussion is relevant since they point out the features that make our approach unique. Furthermore the same arguments apply for the graphics based kinematic analysis and design program, GENKAD, presented in Chapter 5.

The special class of planar lumped parameter mechanical systems addressed by CAMSYD is characterized by rigid bodies interconnected by springs, dampers and revolute joints. The bodies may undergo small angular motions but large translational motions; the forces generated in springs and dampers can be passive or active, linear or nonlinear. The majority of system models in vehicle dynamics, machinery vibration, rotor dynamics, and the like, can be represented by models of this sort. Some examples of this class of models are shown in Figures 2.1 - 2.4.

CAMSYD is based on the analytical methods described in Chapter 2, and is limited to planar systems. As mentioned in Chapter 2, rigid bodies in a plane can be modelled as one, two, or three degree-of-freedom bodies. These DOF may be made up of any combination of two translations and one rotation. The present implementation of CAMSYD allows for only one-DOF (bounce) and two-DOF (bounce and pitch) bodies. The bodies may form free MBS or MBS in tree configuration. The implicit and explicit constraints are automatically taken care of in the formulation so that a minimal set of differential equations is generated. The equations are written in general state-space form and may be linear or nonlinear, depending on the force generator elements used.

For both linear and nonlinear systems, CAMSYD provides time simulation with prescribed displacement or force inputs. Nonlinear models can be linearized about any position and used in other options available for linear models, such as frequency response functions and stochastic response.

3.3 USAGE OF CAMSYD

The program is fully interactive, taking advantage of the interactive graphics facilities of modern engineering workstations. It communicates to the user via on-screen menus and queries, and the user responds with inputs from a mouse or the keyboard. The user need not know any specialized theory of problem formulation or syntax of model description. He simply *draws* the schematic diagram of the mechanical system essentially as those shown in the figures referred to earlier. This is done by assembling the schematic on the graphics screen by selecting system components from a menu. The user also specifies the required outputs and applies inputs by pointing to appropriate elements on the screen. The package is divided into three main modules: the pre-processor, the analysis (solution) stage, and the post-processor. A brief description of the functions of each module is given in Table 3.1. Figure 3.2 shows how, using CAMSYD, one proceeds through the modelling, solution and post-processing stages. Figure 3.3 shows details of CAMSYD in its hierarchical form, along with the contents of important menus.

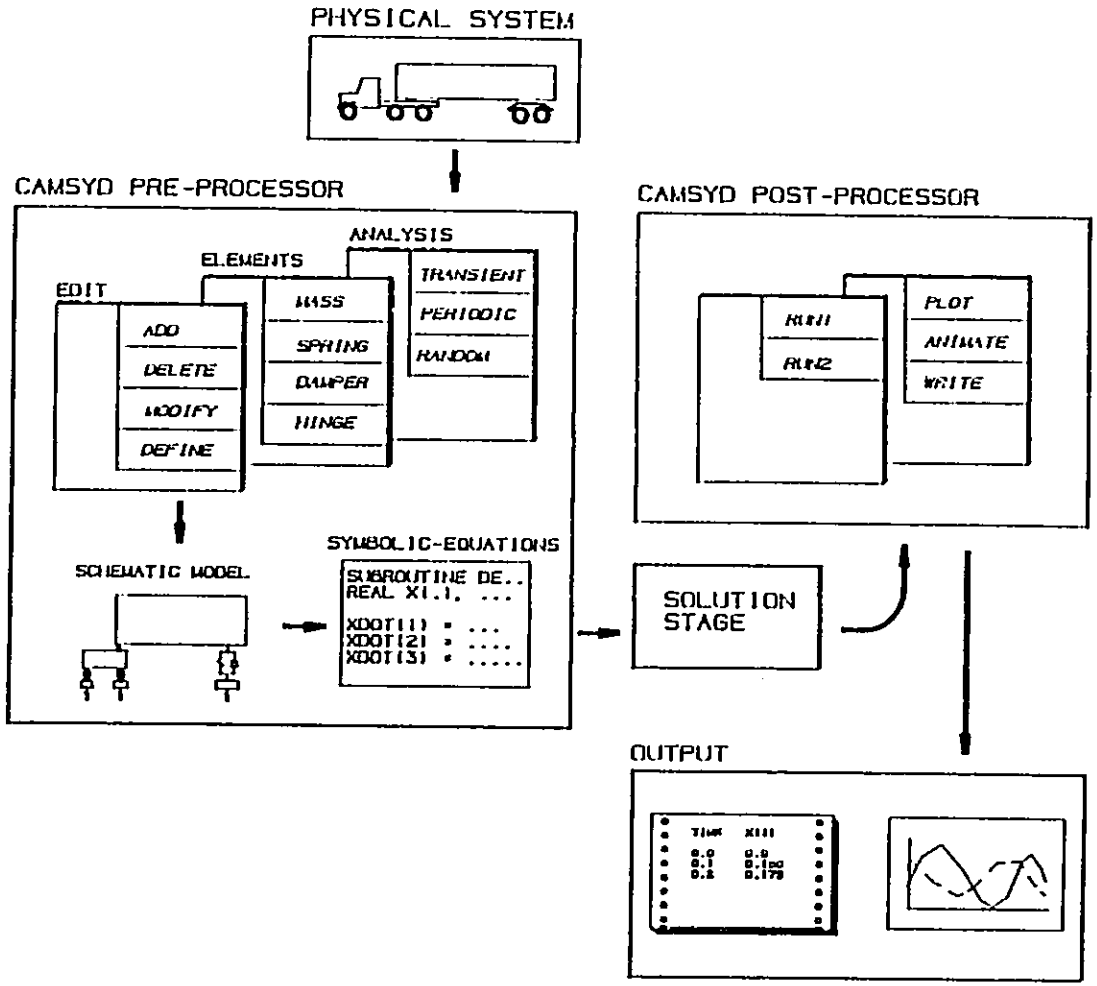

Fig. 3.2: Schematic of the usage of CAMSYD

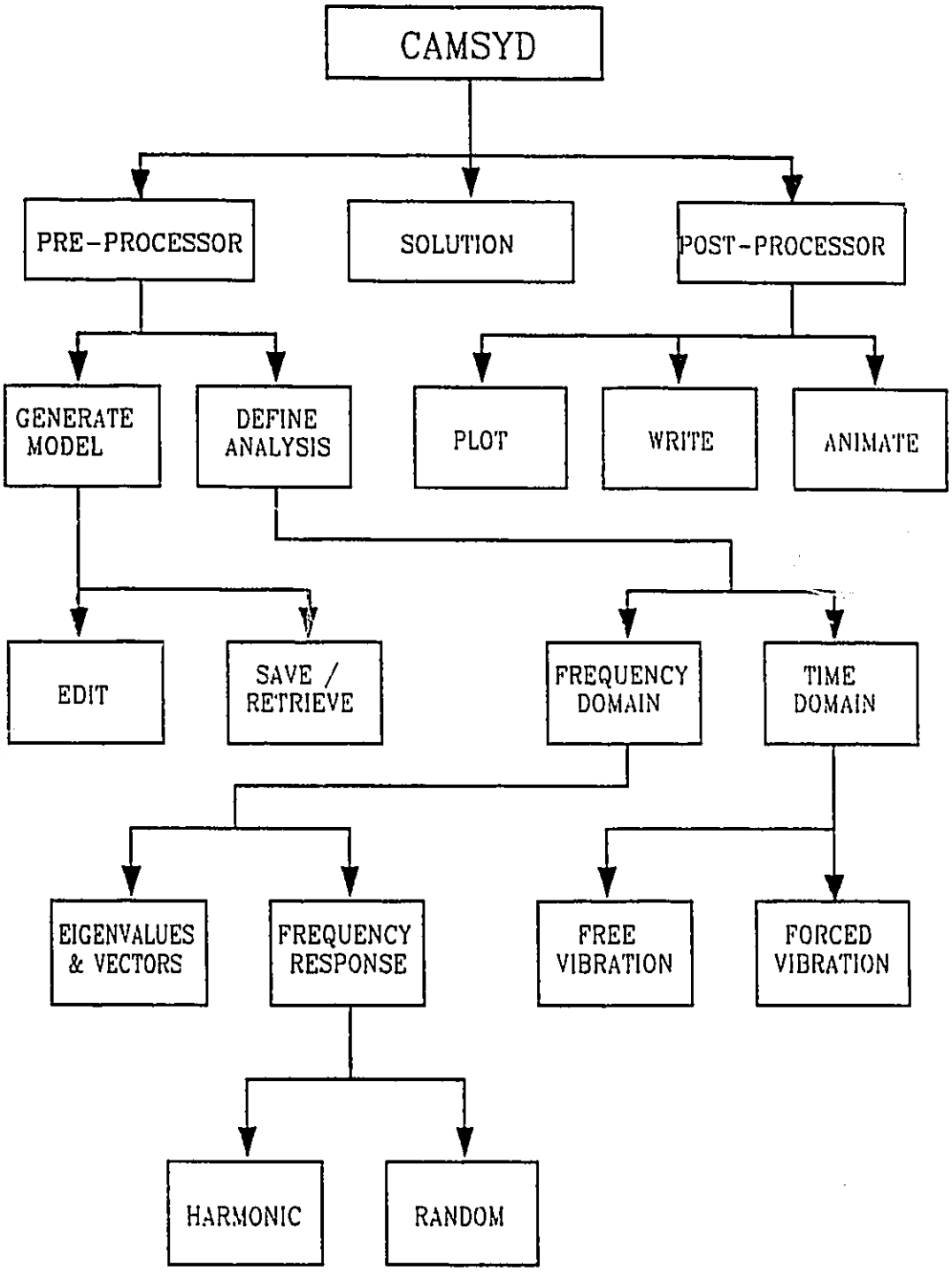

Fig. 3.3: Organization of CAMSYD

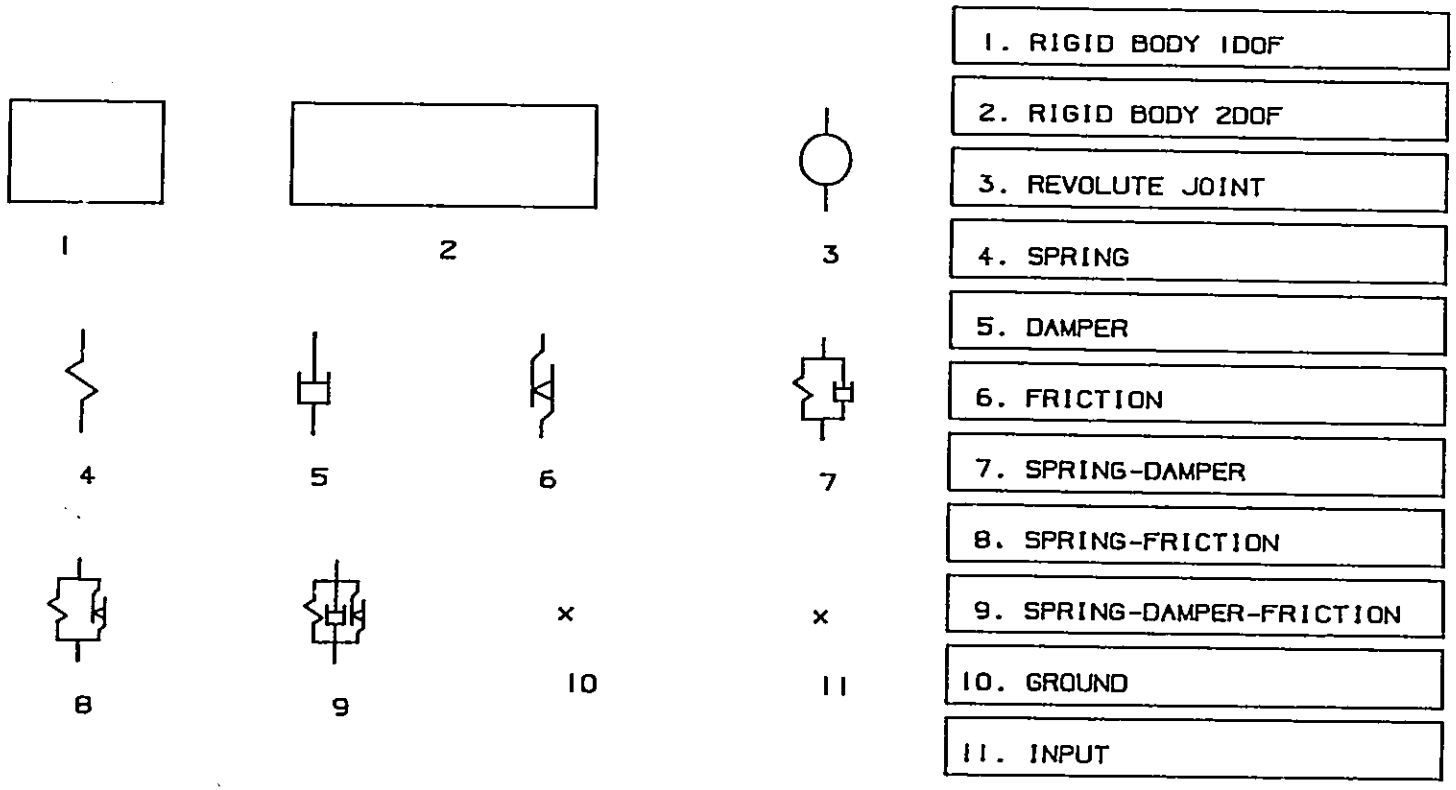

Fig. 3.4: Components in CAMSYD library

Figure 3.4 shows the main CAMSYD menu and the schematic representations of various components. It contains rigid bodies with various degrees of freedom, linear and nonlinear springs and dampers and revolute joints. At a higher stage in the menu hierarchy, the user also has the option of creating user-defined two-port suspension elements whose force generation characteristics can be specified. This feature is useful in modelling components such as oleo-pneumatic suspensions, or active and semi-active isolators. When a new component is defined, it is automatically added to the menu of system elements shown earlier.

Starting with a schematic diagram of the vehicle system such as that shown in Figure 2.4, the user builds his computer model simply by duplicating it on the graphics screen using the components from the CAMSYD menu. The components can be assembled in any order using CAMSYD pre-processor. Once the model creation is complete, the equations of motion are generated after checking for proper topology. Closed kinematic loops are not allowed. The equations are generated symbolically as FORTRAN subroutines. The system parameters are represented symbolically in the equations and their values are supplied at the solution stage. This facilitates easy parameter variations and optimization studies. The equations are written in standard state-space form and the user may use it with any other special analysis program to carry out analysis options which are not provided in CAMSYD. This feature provides tremendous flexibility to the use of CAMSYD.

Once the model generation is complete, the user specifies the

analysis he wishes to perform. This is also carried out in the pre-processor. A wide range of analysis options are available, such as, time simulation for transient inputs, eigenanalysis (frequencies and mode shapes), frequency response functions, stochastic analysis, etc.. A nonlinear model may be automatically linearized about an operating point before it is used in frequency domain analysis. The program has several special features for vehicle system dynamic analysis. For example, various wave forms are available to be used as transient wheel inputs. For vehicles travelling with constant velocity over a given terrain profile, the program automatically computes delayed inputs at each wheel. Similarly, for stochastic analysis with single-variate input process, the input spectral density matrix is also computed from the spectral density of the single input.

A general purpose post-processor helps the user to graphically examine the results. It can select output data and display X-Y plots, mode shapes, write data to files, etc.

3.4 IMPLEMENTATION

Presently the program has been implemented on Apollo workstations running AEGIS operating system, Silicon Graphics IRIS workstations under UNIX, and Digital VAXstation workstations under VMS (partial implementation). All these workstations feature high resolution color screens, three-button mice and good environments for program development. Furthermore they represent a very large segment of

engineering workstations in use.

CAMSYD was originally developed on Apollo workstations and is written entirely in FORTRAN 77. The analysis module of CAMSYD has no user interaction and is therefore fully portable to any machine that supports FORTRAN. However, the pre- and post-processors of CAMSYD make extensive use of interactive graphics. The difficulty of making graphics code portable is the wide variety of graphics hardware and the direct dependence of graphics code on this hardware. There are two approaches to making graphics code portable. The most desirable solution is to write the graphics code in a device-independent graphics standard, such as GKS (Graphics Kernel System) for 2-D, or PHIGS (Programmer's Hierarchical Interactive Graphics System) for 3-D. Both of these provide general device-independent primitives and coordinate systems as well as a set of logical input devices. The second approach is to develop specific graphics libraries on each of the machines. This, of course involves more work. We tried both approaches on Apollo and the experience was that the PHIGS interface had a slower response than the device dependent code. Since fast response is a truly important factor for interactive graphics, PHIGS was abandoned. However, this experience should not be generalized. Thatch and Myklebust [103] have reported a PHIGS-based graphics pre-processor for IMP. Some researchers have chosen to develop their own graphics libraries - e.g. the program LINCAGES [104].

A library of high level graphics subroutines was developed to provide interface between CAMSYD and the graphics hardware on each of

the platforms. This library provides user interfaces such as menus and queries, mouse and keyboard inputs, and graphics primitives such as lines, circles, etc.. CAMSYD makes calls to this library for all device dependent functions. So in this sense the program is device independent.

CAMSYD is designed and built as a collection of modular subpackages for ease in development and addition of new modules. As shown in Table 3.1, the main divisions at the top level are the pre-processor, analysis, and post-processor. The pre-processor is used in defining the system model and analysis options. It then generates the system differential equations and writes them into a file as a set of FORTRAN subroutines. The analysis information as well as the model database are also written into files. The equations are compiled automatically and linked with the analysis program to create an executable image. This is invoked from the main CAMSYD menu to carry out the solution. The post-processor uses the output files created during the analysis run, as well as the model database file created by the pre-processor.

3.5 APPLICATION TO VEHICLE RIDE ANALYSIS

We illustrate the graphics based modelling and analysis of vehicle system dynamics using CAMSYD. Examples are taken from published literature to show the versatility of CAMSYD as a general purpose modelling and analysis tool. The models are built from the system components in the CAMSYD menu and the analysis and the graphical display

Table 3.1: Implementation of CAMSYD

MODULE	FUNCTION
PRE-PROCESSOR (interactive)	- Create / edit system models - Derive equations of motion - Define analysis to be done - specify inputs and outputs
ANALYSIS (no interaction)	- Carry out solution - Capabilities: Nonlinear : linearization, transient response Linear: transient, eigenanalysis, transfer functions, stationary random, etc..
POST-PROCESSOR (interactive)	- Select and plot, write or animate results

Table 3.2: Parameter values for models shown in Fig. 3.5 and 3.8

m_1	200 *kg*
m_2	80 *kg*
m_3	20 *kg*
k_1	30000 *N/m*
k_2	320000 *N/m*
k_3	60000 *N/m*
c_1	4800 *Ns/m*
c_2	0

of results are also carried out. Two examples are presented - automobile ride analysis, and tractor semitrailer ride analysis.

3.5.1 Automobile Ride Analysis

The first example is an automobile vertical vibration problem taken from the textbook by Müller and Schiehlen [105]. Figure 3.5 shows the schematic representation of a two degree-of-freedom quarter car model. The reader may refer to the equations and lengthy solution procedure given in [105. To study this problem using CAMSYD, we recreate this schematic on the graphics screen by picking 2 single-degree-of-freedom rigid bodies from CAMSYD menu (Figure 3.4, item 1), and positioning them using the mouse. We then pick spring-damper combinations (Figure 3.4, item 7), representing the tire and suspension system, and attach them to the rigid bodies appropriately. Next we define the free end of the tire as an input point (item 10); and the model is complete. Figure 3.6 is the schematic of the vehicle model generated using CAMSYD. The parameter values are given in Table 3.2. We can now select the type of analysis to be carried out from a menu of various analysis options. We want to evaluate the eigenvalues and eigenvectors of the dynamic system, and study its transient response for a set of initial conditions.

Using the CAMSYD pre-processor we build the model and specify the analyses that are to be performed. The differential equations are automatically generated in state-space form in terms of the state-vector $[x_1, \ x_2, \ \dot{x}_1, \ \dot{x}_2]^T$. The eigenvalues are : $\lambda_{1,2}$= $-30.2536 \pm 67.003i$, and $\lambda_{3,4}$= $-1.747 \pm 4.578i$. Transient response of

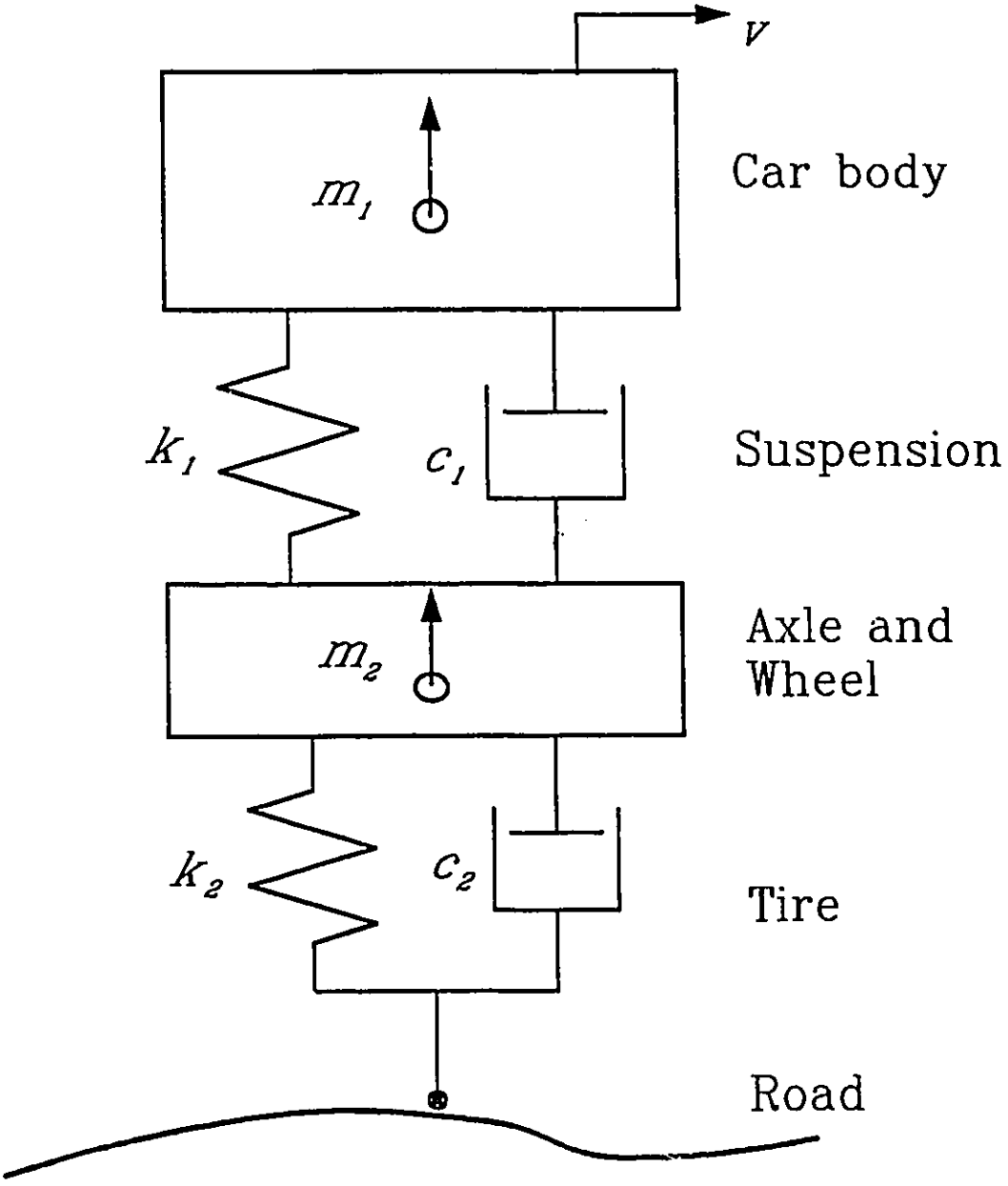

Fig. 3.5: Schematic of two degree of freedom automobile model

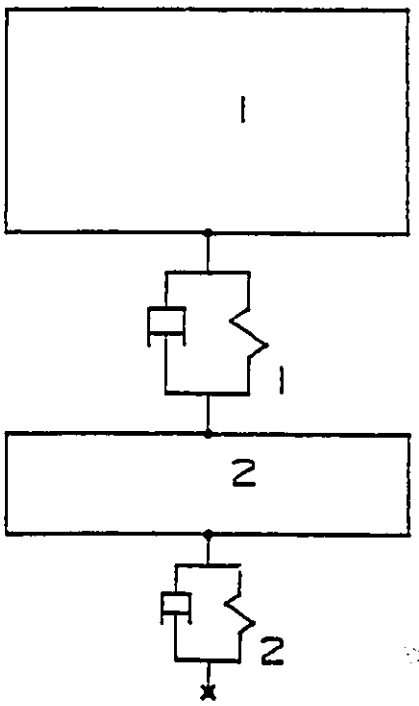

Fig. 3.6: Two DOF automobile model generated using CAMSYD

the system for an initial condition with $x_1(0) = 1.0$ is shown in Figure 3.7. These results are, of course, identical to those given in Ref. [105], but obtained with little pain, and in a matter of minutes.

The model shown in Figure 3.5 is very widely used to evaluate the ride and road holding abilities of passive and active vehicle suspensions. The frequency response function of this 2-DOF system shows a significant vehicle body acceleration at the wheel-hop frequency. One proposal to reduce this vibration is to employ vibration absorbers at the wheel axles [105], as shown in Figure 3.8. The absorber is a relatively small mass elastically attached to the axle. This modification to the earlier model is very easily achieved using CAMSYD. We simply select another single-degree-of-freedom mass from the menu of components and place it on the screen. A spring-damper element is next selected and attached to the absorber mass and the unsprung mass. Figure 3.9 shows the model of the total system, which now has three degrees of freedom. When the user indicates that the model is complete, the equations are automatically generated.

We illustrate another dynamic analysis capability of CAMSYD by using the model developed above. The aim of the analysis is to evaluate the frequency response of the car body vertical acceleration for different values of the absorber damping, C_3. Having created the model we select the analysis options menu of the pre-processor, and select frequency response functions. We ask for the frequency response function relating the vehicle-body acceleration to the base displacement. The response of the system is shown in Figure 3.10. For

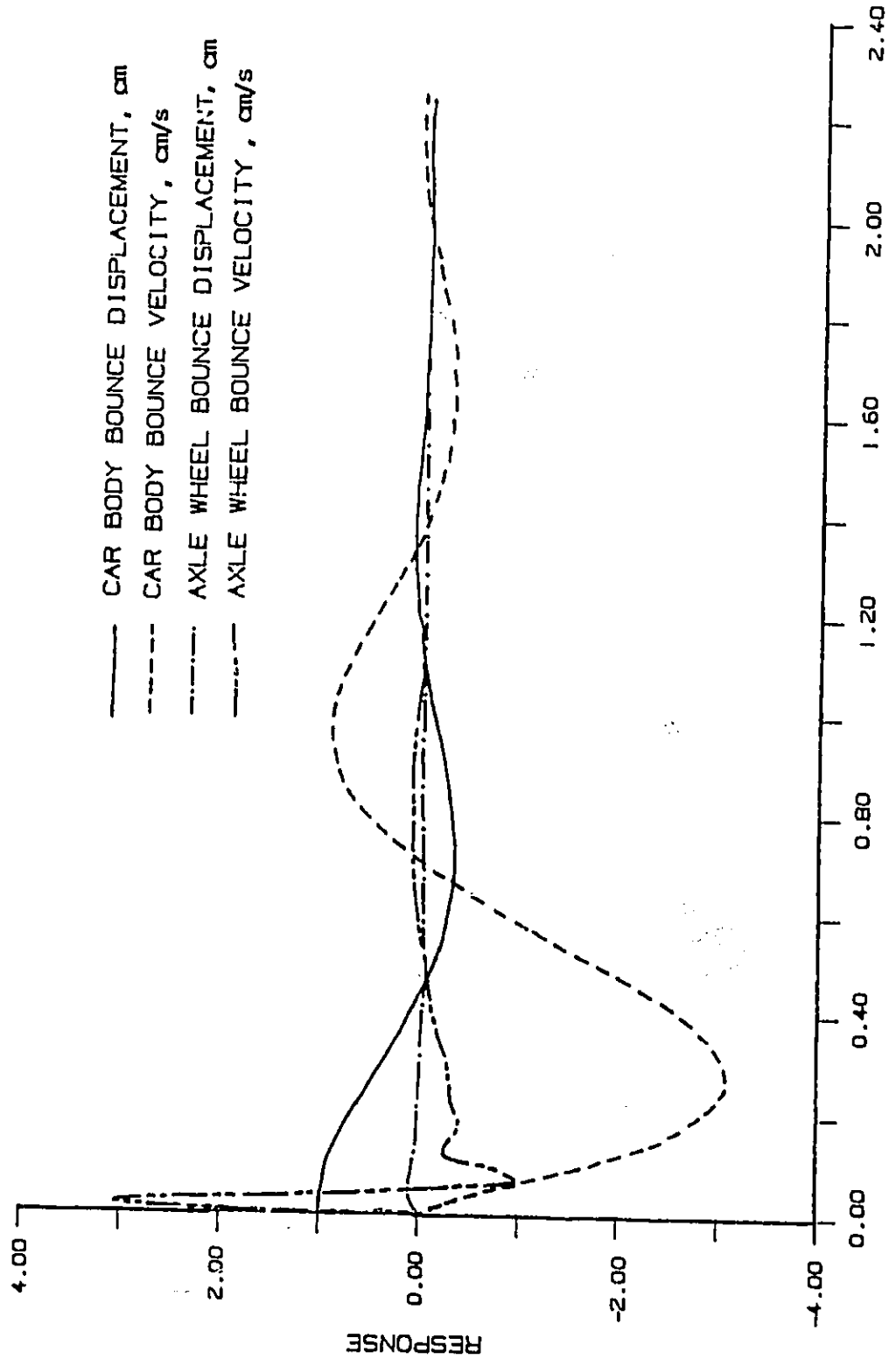

Fig. 3.7: Transient response of system shown in Fig. 3.6

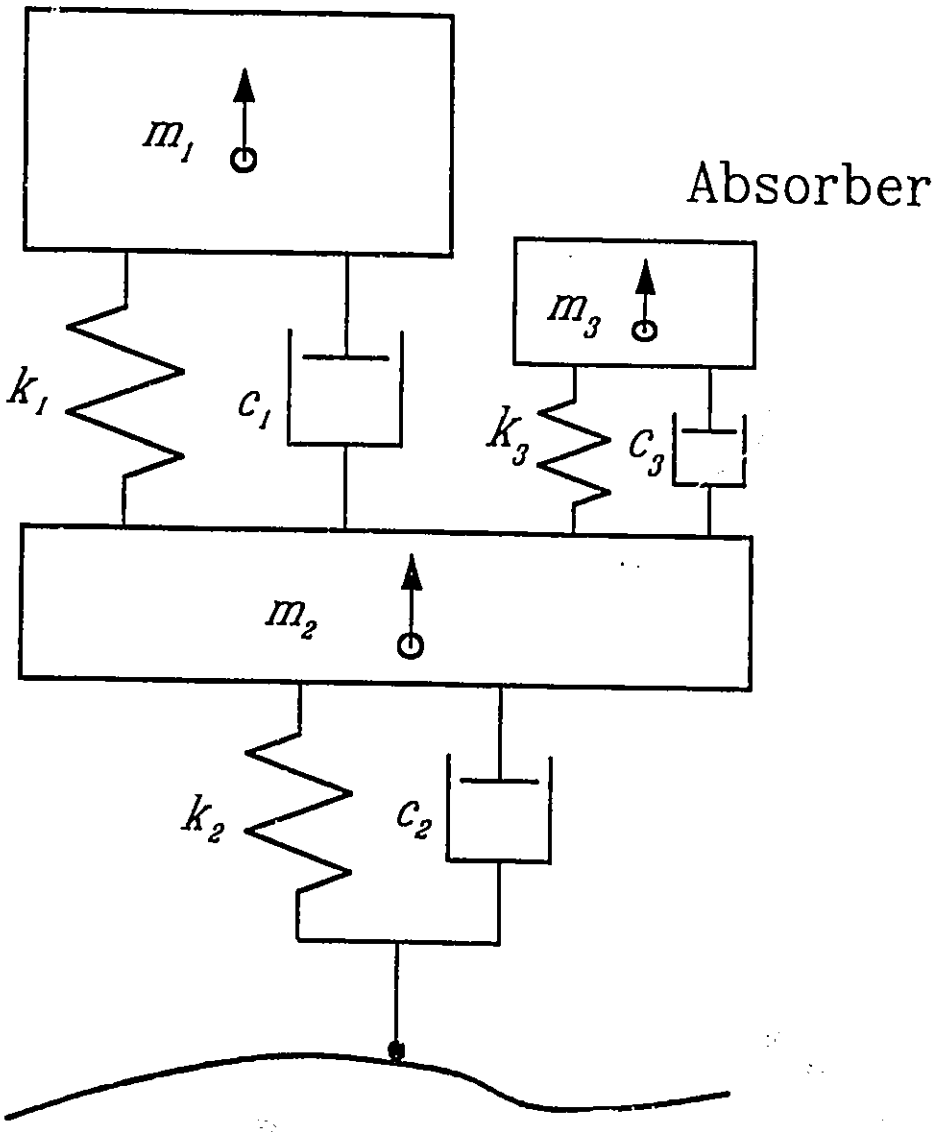

Fig. 3.8: Model of automobile with vibration absorber

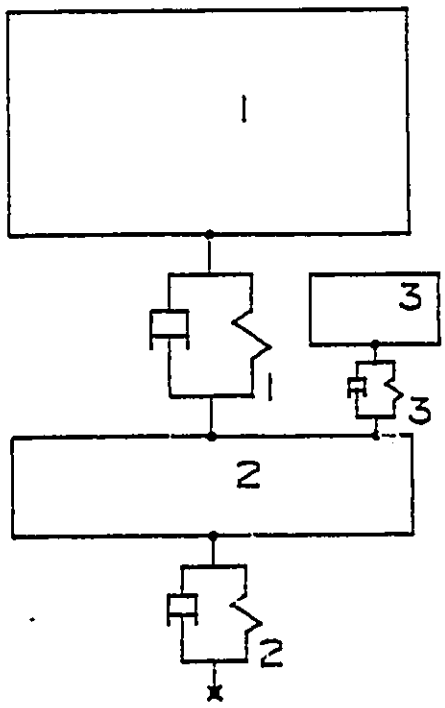

Fig. 3.9: Model of Fig. 3.8 generated using CAMSYD

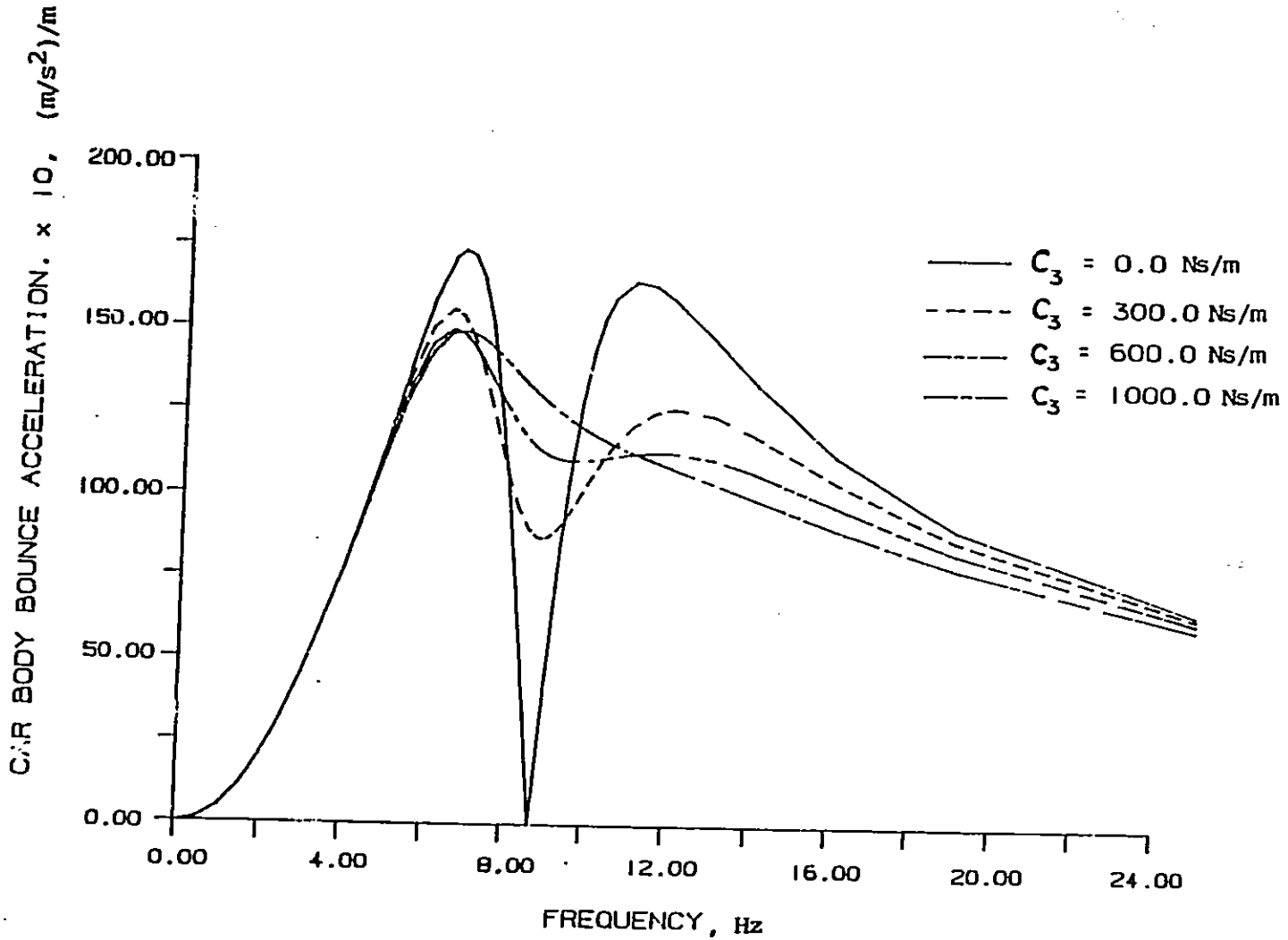

Fig. 3.10: Frequency response of vehicle body acceleration

zero damping, total absorption takes place at the wheel-hop frequency. At other frequencies the amplitude is larger than what we get with damping. With increasing damping one actually loses the effect of total absorption, but this is compensated for by improved performance at other frequencies.

3.5.2 Tractor Semitrailer Ride Analysis

The second example is a tractor semitrailer modelled as a six-degree-of-freedom system as developed in Ref. [106]. Figure 3.11 shows this schematic model. The tractor and the semitrailer are both two-degree-of-freedom (bounce and pitch) rigid bodies. The wheels are single-degree-of-freedom (bounce) rigid bodies. We use the revolute joint element to represent the *fifth-wheel* coupling between the tractor and the semitrailer. Figure 3.12 shows the system schematic model reproduced using CAMSYD pre-processor. The fifth-wheel constraint reduces one degree of freedom from the total of 7. The final six degrees of freedom are: tractor pitch and bounce, trailer pitch, and bounce of each of the three wheels. CAMSYD generates the minimal set of exactly 12 first order differential equations for this system.

CAMSYD recognizes bodies 1 and 2 (Figure 3.12) as a system of constrained bodies in tree configuration and derives equations as given in Section 2.3.4.3. The other 3 rigid bodies are free multi-bodies and their equations are generated separately, as described in Section 2.3.3.2. CAMSYD generates equations of motion as FORTRAN subroutines. Appendix A shows the complete listing of these equations as written by

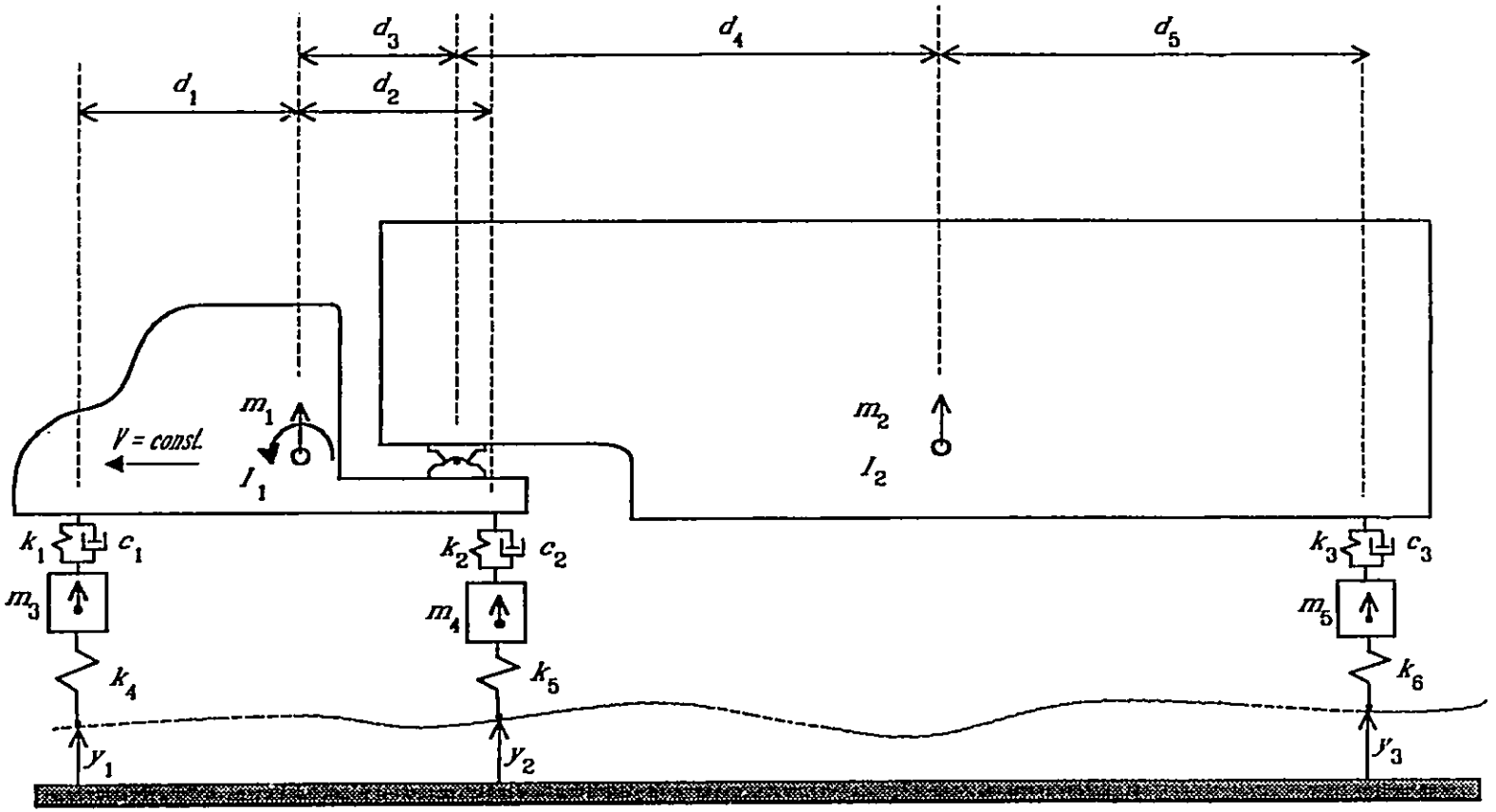

Fig. 3.11: Six degree of freedom tractor-semitrailer model

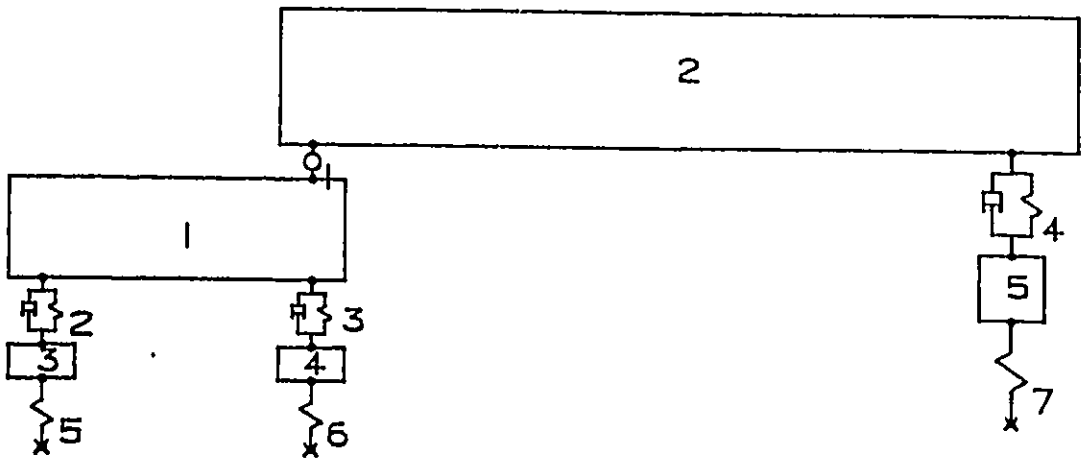

Fig. 3.12: Tractor-semitrailer model generated using CAMSYD

CAMSYD. The assumption of small angular motions for rigid bodies leads to a constant coefficient mass matrix for the hinged pair of bodies. This matrix is evaluated once after data initialization and inverted symbolically (Subroutine INIT). Subroutine DIFEQN represents the actual equations of motion and is repeatedly called by the analysis program during solution. All system parameters are denoted by symbols (REAL arrays MASS, SPAR and DIST), so that equations once generated, can be used for any set of numerical values for these parameters.

To demonstrate the analysis capability of CAMSYD, the eigenvalues and mode shapes of the above example are studied. In Ref. [97], damping in the three main suspension units are optimized considering a stochastic input. We take these parameter values, shown in Table 3.3, and study the effect of varying the location of the fifth-wheel coupling between the tractor and the trailer. This is a very practical design variation and it is expected to have a large influence on the ride performance. To evaluate the real natural modes, we set all damping values to zero, and compute the eigenvalues and eigenvectors. Two variations of the fifth wheel location are studied, 0.5m behind the nominal position (+0.5m), and 0.5m ahead of it (-0.5m). Figures 3.13 and 3.14 show the first 2 modes of vibration, plotted using the CAMSYD post-processor. From the response we see that moving the fifth-wheel rearward leads to generally lower bounce in the first mode and lower pitch in the second mode response of the tractor.

Magnitudes of the bounce and pitch acceleration transfer functions are shown in Figures 3.15 and 3.16. The same two variations of the

Table 3.3: Parameter values for tractor semitrailer model

m_1	2400 kg
m_2	14125 kg
m_3	440 kg
m_4	775 kg
m_5	510 kg
I_1	1660 $kg\ m^2$
I_2	37000 $kg\ m^2$
k_1	290 kN/m
k_2, k_3	960 kN/m
k_4	1450 kN/m
k_5, k_6	2900 kN/m
c_1	9350 Ns/m
c_2	44150 Ns/m
c_3	41390 Ns/m
d_1	0.82 m
d_2	1.84 m
d_3	1.62 m
d_4	2.55 m
d_5	3.02 m

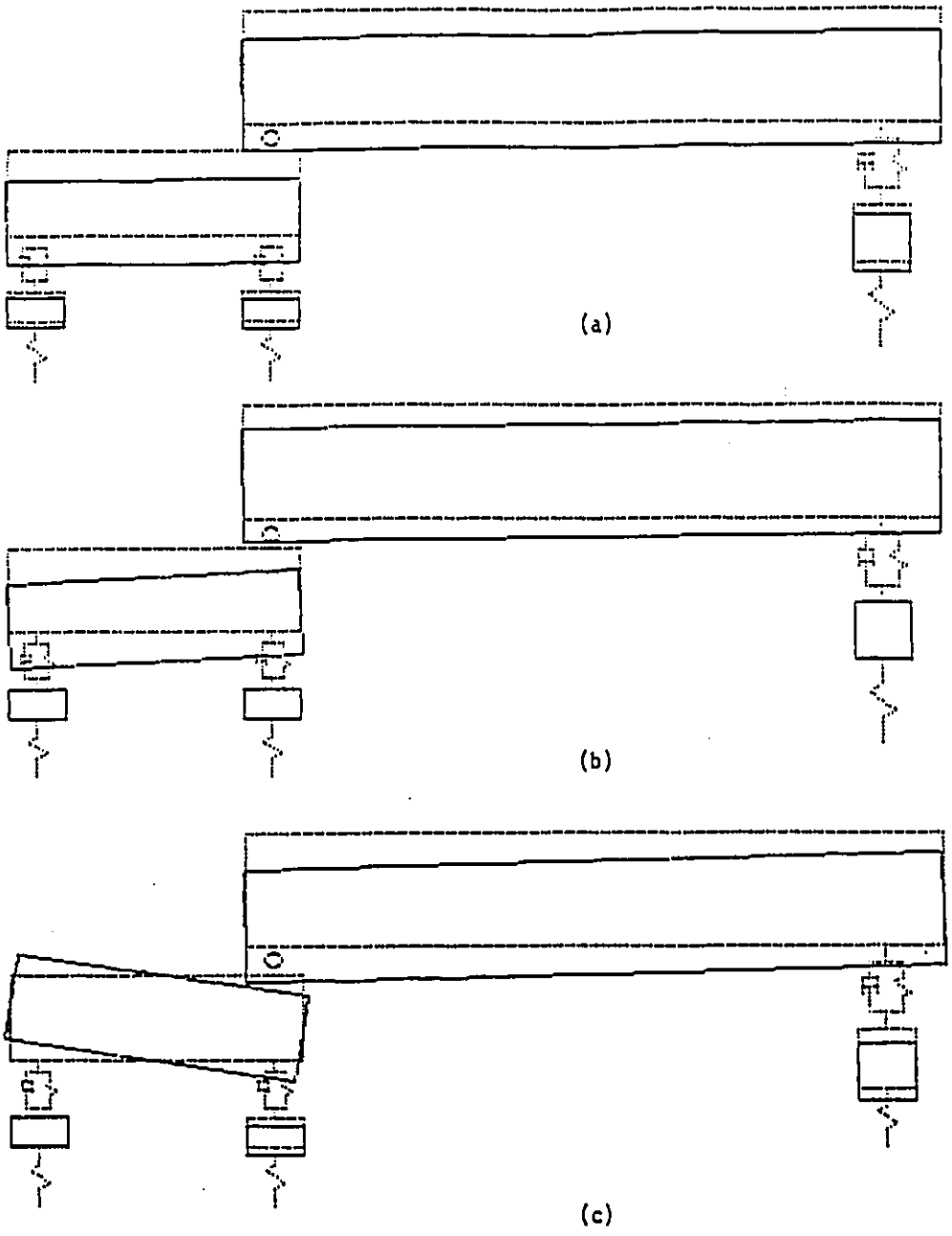

Fig. 3.13: First mode of vibration for 3 different positions of fifth-wheel. (a) 0.5m forward, (b) nominal location (c)t0.5m rearward.

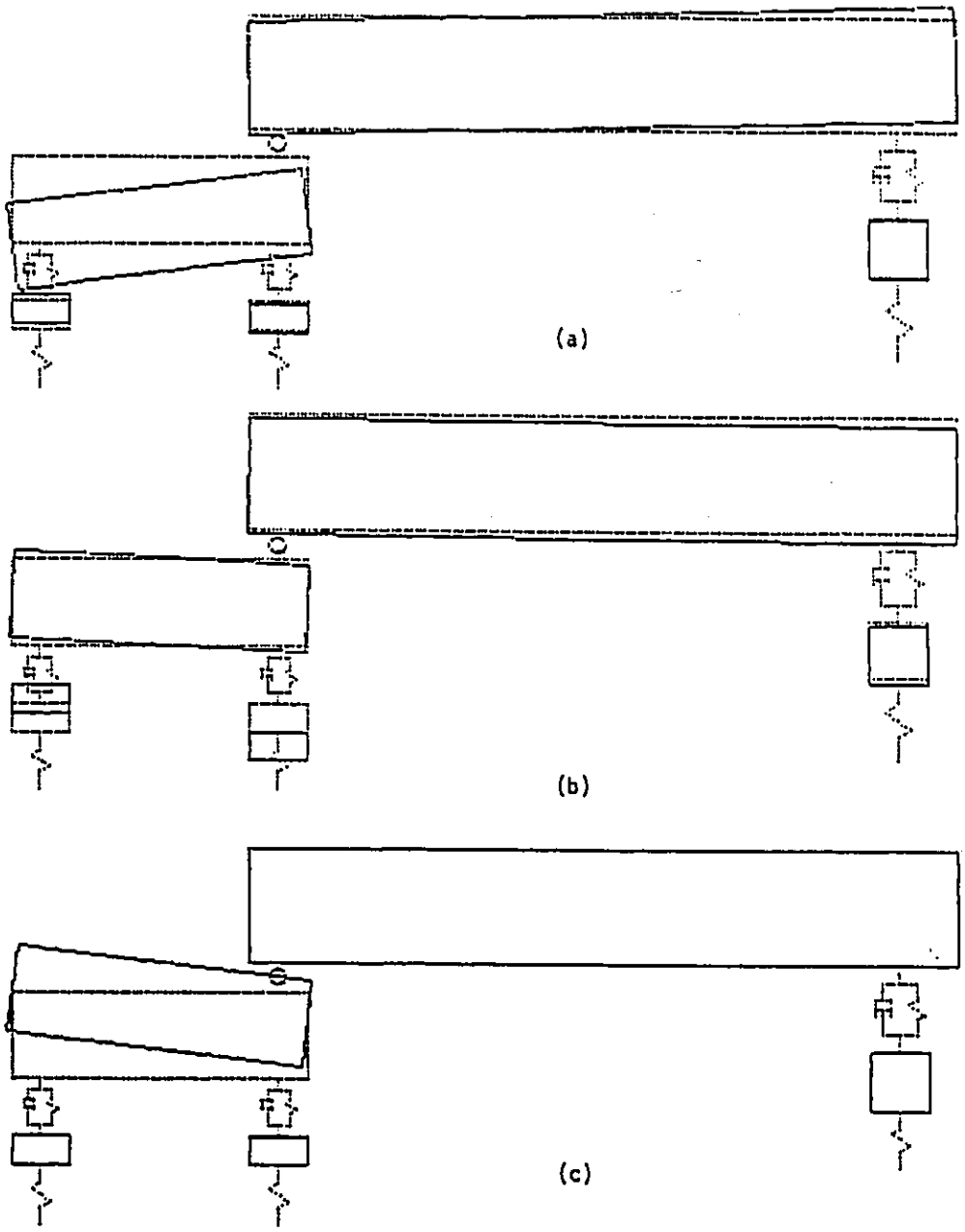

Fig. 3.14: Second mode of vibration for 3 different positions of fifth-wheel. (a) 0.5m forward, (b) nominal location (c)t0.5m rearward.

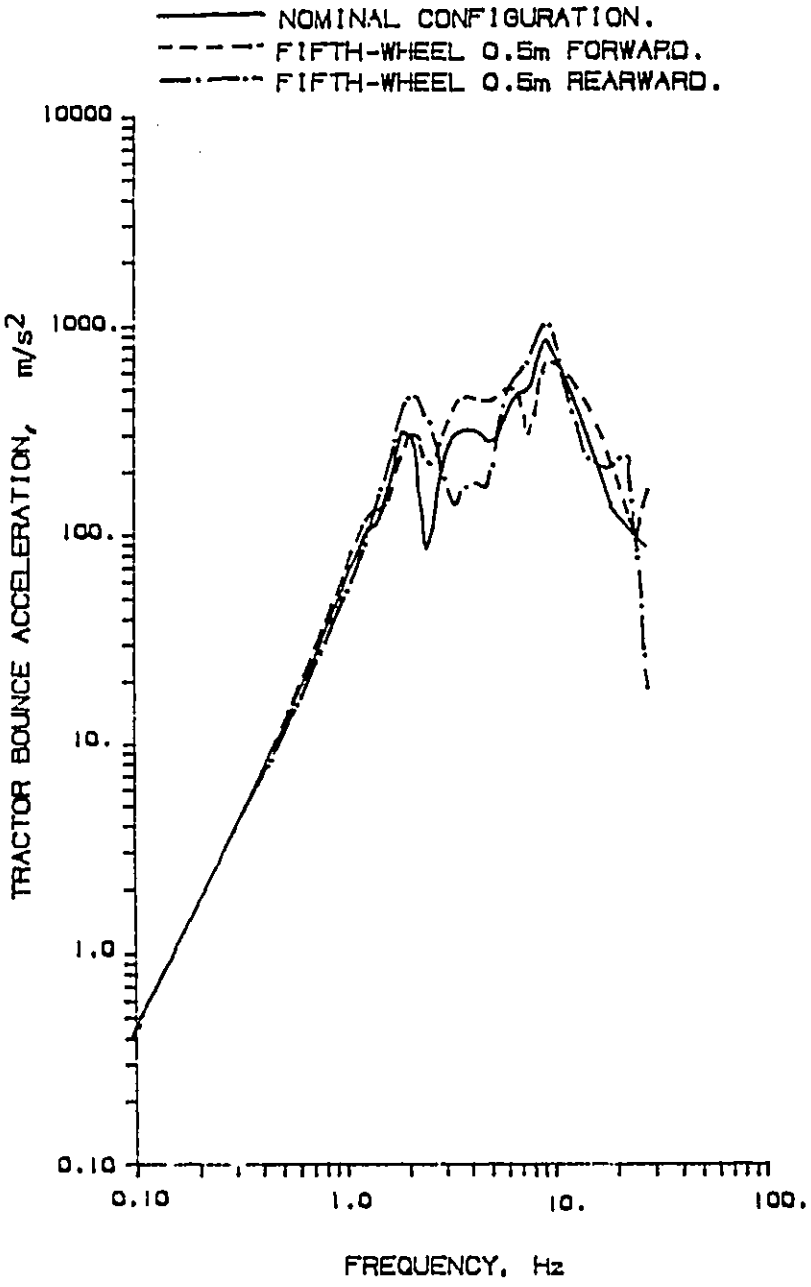

Fig. 3.15: Frequency response of tractor CG bounce acceleration

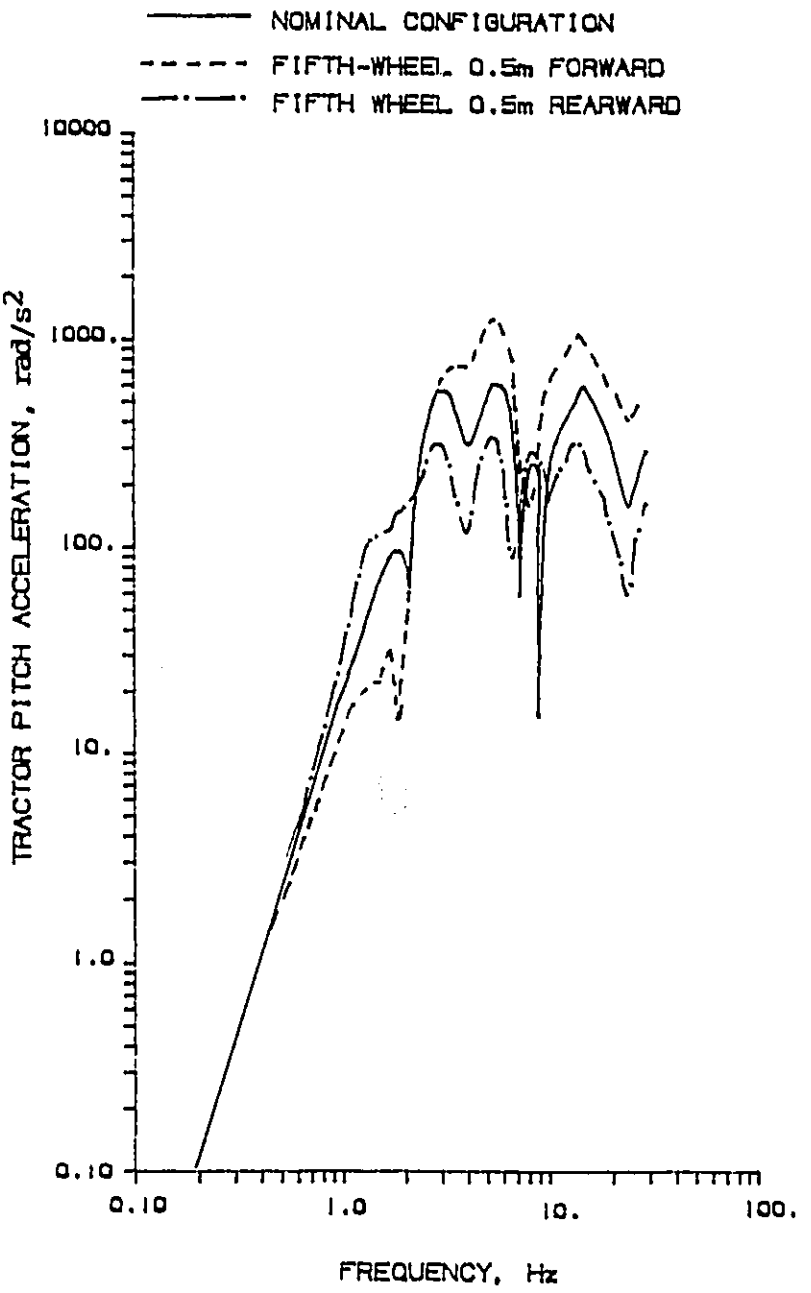

Fig. 3.16: Frequency response of tractor CG pitch acceleration

fifth wheel location are studied for their effect on the frequency response of the vehicle. From Figure 3.15 we see that the -0.5m position leads to higher amplitudes at lower frequencies and lower amplitudes at higher frequencies. In the case of +0.5m position, the situation is reversed. But the pitch acceleration response shown in Figure 3.16 indicates a very different picture. The +0.5 position gives consistently lower amplitudes for the frequency range considered. Similarly, the -0.5 position leads to higher acceleration amplitudes throughout the frequency range.

3.6. SUMMARY

We have presented a general purpose program, called CAMSYD, for the modelling and analysis of lumped parameter mechanical systems. The system models are described to the program by assembling its graphical schematic on the computer screen. The program is self-formulating in that it can automatically generate the dynamic equations from the graphical input. The analysis options implemented in CAMSYD cover a range of analysis techniques. We have illustrated its use by applying it to a number of vehicle dynamics problems.

Using CAMSYD, it is possible to model, and solve complex vehicle system dynamics problems in a matter of minutes, without writing any equations or programming them. Graphics acts as the language of communication between the user and the computer. The computerization of equation generation and solution ensures error-free results and enhances productivity.

Chapter 4

ANALYSIS OF SUSPENSION SYSTEMS USING THE METHOD OF VELOCITY COEFFICIENTS

4.1 INTRODUCTION

In ground vehicles the suspension system performs three essential tasks of providing ride quality, handling, and load support. Ride quality is achieved by isolating the passenger and cargo from ground induced vibration. This aspect of the study concentrates on the bounce, pitch and roll responses of the vehicle sprung mass due to ground excitations. Vehicle handling and stability, on the other hand, depends on its lateral, longitudinal, roll and yaw motions induced due to driving manoeuvres and various surface conditions. The problem of load support falls in the domain of stress analysis, and is not taken up here. The problems of ride and handling are very different and distinct from each other and are therefore studied using different models and analysis techniques. In this chapter we present some new techniques for the analysis and design of vehicle suspension systems using the method of velocity coefficients.

Conventionally vehicle ride dynamicists have used lumped parameter mass-spring-damper models of vehicles for ride dynamics studies [44-47]. Models, such as the one shown in Figure 1.2, have proven to be useful in evaluating vehicle ride quality, and such fundamental vehicle characteristics as natural frequencies and mode shapes. These models

treat the vehicle sprung and unsprung masses as rigid bodies undergoing small deflections. The suspension system is often modelled as linear spring-damper elements interposed between the sprung and unsprung masses. But in reality, it consists of several links and isolator elements such as springs, dampers, and bushings, as shown in Figure 1.3 The criteria that motivate the designers to create the differing linkage geometry are seldom based on ride comfort, but rather on handling and stability characteristics of the vehicle [51]. However, as we will show later, the linkage configurations have a significant effect on the ride behaviour of some vehicles. The large angular motions in suspension linkages produce nonlinear suspension forces, even when the individual isolator elements themselves are linear. In this Chapter, we show how, using the method of velocity coefficients, linkage suspensions undergoing large deflections can be modelled as equivalent force generators for ride analysis.

One of the time-honoured concepts in vehicle handling studies is the one of *roll centres* [52,60-69]. The concept of roll centre is considered to be of primary importance by vehicle suspension designers. The suspension systems play a major role in the vehicle handling and stability by distributing the wheel normal loads. The concept of roll centre provides a concise and simple calculation of this distribution from lateral and longitudinal load transfers during a manoeuvre. But unfortunately there is some confusion in literature as to what exactly a roll centre is, how to determine its location, etc.. In this Chapter we take a fresh look at the problem and clarify several disputed points. For example, it is shown that definition of roll centre given by SAE

[107] is inherently misleading, although it is valid in certain cases. We reestablish roll centre as the instantaneous centre of rotation of the sprung mass, and propose a new, general method of determining its location using velocity coefficients.

Suspension kinematics has been taken into account in several stability studies [52-62], as reviewed in Chapter 1. The *velocity coefficients* we present in this chapter have a resemblance to the *suspension derivatives* presented by Hales [53]. Suspension derivatives are "derived by equating the velocities of the inboard joints of each suspension link expressed in terms of body velocities to velocities of the outboard joints of the same link described in terms of wheel velocities in the direction of the link" [56]. Mathematically the terms *suspension derivatives* and *velocity coefficients* are synonymous. But we prefer the latter because of its wider meaning and accepted usage in kinematic analysis [108]. Some authors have used the term velocity influence coefficient to refer to the same quantity [109].

Textbooks on kinematics of mechanisms define velocity coefficients in the context of kinematic analysis. However, their significance in suspension theory has not been clearly understood. Therefore the aim of this Chapter is twofold - to elucidate the above point, and to show how a suspension system can be modelled so that all the relevant velocity coefficients are computed in the process of doing position analysis. We show how the velocity coefficients can be used to form an equivalent force-generator model of a suspension system for ride analysis; for kinetostatic analysis of vehicle systems; and for determining *roll*

centre locations and roll stiffness of suspension systems for use in handling studies. Once the suspension behaviour is understood in terms of velocity coefficients, the engineer has to carry out kinematic design whereby he seeks to specify a linkage which would provide the desired behaviour. Towards this end, we also derive expressions for the sensitivity of velocity coefficients to design variables. This sensitivity information can be used to manually iterate a design, or it can be used in optimization algorithms. The ideas and procedures presented in the present Chapter are implemented as general purpose computer programs and are illustrated in Chapter 5 by application to suspension systems of racing cars and snowmobiles.

4.2 THE DERIVATION OF VELOCITY COEFFICIENTS

Consider a generic suspension system as schematically shown in Figure 4.1. The first task is to kinematically model the suspension as a mechanism. For this purpose we consider the vehicle chassis as the fixed link and identify a local coordinate system fixed at a convenient reference point on it. Next, all links, joints and force-generator elements (springs dampers, etc.) are identified. Also, we define a convenient set of Lagrangian coordinates which will uniquely determine the configuration of the mechanism. These are typically joint variables and link orientation angles. In kinematic analysis, shock-absorbers are usually modelled using two links, 2 revolute joints and a prismatic joint, as shown in Figure 4.2(a). For the purpose of our analysis, we can make a simpler model by introducing a 'rubber band link', as shown in Figure 4.2(b). We still have the same number of variables, but fewer

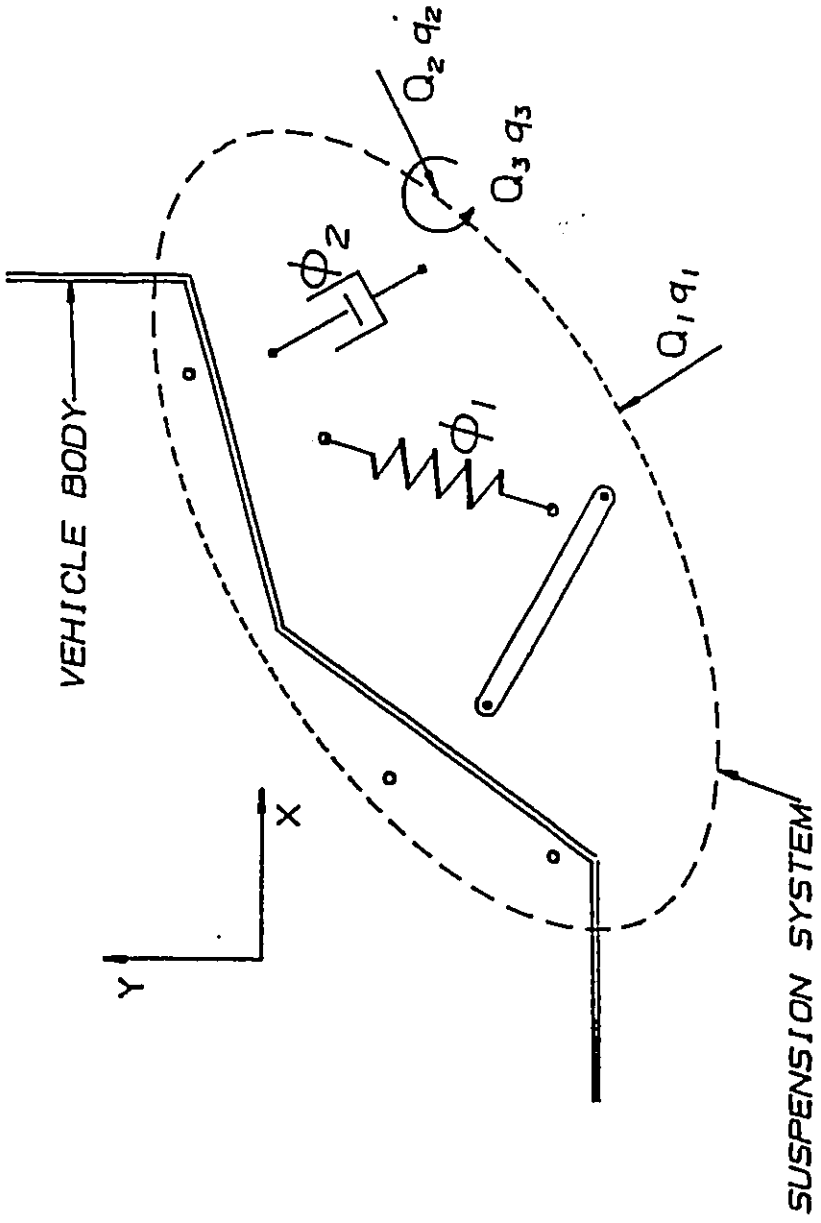

Fig. 4.1: A generic linkage suspension system

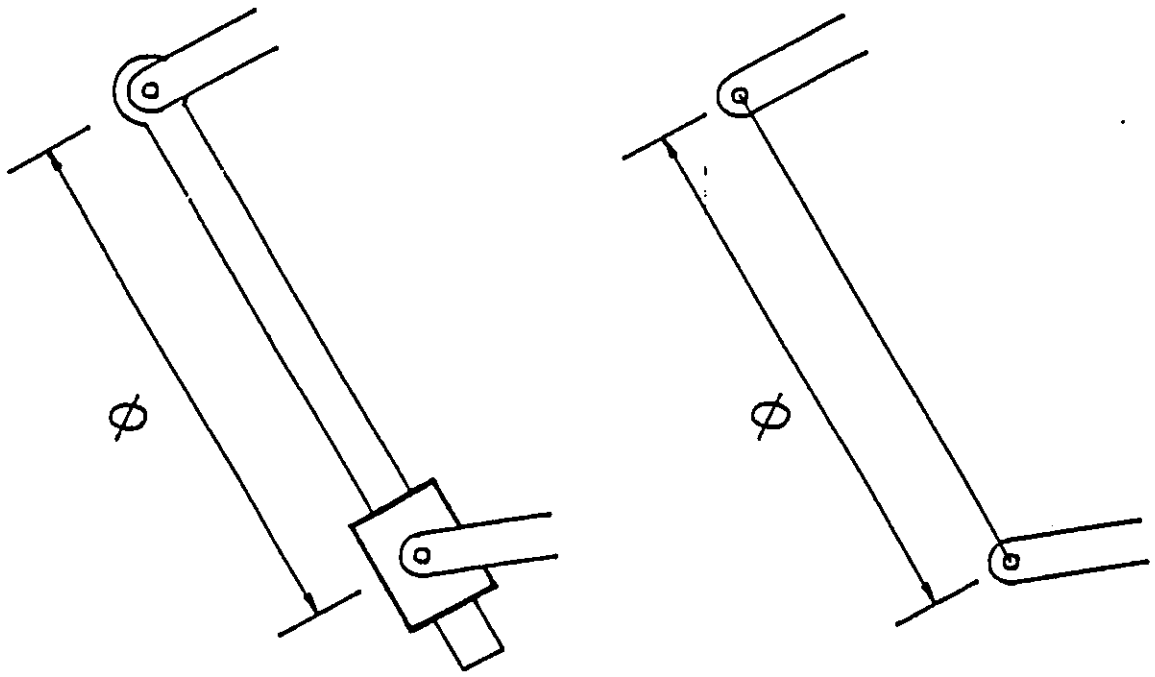

Fig. 4.2: Kinematic model of a shock-absorber (a) conventional model. (b) `rubber band' link model

numbers of joints and links. The set of Lagrangian coordinates chosen must include the deflections across all the force-generating elements. For torsion springs, for example, these are their angular deflections, and for shock-absorbers and coil springs, their length. From kinematic criteria (Gruebler's criterion, or loop-mobility criterion [108]) we determine the number of degrees of freedom of the mechanism. We define that many number of kinematic variables as the *independent* variables or the *generalized coordinates* of the mechanism. These variables should ideally correspond to the motions externally impressed on the suspension system. If such a variable is not readily available from the kinematic modelling, one can always add this variable also to the other kinematic variables, and write a constraint equation relating this new variable to the others.

The suspension system is now characterized by a set of n Lagrangian coordinates, $\underline{\psi}$, among which l of them are identified as the independent variables, $\underline{q}$. The rest $(n-l) = m$ of them are the dependent variables, $\underline{\phi}$. These include the p deflection variables across the force-generator units. We order $\underline{\phi}$ such that the first p of them correspond to these variables. We can partition $\underline{\psi} = (\underline{\phi}^T; \underline{q}^T)^T$. Since there are m dependent variables, we can write m linearly independent constraint equations relating the n kinematic variables $\underline{\psi}$. Assuming all $\underline{q}$ are known, we have a set of m simultaneous nonlinear algebraic equations in m unknowns, $\underline{\phi}$:

$$\underline{f}(\phi_1, \phi_2, \ldots \phi_m; q_1, q_2, \ldots q_l) = \underline{0} \tag{4.1}$$

The variational form of this equation, after rearranging terms,

becomes,

$$\sum_{i=1}^{m} \frac{\partial f_k}{\partial \phi_i} d\phi_i = -\sum_{j=1}^{l} \frac{\partial f_k}{\partial q_j} dq_j \quad , \quad k = 1, 2, \ldots, m \tag{4.2}$$

or, in matrix notation,

$$A\underline{d\phi} = -B\underline{dq} \tag{4.3}$$

where

$$A = \left[A_{ij}\right] = \left[\frac{\partial f_i}{\partial \phi_j}\right] \quad , \quad \text{a } m\text{x}m \text{ Jacobian matrix,}$$

and

$$B = \left[B_{ij}\right] = \left[\frac{\partial f_i}{\partial q_j}\right] \quad , \quad \text{a } m\text{x}l \text{ matrix.}$$

As an illustration of the kinematic modelling procedure, we model the conventional outboard racing car suspension shown in Figure 4.3. The modelling is carried out as outlined above. Figure 4.4 shows the variables and kinematic loops. A coordinate system is fixed on the chassis at the lower inboard joint. Only one generalized coordinate, q_1, is sufficient to specify the motion of the suspension system. This is chosen as the vertical motion of the road-wheel contact point. ϕ_1 denotes the deflection of the spring. c_i are the constants that define

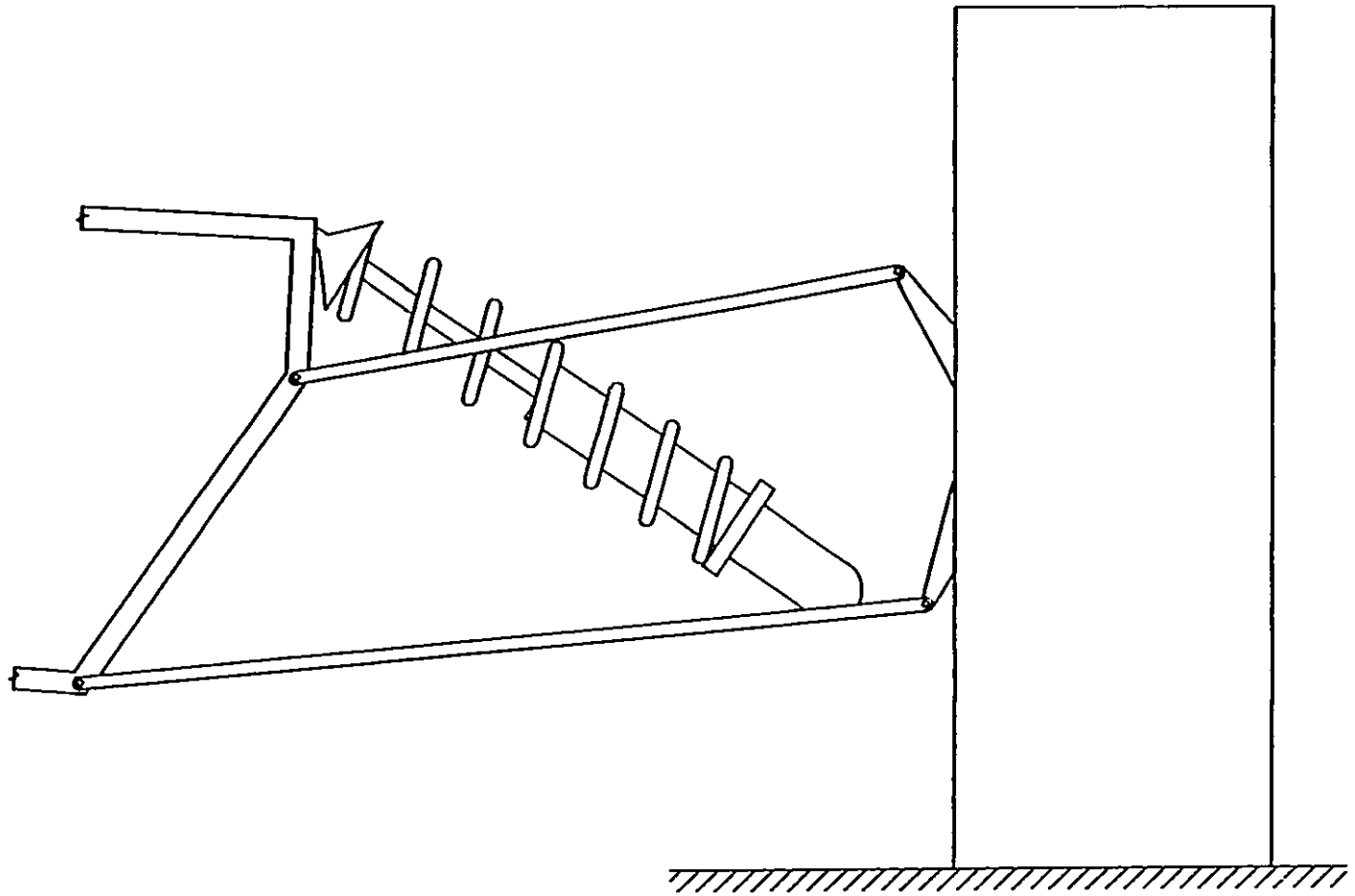

Fig. 4.3: A double wishbone system with conventional outboard shock-absorber and coil-spring

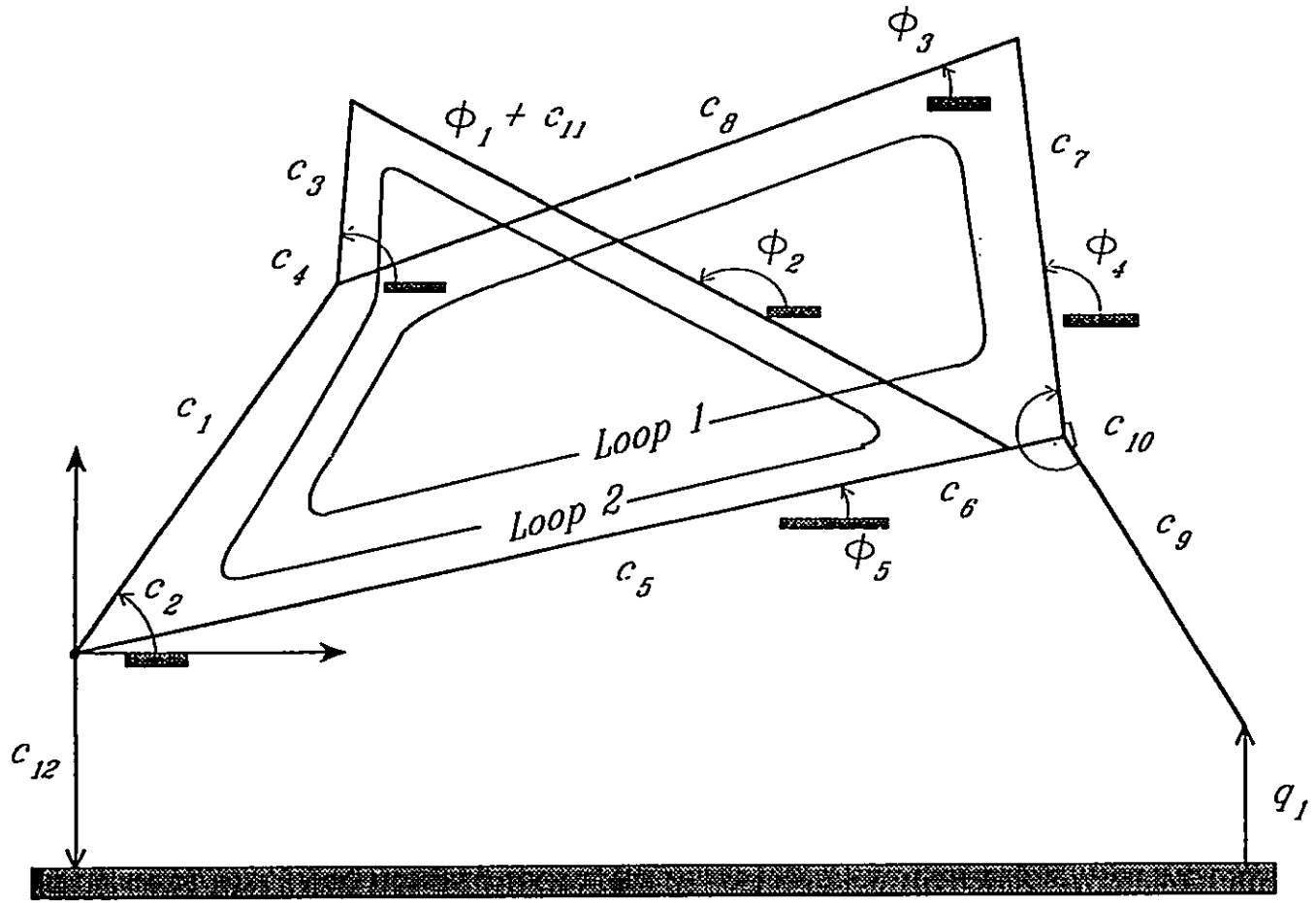

Fig. 4.4: Kinematic model of the conventional double wishbone system shown in Fig. 4.3

the geometry.

We can write two equations corresponding to each of the two loops, and one equation corresponding to the vertical motion, q_1, of the road-wheel contact point. These 5 equations relate 5 Lagrangian coordinates, and one independent coordinate, q_1. The equations are:

$$f_1 = c_5\cos\phi_5 + c_7\cos\phi_4 - c_8\cos\phi_3 - c_1\cos c_2 = 0$$

$$f_2 = c_5\sin\phi_5 + c_7\sin\phi_4 - c_8\sin\phi_3 - c_1\sin c_2 = 0$$

$$f_3 = c_6\cos\phi_5 + (\phi_1 + c_{11})\cos\phi_2 - c_3\cos c_4 - c_1\cos c_2 = 0$$

$$f_4 = c_6\sin\phi_5 + (\phi_1 + c_{11})\sin\phi_2 - c_3\sin c_4 - c_1\sin c_2 = 0$$

$$f_5 = c_5\sin\phi_5 + c_9\sin(\phi_4 + c_{10}) - q_1 + c_{12} = 0$$

Matrices A and B are obtained through direct differentiation as follows:

$$A = \begin{bmatrix} 0 & 0 & c_8\sin\phi_3 & -c_7\sin\phi_4 & -c_5\sin\phi_5 \\ 0 & 0 & -c_8\cos\phi_3 & c_7\cos\phi_4 & c_5\cos\phi_5 \\ \cos\phi_2 & -(\phi_1 + c_{11})\sin\phi_2 & 0 & 0 & -c_6\sin\phi_5 \\ \sin\phi_2 & (\phi_1 + c_{11})\cos\phi_2 & 0 & 0 & c_6\cos\phi_5 \\ 0 & 0 & 0 & c_9\cos(\phi_4 + c_{10}) & c_5\cos\phi_5 \end{bmatrix}$$

$$B = \begin{bmatrix} 0 & 0 & 0 & 0 & -1 \end{bmatrix}^T$$

For a general system, to carry out position analysis we must solve Equation 4.1. For this we assume that the independent coordinates, $\underline{q}$, are known (constants). Then the m simultaneous nonlinear algebraic equations (4.1) in m unknowns, $\underline{\phi}$, can be solved using the popular Newton-Raphson algorithm [108]. The iteration scheme is:

$$\underline{\phi}^{(i+1)} = \underline{\phi}^{(i)} - A^{-1(i)}\underline{f}^{(i)} \tag{4.4}$$

The iteration stops when $\underline{\phi}^{(i)}$ and $\underline{\phi}^{(i+1)}$ are sufficiently close.

The matrix A^{-1} is important for other reasons also. From 4.3 we can write,

$$\underline{d\phi} = -A^{-1}B\ \underline{dq} = K\underline{dq} \tag{4.5}$$

where $K = -A^{-1}B$.

The elements of K are called the *velocity coefficients* of the mechanism [108]. K_{ij} is in fact the partial derivative of the dependent variable, $\phi_i = \phi_i(\underline{q})$, with respect to the independent variable, q_j, since we can write,

$$d\phi_i = \sum_{j=1}^{l} K_{ij}\ dq_j \equiv \sum_{j=1}^{l} \frac{\partial \phi_i}{\partial q_j}\ dq_j \tag{4.6}$$

The Lagrangian coordinates we are particularly interested in are those corresponding to the p force-generator elements, ϕ_1, ϕ_2,...ϕ_p. The velocity coefficients corresponding to these are the elements of the first p rows of K. They play an important role in the many applications of velocity coefficients that we will consider in subsequent Sections.

4.3 DESIGN SENSITIVITY ANALYSIS

In the Sections following this, we show how the force-generation and roll centre characteristics of a complex suspension with several kinematic variables can be described by a few velocity coefficients. In a dynamic analysis model these coefficients appear as system parameters along with other conventional parameters, such as stiffness, damping coefficients, etc.. Optimization may be carried out at this stage, based on some dynamic criteria, to determine desired values for velocity coefficients, generally as functions of the suspension generalized coordinates. Then it is the task of kinematic design to synthesize the suspension mechanism to provide the desired velocity coefficients. During the course of an iterative optimization process, most optimization algorithms require sensitivities of objective and constraint functions to changes in design [110]. Therefore, in this Section we derive expressions for the sensitivities of dependent variables and velocity coefficients to design and input variables. This information can also be used in manual iteration to improve design. As will be seen later, the sensitivities velocity coefficients to input variables are also required for kinetostatic and ride and handling

analyses as well.

The problem of mechanism synthesis has gained considerable attention from researchers in the theory of machines and mechanisms. Detailed reviews can be found in Ref. [111,112], and it is not our intention to go deeply into this subject. Briefly, mechanism synthesis can be divided into two areas: type synthesis, which selects the appropriate mechanism type, and dimension synthesis, where its dimensions are determined. The objective of synthesis can be divided into three areas: kinematics, kinetostatics, or dynamics. In suspension design the linkage kinematics must satisfy the requirements of camber, toe, and caster changes, as well as, produce overall forces as specified functions of suspension travel. Although force generation falls into the area of kinetostatic synthesis, using the velocity coefficients method we have reduced the problem into one of pure kinematics. We restrict our attention to the problem of dimension synthesis.

The objective and constraint functions for kinematic design are dependent on position variables, $\underline{\phi}$, generalized coordinates, $\underline{q}$, velocity coefficients, K, and design variables, $\underline{b}$. In the subsequent discussions one must note the distinction between kinematic constraints and design constraints. The design objective and constraints may be of the form:

$$\Psi_j = \Psi_j(\underline{\phi}, \underline{q}, K, \underline{b}) \tag{4.7}$$

where, as before, $\underline{\phi} \in \mathbb{R}^m$, $\underline{q} \in \mathbb{R}^l$, K is a $m \times l$ matrix, and $\underline{b} \in \mathbb{R}^s$ is the

vector of design variables, and $\underline{\Psi} \in \mathbb{R}^r$ is the vector of objective and constraint functions. $\underline{b}$ is in fact the set of dimensions (constants) that define the geometry of the linkage configuration. As example of an objective function of the type shown above, see Ref. [113], where an off-road motorcycle rear suspension linkage is synthesized to obtain a specified leverage ratio (velocity coefficient) curve.

For use in optimization algorithms we require the derivatives of Equation 4.7 with respect to the design variables, $\underline{b}$. As a necessary first step towards computing these, the expressions for the sensitivities of $\underline{\phi}$ and K with respect $\underline{b}$ and $\underline{q}$ are derived in this Section. From these, the required sensitivity of Ψ_j to $\underline{b}$ can be computed using the chain rule of differentiation.

4.3.1 Sensitivity of ϕ with respect to b

The kinematic constraint equations (4.1) can be rewritten, showing their dependence on $\underline{b}$, as:

$$\underline{f}(\underline{\phi}, \underline{q}, \underline{b}) = \underline{0} \tag{4.8}$$

Taking derivatives, as in Equation 4.2, we have:

$$\left[\frac{\partial f}{\partial \phi}\right]\underline{d\phi} + \left[\frac{\partial f}{\partial q}\right]\underline{dq} + \left[\frac{\partial f}{\partial b}\right]\underline{db} = \underline{0} \tag{4.9}$$

The first two matrices in this equation are A and B defined in Section 4.2. The third one we call C. C_{ij} is the derivative of the i^{th}

kinematic constraint equation with respect to the j^{th} design variable. For a given design $\underline{b}$ is constant and hence $\underline{db} \equiv \underline{0}$. In this case 4.9 is identical to 4.3. From Equation 4.5, K_{ij} can also be interpreted as the sensitivity of the position variable ϕ_i with respect to the input q_j.

For a given configuration, $\underline{dq} \equiv \underline{0}$, and therefore, from Equation 4.9 we have:

$$A\underline{d\phi} = -C\underline{db} \tag{4.10}$$

or

$$\underline{d\phi} = -A^{-1}C\underline{db} = P\underline{db} \tag{4.11}$$

where $P = -A^{-1}C$ is sensitivity matrix of the position variables, $\underline{\phi}$, with respect to the design variables.

4.3.2 Sensitivity of K with respect to b

By definition (Equation 4.5),

$$K = -A^{-1}B$$

$$\Rightarrow \quad AK = -B$$

Differentiating with respect to a design variable b_i, we have,

$$\frac{d}{db_i}(AK) = -\frac{d}{db_i}(B)$$

$$\Rightarrow \quad \frac{dA}{db_i}K + A\frac{dK}{db_i} = -\frac{dB}{db_i}$$

$$\Rightarrow \quad \frac{dK}{db_i} = -A^{-1}\left[\frac{dA}{db_i}K + \frac{dB}{db_i}\right] \tag{4.12}$$

This is the expression for the sensitivity of K. However, it needs to be further simplified because the derivatives, $\frac{dA}{db_i}$ and $\frac{dB}{db_i}$, are not explicitly known. Since $A = A(\underline{\phi}, \underline{q}, \underline{b})$,

$$\frac{dA}{db_i} = \frac{\partial A}{\partial b_i} + \frac{\partial A}{\partial \phi}\frac{d\phi}{db_i} + \frac{\partial A}{\partial q}\frac{dq}{db_i} \tag{4.13}$$

The last term drops because q is independent of b ($\frac{dq}{db_i} = 0$). From Equation 4.11 we can write $\frac{d\phi}{db_i} = P_i$, where P_i is the i^{th} column of the matrix $P = -A^{-1}C$. Equation 4.13 now becomes,

$$\frac{dA}{db_i} = \frac{\partial A}{\partial b_i} + \frac{\partial A}{\partial \phi}P_i \tag{4.14}$$

Similarly,

$$\frac{dB}{db_i} = \frac{\partial B}{\partial b_i} + \frac{\partial B}{\partial \phi}P_i \tag{4.15}$$

Substituting these in Equation 4.12, we get,

$$\frac{dK}{db_i} = -A^{-1}\left[\left(\frac{\partial A}{\partial b_i} + \frac{\partial A}{\partial \phi}P_i\right)K + \frac{\partial B}{\partial b_i} + \frac{\partial B}{\partial \phi}P_i\right] \tag{4.16}$$

Note that $\frac{\partial A}{\partial \phi}$ is a 3-dimensional array, $m \times m \times m$, since A is a $m \times m$

matrix and $\underline{\phi}$ is a m-vector. Similarly, $\frac{\partial B}{\partial \phi}$ is $mx1xm$.

4.3.3 Derivative of K with respect to q

This derivative is the rate of the change of the velocity coefficients with respect to the input deflections. Its derivation parallels that of $\frac{dK}{db}$. Similar to Equation 4.16 we have,

$$\frac{dK}{dq_i} = -A^{-1}\left[\left(\frac{\partial A}{\partial q_i} + \frac{\partial A}{\partial \phi} K_i\right)K + \frac{\partial B}{\partial q_i} + \frac{\partial B}{\partial \phi} K_i\right] \qquad (4.17)$$

where K_i is the i^{th} column of the matrix K.

4.4 APPLICATION TO VEHICLE RIDE AND HANDLING ANALYSIS

The general purpose programs, such as IMP, ADAMS, DADS and MEDYNA, have been used in several vehicle dynamics studies that include the suspension kinematics [72-84]. Most applications of IMP, ADAMS and DADS have been especially for suspension load determination. While these were developed by researchers in machine dynamics, and are more relevant to that area, MEDYNA was developed with high-speed transportation systems in mind. It has analysis options useful for vehicle ride and stability studies, and special modules for vehicles on rails [83-85].

MEDYNA does not take into account large rigid body motions in suspensions. The two most popular programs, ADAMS and DADS, which do this, are based on formalisms that generate a maximal set of equations

for the multi-body system. For example, even a simplified model of a MacPherson strut suspension unit, as shown in Figure 4.5, gives rise to 35 second order differential equations together with 33 algebraic constraint equations [81]. Full vehicle models may have hundreds of equations and may take an hour or more of main-frame CPU time for a single second of vehicle dynamic simulation. These programs also require large amounts of geometrical and physical data, and require a high level of modelling expertise and time. Furthermore, due to the complexity of the model, little physical insight can be gained about the effect of various components on the overall system performance.

Important kinematic parameters affecting handling dynamics are toe, camber and scrub, and their derivatives with respect to wheel travel. Besides these, the movements of suspension links also affect bounce and roll stiffnesses. These effects are especially important to consider in the case of racing applications. By using different linkage arrangements to mount the springs and dampers in the suspension system, one has the possibility of shaping the stiffnesses as functions of the relative motion between the body and the wheel as desired. In Figure 4.6 we see the double wishbone linkage as the basic suspension concept with variations in the way the spring-damper unit is mounted. Similarly, in Figure 4.7 we see several variations on the rear swing-arm suspension system employed in off-road motorcycles. In each of these figures, the kinematic relation between the vehicle body and wheel movements are the same while the effective stiffness properties have been modified. In four-wheeled vehicles, the roll stiffness of front and rear suspensions are related to vehicle understeer and oversteer

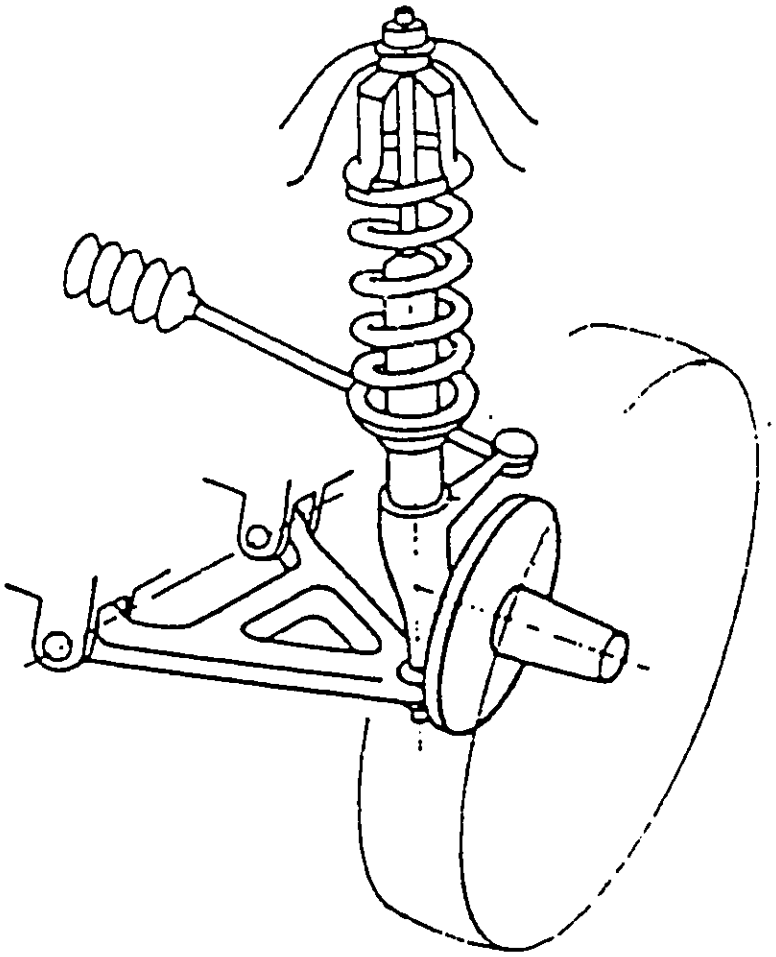

Fig. 4.5: MacPherson strut type front suspension

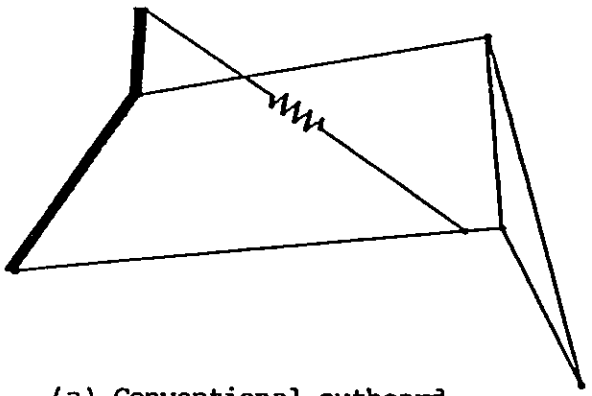

(a) Conventional outboard

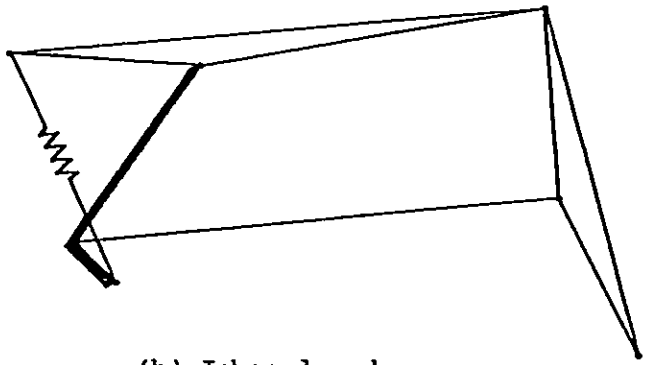

(b) Inboard rocker

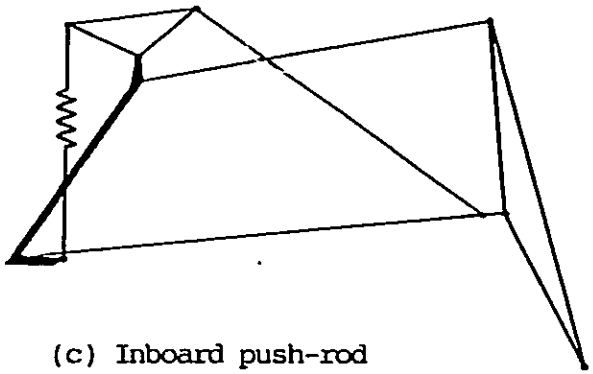

(c) Inboard push-rod

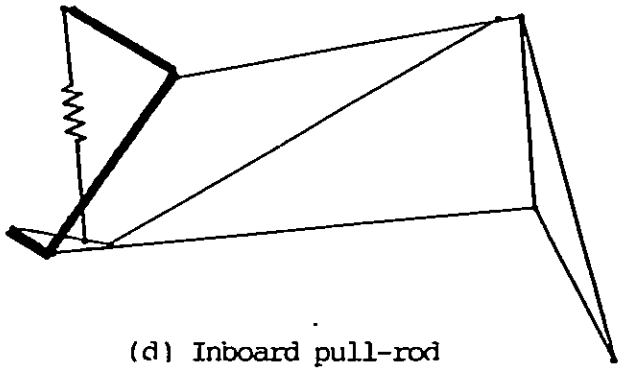

(d) Inboard pull-rod

Fig. 4.6: Variations of double wishbone suspension system in racing cars

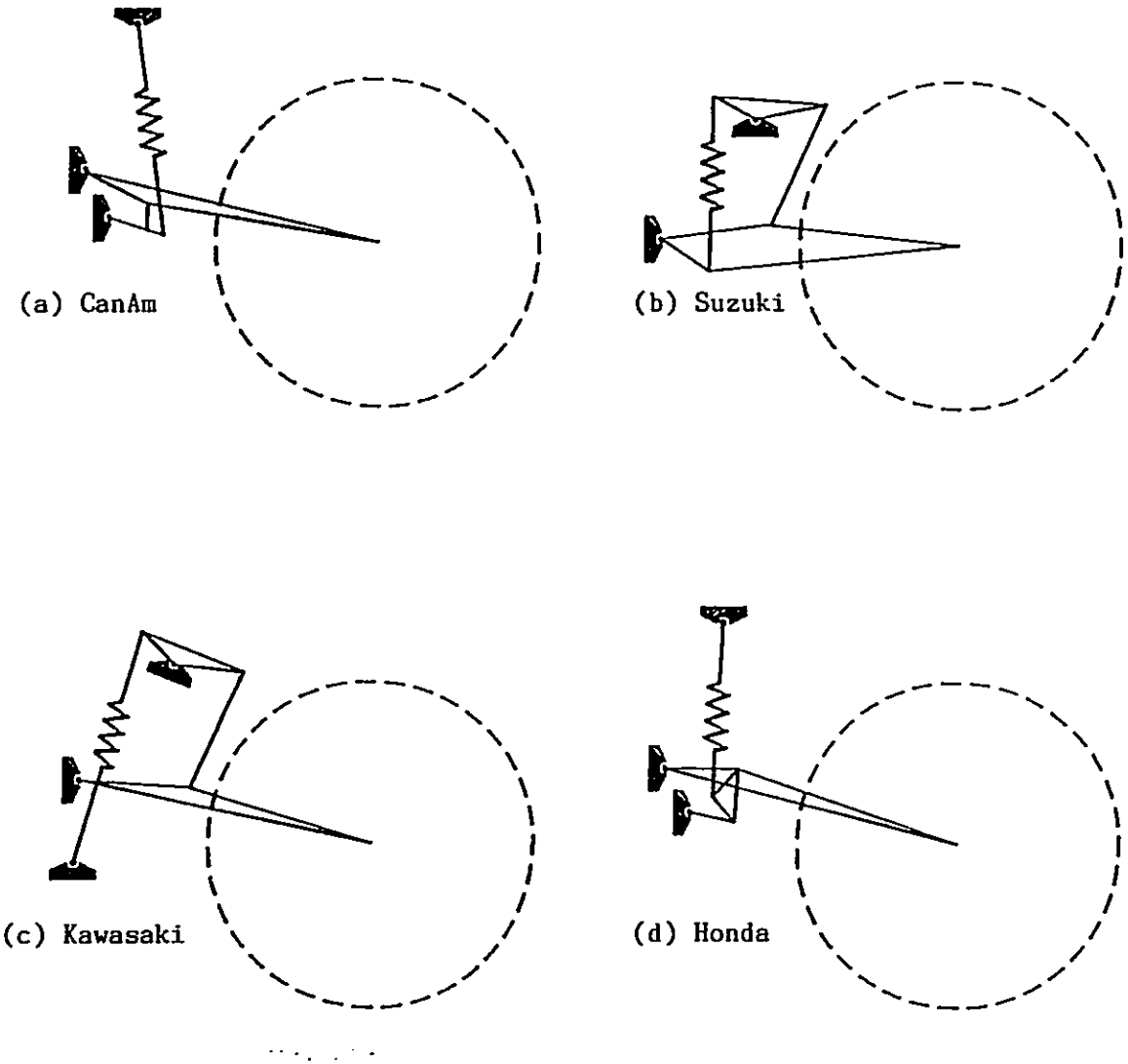

Fig. 4.7: Variations of swing-arm rear suspension system in off-road motorcycles

characteristics [52]. Although many studies have assumed constant roll stiffness, it has been shown that this can vary considerably depending on suspension movement [67]. The velocity coefficient approach we propose provides a convenient way of analyzing and understanding these effects.

In this Section, we present an approach to modelling linkage suspensions that fits in with traditional methodology where suspension systems are modelled as two-port force generators. At the same time this approach incorporates nonlinearities in springs and dampers, and large deflections in suspension linkages. We do not have to model the entire vehicle-terrain system as one spatial mechanism, as would be required by certain general purpose mechanism programs. Forces generated in the elements of the suspension assembly may be passive or active, linear or nonlinear. They may also be experimentally evaluated 'black-box' elements. In our approach, a kinematic analysis is performed *a priori*, to extract precisely and completely, the information required for a separate dynamic analysis.

The information obtained from kinematic analysis is independent of isolator parameters such as spring stiffness, damping characteristics etc.. The parameters of these elements can be varied and optimized during the dynamic analysis/design stage without having to redo kinematic analysis. The optimum variation of velocity coefficients and isolator deflections can also be computed at this stage. This information can then be used to solve the problem of kinematic design, whereby one tries to synthesize these curves. This modular approach

affords the engineer a better understanding of the problems, thereby leading to better design solutions.

4.4.1 Suspension Forces Using Velocity Coefficients

We continue with the kinematic modelling and analysis procedure described in Section 4.2. As noted there, the vehicle suspension system is modelled as a mechanism. Among the p force generating elements in this mechanism, let the forces generated in the i^{th} element be denoted F_i. The corresponding deflections in the direction of these forces are ϕ_i. In order to model the suspension system as an equivalent force-generator, we seek to find the set of *generalized forces*, Q_j, corresponding to the generalized coordinates, q_j. Using the principle of virtual work we can write,

$$\delta W = \sum_{i=1}^{p} F_i \delta\phi_i \tag{4.18}$$

Using velocity coefficients (Equation 4.6), this becomes,

$$\delta W = \sum_{i=1}^{p} \left(F_i \sum_{j=1}^{l} K_{ij} \delta q_j \right) = \sum_{j=1}^{l} \sum_{i=1}^{p} F_i K_{ij} \delta q_j \tag{4.19}$$

which implies

$$Q_j = \sum_{i=1}^{p} F_i K_{ij} \tag{4.20}$$

This means that all Q_j can be evaluated, once the input motions,

q_j, are known. Thus we have a complete description of the force displacement characteristics of the suspension. In particular, if the force generators are passive elements,

$$F_i = F_i(\phi_i, \dot{\phi}_i) \tag{4.21}$$

Variables, ϕ_i, are known from the solution of Equation 4.1, for a given $\underline{q}$. $\dot{\phi}_i$ can be evaluated as (Equation 4.6), knowing $\dot{\underline{q}}$, as

$$\dot{\phi}_i = \sum_{j=1}^{l} K_{ij} \dot{q}_j \tag{4.22}$$

Therefore we can write

$$Q_j = Q_j(\underline{q}, \dot{\underline{q}}) \tag{4.23}$$

This expression is valid for active force-generators as well, since the full state of the system is known once $\underline{q}$ and $\dot{\underline{q}}$ are specified. Since K is known once the positions $\underline{\phi}$ and $\underline{q}$ are known, a position analysis alone is sufficient to compute the overall suspension forces.

Note that $\underline{q}$ is a vector describing the relative motion between two ends of a suspension system, and $\underline{Q}$ is the vector of corresponding forces. Since, using Equation 4.23, the forces can be expressed in terms of the relative motion, a linkage suspension can be modelled as an equivalent two-port force generator in conventional vehicle dynamic models. The kinematic analysis can be done once, to evaluate the required variables (spring deflections and velocity coefficients) for a

full range of input motion. These values can then be used during a subsequent dynamic analysis either as a look-up table with interpolation or as a functional approximation. In this manner, we can carry out large-deflection dynamic analysis of the vehicle system without having to solve the kinematics repeatedly in each integration step of the dynamic equations of motion. If a small-deflection analysis is required, the kinematic analysis carried out at the operating height provides the necessary information to determine equivalent stiffness and damping coefficients. This procedure is described in the next Section.

A further advantage of the velocity coefficient method is that it helps us to characterize a suspension system using a set of fewer number of parameters than those of the original system. For example, to define the suspension system shown in Figure 4.3, one must specify the interconnection structure of the different links and their dimensions. In characterizing the forces generated in this suspension, these individual parameters are relevant only to the extent to which they affect this force generation. The method of velocity coefficients summarize the overall force generation characteristics in terms of a few parameters. Since the dynamics of the sprung mass is determined only by the forces acting on it, a kinematic analysis is not relevant at that stage. This division of kinematic and dynamic analyses helps to give better understanding of the system. It also helps by separating the design problem into manageable sizes. For example, during dynamic analysis, optimization may be carried out using a cost function of dynamic response variables to determine optimum variation of velocity coefficients for a particular set of inputs. A kinematic synthesis may

be carried out subsequently to design an appropriate suspension configuration which will achieve this criterion as well as other relevant ones.

4.4.1.1 Special Cases

We will now consider suspensions with each force-generator element being a linear, passive spring in parallel with a damper. The stiffness and damping coefficients are k_i and c_i, and the spring has an unstretched length of ϕ_i^0. Then, using Equations 4.20 and 4.22, the generalized forces corresponding to each of the generalized coordinates can be written as:

$$Q_j = \sum_{i=1}^{p} K_{ij} \left\{ k_i\left(\phi_i - \phi_i^0\right) + c_i \sum_{j=1}^{l} K_{ij} \dot{q}_j \right\} \tag{4.24}$$

Note that Q_j are in general nonlinear, due to nonlinear ϕ_i and K_{ij}, although the forces generated in the isolator elements themselves are linear with respect to motions across them.

The linearized (small deflection) force-generation characteristics of the linkage suspension can be written in terms of constant-coefficient $l \times l$ stiffness and damping matrices, $\mathcal{K}$ and $\mathcal{C}$, as:

$$\underline{Q} = \mathcal{K}\underline{q} + \mathcal{C}\dot{\underline{q}} \tag{4.25}$$

where

$$\mathcal{K}_{ij} = \frac{\partial Q_i}{\partial q_j}\bigg|_{\underline{q}=\underline{q}^0} = \sum_{s=1}^{p} k_s \left\{ K_{sj}K_{si} + \left(\phi_i - \phi_i^0\right)\frac{\partial K_{si}}{\partial q_j} \right\}\bigg|_{\underline{q}=\underline{q}^0} \tag{4.26}$$

and

$$\mathcal{C}_{ij} = \frac{\partial Q_i}{\partial \dot{q}_j}\bigg|_{\underline{q}=\underline{q}^0} = \sum_{s=1}^{p} c_s K_{sj}K_{si}\bigg|_{\underline{q}=\underline{q}^0} \tag{4.27}$$

where $\underline{q}^0$ is the position of the generalized coordinates about which linearization is carried out. If at this position $\underline{\phi} = \underline{\phi}^0$, then the second term inside brackets in Equation 4.26 vanishes. However, this is often not the case since suspension springs will have a nonzero deflection at static ride height due to vehicle weight. This means that unless the velocity coefficients are constant with respect to wheel motions, the rate of change of velocity coefficients, $\frac{\partial K}{\partial q}$, must also be taken into account in computing effective wheel rates. This fact is neglected in books on car suspension design [65,66,68]. Analytical expression for computing $\frac{\partial K}{\partial q}$ is given in Section 4.3.3. There, this same quantity is represented by the notation $\frac{dK}{dq}$.

4.4.2 Vehicle Handling Analysis

The main objective of handling analysis is to determine the vehicle performance in cornering and braking. These are largely determined by

the forces developed at the road-tire contact patches. Therefore the most important components of a vehicle system affecting its handling performance are the tires. Next in line is the suspension system, since it transmits the forces between the vehicle sprung mass and the tires, and determines the kinematics of wheel motion with respect to the chassis and the road. The methodology for analyzing suspension forces has been explained in Section 4.4.1.

Among the suspension system kinematic variables, the wheel camber angle and its rate of change with respect to wheel travel are very important in determining the cornering performance. Other variables such as toe, bump-steer, roll-steer, and wheel scrub are also required for vehicle handling analyses. All these quantities can be computed using the kinematic modelling and analysis procedure described above. The 'rate' quantities (camber rate, bump-steer rate etc.) are nothing but velocity coefficients when the suspension system is appropriately modelled. These can therefore be computed from a kinematic analysis, prior to a dynamic analysis, for the full range of input variables.

4.4.3 Kinetostatic Analysis

In mechanism theory the terms *kinetostatic* and *quasistatic* are used to refer to static analysis that includes applied forces, as well as, d'Alembert forces [108]. The problem may the determination of joint reaction forces for a given state of the system and/or the determination of equilibrium position under the action of applied and inertia forces. Knowing the spring/damper forces (Equation 4.21) and generalized

external forces (Equation 4.20), determination of joint reaction forces can be achieved using static force analysis methods given in References [10,108]. In this Section we describe the determination of kinetostatic equilibrium position using velocity coefficients. This computation is often required in vehicle suspension analysis, for example, to determine steady-state roll angle for a given centrifugal force [52,60,66].

Ellis [52] has presented a procedure for determining steady-state roll angle using the concept of roll centre. This procedure, which is widely used in practice, assumes constant roll stiffness and fixed roll centre location, and gives a closed form solution. Nalecz [60] has shown that roll centre movements can cause changes in roll moment arm of up to 20% for some suspension systems. This means that error in roll angles computed using Ellis' equations would not be insignificant Nalecz used essentially the same equation as those in [52] but implemented an iterative procedure to take care of roll centre movements. However, a constant roll stiffness value was assumed. George and Sadler [67] actually solved for link forces and computed steady-state position from force equilibrium, without reference to a roll centre or roll stiffness. A set of simultaneous nonlinear algebraic equations representing kinematic constraints and force balance is solved numerically. The partial derivatives required in Newton-Raphson algorithm are computed using numerical differentiation.

We present a method of kinetostatic analysis using velocity coefficients. This procedure makes use of the expression for generalized forces (Equation 4.20) and linear stiffness matrix (Equation

4.26) derived earlier. Let $\underline{R} \in \mathbb{R}^l$ be the vector of external forces applied along the generalized coordinates $\underline{q}$. If there are other external forces, they can be included as one of the p forces, F_i, already considered in Equation 4.20. In the case of inertial forces, we apply the corresponding d'Alembert force at the CG of that particular link, and treat it like an external force. For each external force, F_i, there is a corresponding Lagrangian coordinate, ϕ_i, included in the kinematic constraint equation, so that the velocity coefficient relating it to the input motion, q_j, are computed as K_{ij}. For static equilibrium,

$$g_i(\underline{q}) = Q_i - R_i = 0 \quad , \; i = 1,2, \ldots, l \tag{4.28}$$

$\underline{R}$ is a known, since it is a constant vector. $\underline{Q}$ is in general a nonlinear function of $\underline{q}$ as given in Equation 4.20. Therefore Equation 4.28 represents a set of l simultaneous nonlinear algebraic equations in l unknowns, $\underline{q}$. As in the case of Equation 4.1, this can also be solved using Newton-Raphson algorithm. The iteration scheme is:

$$\underline{q}^{(s+1)} = \underline{q}^{(s)} - \mathcal{K}^{-1(s)}\underline{g}^{(s)} \tag{4.29}$$

where,

$$\mathcal{K}_{ij}^{(s)} = \left.\frac{\partial g_i}{\partial q_j}\right|_{\underline{q}=\underline{q}^{(s)}} = \left.\frac{\partial Q_i}{\partial q_j}\right|_{\underline{q}=\underline{q}^{(s)}} \tag{4.30}$$

For the case of linear springs, this stiffness matrix is given in

Equation 4.26. The expression involves velocity coefficients and their derivatives as given in Equations 4.5 and 4.17 respectively. All these quantities can be evaluated for a given $\underline{q}$ from a kinematic analysis as explained in the previous Sections. The flow chart of the kinetostatic procedure is shown in Figure 4.8. It involves 2 nested iteration loops. The inner loop is the kinematic analysis stage which computes positions (solution of Equation 4.1) and stiffness matrix, for a given $\underline{q}$. The outer loop varies $\underline{q}$ to solve for Equation 4.28. The method is general and does not involve numerical differentiations. The stiffness matrix derived in the last stage may be used for a subsequent computation of roll centre location and roll stiffness as explained in Section 4.5.

4.5 ROLL CENTRE LOCATION AND ROLL STIFFNESS

Roll axis of a suspension system is generally taken to be the line about which the sprung mass rolls when it is acted upon by a lateral force. This is the line joining the front and rear suspension *roll centres*. It is presumed that the vehicle rolls about this line during cornering. The concept of roll centre is a very old one. Dixon [69] traces its roots to 1908. The term is very widely used in discussing vehicle handling dynamics [52,65-69]. Its primary purpose has been to aid in the computation of the load transfer that occurs between inner and outer wheels during steady-state cornering manoeuvre. This in turn may be used to determine the vehicle understeer or oversteer characteristics. Therefore, the concept of roll centre is considered to be of great importance by vehicle suspension designers.

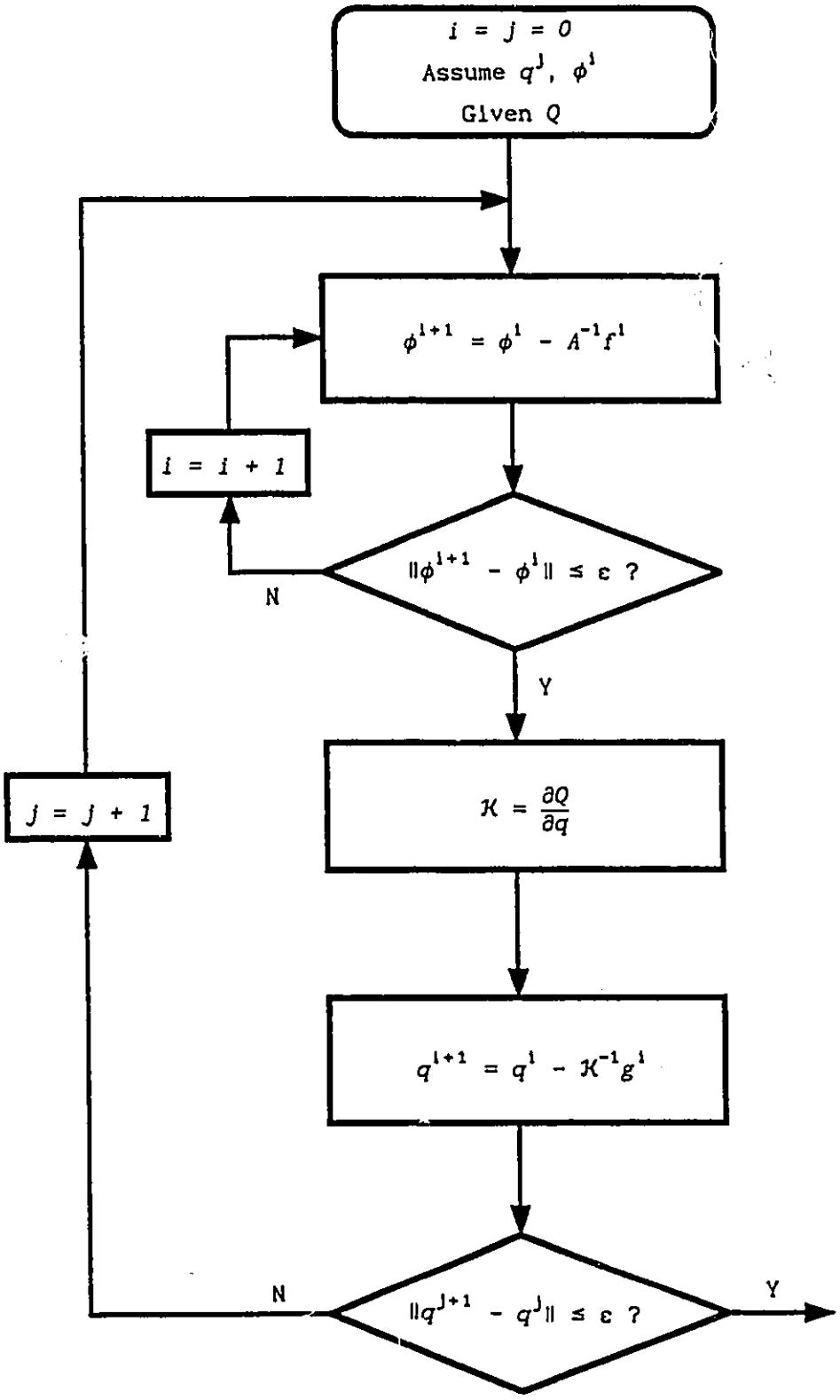

Fig. 4.8: Flowchart of kineto-static analysis procedure

It is possible to perform computer simulation and analysis of vehicle dynamics without explicit reference to roll centres. It is recognized that the roll centre approach is only an approximation which gives first order estimates of suspension loads [52]. However, the concept of roll centre is still popular because it very neatly summarizes some important characteristics of the suspension system. But unfortunately there has been some confusion in literature as to what exactly a roll centre is, how to determine its location, etc..

In this Section we take a fresh look at the concept of roll centres and clarify some disputed points. For example, it is shown that the definition of roll centre given by Society of Automotive Engineers [107] is inherently misleading, although it is valid in certain cases. We reestablish roll centre as the instantaneous centre of rotation of the sprung mass, and propose a new, general method of determining its location based on velocity coefficients. The method is illustrated in Chapter 5, where several racing car suspension geometries are analyzed. It is shown that many suspension systems have a variable roll stiffness as well as varying location of the roll centre.

4.5.1 Definition of Roll Centre

Ellis [52] defines roll centre as "kinematic centre of rotation of the suspension assuming that the wheels are rigid and do not move sideways on the road surface". The Society of Automotive Engineers [107] defines it as the "point in the transverse vertical plane through

any pair of wheel centres at which lateral forces may be applied to the sprung mass without producing suspension roll". vanValkenburgh [68] says it is the "single point at which resultant (lateral) force vector acts on the chassis centreline".

We have briefly listed above some of the conflicting definitions of roll centre advanced in literature. These definitions do indeed conflict, because it is not necessarily true that a lateral force applied at the instantaneous centre of rotation will not produce suspension roll. Similarly, instantaneous centre is not necessarily the point at which the resultant suspension force acts on the body. Thirdly, a point where a lateral force may be applied without causing suspension roll is not necessarily the same point where suspension forces are effectively applied to the body. We have repeatedly used the term *not necessarily* in pointing out the deficiency in all the three above definitions because these definitions are not *always* valid or equivalent. It so happens that the procedure for determination of roll centre location is almost always illustrated with the aid of a conventional double wishbone suspension system. In this particular case all the above definitions are correct since they refer to the same point. However, this is not the general case.

Recognizing the apparent differences in definition, Dixon [69] makes a distinction between *kinematic* roll centre and *force* roll centre. He refers to the generally understood definition of roll centre (instantaneous centre of rotation) as the kinematic roll centre and the SAE definition as force roll centre. He proposes the definition that

the roll centre "is the point at which suspension link forces are effectively applied to the body". He presents a geometrical construction for determination of force roll centre, which is identical to the construction procedure for the kinematic roll centre. However, the procedure is now explained in terms of forces rather than kinematics. The method is illustrated and explained with a double wishbone suspension as the principal example. He points out the ambiguity in the SAE definition, where, it refers to "the *point* . . at which lateral forces may be applied", while what we have is a *line* of application of force. Dixon suggests that we do away with a graphical construction altogether and use an abstract definition of roll centre height as the product of actual load transfer factor and vehicle track width. In this case the load transfer will somehow have to be computed first, before the roll centre height can be deduced. However, the general procedure [52] is to compute the roll centre height first, so that it can be used to compute the actual load transfer.

Dixon is the only person who has pointed out the apparent differences between the general understanding of roll centre and the SAE definition. But he does not notice a conflict. This conflict is not obvious in the case of a double wishbone, or MacPherson strut suspensions with the wheels assumed to be rigid and pinned to the ground. These kinematic models have only one degree of freedom each. Therefore, at any given position there is a unique point about which the body is free to rotate, no matter where and how external forces or moments are applied to it. This is, of course, the instantaneous centre (IC) of rotation. In this case any force applied at the IC will not

cause any body roll, and therefore the IC is identical to SAE definition of roll centre. To illustrate the deficiency if this definition, we take a more general case of a 2 DOF body as shown in Figure 4.9, which has rotational and vertical degrees of freedom in this plane. An applied vertical force at P causes a translation and rotation. The instantaneous centre is located at C as shown in the figure. It is obvious from inspection that a vertical force applied at C will not fail to cause a rotation of the body. Therefore in this case the SAE roll centre is not the instantaneous centre of rotation. Note that there is no unique IC, since its location will vary depending on the point of application and direction of the external load.

As we noted earlier, the practical use of roll centres is to determine the lateral load transfer occurring during a steady-state turn or to determine the steady-state roll angle. This calculation involves the roll stiffness of the suspension about the roll centre and the moment of the centrifugal force about the roll centre. This requires a pure angular deflection of the body about the roll centre and therefore this point must be the instantaneous centre of rotation of the body. Hence we define roll centre as follows: it is the instantaneous centre of rotation of the body for a lateral force applied at the centre of gravity. This is the only valid definition for use in determining suspension lateral properties. It incorporates *both* kinematic and force parameters as opposed to the IC definition of Ellis [52] or the SAE definition [107].

Using the above definition, roll centre location and roll stiffness

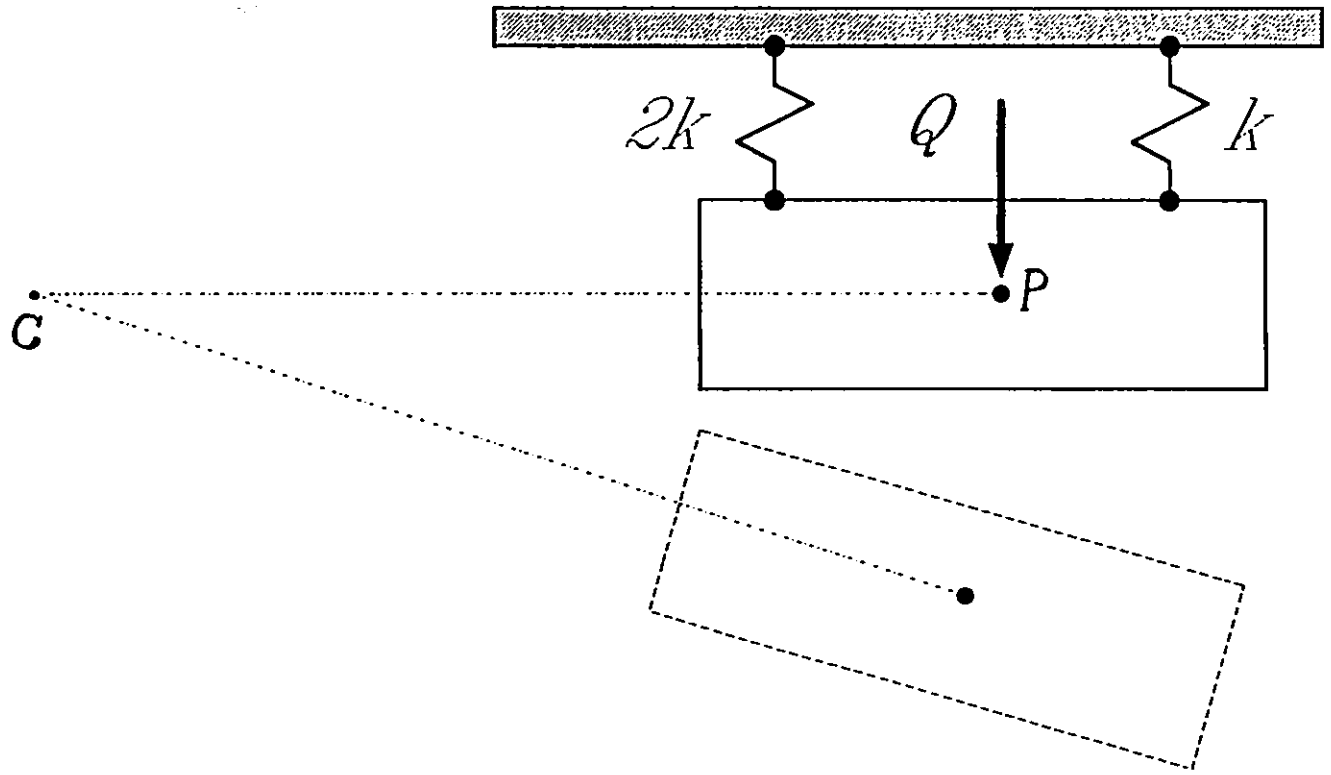

Fig. 4.9: Instantaneous centre location for a 2 DOF body acted upon by a vertical load

are very easily determined using the method of velocity coefficients. This is in contrast with graphical methods [42], and other numerical methods [88]. The graphical method for independent suspensions is fairly well known. The method does not make any reference to forces, but rather it is based on kinematics of single degree of freedom mechanisms. When it comes to multiple degree of freedom suspension system models there is some confusion as to how the roll centre is located. For example there is clear discrepancy between Smith [86] and Bastow [87] as to roll centre locations of various beam axle suspension systems. The method we present is more general. It does not have the limitations of the graphical method, or the complexities and inaccuracies of an ad hoc numerical method. Exact analytical expressions are presented for the roll centre location and roll stiffness. The method is a logical extension of the velocity coefficient method of suspension analysis presented earlier, and involves only a kinematic analysis.

4.5.2 Determination of Roll Centre

The approach is simply to apply a small lateral force, δQ_y at the body centre of gravity, and determine the point on the body which has zero translational velocity, i.e., the instantaneous centre (IC). Roll stiffness is then the moment of this force about the IC divided by the roll deflection, $\delta\theta$, caused by δQ_y. The method is general enough to be applied to any system, no matter how many degrees of freedom it has. For example, we can analyze the 5 DOF suspension system model shown in Figure 4.10, or the 3, 2 or 1 DOF models shown in 4.11 - 4.13. We

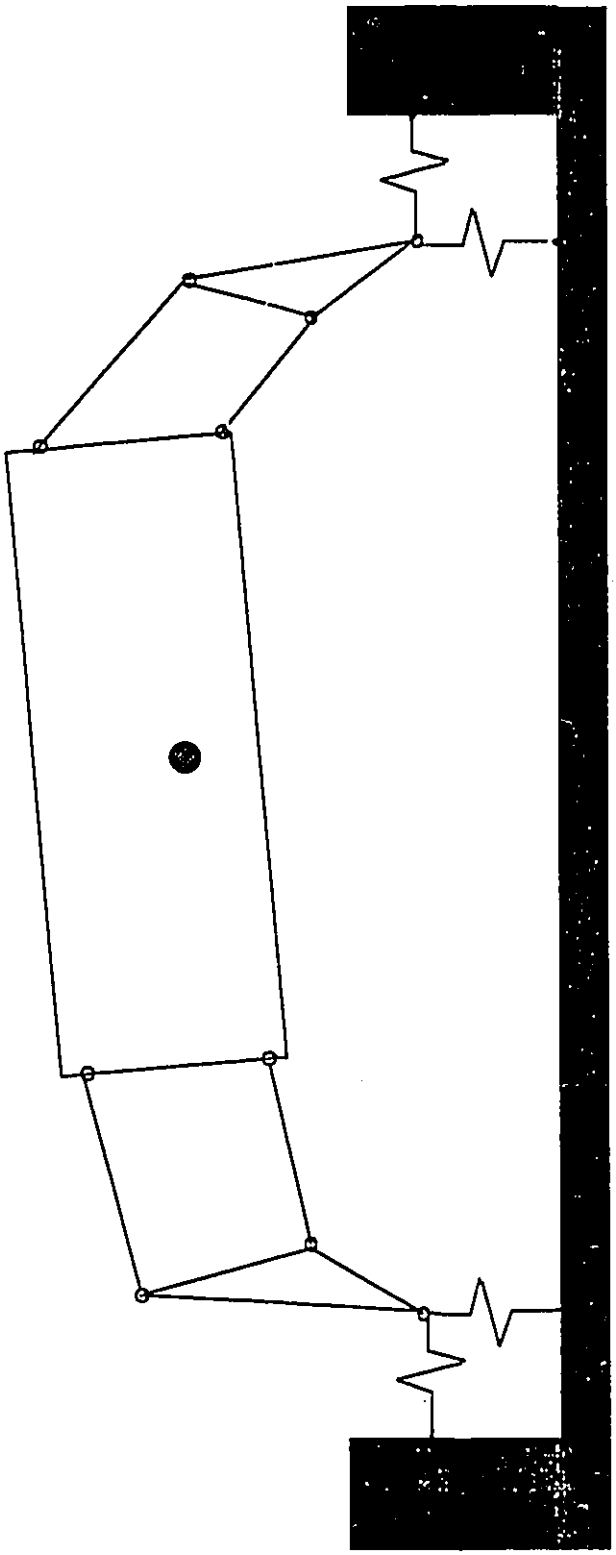

Fig. 4.10: Suspension system model with 5 degrees of freedom

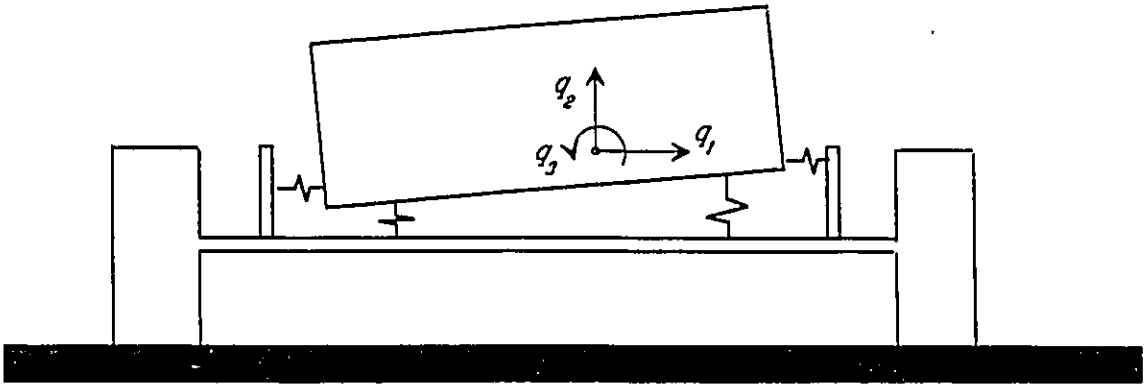

(a)

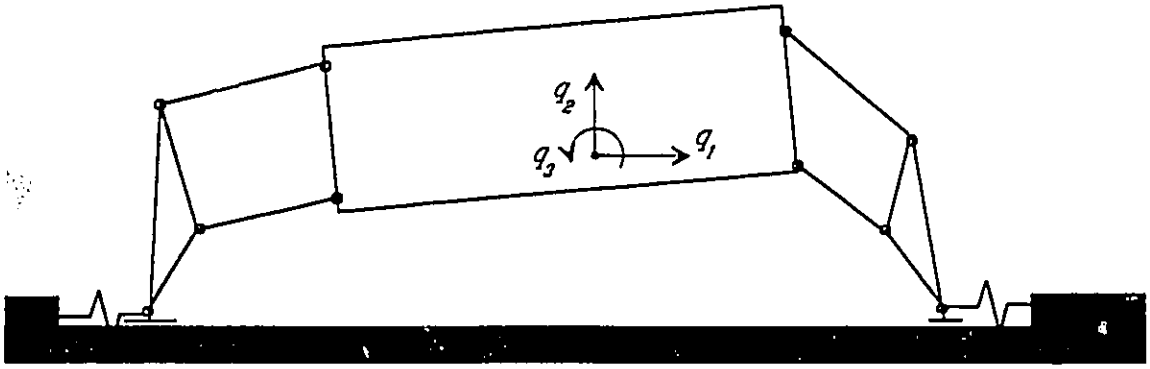

(b)

Fig. 4.11: Suspension system models with 3 degrees of freedom

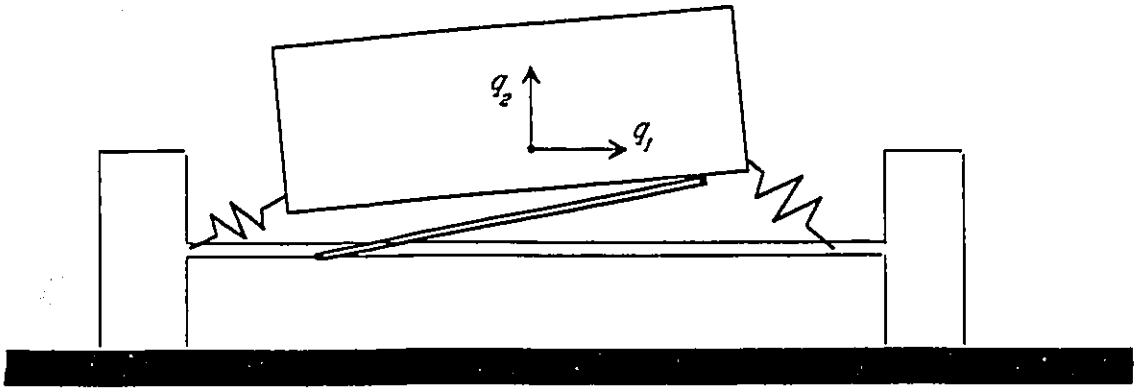

Fig. 4.12: Suspension system model with 2 degrees of freedom

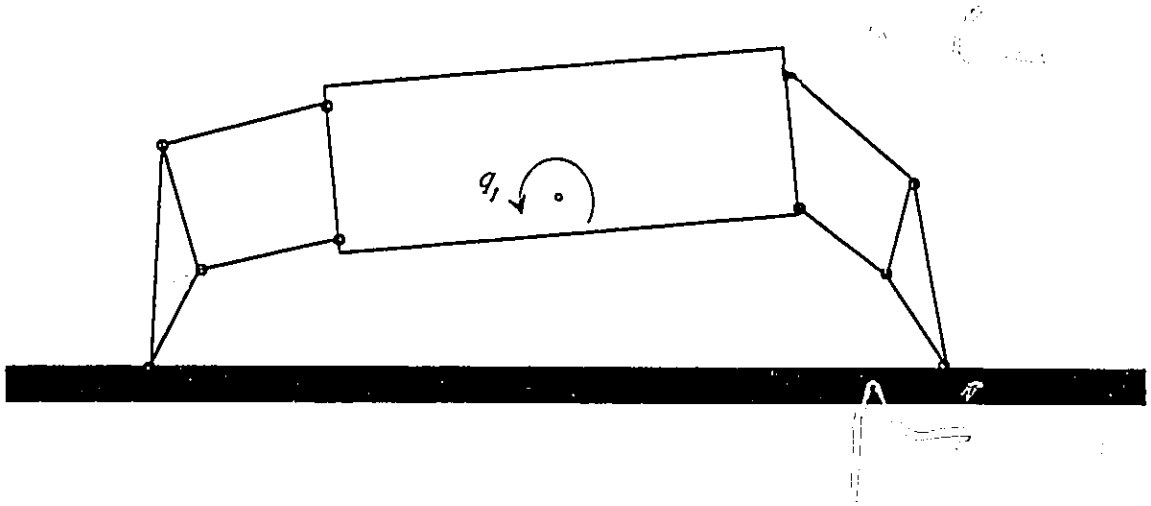

Fig. 4.13: Suspension system model with 1 degree of freedom

present detailed derivations for bodies with degrees of freedom 3, 2, and 1.

Figure 4.14 shows the general notation for derivations that follow. The body is in generalized equilibrium under the action of all applied and effective forces. x_{cg}, y_{cg}, and θ are the location and rotation of the vehicle body centre of gravity in the inertial frame. x_p and y_p specify the position of the roll centre in the inertial frame. ξ and η are its coordinates in the body-fixed coordinate system, which is parallel to the inertial frame when $\theta = 0$. Then, $\alpha = (\xi\cos\theta - \eta\sin\theta)$ and $\beta = (\xi\sin\theta + \eta\cos\theta)$ are the x and y distances to the roll centre from the body CG, measured in the inertial frame. We can write,

$$\left.\begin{aligned} x_p &= x_{cg} + \xi\cos\theta - \eta\sin\theta \\ y_p &= y_{cg} + \xi\sin\theta + \eta\cos\theta \end{aligned}\right\} \tag{4.31}$$

$$\Rightarrow \quad \left.\begin{aligned} \dot{x}_p &= \dot{x}_{cg} - (\xi\sin\theta + \eta\cos\theta)\dot{\theta} = \dot{x}_{cg} - \beta\dot{\theta} \\ \dot{y}_p &= \dot{y}_{cg} + (\xi\cos\theta - \eta\sin\theta)\dot{\theta} = \dot{y}_{cg} + \alpha\dot{\theta} \end{aligned}\right\} \tag{4.32}$$

4.5.2.1 Bodies with 3 Degrees of Freedom

Figure 4.11(a) and (b) show models of suspension systems with 3 degrees of freedom. In (a) this is a general 'free' body in 2D. In (b) this is the model of a conventional double wishbone suspension system

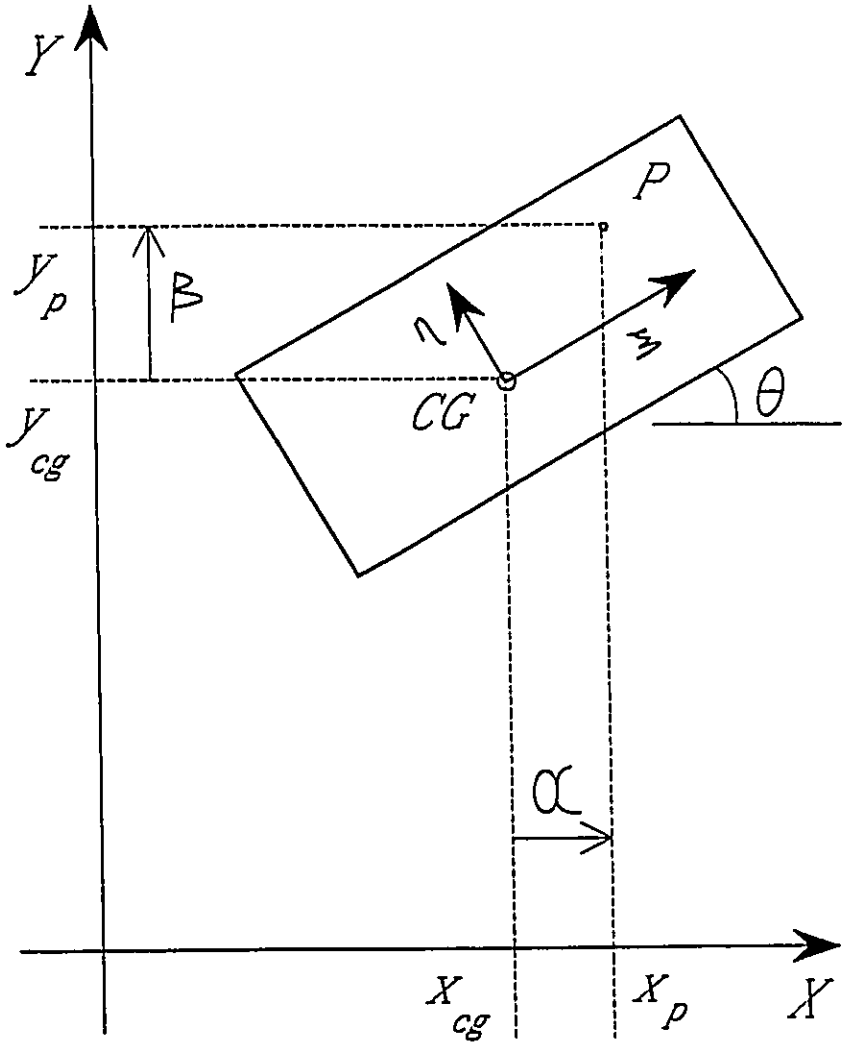

Fig. 4.14: General notation for determination of roll centre location

with the tires modelled with their lateral stiffnesses. In any case we can kinematically model the system with the 3 independent coordinates, q_1, q_2 and q_3, as x_{cg}, y_{cg}, and θ, respectively. For small deflections, $\underline{\delta q}$, we can write,

$$\begin{bmatrix} \delta Q_1 \\ \delta Q_2 \\ \delta Q_3 \end{bmatrix} = \begin{bmatrix} \mathcal{K}_{11} & \mathcal{K}_{12} & \mathcal{K}_{13} \\ \mathcal{K}_{21} & \mathcal{K}_{22} & \mathcal{K}_{23} \\ \mathcal{K}_{31} & \mathcal{K}_{32} & \mathcal{K}_{33} \end{bmatrix} \begin{bmatrix} \delta q_1 \\ \delta q_2 \\ \delta q_3 \end{bmatrix} \tag{4.33}$$

To find the roll centre due to a lateral force, δQ_1 (corresponding to generalized coordinate $q_1 = x_{cg}$), we set $\delta Q_2 = \delta Q_3 = 0$ and solve for the deflections δq_1, δq_2 and δq_3 from above. Then we get,

$$\left.\begin{aligned} \delta q_1 &= \delta Q_1 (\mathcal{K}_{22}\mathcal{K}_{33} - \mathcal{K}_{32}\mathcal{K}_{23}) \;/\; \Delta \\ \delta q_2 &= -\delta Q_1 (\mathcal{K}_{21}\mathcal{K}_{33} - \mathcal{K}_{31}\mathcal{K}_{23}) \;/\; \Delta \\ \delta q_3 &= \delta Q_1 (\mathcal{K}_{21}\mathcal{K}_{32} - \mathcal{K}_{31}\mathcal{K}_{22}) \;/\; \Delta \end{aligned}\right\} \tag{4.34}$$

where, $\Delta = \det(\mathcal{K})$. Substituting Equation 4.34 in 4.32, we get,

$$\left.\begin{aligned} \dot{x}_p &= \delta Q_1 \left[(\mathcal{K}_{22}\mathcal{K}_{33} - \mathcal{K}_{32}\mathcal{K}_{23}) - \beta(\mathcal{K}_{21}\mathcal{K}_{32} - \mathcal{K}_{31}\mathcal{K}_{22})\right] \;/\; \Delta \\ \dot{y}_p &= \delta Q_1 \left[(\mathcal{K}_{31}\mathcal{K}_{33} - \mathcal{K}_{21}\mathcal{K}_{33}) + \alpha(\mathcal{K}_{21}\mathcal{K}_{32} - \mathcal{K}_{31}\mathcal{K}_{22})\right] \;/\; \Delta \end{aligned}\right\} \tag{4.35}$$

Setting $\dot{x}_p = \dot{y}_p = 0$ we can solve for (α, β), the location of roll centre. We then get,

$$\left.\begin{aligned} \alpha &= (\mathcal{K}_{21}\mathcal{K}_{33} - \mathcal{K}_{31}\mathcal{K}_{33}) \;/\; (\mathcal{K}_{21}\mathcal{K}_{32} - \mathcal{K}_{31}\mathcal{K}_{22}) \\ \beta &= (\mathcal{K}_{22}\mathcal{K}_{33} - \mathcal{K}_{32}\mathcal{K}_{23}) \;/\; (\mathcal{K}_{21}\mathcal{K}_{32} - \mathcal{K}_{31}\mathcal{K}_{22}) \end{aligned}\right\} \qquad (4.36)$$

We note that the roll centre location depends only on the stiffness coefficients, $\mathcal{K}_{ij}$. These are, in turn, dependent only on the generalized coordinates and spring stiffnesses, and can be computed using velocity coefficients as in Equation 4.26. Therefore, we can determine the roll centre location for any given position from a kinematic analysis. We also note that the above computation of roll centre location was for an incremental lateral force application. The roll centre will, in general, be different if other force components are present.

4.5.2.2 Bodies with 2 Degrees of Freedom

Figure 4.12 shows the model of suspension systems with 2 degrees of freedom. This is the model of a beam axle suspension of Panhard rod type. In this case we choose $q_1 = x_{cg}$, and $q_2 = y_{cg}$, as the two degrees of freedom. Setting $\delta Q_2 = 0$, we get,

$$\left.\begin{aligned} \delta q_1 &= \delta Q_1 \mathcal{K}_{22} \;/\; \Delta \\ \delta q_2 &= -\delta Q_1 \mathcal{K}_{21} \;/\; \Delta \end{aligned}\right\} \qquad (4.37)$$

where $\Delta = \det(\mathcal{K}) = (\mathcal{K}_{11}\mathcal{K}_{22} - \mathcal{K}_{21}\mathcal{K}_{12})$. During kinematic analysis θ is chosen as one of the dependent variables, so that we can write,

$$\delta\theta = K_{t1}\delta q_1 + K_{t2}\delta q_2 \tag{4.38}$$

where K_{t1} and K_{t2} are the velocity coefficients relating the body roll angle, θ, to to the inputs, q_1 and q_2. Substituting Equations 4.37 and 4.38 in 4.32, and solving for α and β we get,

$$\left.\begin{aligned} \alpha &= \mathcal{K}_{21} \,/\, (K_{t1}\mathcal{K}_{22} - K_{t2}\mathcal{K}_{21}) \\ \beta &= \mathcal{K}_{22} \,/\, (K_{t1}\mathcal{K}_{22} - K_{t2}\mathcal{K}_{21}) \end{aligned}\right\} \tag{4.39}$$

4.5.2.3 Bodies with 1 Degree of Freedom

Figure 4.13 shows the model of a suspension system with 1 degree of freedom. This is the model of a conventional double wishbone suspension system with rigid tires, assumed to be pinned at the contact patch. Since the body has only one degree of freedom, it has a unique roll centre no matter what the direction of applied forces. For kinematic analysis, it is convenient to take $q_1 = \theta$. For the one degree of freedom system, we can arbitrarily choose δq_1. During kinematic analysis x_{cg} and y_{cg} are chosen as dependent variables, so that we can write,

$$\left.\begin{aligned} \delta x_{cg} &= K_{x1}\delta q_1 \\ \delta y_{cg} &= K_{y1}\delta q_1 \end{aligned}\right\} \tag{4.40}$$

where K_{x1} and K_{y1} are the velocity coefficients relating the body lateral and vertical deflections to the body roll. Substituting Equation 4.40 in 4.32, and solving for α and β we get,

$$\left.\begin{aligned} \alpha &= -K_{y1} \\ \beta &= K_{x1} \end{aligned}\right\} \qquad (4.41)$$

4.5.3 Roll Stiffness

Roll moment, M_r, is the sum of all moments about the roll centre. In a vehicle roll plane model, this is the moment due to the vertical and lateral forces. The roll stiffness, $\mathcal{K}_r$, is the rate of change of the roll moment with respect to the roll angle, $\delta\theta$, and reflects the resistance of the vehicle body to roll about the roll centre [88]. Then we have,

$$M_r = Q_1\beta - Q_2\alpha + Q_3 \qquad (4.42)$$

Therefore,

$$\delta M_r = \delta Q_1\beta + Q_1\delta\beta - \delta Q_2\alpha - Q_2\delta\alpha + \delta Q_3 \qquad (4.43)$$

Then the roll stiffness is,

$$\mathcal{K}_r = \frac{\delta M_r}{\delta\theta} = \frac{\delta Q_1}{\delta\theta}\beta + Q_1\frac{\delta\beta}{\delta\theta} - \frac{\delta Q_2}{\delta\theta}\alpha - Q_2\frac{\delta\alpha}{\delta\theta} + \frac{\delta Q_3}{\delta\theta} \qquad (4.44)$$

As in the case of roll centre determination, we look at the case of $\delta Q_2 = \delta Q_3 = 0$, i.e., roll stiffness due to an incremental lateral force. As before, we note that the stiffness will be different when other force components are present. In the above expression, we can substitute for $\frac{\delta\alpha}{\delta\theta}$ and $\frac{\delta\beta}{\delta\theta}$ as follows:

$$\left.\begin{aligned} \alpha = x_p - x_{cg} \quad &\Rightarrow \quad \delta\alpha = -\delta x_{cg} = \delta q_1 \\ \beta = y_p - y_{cg} \quad &\Rightarrow \quad \delta\beta = -\delta y_{cg} = \delta q_2 \end{aligned}\right\} \tag{4.45}$$

This is so because $x_p = y_p = 0$, since the roll centre does not move by definition. Also from the definition of roll centre (Equation 4.32), we have,

$$\delta q_1 = \beta\ \delta\theta, \quad \text{and} \quad \delta q_2 = -\alpha\ \delta\theta \tag{4.46}$$

Hence,

$$\left.\begin{aligned} \frac{\delta\alpha}{\delta\theta} &= -\frac{\delta q_1}{\delta\theta} = -\beta \\ \frac{\delta\beta}{\delta\theta} &= -\frac{\delta q_2}{\delta\theta} = \alpha \end{aligned}\right\} \tag{4.47}$$

Substituting this in Equation 4.44 and setting $\delta Q_2 = \delta Q_3 = 0$ we get,

$$K_r = \frac{\delta Q_1}{\delta\theta}\beta + Q_1\alpha + Q_2\beta \tag{4.48}$$

For the 3 DOF system in Section 4.5.2.1 this becomes,

$$K_r = \Delta\ (K_{22}K_{33} - K_{32}K_{23})\ /\ (K_{21}K_{32} - K_{31}K_{22})^2 + Q_1\alpha + Q_2\beta \tag{4.49}$$

where, α and β are given in Equation 4.36, and Δ is the determinant of the 3x3 stiffness matrix $\mathcal{K}$.

For the 2 DOF system in Section 4.5.2.2 we get,

$$\mathcal{K}_r = \frac{\mathcal{K}_{22}\,(\mathcal{K}_{11}\mathcal{K}_{22} - \mathcal{K}_{21}\mathcal{K}_{12})}{(K_{t1}\mathcal{K}_{22} - K_{t2}\mathcal{K}_{21})^2} + \frac{\mathcal{K}_{21}Q_1 + \mathcal{K}_{22}Q_2}{(K_{t1}\mathcal{K}_{22} - K_{t2}\mathcal{K}_{21})} \qquad (4.50)$$

For the 1 DOF system, with $q_1 = \theta$, the roll stiffness is simply,

$$\mathcal{K}_r = \mathcal{K}_{11} - Q_1 K_{y1} + Q_2 K_{x1} \qquad (4.51)$$

A curiosity in the expressions for the roll stiffness is that the stiffness depends on *external* forces. This seems peculiar since we usually think of *stiffness* as an *intrinsic* property of a system without any regards to the external stimuli. This is indeed the case here also because Q_1 and Q_2 only serve to keep the system under equilibrium, or in other words, to determine the position of the system. Indeed we can express these forces in terms of the intrinsic properties of the system as in Equation 4.20 or 4.24. Therefore roll stiffness, as well as roll centre locations can be determined purely from a kinematic analysis. Once again we see that although the roll centre and roll stiffness are defined with reference to forces, these can be determined without a force analysis, using the method of velocity coefficients.

4.6 SUMMARY

In this Chapter we have presented a computer-aided analysis methodology for vehicle suspension linkages. The approach allows the modelling, analysis and design of various subsystems in a modular fashion as opposed to a scheme where the complete system is studied as one mechanism. Using the velocity coefficients method we propose, a kinematic analysis program can determine precisely and completely, the information required for a separate dynamic analysis. This approach affords the engineer a better understanding of the problems, thereby leading to better and faster solutions.

We have presented the velocity coefficient method of kinematic analysis to determine the equivalent force generation characteristics of linkage suspension. This method helps to represent the suspension system by a few parameters which may be optimized during a dynamic analysis. Kinematic synthesis may then be carried out independently to obtain the actual mechanism which will yield these parameters. To aid this process, expressions for the design sensitivity of velocity coefficients and deflections have also been presented.

The procedure can be used to determine both handling and ride characteristics of a linkage suspension. For ride the suspension system is modelled to determine its vertical force deflection characteristics in terms of velocity coefficients. For handling analysis, the method

yields variations of all kinematic parameters, as well as, the location of roll centre and roll stiffness. We have discussed and clarified several confusing points with regard to the concept of roll centre, and presented a new definition as well as a convenient way of computation based on velocity coefficients.

Chapter 5

APPLICATION OF VELOCITY COEFFICIENT METHOD IN THE ANALYSIS OF VEHICLE SUSPENSION SYSTEMS

5.1 INTRODUCTION

In the previous Chapter, we discussed the method of kinematic analysis and characterization of suspension properties using velocity coefficients. In the present Chapter we discuss the implementation of this theory in a general purpose software package and its application to a number of suspension system analysis problems. The software implementation is presented in the context of other kinematic analysis programs already available as well as the multi-body dynamic analysis program, CAMSYD, presented in Chapter 3. The new software, GENKAD, for *Gen*eral-Purpose *K*inematic *A*nalysis and *D*esign, is a set of programs that allow modelling and analysis of general, multi-loop, multi-degree-of-freedom planar mechanisms for positions, velocity coefficients, force characterization, and kineto-static and roll centre calculations. It features interactive graphics, symbolic equation derivation, and display of animated motion.

The commercial general purpose mechanism programs mentioned in Chapters 1-3, such as ADAMS, DADS and IMP, can carry out dynamic as well as kinematic analyses. Other commercial general purpose programs for kinematic analysis include KINMAC (*Kin*ematics of *Mac*hinery) and STATMAC

(*Statics of Machinery*) developed by B. Paul and associates [108]. There is an inexhaustible supply of special purpose programs for the basic mechanisms such as the four-bar linkage [114-115]. Research and development in this area is by no means static as we witness new programs and techniques appearing every year. Recently presented general purpose kinematic analysis codes include MECHAN [116] and CINPLA [117].

Modelling and analysis techniques that may be applied to a mechanism problem depend on the complexity of the problem. The graphical method which uses drawing instruments and a calculator is still popular in practice because of its simplicity. Fabrikant and Sankar [118] has presented a computer program which emulates the geometrical constructions on a graphical screen to solve the four-bar linkage problem. The solution method must be preprogrammed for particular mechanism types and is therefore not a general purpose scheme. For simple mechanisms of known types, closed-form algebraic solutions are available. These can be easily solved on a calculator or computer, and are mostly restricted to single-loop, single-degree-of-freedom systems, for which algebraic displacement equations can be derived [114-115]. Closed-form solutions can also be derived for many multi-loop mechanisms if they can be assembled as a sequence of simple mechanisms [119]. This concatenation must be such that one would be able to solve for one block after another with the outputs from one forming the inputs for the next. The program MECHAN [116] is based on this modular approach. Kinematically complex

mechanisms which require the simultaneous solution of a set of nonlinear equations cannot be analyzed by MECHAN.

General purpose programs capable of solving multi-loop, multi-degree-of-freedom mechanisms use iterative numerical methods to solve a set of nonlinear algebraic equations. A small set of tightly coupled equations usually result from the use of Lagrangian coordinates and loop-closure techniques [108], while a large number of sparse equations is the result of Cartesian coordinates and joint compatibility equations. IMP, KINMAC use the former approach where vector loop equations are derived for each closed kinematic loop in the mechanism. The method used in KINMAC is explained by Paul in his popular textbook [108]. This is essentially what has been implemented in CINPLA [117]. These programs cannot directly handle open kinematic chains. To analyze such systems, the user must first close all loops using additional links. The general purpose programs ADAMS and DADS derive one vector equation for each joint expressing the constraint imposed by it in terms of the Cartesian coordinates of the two bodies, resulting in a large number of sparse equations. These programs have no difficulty analyzing open or closed chains.

5.2 A NEW SOFTWARE IMPLEMENTATION, *GENKAD*

5.2.1 Scope of the Software

The kinematic analysis programs mentioned earlier are intended for

general machine mechanisms and do not address the special needs of vehicle suspension studies. Besides position analysis, these needs include determination of rate of change of certain kinematic variables with respect to suspension travel (velocity coefficients), characterization of forces, kineto-static analysis and roll centre calculations. Researchers who have used the general purpose mechanism programs such as IMP, ADAMS and DADS [72-82] model their systems as complex mechanisms without reference to such concepts are roll centres, bump-steer etc.. Therefore the results from such dynamic analysis do not yield good insights into system behaviour. We seek to redress this deficiency using the present software, GENKAD.

GENKAD is a comprehensive set of programs for the kinematic, kineto-static, roll centre, and design sensitivity analysis of vehicle suspension systems modelled as planar mechanisms. The analysis can, of course, be applied to any planar mechanism. The mechanism may consist of any number of rigid links interconnected in whatever fashion using revolute and sliding joints. GENKAD automatically generates the equations of motion from a topological description of the system configuration. It can carry out position analysis and determine the velocity coefficients. The velocity coefficients may be used to determine generalized forces at input points as well as reaction forces at link joints. It can also determine the sensitivities of positions and velocity coefficients with respect to any of the system parameters. Using this sensitivity information, the engineer can carry out iterative design modifications to arrive at an improved design. For vehicle

systems, it determines suspension force generation characteristics as functions of the generalized coordinates to be used in dynamic analysis. It can also carry out kineto-static analysis, determine roll centre location and roll stiffness. The post-processing features in GENKAD allow the user to animate the motion of the mechanism, and to obtain graphs and tabular listings of the analysis results.

5.2.2 Usage of GENKAD Package

Figure 5.1 shows schematic of the overall structure of GENKAD package. It consists of the main modules GENMODEL, GENEQN, ANALYSIS, KINETIC, EQUALS, GENPOST, and ANIM. GENMODEL is envisaged to be a graphic pre-processor which will help the analyst to communicate a *schematic* description of the mechanism to the package. It is a sketch pad for modelling and data entry system as in CAMSYD, described in Chapter 3. Its development is presently not complete. Currently, the model description must be supplied in text files to be processed by GENEQN, which generates the system equations in symbolic form as described in Section 5.2.2.2. The equations are derived based only on the topology of the system, and geometric parameters, and Lagrangian coordinates appear as symbolic variables in the equations. Their numerical values are either supplied by the user or computed by the program, as the case may be, during the analysis phase. ANALYSIS is a general module which carries out position and velocity analysis, design sensitivity computations and generates files for animation and general post-processing. KINETIC is for kineto-static and roll centre

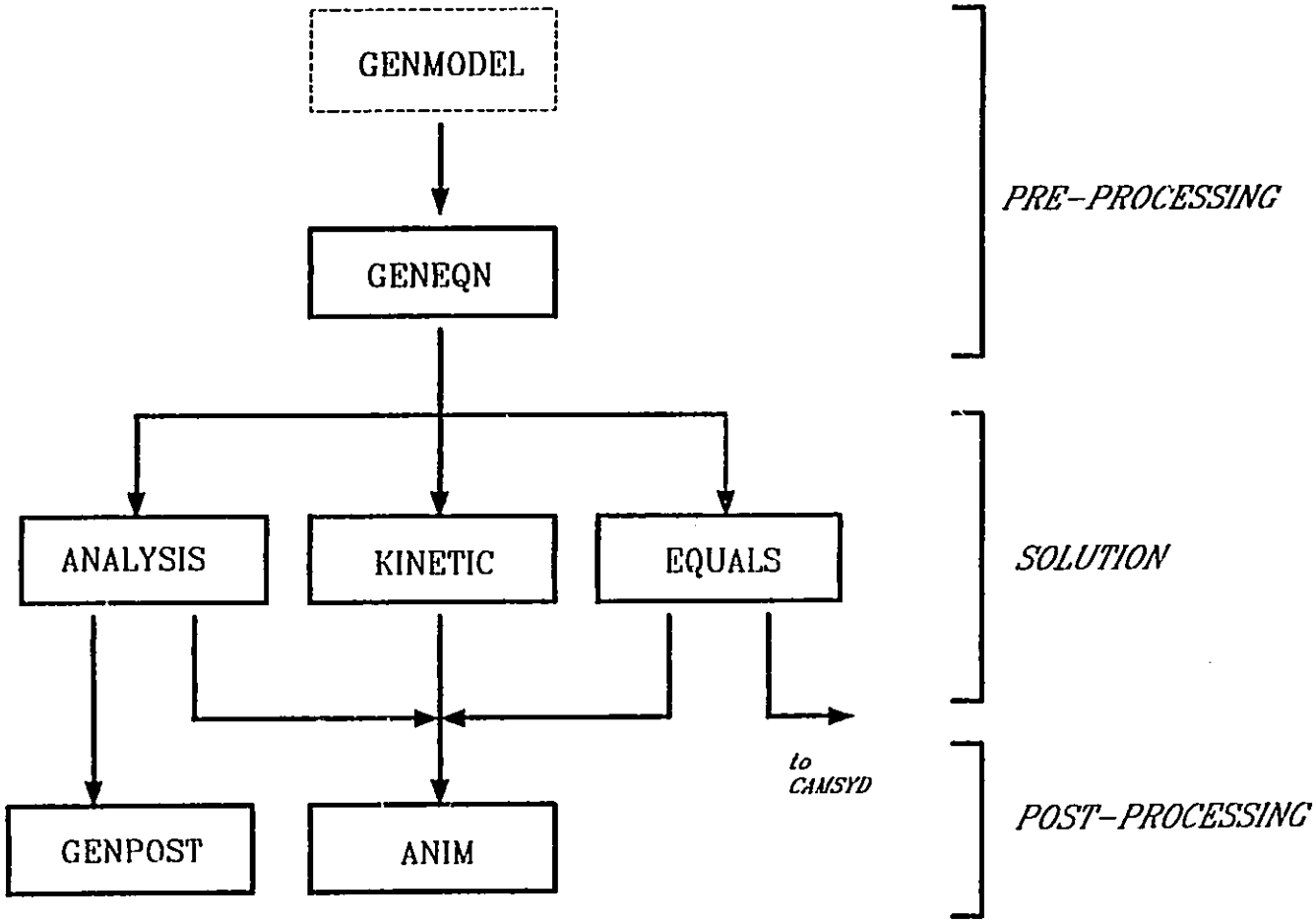

Fig. 5.1: Schematic of the overall structure of GENKAD

calculations of vehicle suspensions, and EQUALS derives the equivalent force generation characteristics to be used in dynamic analysis. ANIM and GENPOST are used for post-processing.

The software package is still in a stage of improvement and integration. However, in its present state it still forms a comprehensive tool for analysis and design of vehicle suspension linkages as we will illustrate in Section 5.3. The package is now operational on Apollo workstations running AEGIS operating system, and on Digital VAXstation workstations under VMS. The software is for the most part device-independent since graphics interface is achieved through libraries developed on both systems, as described in Chapter 3. Since quick turnaround is important for animation, the module ANIM directly uses graphics native to each platform.

5.2.2.1 Modelling of Mechanisms

The mechanism may be any regular, planar mechanism. Regular means that all joints are lower pairs (revolute and slider joints) and that there are no closed kinematic loops containing only slider joints. The mechanism may be made up of any number of links and any number of joints. It can be a simple 4-bar mechanism or a complex multi-loop multi-degree-of-freedom mechanism. Mechanisms with open kinematic chains, such as robots and manipulators, can also be analyzed. In addition to rigid links there can be 'rubber-band' links. These can represent coil springs, actuators or shock-absorbers, as mentioned in

Section 4.2.

The system must be modelled as outlined in Section 4.2. The first step is to model the mechanism as a network of oriented edges. The orientation is an arbitrary direction assigned to an edge. The next step is to identify the kinematic variables and constants of the system, as well a set of *independent* kinematic loops. Edges and variables/constants are identified such that each edge, i, possesses a length, r_i, inclined at an angle, α_i, to the inertial X-axis. Both r and α may have a variable part and a constant part so that we can write,

$$r_i = v_i^r + c_i^r \tag{5.1}$$

$$\alpha_i = v_i^a + c_i^a \tag{5.2}$$

where v_i^r is the variable part of r_i and c_i^r is the constant part of r_i. Similarly v_i^a and c_i^a are the variable and constant parts, respectively, of α_i. The user must supply a table of indices of these constants and variables for each edge, in the *Edge Data Table*. He must also supply, for each edge, a list of edges that make up the path from the origin of XY to the base of that edge (*Ground Path Table*), as well lists of edges that make up individual loops (*Loop Table*). This data structure is essentially the same as that described by Paul for the program KINMAC [108]. However, in our implementation, the equation are derived symbolically and there are more analysis options. We also have the facility of specifying additional constraint equations. An additional

constraint equation specifies either the *x* or *y* coordinate of any point on a link as a new variable. This can be used to model *open* kinematic chains, such as robots, or to denote the motion of specific points on a mechanism, such as the road-tire contact point in Figure 4.4, or to generate coupler curves. Whereas two scalar equations are generated for each loop, a single equation is generated for a node specified in a *Node Data Table*.

5.2.2.2 Equation Derivation

The topological description of the mechanism contained in the tables described above are sufficient to generate the system equations for kinematic analysis. The first stage of equations are the kinematic position constraint equations. These are the loop closure equations and additional constraint equations. These equations are the summation of the lengths of a list of edges in either the *X* or *Y* direction. Each term in this equation has a very simple form. For the *X* direction, it is

$$\pm\ (v_i^r + c_i^r)\ Cos\ (v_i^a + c_i^a) \qquad (5.3)$$

Similarly, for the *Y* direction we have *Sin* instead of *Cos*. These equations are symbolically generated by GENEQN. Derivatives of the position equations with respect to the position variables form the elements of the matrices *A* and *B* (Equation 4.3). Similarly their derivatives with respect to the design variables (constants) form the

matrix C, required in design sensitivity analysis (Equation 4.9). Derivatives of A and B with respect to the design variables are required in sensitivity analysis (Equations 4.16, 4.17). These equations are also made up of term with the simple form of Equation 5.3. GENEQN carries out the symbolic derivations of all these equations as well.

In the equations generated by GENEQN all the system parameters appear as symbols. During analysis, these parameters are given numerical values. Since the equations are derived symbolically, they need to be generated only once for a given topology. The symbolic equations also lead to exact symbolic derivation of velocity coefficients and sensitivity coefficients. This is very desirable since numerical methods for computing derivatives are very error prone.

If the mechanism has n variables and a total of m equations, then it has $(n-m) = l$ degrees of freedom. Therefore l of the variables must be specified as the *degrees of freedom*. The equations are derived such that the user does not have to specify this information at this stage. During analysis, he has the choice of selecting any of the variables as the degrees of freedom.

5.2.2.3 Analysis Options

The equations generated by GENEQN are used by the three solution modules ANALYSIS, KINETIC and EQUALS. ANALYSIS is a general kinematic analysis program and it does not require any further information about

the model except for the numerical values of the constants and initial, approximate values for the variables. Kineto-static and roll centre analysis module, KINETIC, requires additional information such as external forces, and spring stiffness. EQUALS computes the equivalent force generator models of the suspension unit to be used in a separate dynamic analysis of the vehicle system. This program asks for the unstretched lengths of springs.

ANALYSIS module asks the user to identify the required number of variables as degrees of freedom. Analysis is carried out subsequently for a specified range of numerical values for these control variables at constant intervals. At each step position analysis is performed to solve for all the other variables as well as to compute the velocity coefficients of all these variables with respect to the degrees of freedom (Equation 4.5). Optionally, sensitivity analysis can also be performed for selected variables and velocity coefficients with respect to selected design constants and inputs.

Velocity coefficients can be used to compute the generalized forces corresponding to the generalized coordinates (degrees of freedom) as given in Equation 4.20. This can be used to determine effective suspension forces at the input points, or in the case of other mechanisms, driving torques or forces required to keep the mechanism in equilibrium at a given position and given applied loads. Since ANALYSIS performs only kinematic analysis, it does not directly solve this problem. However, the force analysis can be carried out using the

post-processor, GENPOST. This is really a positive aspect of our software implementation. Using the velocity coefficient method we can compute the generalized forces for *any* set of external forces without doing a static force analysis. Commercially available programs require the forces to be numerically specified before the solution. Using the present software, kinematic analysis can be performed independently, and the post-processor GENPOST can be used to compute generalized forces by specifying the external forces, either as numbers, or as functions of the kinematic variables themselves.

Reaction forces in hinges are often required for stress analysis. Since stresses are generally nonlinear with respect to large motions in mechanisms, forces are to be computed as part of kinematic analysis stage and then used in a finite element stress analysis. The discussion above showed how the generalized forces corresponding to the generalized coordinates can be computed using velocity coefficients. Internal reaction forces in hinges can also be computed in a similar manner. This requires the mechanism to be modelled with some additional details. The trick is to create additional *degrees of freedom* corresponding to each of the internal forces we wish to compute. This means that links must be separated at the hinges and connected using edges in the same direction as the force we wish to compute. These edges will have lengths defined as additional variables. Since we are adding new variables without increasing the number of equations, we have more than the initial number of degrees of freedom. The hinge variables are given zero lengths, and a kinematic analysis is performed. The velocity

coefficients corresponding to the hinge variables can now be used to determine the generalized forces corresponding to each of them, which are the internal hinge forces. This method has the advantage that a static analysis need not be carried out for specific values of forces. Any set of applied forces can be specified at the post-processing stage to compute the corresponding reaction forces.

If reaction forces are to be computed the system must be modelled with a large number of extra degrees of freedom. This causes an additional computational burden and unnecessary outputs when only a position analysis is required. This problem is circumvented in ANALYSIS as well as KINETIC and EQUALS by giving the user the choice at run-time to specify any of the degrees of freedom as constants. The numerical solution then treats these variables just like constants with their specified numerical values.

The module KINETIC is based on the flowchart given in Figure 4.8. It determines the static equilibrium position of a planar mechanism, given the external forces acting on it. These forces may be applied along any of the kinematic variables, including the degrees of freedom. Springs are assumed linear with respect to the motion across them, although nonlinearities can easily be included. The program can also determine the roll centres location and roll stiffness as detailed in Section 4.5.

EQUALS is a module in GENKAD used to generate a data file

describing the deflections and the corresponding velocity coefficients of the force generating elements in a suspension. This file is used by the dynamic analysis program, CAMSYD, to compute the equivalent suspension forces. Computationally, EQUALS is a subset of ANALYSIS. The necessary quantities are computed at equally spaced grid points along each of the degrees of freedom. An interesting point that occurs in the program logic is the determination of the order in which these grid points are to be visited. At each point, the iterative solution procedure requires an approximate starting value for the kinematic variables. The user supplies it for an arbitrary position in the beginning. The program uses it as the starting value for the nearest grid point. It then determines an order such that each grid points can be visited from an adjacent point that has already been solved for. This adjacent point supplies the starting values to be used for the Newton-Raphson iteration.

5.2.2.4 Post-Processing

As we saw in the preceding Section, the analysis program computes positions, velocity coefficients and their sensitivities to design and input variables. There is a wide variety of ways in which these can be used depending on the particular application, as seen in Chapter 4. Therefore a general purpose post processor was designed with a functionality similar to that of a calculator, together with file manipulation and plotting capabilities. It can extract any set of results from an analysis output and perform a variety of mathematical

operations on it. Values can be stored and combined with other data sets to perform complex operations. For example, it can be used to compute suspension forces as in Equation 4.24, or wheel rates as in Equation 4.26. It can also be employed to compute possible performance variations due to design changes using the sensitivity analysis results, or to compute reaction forces in joints as described in Section 5.2.2.3.

Another post processing feature is the module ANIM, which displays the animated motion of the mechanism. This program has also been extremely useful in the preprocessing stage to display the initial position in order to visually verify the input data. The mechanism is shown as a collection of lines. The number of lines used can be more than what is required for the purpose of kinematic analysis, so that the visual representation is satisfactory. The animation can be smooth or frame by frame. It can be speeded up or slowed down. The image can be zoomed in and out, panned, and reproduced on a printer. On a color graphics screen, the link colors can be modified.

5.3 APPLICATION TO VEHICLE SUSPENSIONS

We illustrate the use of GENKAD using two types of analysis applied to vehicle suspension systems. These are suspension force analysis using ANALYSIS, and kinetostatic and roll centre calculations using KINETIC. All the results presented in this Section, including graphs and plots of animation sequences, are generated using GENKAD. First we

show how suspension systems are modelled and analyzed to characterize their force generation behaviour. Analysis is performed on four variations of the double wishbone suspension system, and comparisons are made. The program is also applied to a more complex snowmobile suspension system which has two degrees of freedom. Secondly, kineto-static and roll centre calculations are carried out for racing car beam-axle suspension systems. The accuracy of the software implementation is validated by comparing the results obtained from this general purpose program with published data from other sources. The analysis also leads to several original observations.

5.3.1 Suspension Force Analysis

By force analysis we mean the characterization of a suspension's force generating behaviour using velocity coefficients are detailed in Section 4.4.1. Various suspension systems were kinematically modelled as described in Section 5.2.2.2. Corresponding data files were then prepared and passed to GENEQN for equation generation. This is the only major effort required from the user. Once the equations are successfully generated, they are used by subsequent analysis modules to perform a variety of tasks as we will illustrate through examples.

Vehicle ride comfort analysis is often carried out using small deflection linear analysis. Suspensions must however, be designed to perform under a wide range of inputs. In extreme cases it must not

allow metal-to-metal contact and consequent damage. One way to achieve this is by increasing the force generated in the suspension as it reaches the limit of its travel. To this end one may employ a combination of rubber 'bump' stops, 'rising rate' springs, or suspension linkage with a 'rising rate' leverage ratio. Leverage ratio is the term used in racing circles to refer to the negative value of the velocity coefficient which relates the shock-absorber travel to the wheel vertical motion. Suspension springs are designed for a desired static wheel-rate, and it is assumed that the wheel rate is the product of the spring rate and the square of leverage ratio [65,66]. We will show that this expression is not always valid and can lead to gross errors. The correct expressions are derived and design guidelines are established.

5.3.1.1 Racing Car Independent Suspension

As an example, consider the four variations of double wishbone suspension, as shown in Figure 4.6. The four configurations vary only in the manner in which the spring-damper unit is mounted. We assume that they all support the same weight and have identical static ride height. We will examine the effect of the suspension geometry variations on the vertical force generated at the wheel, and also comment on how the springs are to be selected for proper wheel-rate.

The suspensions are kinematically modelled as outlined earlier. For example, Figure 4.4 shows the variables and kinematic loops for the conventional outboard system. A coordinate system is fixed on the

chassis at the lower inboard joint. Only one generalized coordinate, q_1, is sufficient to specify the motion of the suspension system. This is chosen as the vertical motion of the road-wheel contact point. ϕ_1 denotes the deflection of the spring from the unstretched position so that $\phi_1^0 = 0$. The force generation characteristics are completely defined by the variables ϕ_1 and K_{11}. Since we are dealing with a single spring and a single input variable, we will omit the subscript, 1, in the subsequent discussions, and simply refer to ϕ, ϕ^0, q, Q, K and k.

We consider a wheel vertical motion of ±2.5 inches about the static ride position. Figure 5.2 shows some frames from the animated motion generated by ANIM for the inboard rocker configuration for this range of input motion. The shock absorber deflections with respect to the static position are shown in Figure 5.3 for the four configurations. We note that there is no significant variation from one configuration to another.

Figure 5.4 shows the leverage ratio (the negative value of the velocity coefficient relating the shock-absorber motion to the wheel vertical motion) as a function of the wheel vertical motion, q, for all the four configurations. The vertical force at the wheel is (from Equation 4.24),

$$Q = K\,k\,\phi + K^2\,c\,\dot{q} \tag{5.4}$$

Since at static equilibrium ($q = 0$), the spring force must support the

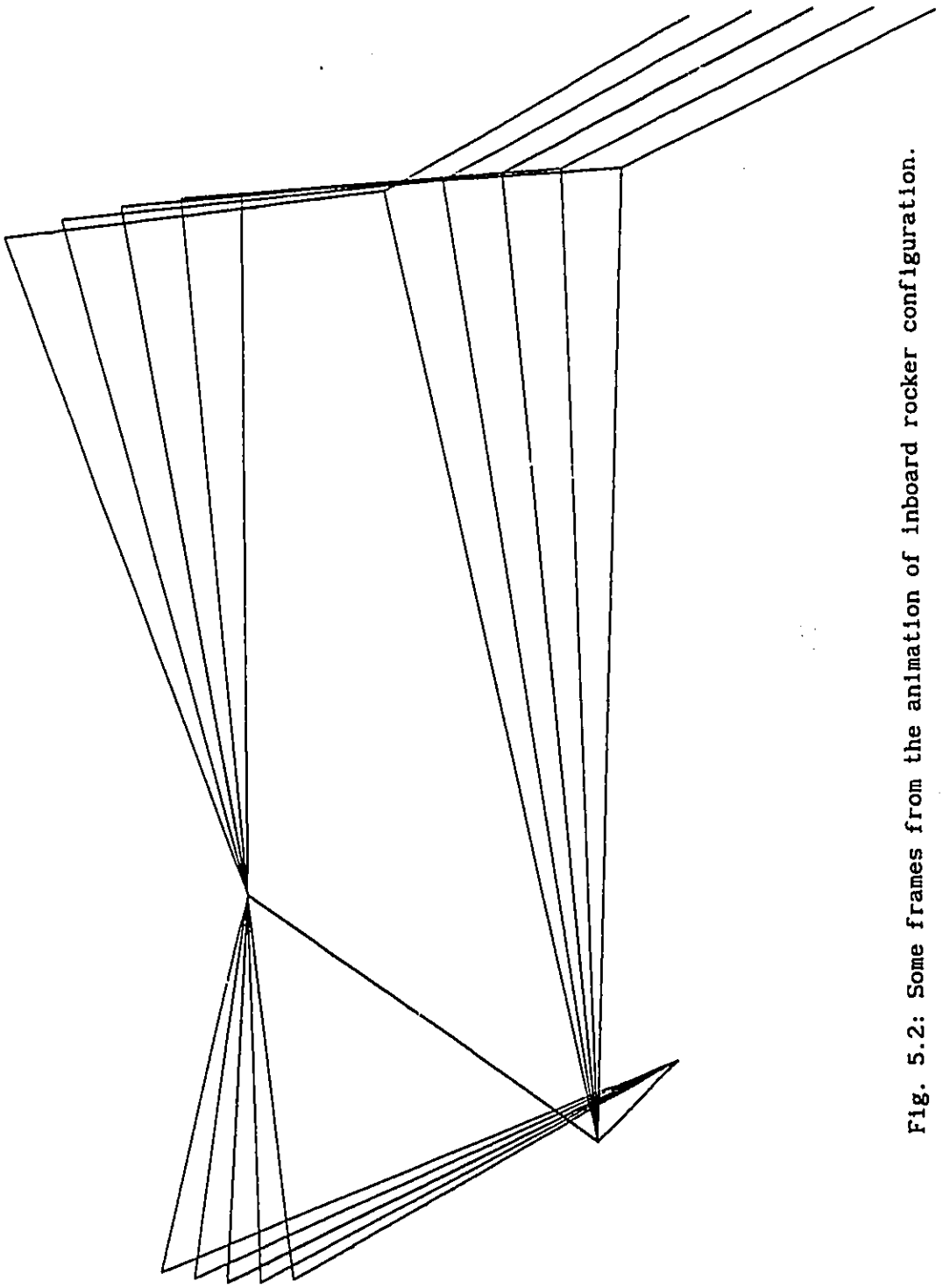

Fig. 5.2: Some frames from the animation of inboard rocker configuration.

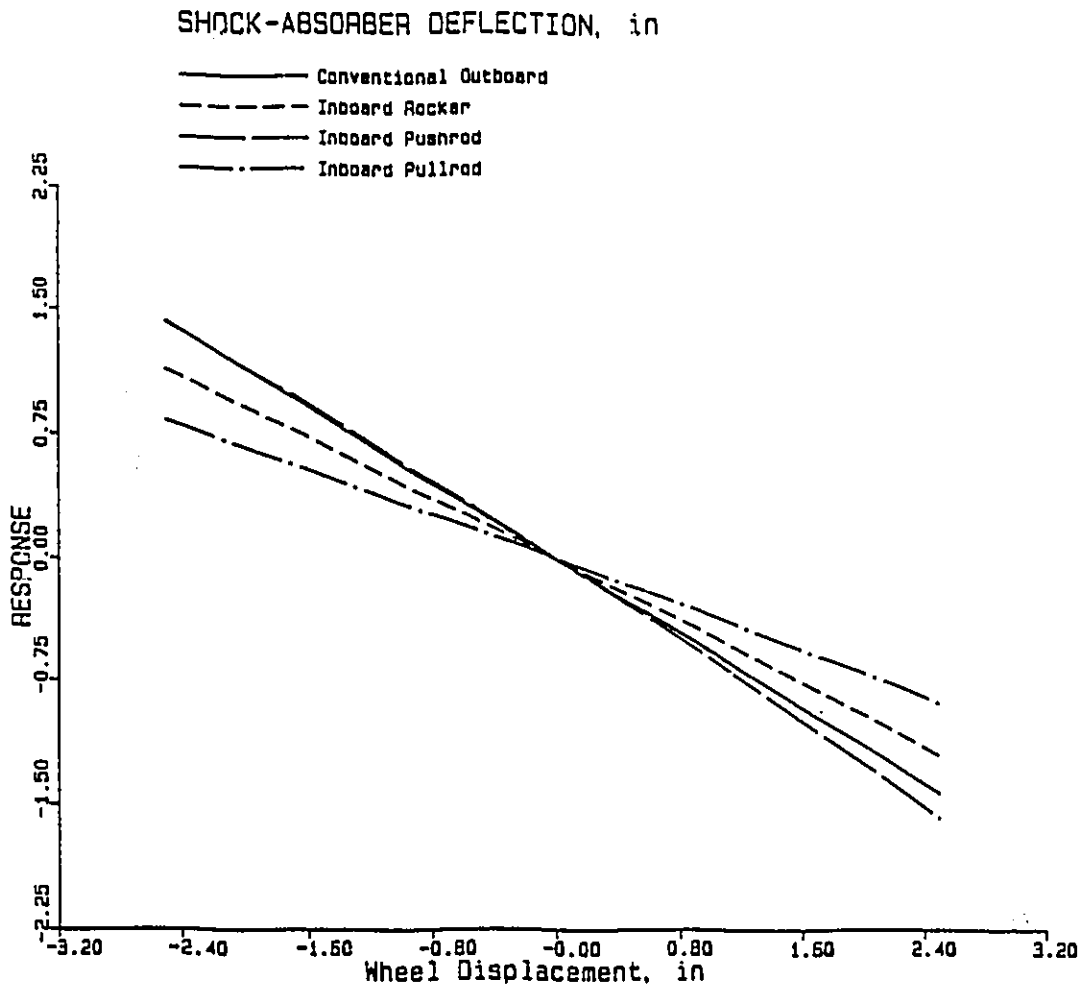

Fig. 5.3: Deflection of spring/shock-absorber vs wheel vertical motion

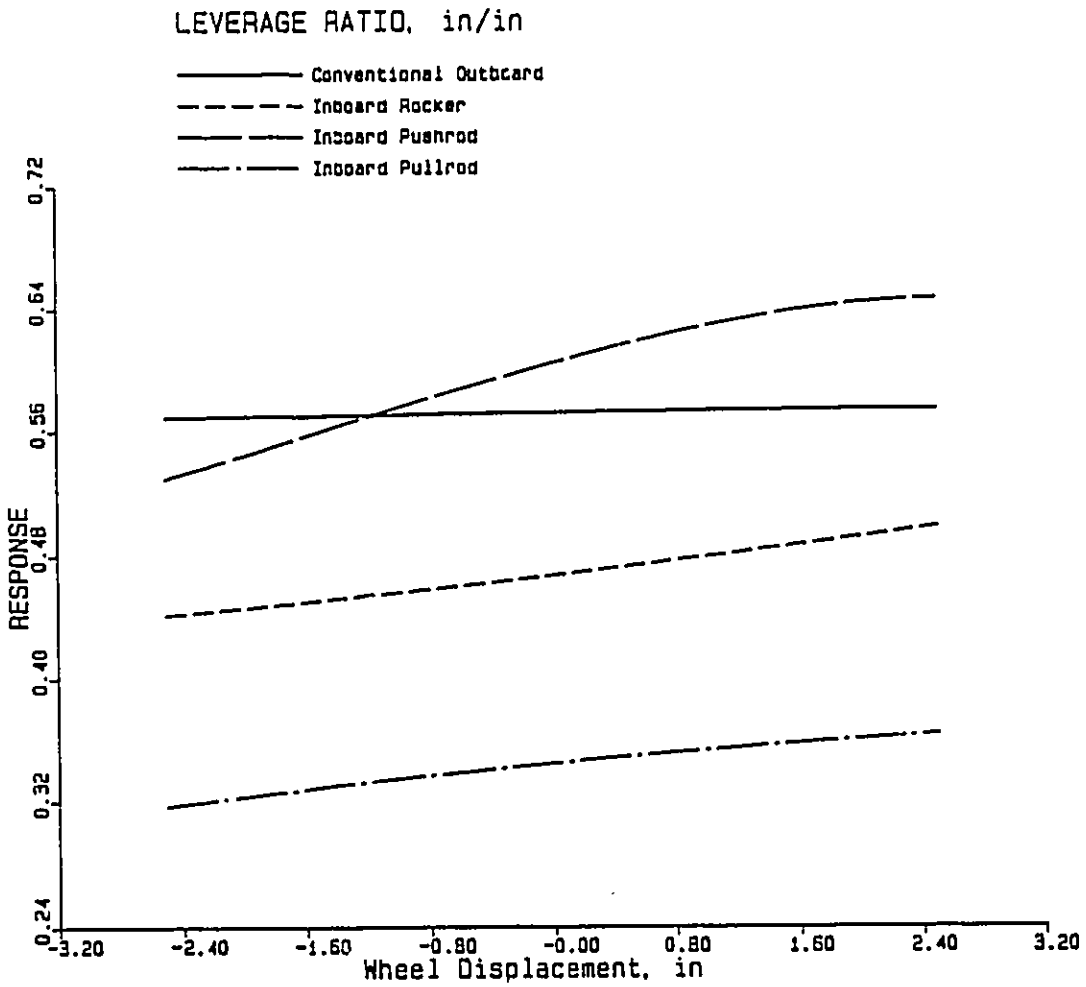

Fig. 5.4: Leverage Ratio vs wheel displacement for four configurations of double wishbone suspension

vehicle weight, W, we have

$$W = kK(0)\ \phi(0) \tag{5.5}$$

Since, in general, the leverage ratios are different for each of the four configurations, k and/or the static spring deflection, $\phi(0)$, may be different for each.

The wheel-rate of the suspension is the effective stiffness at the wheel. This is, from Equation 4.26,

$$\mathcal{K}(q) = k\left(K^2(q) + \phi(q)\ \frac{\partial K}{\partial q}(q)\right) \tag{5.6}$$

Suspension springs are designed for a desired static wheel-rate, $\mathcal{K}(0)$ [65,66]. Once the geometry is designed, K and $\partial K/\partial q$ are known. What we need to find are the spring stiffness k and the static spring deflection, $\phi(0)$. These can be solved for from Equations 5.5 and 5.6, and we get,

$$\phi(0) = \frac{W\ K^2(0)}{\mathcal{K}(0)\ K(0) - W\ \frac{\partial K}{\partial q}(0)} \tag{5.7}$$

and

$$k = \frac{\mathcal{K}(0)}{K^2(0)} - \frac{W\ \frac{\partial K}{\partial q}(0)}{K^3(0)} \tag{5.8}$$

During the design stage if we find either k or $\phi(0)$ to be practically infeasible, we must redesign the linkages. As we noted earlier, this expression for finding the stiffness, k, is different from that given in many books, where the second term in Equation 5.8 is ignored. This factor may be ignored only if the leverage ratio remains constant as the wheel input is varied. Furthermore it is clear from Equation 5.5 and 5.6 that the wheel-rate does not vary proportionately with the spring-rate, since $\phi(0)$ also varies with the spring rate.

The effective stiffness at the wheel is generally a nonlinear function of the wheel displacement. If this stiffness increases with increasing wheel deflection, one has a *rising rate* suspension. Figure 5.5 shows the wheel rate for the four suspension configurations, normalized with respect to the static wheel rate, $K(0)$. Using numerical values for a typical Formula Ford vehicle, we have selected each of the springs so that all the configurations have the same static wheel rate. The conventional outboard system has nearly constant wheel rate because it had a nearly constant leverage ratio as seen in Figure 5.4. The inboard rocker and pull-rod configurations have wheel rates that vary ±15 to ±20 % of the static value. The push-rod configuration, curiously, has a wheel rate that at first increases, and then decreases with wheel travel. This is despite the fact that the leverage ratio is monotonically rising. The reason for this is the second term in Equation 5.6. It must be pointed out that the behaviour shown in Figure 5.4 and 5.5 are true only for the particular geometrical dimensions that we have used and cannot be generalized for each of the suspension

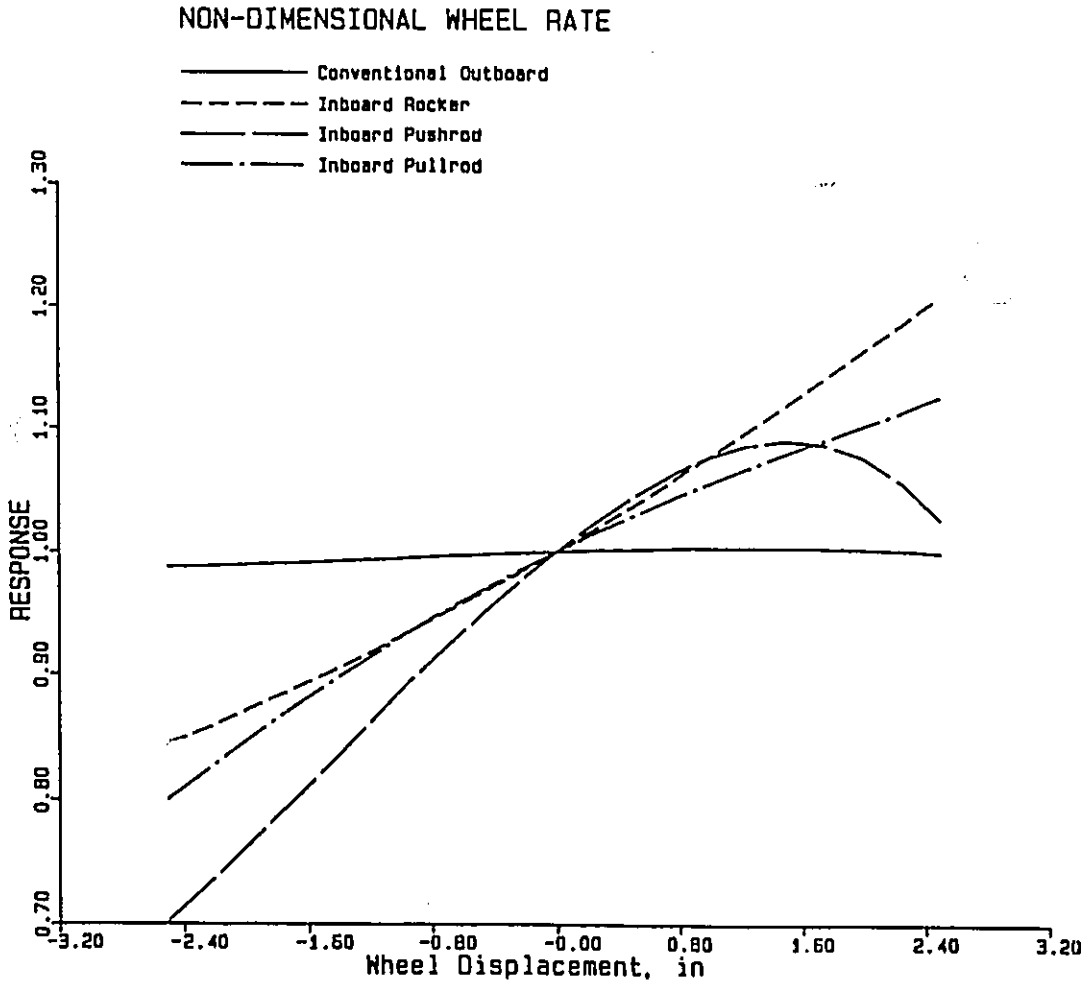

Fig. 5.5: Non-dimensional effective wheel rate for four configurations of double wishbone suspension

categories.

Ignoring the second term in Equation 5.8 in calculating the spring stiffness can lead to substantial errors if the leverage ratio is not nearly constant. In the examples we considered above, this would lead to the springs being over designed by 0.45% for the conventional outboard, 6.33% for the inboard rocker, 12.25% for the inboard pushrod, and 6.85% for the inboard pull-rod configurations. If the leverage ratio decreases with wheel travel the springs would have been under-designed.

From Equation 5.4 we note that while spring force is only position dependent, the damping force depends on *position* and velocity. Figure 5.6 shows a nondimensional parameter representing the effective damper force experienced at the wheel, as a function of the wheel bounce velocity for a sinusoidal input at the wheel, assuming linear viscous damping across the damper unit. For systems that have nearly constant leverage ratio, the damping wheel damping force is also nearly linear. Otherwise, the magnitude of the damping force is strongly position dependent.

5.3.1.2. Snowmobile Rear Suspension

As an example of a more complex suspension system we examine the track suspension geometry of a performance snowmobile. Figure 5.7 shows an overall view of the rear suspension system and Figure 5.8 shows a

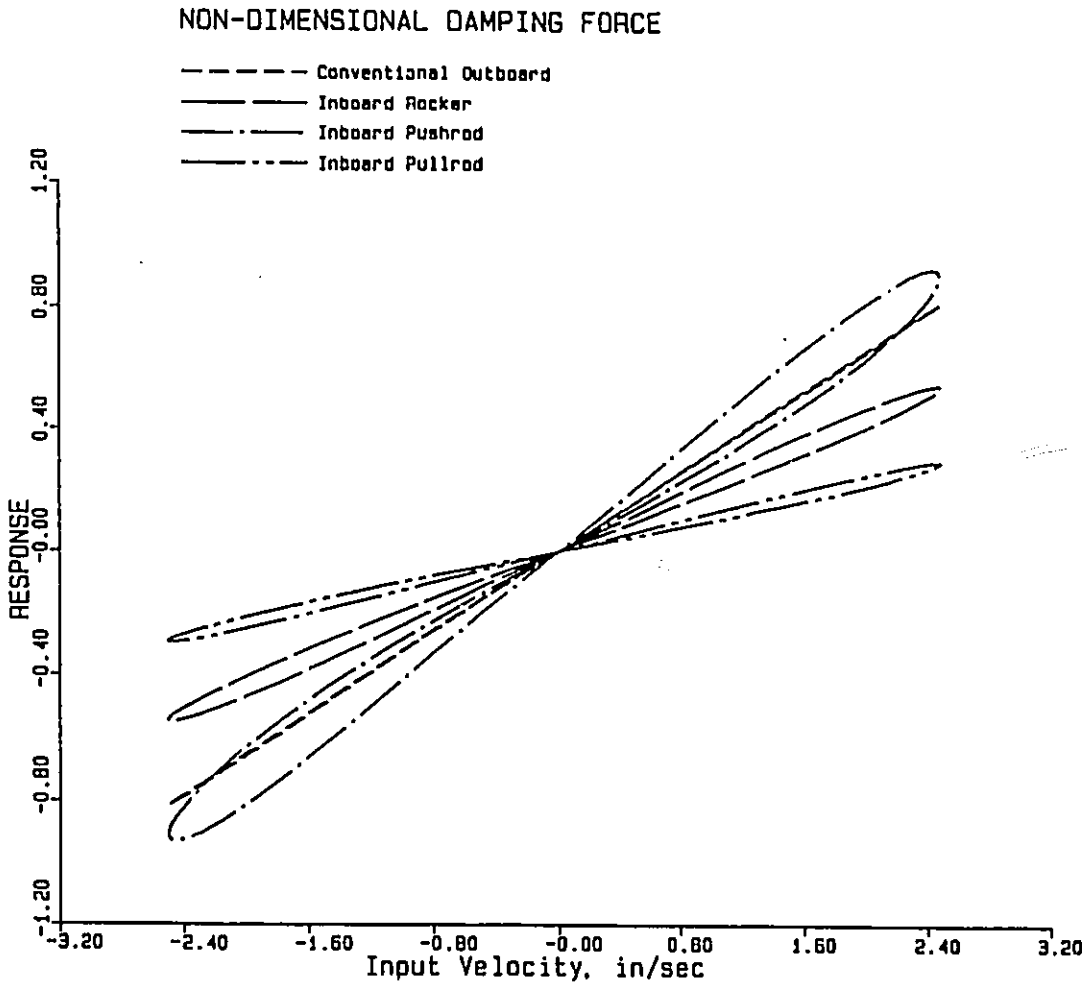

Fig. 5.6: Non-dimensional effective damping force for four configurations of double wishbone suspension

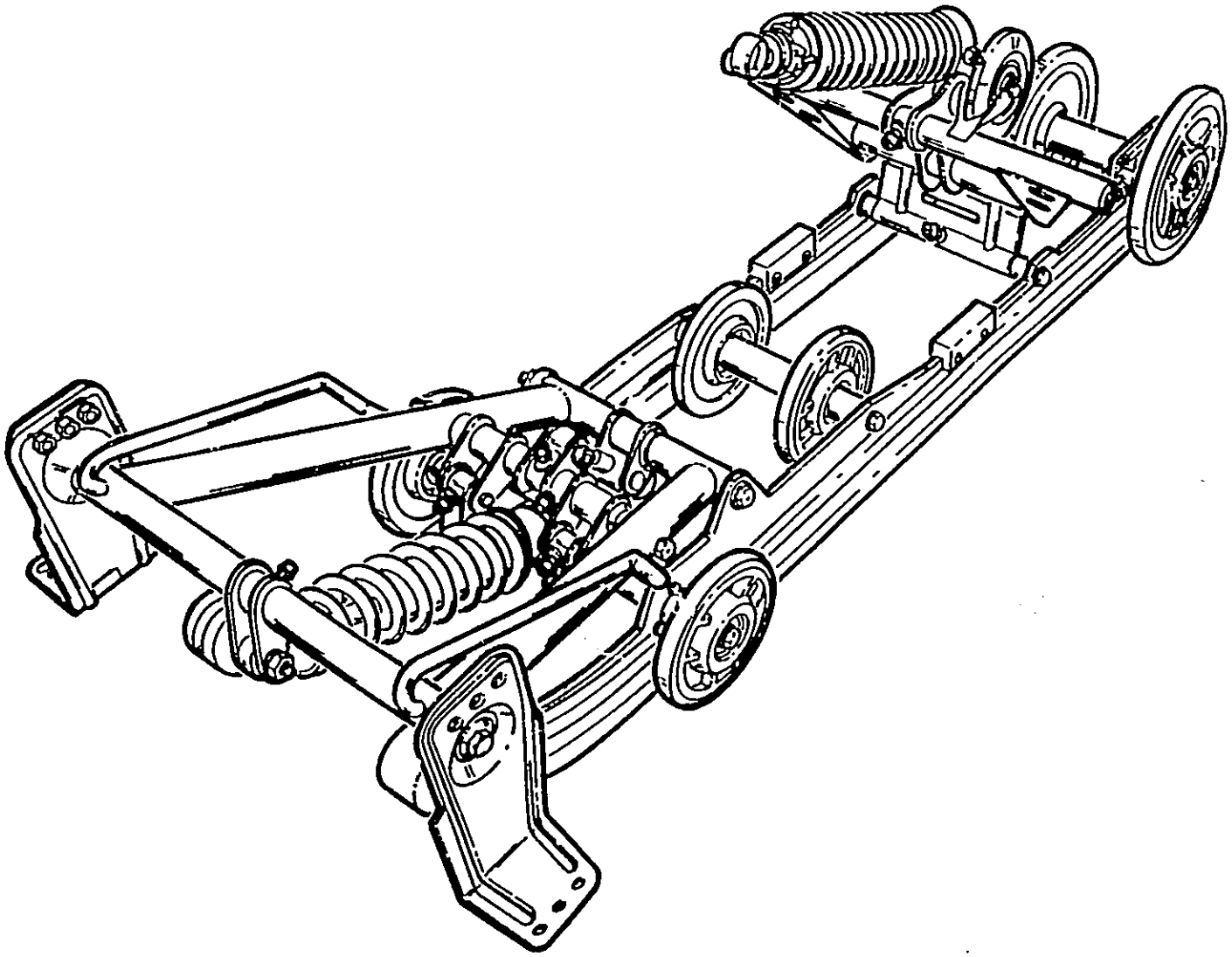

Fig. 5.7: View of a snowmobile rear suspension system

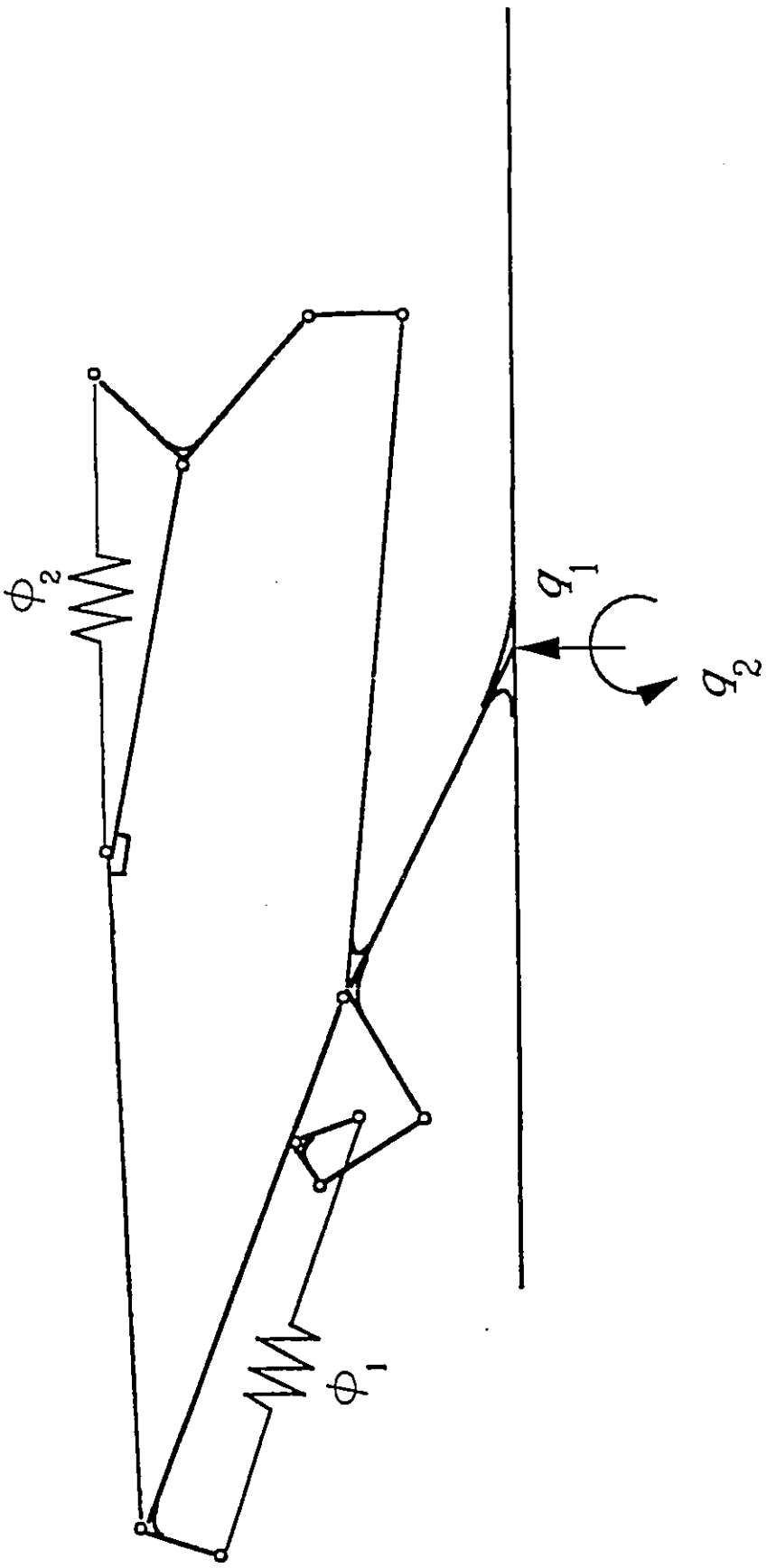

Fig. 5.8: Schematic of snowmobile rear suspension system linkages

schematic of its linkage geometry. At the bottom , the track runs on a pair of rails called *runners*. These are connected to the vehicle body through a linkage arrangement allowing bounce and pitch motions of the runners with respect to the vehicle body. Two sets of shock-absorbers are also incorporated into the linkage assembly in the front and rear of the runners.

Unlike the automobile independent suspension system, this snowmobile suspension has two degrees of relative motion between the base and the vehicle body. These are q_1, the vertical motion of a reference point on the track, and q_2, its rotation. Corresponding to these coordinates are the generalized forces, vertical force Q_1 and a torque Q_2. The deflections across each of the spring-shock-absorber units from their unstretched position are ϕ_1 and ϕ_2 as marked in Figure 5.8. The corresponding forces at these units are F_1 and F_2 respectively. Using the velocity coefficients method, we can express the forces at the base of the suspension unit as:

$$Q_1 = K_{11}F_1 + K_{12}F_2 \tag{5.9}$$

$$Q_2 = K_{12}F_1 + K_{22}F_2 \tag{5.10}$$

where K_{11}, K_{12}, K_{21} and K_{22} are the velocity coefficients relating the deflections of the front and rear shock-absorbers to the two input motions, such that:

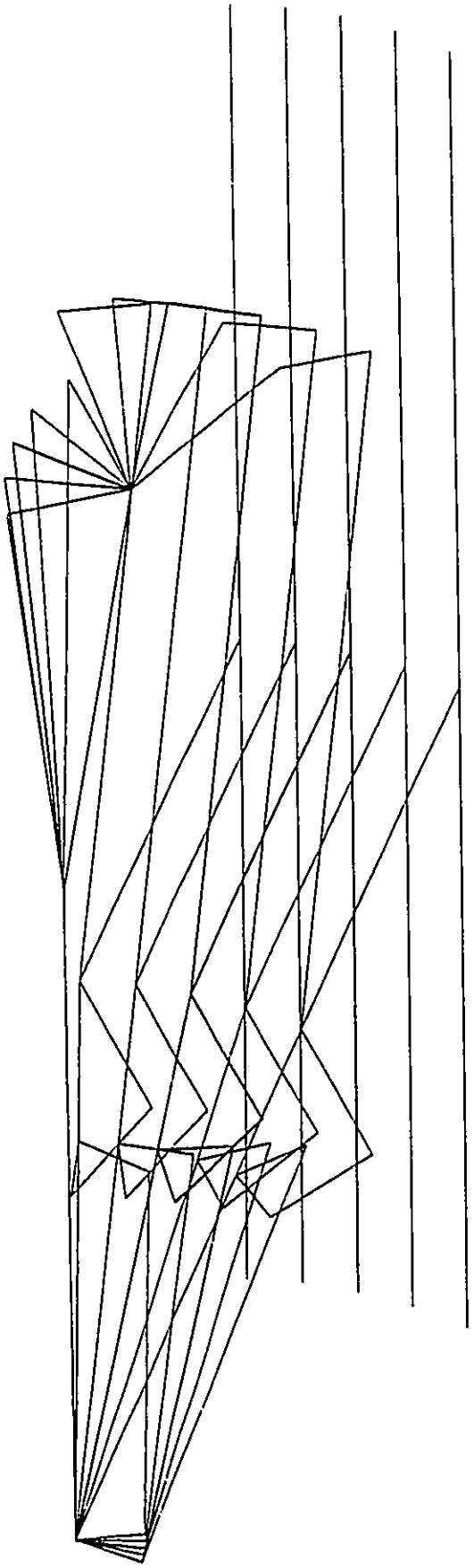

Fig. 5.9: Frames from the animation of rear suspension with track moving up

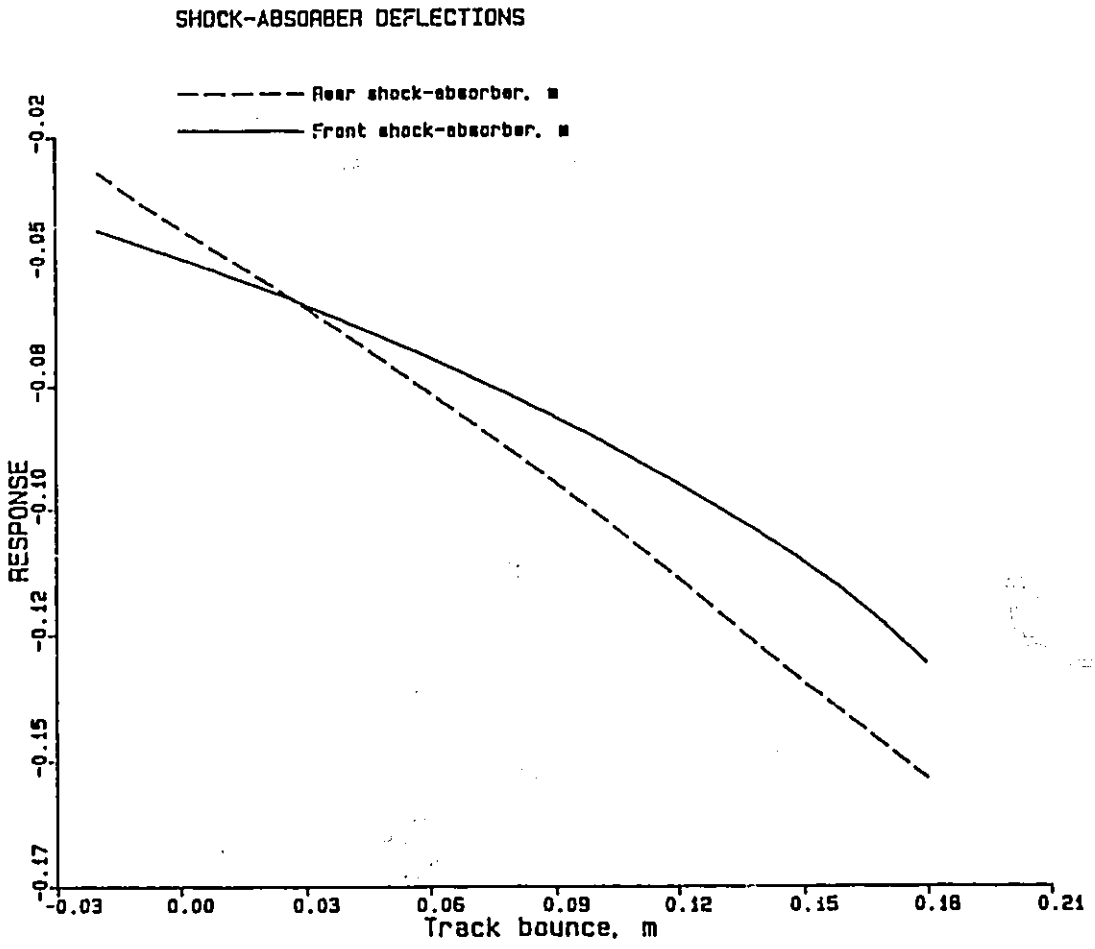

Fig. 5.10: Deflection of springs vs track vertical motion

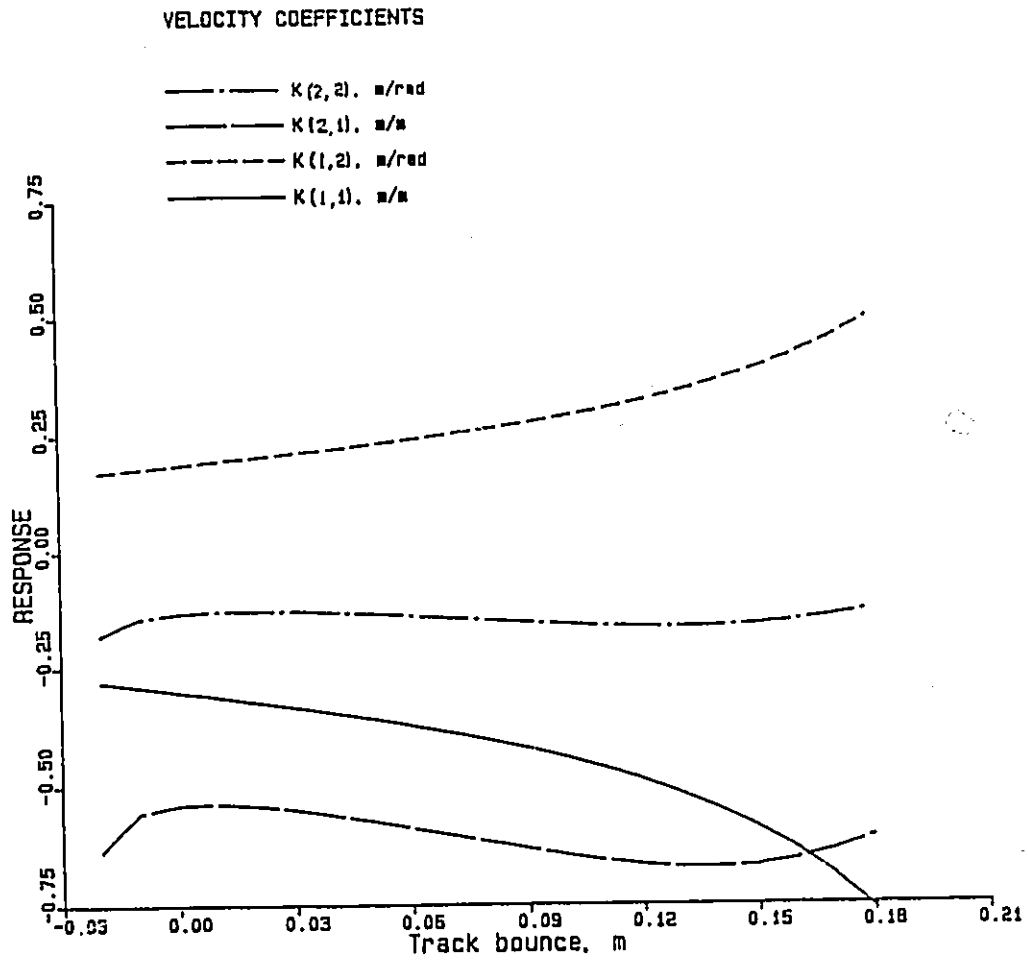

Fig. 5.11: Velocity coefficients of shock-absorbers/spring motion vs track vertical motion

$$\dot{\phi}_1 = K_{11}\dot{q}_1 + K_{12}\dot{q}_2 \tag{5.11}$$

$$\dot{\phi}_2 = K_{21}\dot{q}_2 + K_{22}\dot{q}_2 \tag{5.12}$$

The kinematic analysis was carried out for a complete range of inputs, q_1 and q_2. Figure 5.9 shows the linkage geometry for different positions of the track vertical displacement. These are superimposed frames from animation using the post-processor ANIM. Variables ϕ_1 and ϕ_2, and K_{11}, K_{12}, K_{21} and K_{22}, have also been evaluated for all combinations of the inputs q_1 and q_2. These show that the motion of the linkages cause nonlinear suspension effects. Figure 5.10 shows the deflection of the front and rear springs of the track suspension for the bounce deflection of the track. Figure 5.11 shows the 4 velocity coefficients for the same input motion.

The equivalent force generator model of the linkage suspension was extracted using the module EQUALS. This is used in the dynamic analysis of a pitch plane vehicle model, which includes the front ski suspension as well. The dynamic analysis methodology and results are presented in Chapter 6, along with correlation to test data.

5.3.2 Kineto-Static Analysis and Roll Centres

In Chapter 4, we have presented the theory of suspension roll centre. We have defined the roll centre as the instantaneous centre of rotation for an incremental lateral force applied at the centre of

gravity. It was pointed out that, although the roll centre and roll stiffness are defined with reference to forces, they can be computed from a *kinematic* analysis alone. Using the software package GENKAD, we can compute roll centre location and roll stiffness by post-processing the analysis results from ANALYSIS module. Alternately, the module KINETIC can be used to compute these also, given a set of applied forces on the body. In this Section we use both these methods to determine these quantities for a racing car rear suspension system.

George and Sadler [67] have presented detailed descriptions of modelling, analysis procedures, as well as numerical data and results, for three types of racing car beam-axle suspensions. They derived the equations manually and wrote special-purpose programs for each case. The nonlinear algebraic equations represent a set of equations describing the kinematics, and another set describing the force-equilibrium conditions. For a given set of numerical parameters and applied forces, these equations are solved using the Newton-Raphson scheme. For this calculation they derived the expressions for the partial derivatives of force and displacement equations and programmed them. Numerical results were presented for roll centre locations and roll stiffness of the three types of suspensions acted upon by various combinations of lateral and vertical loads.

We use the suspension models and numerical data given in Ref. [67] to validate the theory presented in Chapter 4, as well as to demonstrate how effortless it is to carry out such analysis using the new general

purpose software, GENKAD. Using this program, the user does not have to write any equations. Furthermore, since the generation of equations and their partial derivatives are carried out symbolically, the numerical solution does not involve the errors associated with finite difference approximation of derivatives. We compare the results obtained from GENKAD with those presented in [67]. It is found that they are identical, except for some minor discrepancies, although the methods employed for the calculations are entirely different. We also present some further analysis and discussions.

5.3.2.1 Racing Car Beam-Axle Suspensions

The three suspensions considered are the Panhard Bar, Watt, and Roberts linkages. These linkage geometries are used for the lateral location of the vehicle body with respect to the axle, and are contained in the transverse vertical plane through the two wheel centers. Figure 5.12 shows these layouts. The figure also shows some additional links used to restrain the fore-aft motions as well. The Panhard bar suspension is very common in passenger cars. The Watt linkage is used in some high performance sports cars. The Roberts linkage, also known as *Jacob's Ladder*, is used only on oval track race cars because of its asymmetrical properties. Although independent suspensions are gaining popularity, beam axle suspensions have certain definite advantages - they are less expensive, rugged and camber-free with vehicle roll.

We consider motions in the roll-plane (i.e., the vertical plane

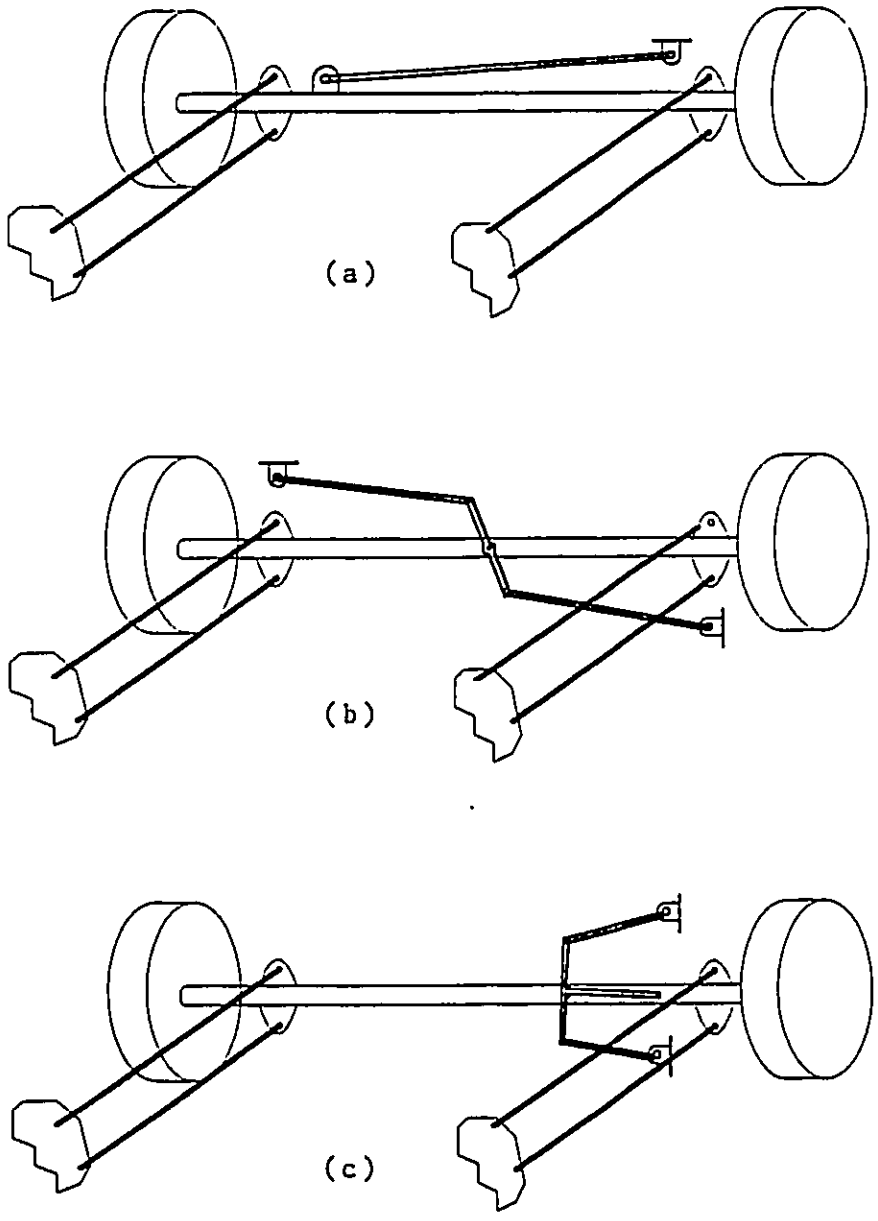

Fig. 5.12: Three types of beam axle suspensions - (a) Panhard bar, (b) Watt linkage, and (c) Roberts linkage

through the wheel centres). In all three configurations, the isolation units are coil spring and damper combinations connected between the axle and the sprung mass on either side. Each of the linkages are such that the sprung mass has two degrees of freedom with respect to the axle. If we consider another degree of freedom for the axle with respect to the the level ground, we have 3 degrees of freedom. In the analysis that follows, we consider that the axle is rigidly connected to the ground so that the motion of the sprung mass alone is studied with its two degrees of freedom. However, it is noted that the models are built with all 3 degrees of freedom. The axle freedom is treated as a constant at the analysis stage to simplify calculations, as mentioned in Section 5.2.2.3. The body has two degrees of freedom and the applicable equations for roll centre calculations are those given in Section 4.5.2.2.

Each of the suspension systems are modelled as described in Section 5.2.2.2. For the sake of convenience all the constants and variables common to the three systems are labelled by the same variables and constants. Figure 5.13 shows the main ones in the case of the Panhard bar suspension system. This model has a total of 9 kinematic variables. The Watt and Roberts linkages have 11 variables each. Our notations for all three configurations, corresponding to those used in Ref. [67] are as follows: $Q_1 = F$, $Q_2 = -W$, and $\phi_7 = \phi$.

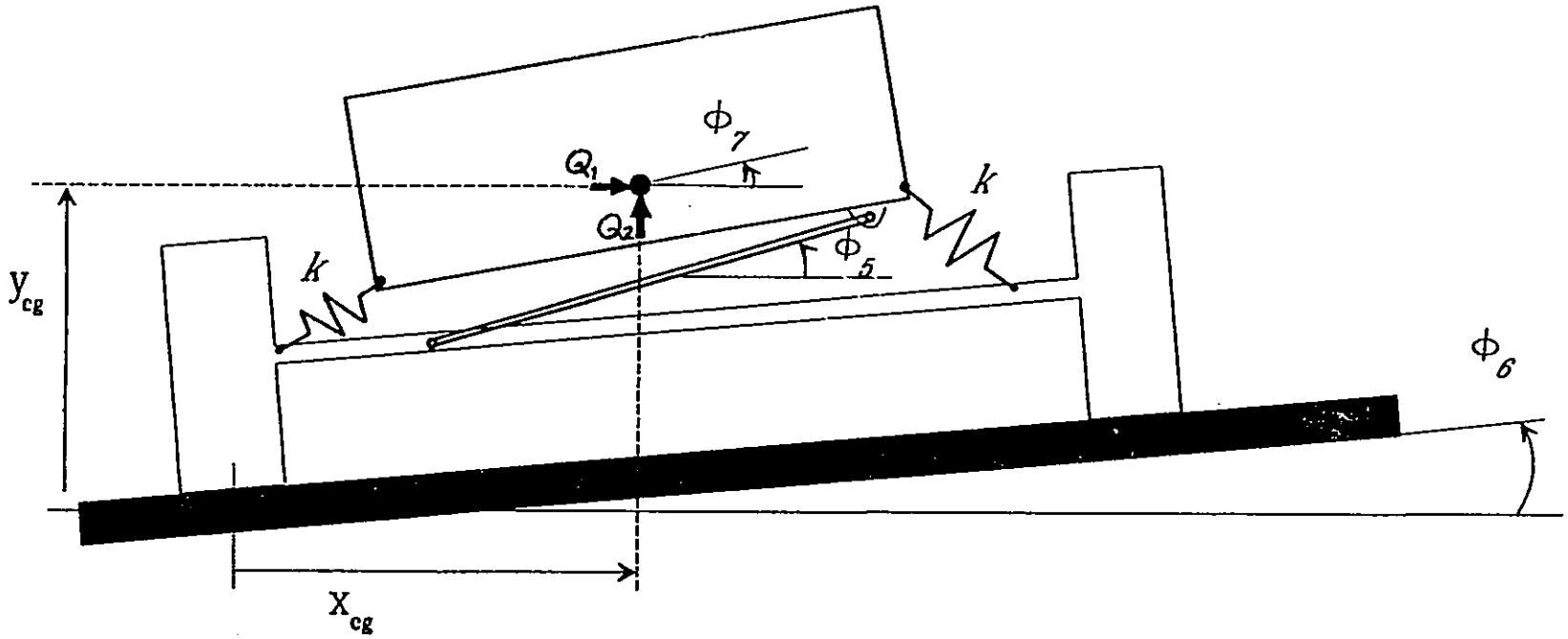

Fig. 5.13: Kinematic model of Panhard bar beam axle suspension

5.3.2.2 Analysis Results and Comparison

The object of the analysis is to duplicate the kineto-static and roll centre calculations reported in Ref [67], in order to demonstrate the capabilities of GENKAD. All the linkage dimensions as well as other numerical parameters are used as given in Ref. [67], after converting to SI units. First of all position analysis was performed in each cases to visually confirm that the modeling is correct by animating the motion using the post-processor module, ANIM. Figure 5.14, 15 and 16 show some frames from the vertical motion of Panhard, Watt and Roberts configurations, respectively. One disadvantage of the Panhard bar systems compared to the other two is clear from these figures - namely the fact that for the Panhard beam, a vertical motion is accompanied by an undesirable lateral motion.

Results presented in Tables I, II and III of Ref. [67] were duplicated using the kineto-static and roll centre calculation module, KINETIC. It was found that for all three suspension configurations the results obtained using the present program is almost identical to those already published. For example, Table 5.1 shows the comparison of results for 9 combinations of loads on the sprung mass for the Panhard bar type suspension. In each case results from Ref. [67] are indicated in parenthesis. Three values for vertical load and three values for horizontal load make up the nine combinations of inputs. Six output quantities are also given in the table. The results are almost identical, often differing only in the third decimal place. The

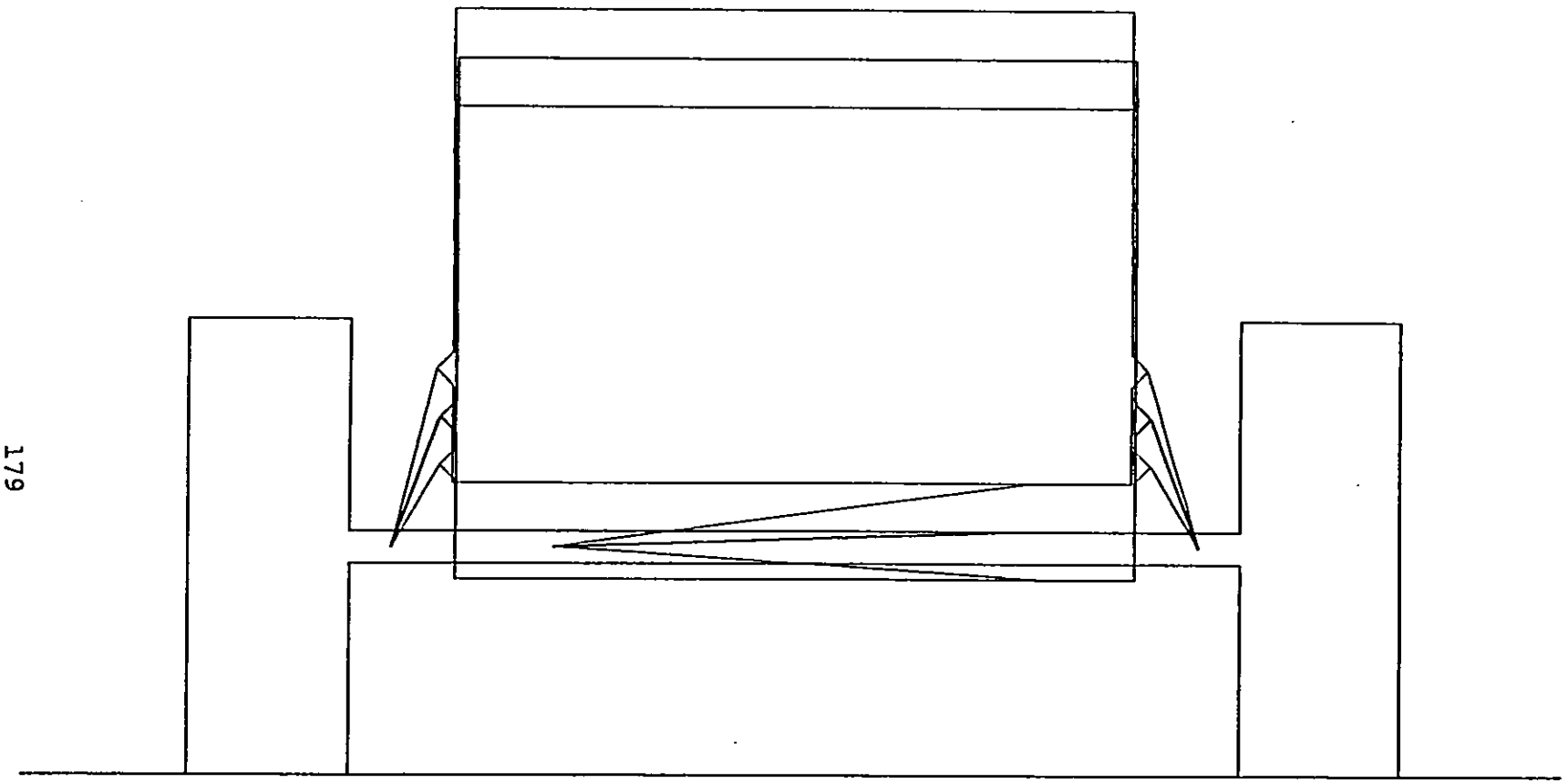

Fig. 5.14: Animation of Panhard bar suspension vertical motion

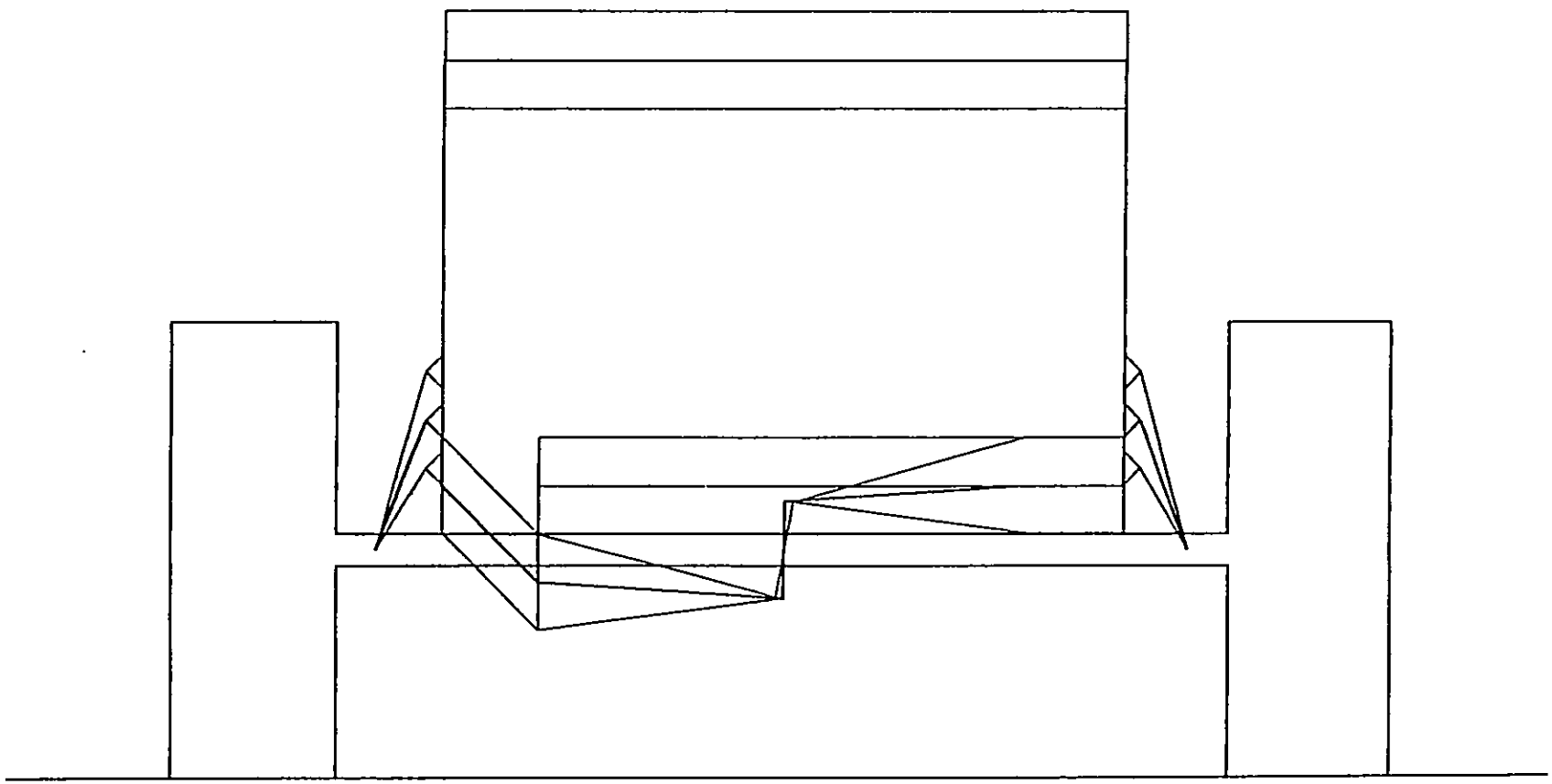

Fig. 5.15: Animation of Watt linkage suspension vertical motion.

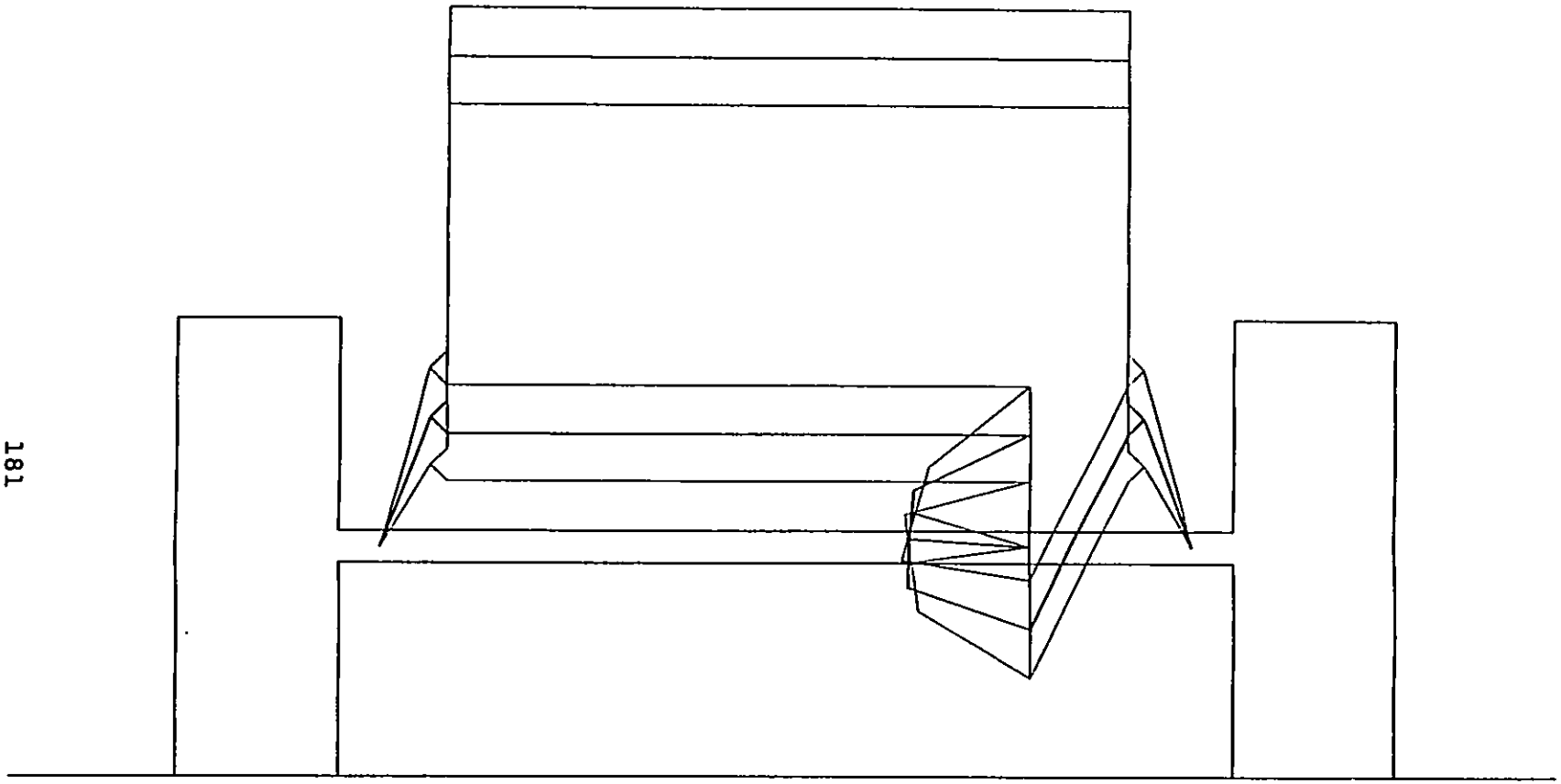

Fig. 5.16: Animation of Roberts linkage suspension vertical motion

Table 5.1 Results for Panhard bar, and comparison with [67]

Q_1 lb	Q_2 lb	*Roll*, θ deg	x_{cg} in	y_{cg} in	x_p in	y_p in	K_r lb.ft/deg
-1000.0	-1650.0	1.9885 (1.99)	32.266 (32.27)	20.473 (20.46)	32.306 (32.34)	13.999 (13.99)	292.18 (292.0)
0.0	-1650.0	-0.0058 (0.00)	32.497 (32.50)	20.498 (20.49)	33.857 (33.88)	13.726 (13.72)	291.97 (291.0)
1000.0	-1650.0	-2.1229 (-2.12)	32.753 (32.75)	20.567 (20.56)	35.015 (35.02)	13.425 (13.42)	291.32 (291.2)
-1000.0	-1500.0	1.9923 (1.99)	32.260 (32.26)	21.042 (21.04)	30.040 (30.07)	14.237 (14.23)	309.66 (309.5)
0.0	-1500.0	0.0001 (0.00)	32.500 (32.50)	21.006 (21.00)	32.484 (32.50)	14.003 (14.00)	300.43 (300.3)
1000.0	-1500.0	-2.1155 (-2.12)	32.764 (32.76)	21.035 (21.03)	34.246 (34.26)	13.713 (13.71)	296.46 (296.4)
-1000.0	-1350.0	2.0027 (2.00)	32.244 (32.24)	21.575 (21.57)	28.232 (28.25)	14.395 (14.39)	325.05 (324.8)
0.0	-1350.0	-0.0041 (0.00)	32.497 (32.50)	21.486 (21.48)	31.265 (31.28)	14.223 (14.22)	308.17 (308.1)
1000.0	-1350.0	-2.1303 (-2.13)	32.770 (32.77)	21.479 (21.47)	33.469 (33.48)	13.961 (13.96)	300.52 (300.5)

Table 5.2: Panhard bar roll centre results for incremental vertical load

Q_1 lb	Q_2 lb	x_p in	y_p in	K_r lb.ft/deg
-1000.0	-1650.0	25880.	11.682	244.76×10^6
0.0	-1650.0	-2273.4	52.431	2.2040×10^6
1000.0	-1650.0	-1139.8	51.983	0.6161×10^6
-1000.0	-1500.0	-3993.9	-61.972	6.4574×10^6
0.0	-1500.0	$233. \times 10^6$	62.201	$24026. \times 10^6$
1000.0	-1500.0	4576.0	-64.033	9.9196×10^6
-1000.0	-1350.0	-2363.7	-73.618	2.4196×10^6
0.0	-1500.0	3615.5	72.188	5.9684×10^6
1000.0	-1500.0	1137.2	11.243	0.6151×10^6

discrepancies can be attributed to numerical round-off errors.

The roll centre location and roll stiffness given in Table 5.1 are for an incremental horizontal load, as described in Section 4.5. In Ref. [67] the roll centre location is computed numerically by applying a small extra lateral force at an equilibrium position, and then applying the perpendicular bisector approach for these closely spaced positions. Roll stiffness is computed by dividing the resulting incremental moment about the roll centre by the incremental rotation. The comparison in Table 5.1 shows that the general purpose program, GENKAD, using the new analytical expressions derived in Section 4.5 gives the same results as the special purpose code developed in Ref. [67].

We defined roll centre with reference to an incremental *horizontal* force. It was pointed out that the distinction is necessary because the roll centre may be different for other force directions. To illustrate this point we present the results from GENKAD for an incremental *vertical* load. Table 5.2 shows these results for the same 9 load combinations used in Table 5.1. The results for the x coordinate of roll centre location show large magnitudes, indicating, as expected, that the body motion is essentially pure bounce. Consequently the roll stiffness is quite high. This means that roll motion is determined almost entirely by lateral loads, as one would expect. The present analysis method and software makes these ideas more explicit and quantifiable.

From Table 5.1 we see that the roll centre location and roll stiffness vary with each load case. This is in contrast to the fact that many studies ignore this effect. It was pointed out in Chapter 4 that roll centre location and roll stiffness are of necessity qualities intrinsic to the system, and do not explicitly depend on the external loads applied on it. In Ref. [67], these quantities were presented in terms of the lateral or vertical loads acting on the body. This presentation is also valid, since the external loads determine the actual spatial coordinates assumed by the body, which in turn determines the roll centre location, roll stiffness etc.. In this Chapter, we show these quantities as functions of two spatial quantities - the vertical bounce of the vehicle CG and its roll angle. The results are essentially the same if one thinks of these plots in terms of vertical and lateral loads, since we have shown that vertical loads cause little roll (Table 5.2).

Figures 5.17 and 18 show the roll centre x and y coordinates for the Panhard bar suspension plotted as a function of the roll angle for 5 different values of vehicle CG bounce. It is clear that the roll centre moves over a wide range in both horizontal and vertical directions. These movements are nearly linear with respect to both the roll angle and bounce. Note that the system has two degrees of freedom and therefore a combination of bounce and roll uniquely determines the position of the system. Similarly the roll stiffness is not a constant as it is often assumed to be. Figure 5.19 shows this plotted for various roll and bounce values. This illustrates the asymmetric nature

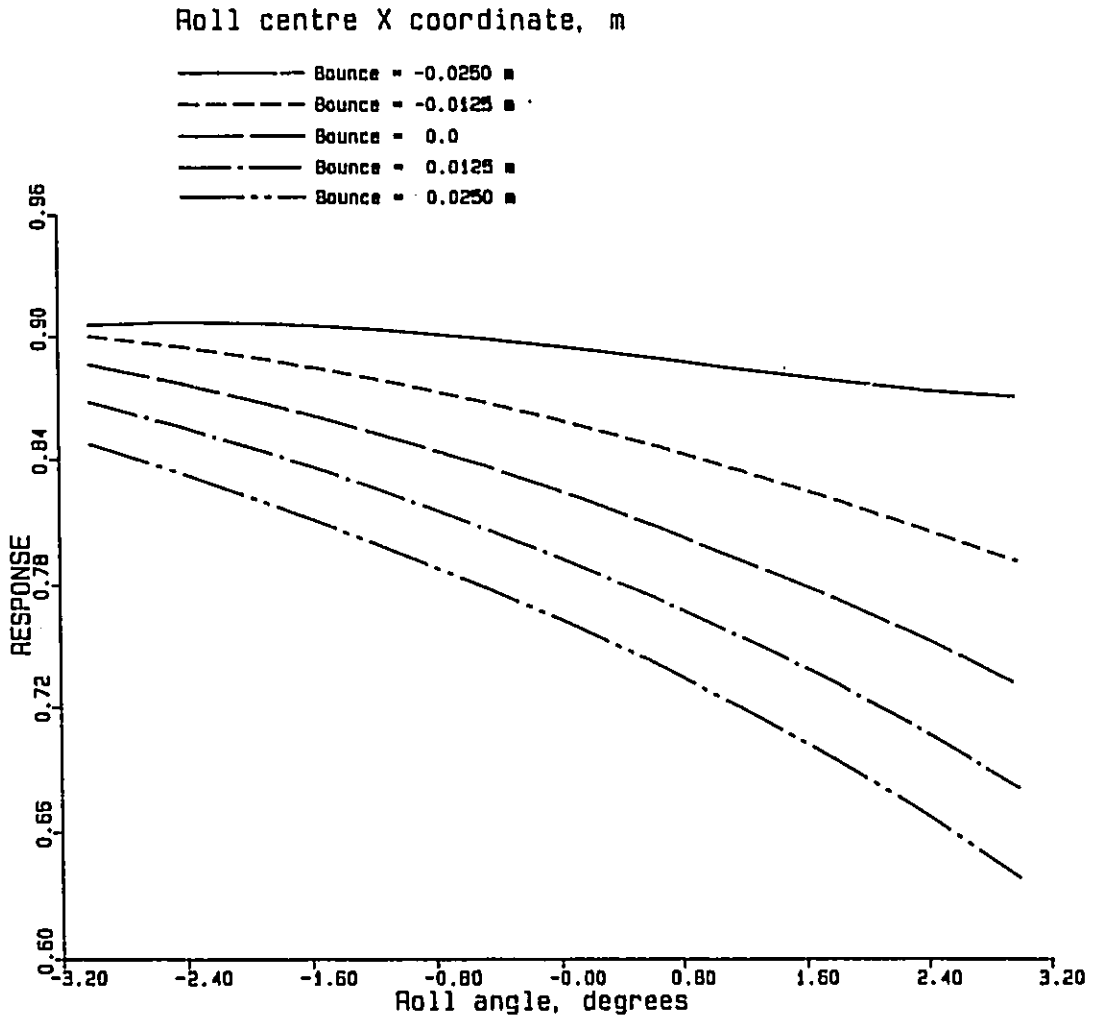

Fig. 5.17: Roll centre x coordinate of Panhard bar suspension

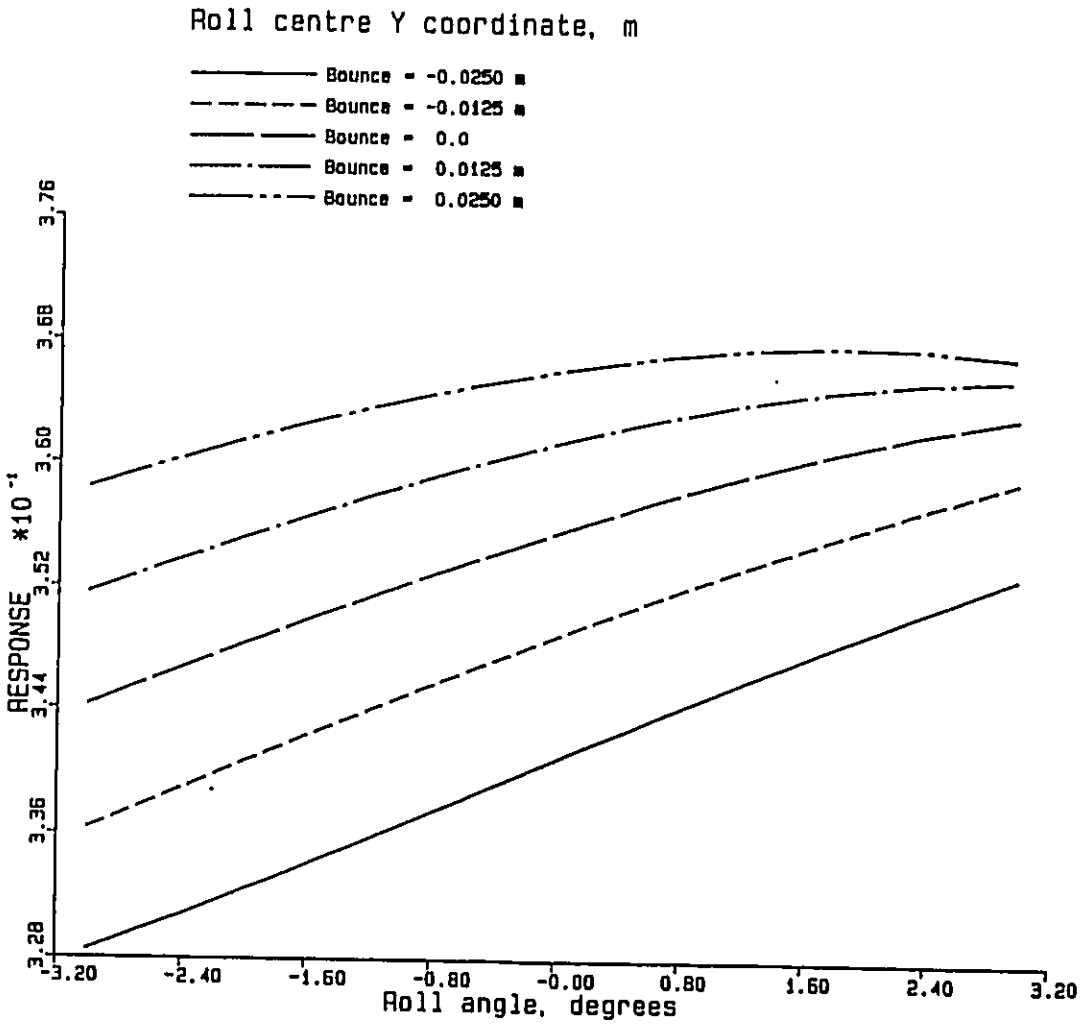

Fig. 5.18: Roll centre y coordinate of Panhard bar suspension

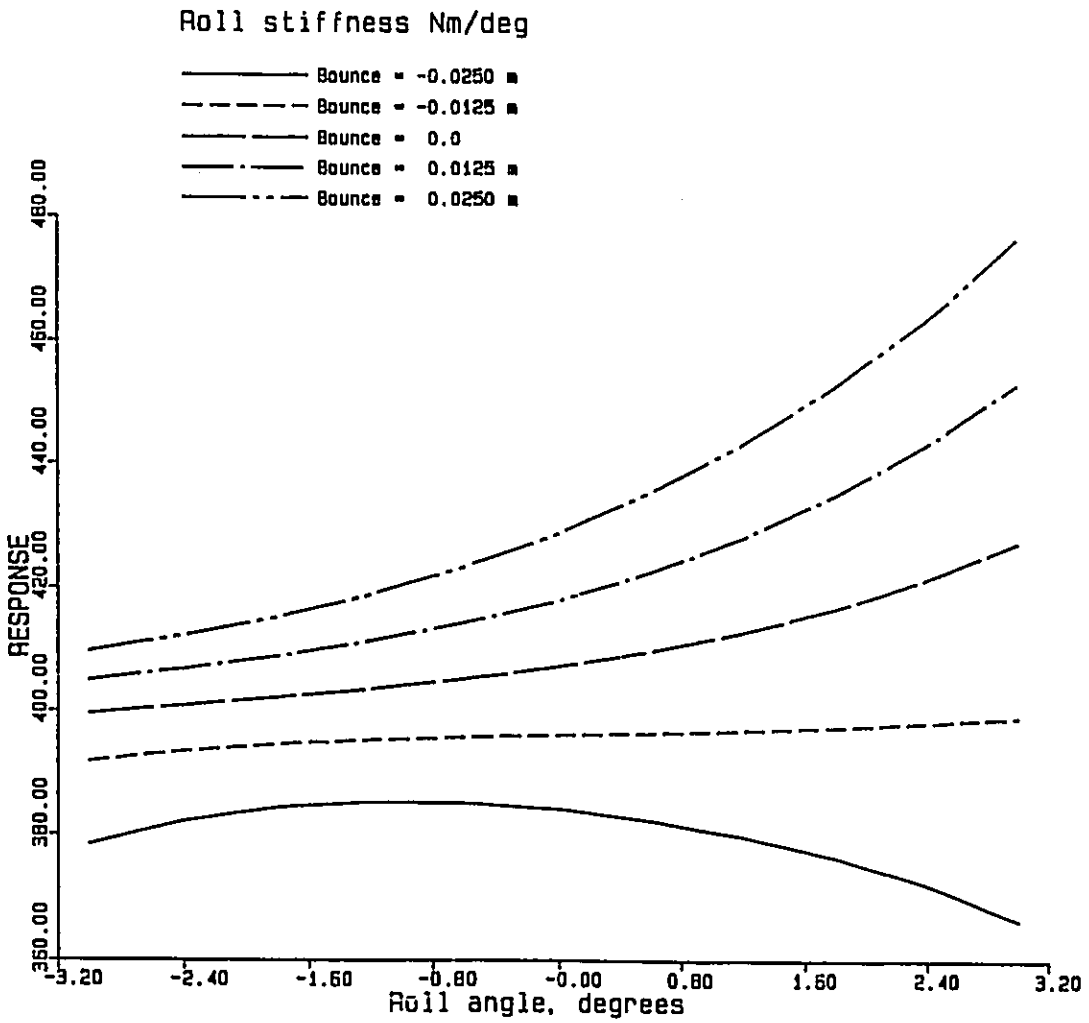

Fig. 5.19: Roll stiffness of Panhard bar suspension

of the Panhard bar suspension roll stiffness. The figure shows that generally speaking, the vehicle has more roll stiffness in left-turns than in right-turns, assuming that Figure 5.12 shows the front view of the vehicle. Furthermore, this difference is more pronounced as the vehicle static ride height is varied. Another point to note is that the roll stiffness decreases as the vehicle CG is lowered. This could imply that the roll natural frequency is significantly altered.

Figures 5.20 and 21 show the roll centre location for the Watt linkage suspension. These indicate that the roll centre location is almost insensitive to the vertical motion of the vehicle CG. The x coordinate varies by a significant amount as the roll angle is changed, and in linear fashion. However, there is very little movement of the roll centre in the vertical direction. Whatever variation is there, is symmetric with respect to the level position (roll = 0). Figure 5.22 shows the roll stiffness. This is also symmetric with respect to the zero roll position. This is the reason why the Watt linkage is often preferred over the Panhard bar.

Figures 5.23, 24 and 25 show the roll centre x and y coordinates, and roll stiffness, respectively, for the Roberts linkage. This is also an asymmetric system, designed for use in an asymmetric environment - oval tracks with right-turns only. Variation of roll centre locations fall between those of the Panhard bar and the Watt linkage. From Figure 5.25 we see that the roll stiffness variation, as a function of roll angle, is more severe than the other two types of suspension. However,

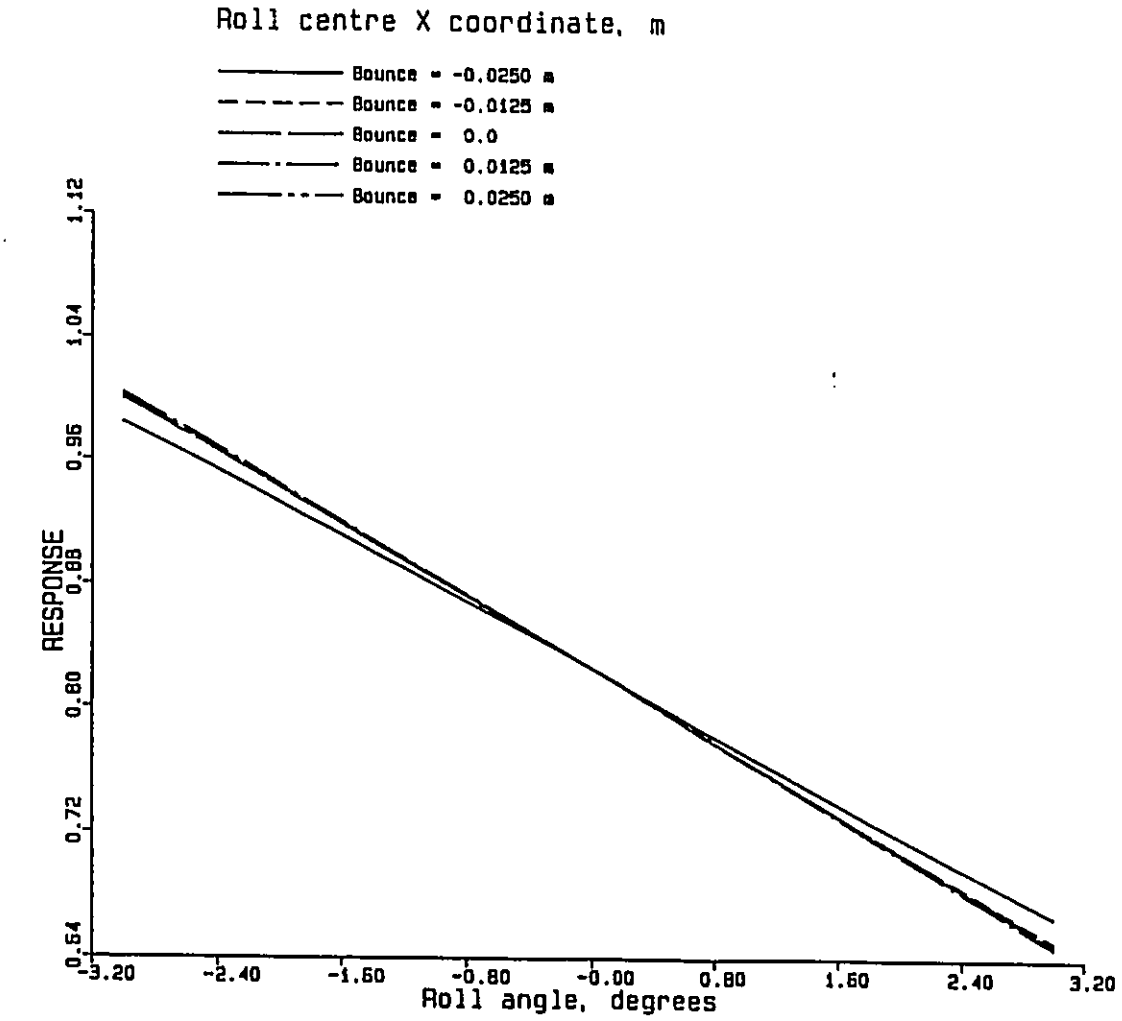

Fig. 5.20: Roll centre x coordinate of Watt linkage suspension

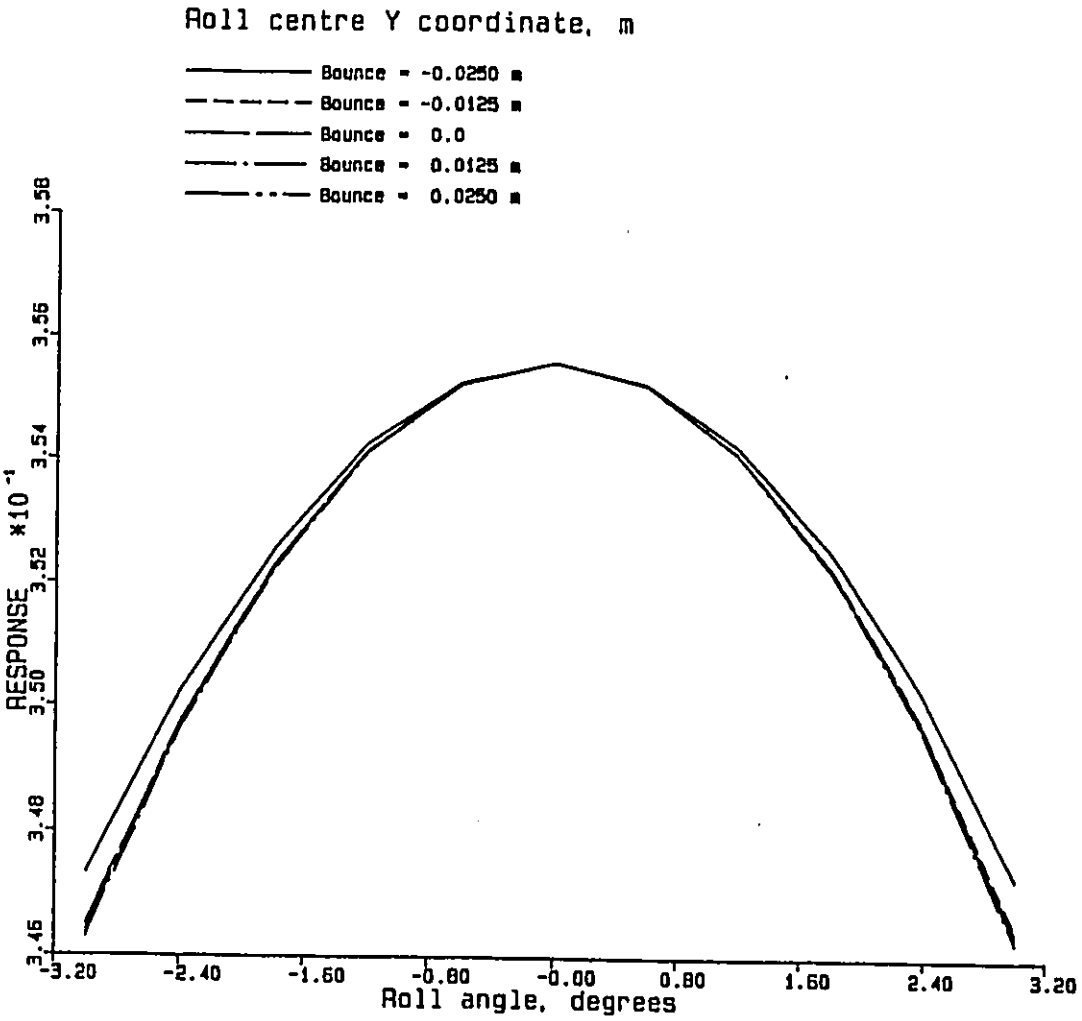

Fig. 5.21: Roll centre y coordinate of Watt linkage suspension

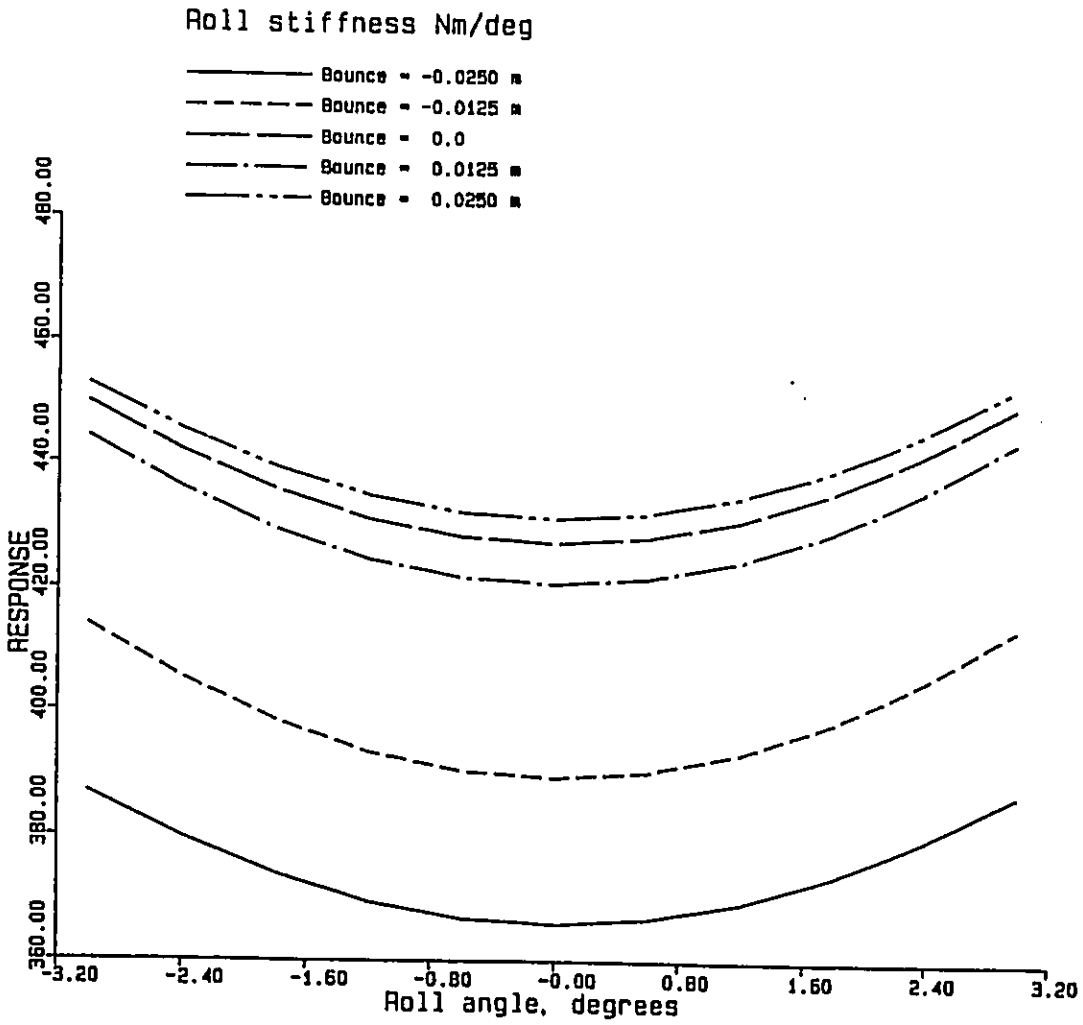

Fig. 5.22: Roll stiffness of Watt linkage suspension

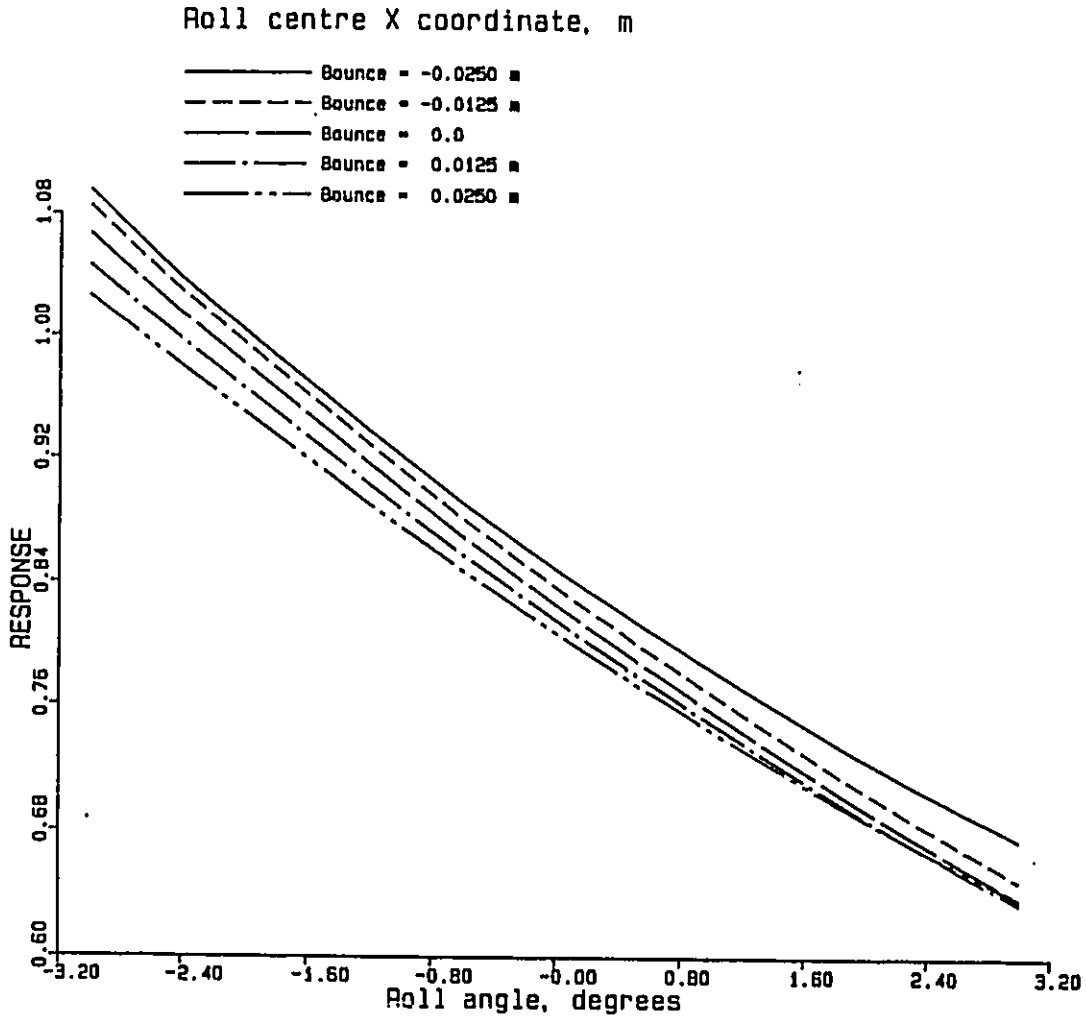

Fig. 5.23: Roll centre x coordinate of Roberts linkage suspension

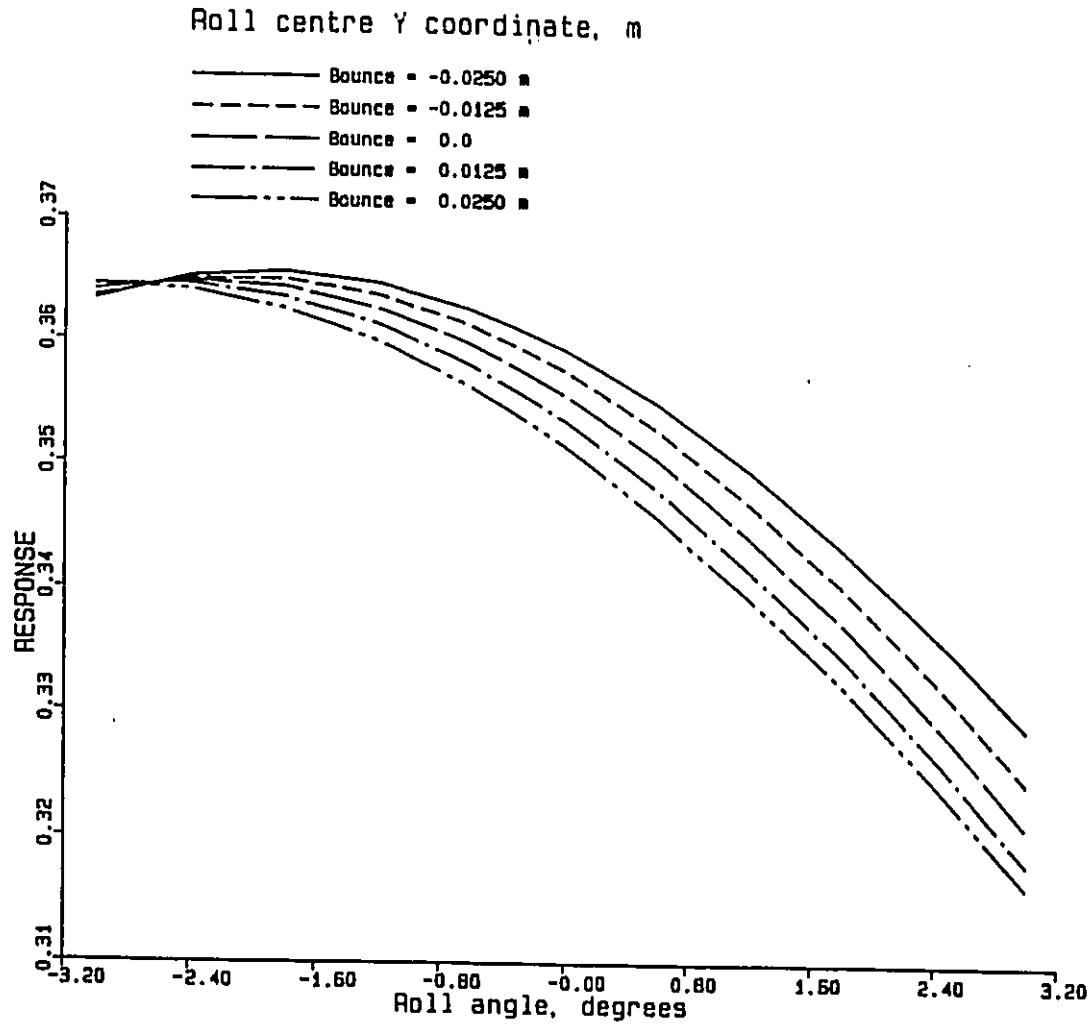

Fig. 5.24: Roll centre y coordinate of Roberts linkage suspension

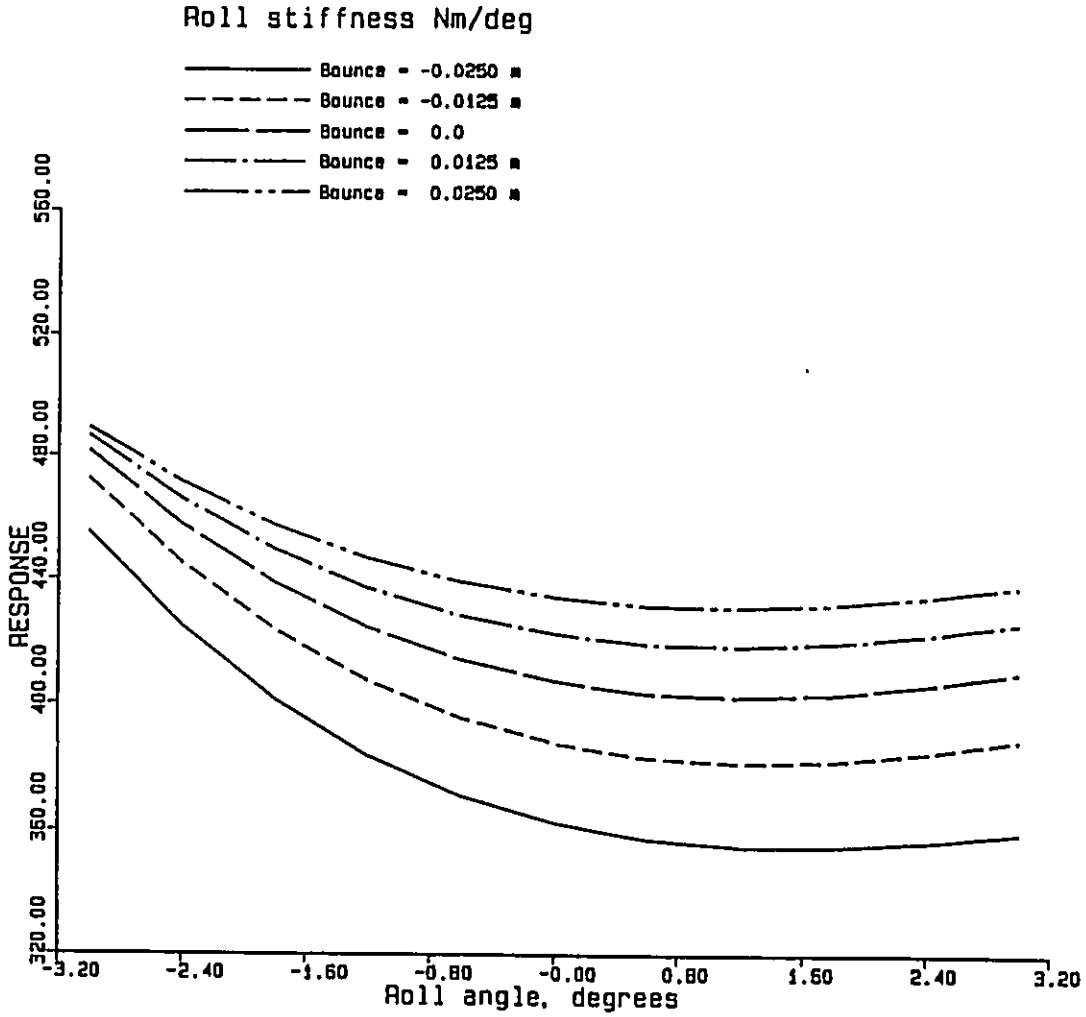

Fig. 5.25: Roll stiffness of Roberts linkage suspension

unlike the Panhard bar, Roberts linkage bounce is not accompanied by lateral shift, as seen in Figure 5.16.

The results obtained for roll centre locations and roll stiffnesses are very nearly the same as those presented in Ref. [67]. The results we have obtained are based on more general theory and obtained using the general purpose program GENKAD. The excellent correlation obtained validates the theoretical development presented in Chapter 4, as well as its numerical implementation in the form of the software packages.

5.4 SUMMARY

In this Chapter we have presented a new general purpose software package for the kinematic and kineto-static analysis of planar mechanisms. It differs from the many other programs already in the market in two important aspects. First, it is based on a *sketchpad* approach to system modelling, so that the model is described to the program in an *abstract*, symbolic form, without any explicit reference to joints or dimensions. This is in contrast to many other programs where more explicit descriptions are required. This program can therefore precompute derivatives and sensitivity coefficients symbolically, leading to accurate computations, as well as fast design evaluations. The second main feature of the software package is that it can be used in many specific vehicle suspension system application, as illustrated in this Chapter. The velocity coefficient method is used to perform

kinematic position analysis, to represent linkage suspensions as equivalent force generators, and for kineto-static and roll centre analyses.

Chapter 6

COMPUTER SIMULATION AND TESTING OF SNOWMOBILE RIDE DYNAMICS

6.1 INTRODUCTION

In the previous chapters we have presented theory and software implementations for the computerized analysis of lumped parameter vehicle systems. In this Chapter, we present the application of these to the modelling and ride dynamic analysis of a snowmobile, and the validation of the analysis results using field testing.

In Chapter 1 we have reviewed some of the vast amount of research conducted in the area of vehicle suspensions [44-47]. Although there are many common aspects between suspension systems of other ground vehicles and snowmobiles, there are many obvious differences as well. Snowmobiles use tracks in the rear, and skis in front. There is very little published material in the area of snowmobile dynamics. Much of the work related to tracked military vehicles [120,121] are not considered to be applicable for two reasons. First, the tracks of these vehicles move under a set of wheels, each of which is suspended on the chassis, while on the snowmobile, the track moves under a rigid rail, which is suspended from the chassis in such a way that it can bounce and pitch. Second, in the other types of tracked vehicles, the track-terrain interaction is considered to be very important [120,121].

Recreational snowmobiles, for the most part, operate on groomed trails of packed snow, and experience has shown that snow compaction is not a major factor. The suspension system of a snowmobile used in racing that we analyze is quite complex, and very different from conventional automobile suspensions and tracked vehicle suspensions.

Newman et al. [122] studied the dynamic behaviour of a snowmobile as it traverses a bumpy terrain using a high speed motion picture camera. A hybrid computer simulation was later conducted to simulate the vehicle behaviour [123]. The snowmobile model used had leaf-spring suspensions for skis and and a bogie-wheel suspension system for the rear track. The performance snowmobile we study has linkage suspensions for the skis and a linkage suspension that couples a rigid rail to the chassis, under which moves the rail. Leaf-spring ski suspensions are still widely used in popular models, while the bogie-wheel suspension has all but disappeared. Hollnager [124] has studied many design aspects of snowmobile ski suspensions. Due to the recreational, off-road operation of snowmobiles, safety has been a very serious concern. This aspect is studied by Kho and Newman [125] and by Smith [126]. A 1973 conference [127] addressed the environmental and social impacts of recreational snowmobile use. As we see from the above review, very little theoretical effort is presently directed at studying the ride dynamics and suspension system design of snowmobiles.

We have discussed earlier how, for ride dynamics studies, a lumped parameter mass-spring-damper model of a vehicle is preferable to a

complex mechanism model of the vehicle-terrain system. Using the methodology described in Chapters 2 and 4, we can model vehicle sprung masses undergoing small angular deflections and suspensions with large deflections. The software, GENKAD, presented in Chapter 5, helps to model any general planar suspension system as equivalent force-generators which can be used in the general purpose dynamic analysis program CAMSYD. We have made use of both these programs in the dynamic analysis of snowmobile ride that is presented in this Chapter. The force-generation characteristics of the suspensions derived from GENKAD are used in a 2-degrees-of-freedom (bounce and pitch) vehicle model, generated in CAMSYD, to evaluate driver ride comfort. The enveloping action of the ski and track are taken into account by using a separate terrain pre-processor. 'Discrete event simulation' is carried out for the vehicle traversing a bump at various speeds. The vehicle is considered to have constant velocity forward motion, with the ski and track always in contact with the ground profile. The main purpose of this study is to analyze the ride dynamics using equivalent force generator models employing the method of velocity coefficients advanced in Chapter 4.

The general methodology we follow is a very traditional one. At the same time it incorporates nonlinearities in springs and dampers, and large deflections in suspension linkages. Figure 6.1 shows the steps involved in the present methodology. We do not model the snowmobile-terrain system as one spatial mechanism, as would be required if some other general purpose mechanism programs were to be used.

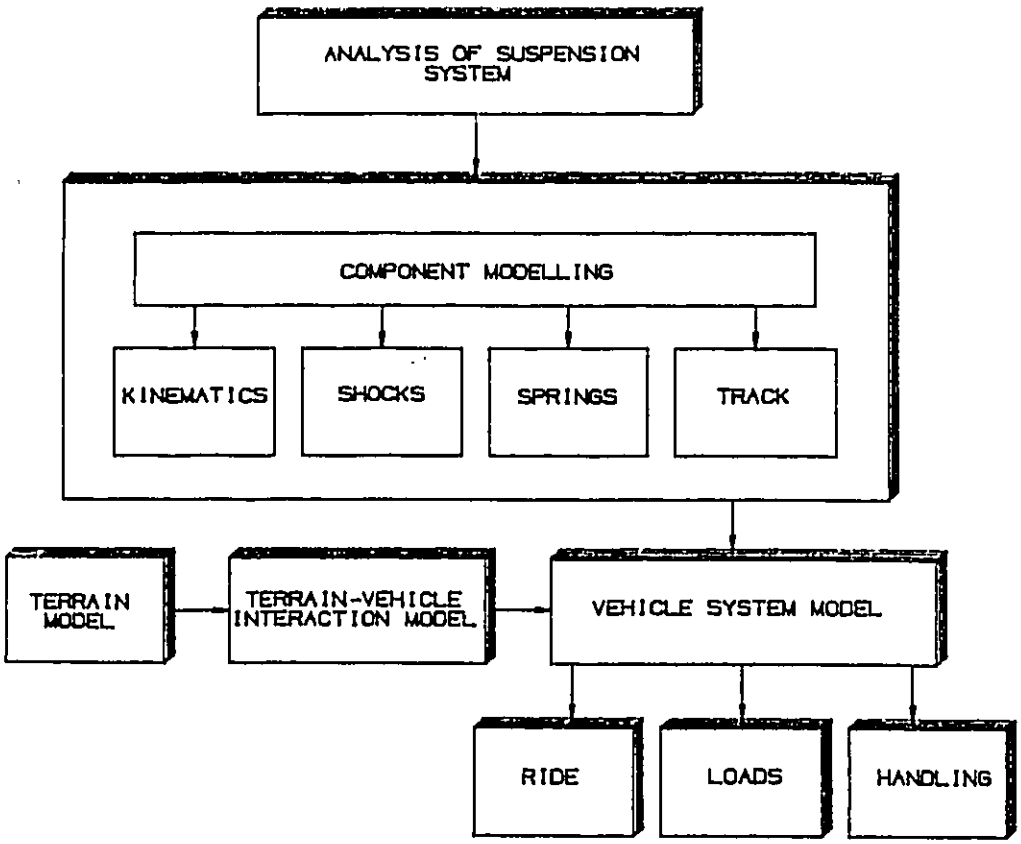

Fig. 6.1: Schematic of analysis methodology

Nonlinear characteristics of spring and shock-absorbers are experimentally determined. Kinematic analysis is performed *a priori*, to characterize the force generation characteristics of the suspensions required for a lumped parameter dynamic analysis to follow. A terrain pre-processor is used to compute the equivalent path to be followed by various points on the ski and track. This modular approach enables one to understand the problems more clearly.

Field testing was conducted at Bombardier Inc. to validate the computer simulation results. We present the analysis of test data and their correlation with simulation results. It is seen that there is a good correlation between the two sets of data, despite the fact that this is the first time such analysis and testing has been attempted. As anticipated, the computer program fails to predict response at higher vehicle speeds because of the vehicle losing contact with the ground profile. However, at lower speeds, predicted values of displacement as well as acceleration time histories are very close to what was recorded in field tests. There are several factors which may have contributed to poor correlation in some instances. It is surmised that the main ones are noise and vehicle speed variation.

6.2 DESCRIPTION OF THE SNOWMOBILE

The snowmobile under study is a Ski-doo FORMULA MACH 1 model manufactured by Bombardier Inc. of Valcourt, Québec. Figure 6.2 shows a

Fig. 6.2: Ski-Doo FORMULA MACH I snowmobile

picture of the vehicle. This is a performance vehicle, operating at high speeds over harsh, snow and ice covered off-road terrains.

The front suspension of this vehicle involves a spatial linkage geometry similar to a *double-A arm* type automobile suspension. The skis are free to pivot in a vertical plane. The vertical motion of the pivot point is transmitted to the shock-absorbers, mounted under the hood in a nearly horizontal attitude. Figure 6.3 shows a view of the front suspension system. A schematic of the linkage configuration is shown in Figure 6.4.

To provide traction in snow, the snowmobile has a track in the rear. At the bottom this runs on a pair of rails called runners. These are connected to the vehicle body through a five-link linkage arrangement allowing bounce and pitch motions of the runners with respect to the vehicle body. Two sets of shock-absorbers are also incorporated into the linkage assembly in the front and rear of the runners. A view of the rear suspension system, as well as schematic of the linkage arrangement were shown in Figures 5.7 and 5.8.

6.3 MATHEMATICAL MODELLING AND COMPUTER SIMULATION

The modelling and analysis are carried out in two phases. In phase 1, the various components such as shock-absorbers, springs, and suspension linkage arrangements are modelled and studied separately. In

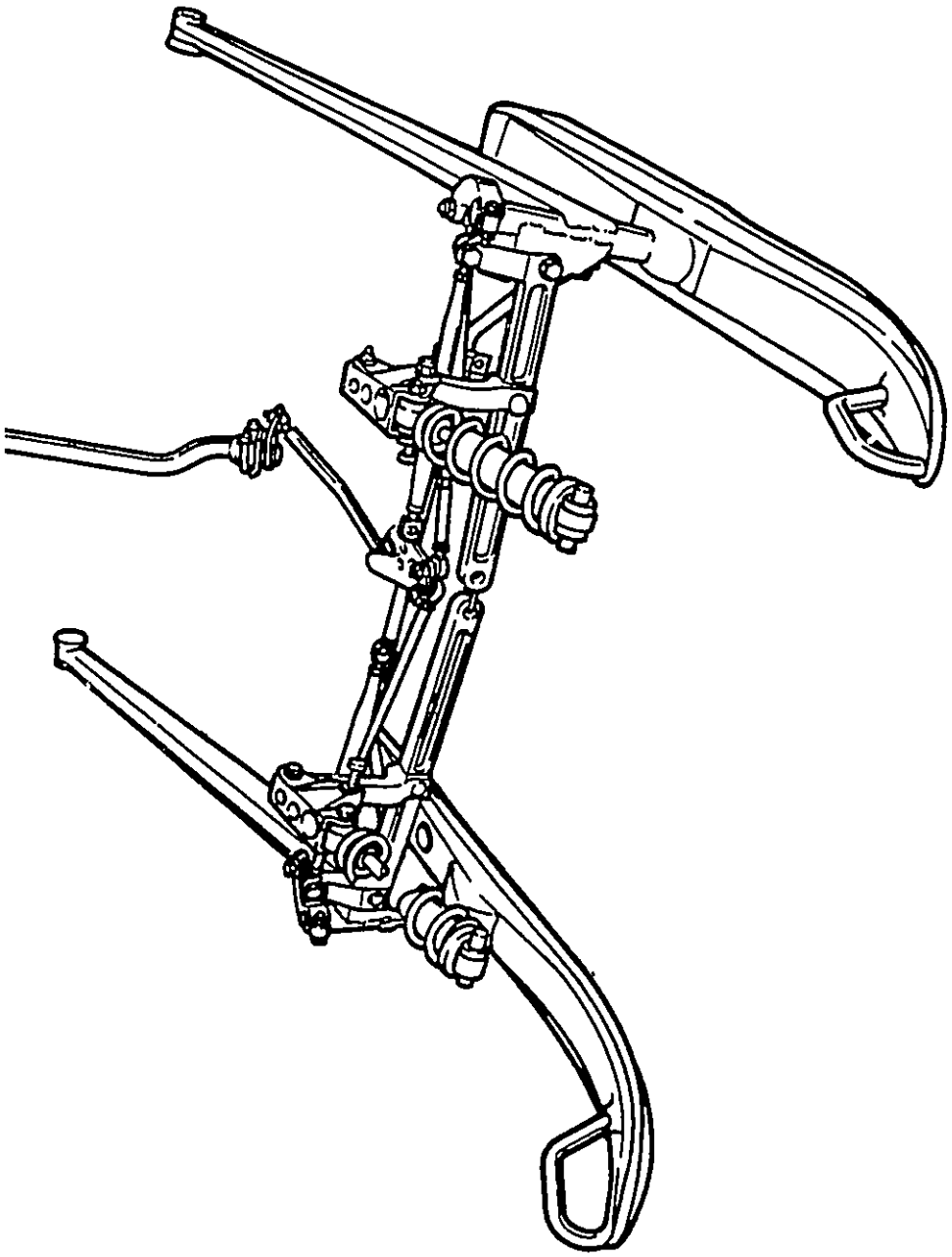

Fig. 6.3: A View of the front suspension system

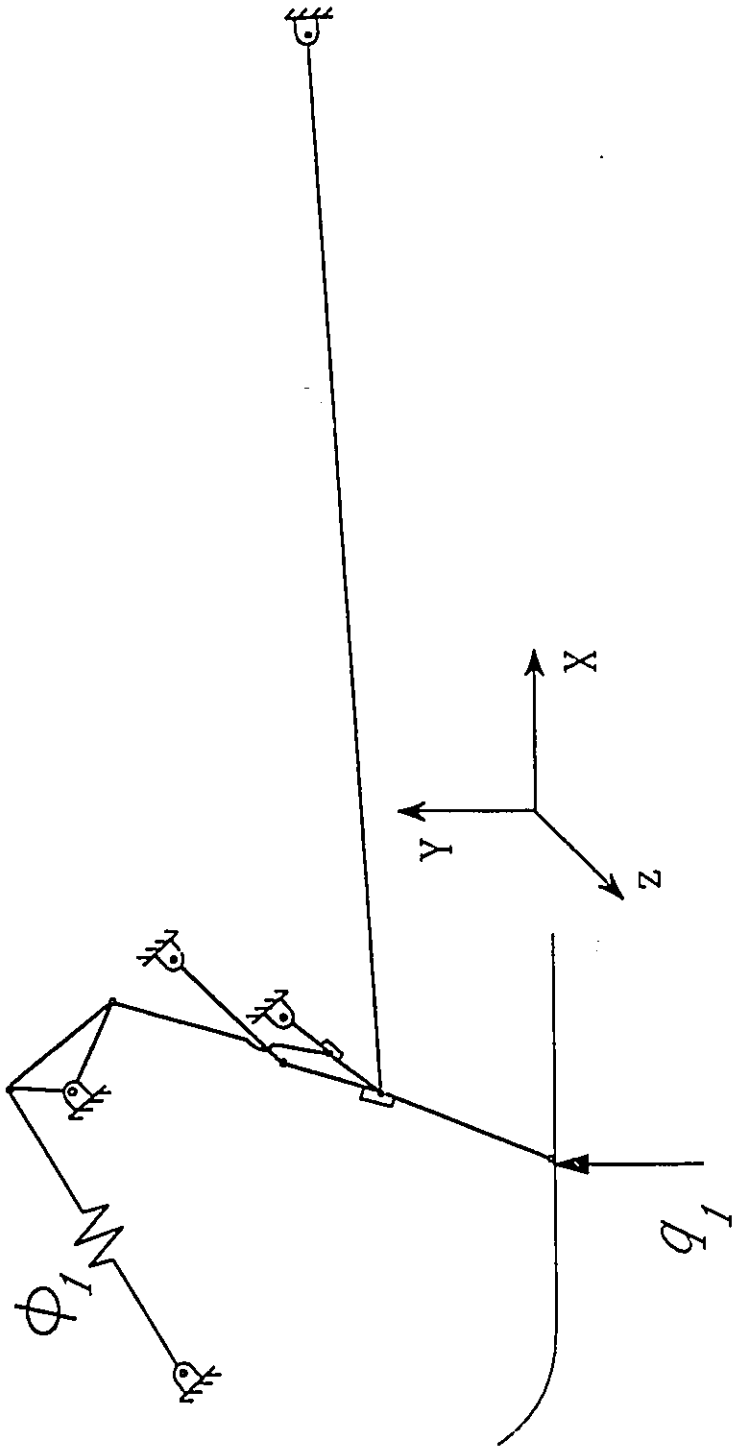

Fig. 6.4: Schematic of front suspension linkage

the second phase, the mathematical model of the complete snowmobile is created which includes the component models created in phase 1. Component modelling is carried out using both analytical and experimental methods. The kinematic analysis of the rear suspension linkages are carried out using the newly developed general purpose program, GENKAD. The front suspension, which is a spatial mechanism, is modelled and analyzed using the commercially available program, IMP [38], used as part of I-DEAS [39] software package. From the kinematic analyses, the force generation characteristics of the complex suspensions are summarized in terms of a few parameters.

The vehicle suspension component models are then incorporated into a full vehicle dynamic model used to evaluate driver ride comfort. For this purpose, a two degree of freedom (bounce and pitch) model is developed. This model takes into account the suspension nonlinearities due to large motions at linkages. 'Discrete event simulation' is carried out for the vehicle traversing a bump at various speeds. Unlike wheeled vehicles, the contact between the ski or track to the snow terrain cannot be adequately represented by a 'point contact' model. We have taken into account the enveloping action of the ski and track by using a terrain pre-processor.

6.3.1 Subsystem Models

The snowmobile is conceptually divided into 3 main subsystems: shock-absorbers and springs, suspension linkages, and

chassis-body-driver subsystems. Each one is modelled separately and brought together in the full vehicle model.

6.3.1.1 Shock-Absorbers and Springs

The suspensions use shock-absorbers with coiled-over springs. The shocks are manufactured by Monroe and Marzocchi. The mathematical model requires the force vs velocity characteristics of the shock-absorber. Springs have been manufactured to give linear force-deflection curves. For the shock-absorbers, we do not model the complex oil-flows and analytically predict the force-deflection characteristics, but rather determine these experimentally. From the force-deflection curves produced by sinusoidally stroking the shock-absorber at different frequencies, average damping constants for compression and extension are identified. Using these constants, the shock-absorbers are modelled as bilinear dampers.

6.3.1.2 Suspension Linkages

Since the springs and shock-absorbers appear as part of a linkage assembly in the suspension, the forces acting on a vehicle sprung mass are not the same as those developed locally across these elements. The manner in which these forces are modified by the linkages is represented by a set of *velocity coefficients*, as explained in Chapter 4. These velocity coefficients and deflections, which determine the local element forces, are evaluated from a kinematic analysis. This data is stored

and used during dynamic analysis to compute the forces across the suspension units. This leads to a computational efficiency several magnitudes higher than what would be possible if the total system was modelled as a mechanism. The information obtained from kinematic analysis is independent of shock-absorber parameters such as stiffness, damping etc.. These are supplied during the dynamic analysis stage.

Figure 6.5 shows a side view of the snowmobile with the deflections and forces at the base of front and rear suspension systems. If we ignore the inertias of the suspension links, the suspension forces depend only on the relative motion between the vehicle body and the base of the suspensions. To evaluate this, we consider the vehicle body fixed, and apply deflections at the ski and track. The ski has one input, q_1, the vertical deflection of the ski-pivot point. The track has two degrees of relative motion, q_2, the vertical motion of a reference point on the track, and q_3, its rotation. Using the velocity coefficients method, we can express the forces at the base of the suspension units as:

$$Q_1 = Q_1(q_1, \dot{q}_1) \tag{6.1}$$

$$Q_2 = Q_2(q_2, \dot{q}_2, q_3, \dot{q}_3) \tag{6.2}$$

$$Q_3 = Q_3(q_2, \dot{q}_2, q_3, \dot{q}_3) \tag{6.3}$$

Kinematic analysis of the ski suspension, which is a spatial mechanism, was carried out using IMP. The program cannot directly

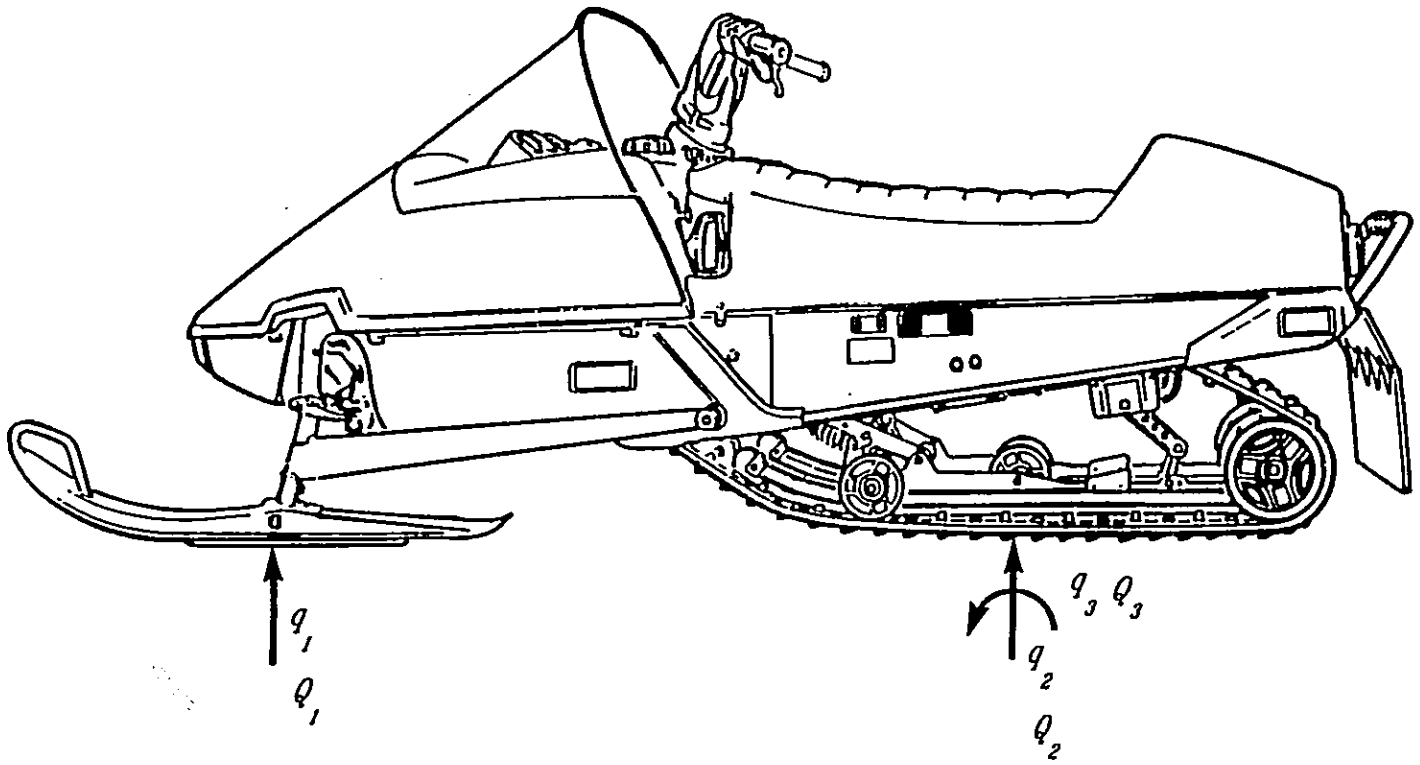

Fig. 6.5: Deflections and forces at the base of suspensions

handle open kinematic chains. Therefore the schematic shown in Figure 6.4 was modified so that the ski pivot point is connected to the ground by a series of links and 3 prismatic joints, and one ball joint. This creates a path for artificial loop closure. To input the model the initial position must be precisely known. It is important to model the mechanism so that it does not have any redundant constraints or any unrestrained motion other than the degree of freedom. Position analysis was carried out by specifying the vertical motion of the ski pivot point as the primary motion. The analysis gives the solution of various joint variables as a function of the primary motion. From this result, the velocity coefficients were determined by numerical differentiation. Figure 6.6 shows the deflection of the shock-absorber as a function of the ski vertical motion. The corresponding velocity coefficient is shown in Figure 6.7. It must be noted that this quantity has a significant variation with ski travel, and therefore the effective spring stiffness is highly nonlinear. The shock-absorber deflection and velocity coefficient is tabulated for use in the dynamic analysis program. There the spring and damping characteristics are combined with these to calculate the effective vertical force, Q_1, as experienced at the ski pivot.

Kinematic modelling and analysis of the rear suspension linkage was carried out using GENKAD as detailed in Chapter 5. The shock-absorber deflections and four velocity coefficients are given in Figure 5.10 and 5.11. Using the EQUALS module of GENKAD, these six quantities are tabulated for a range of values of rail relative bounce and rotation.

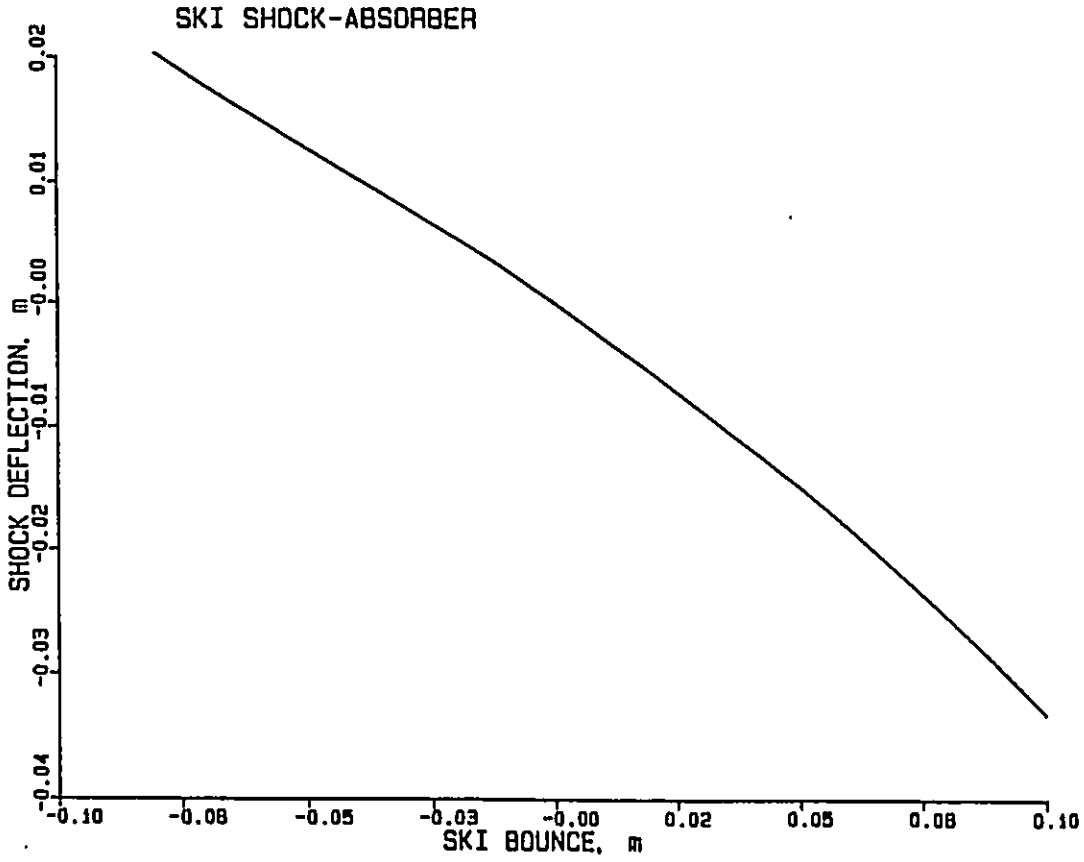

Fig. 6.6: Shock-absorber deflection vs ski vertical deflection

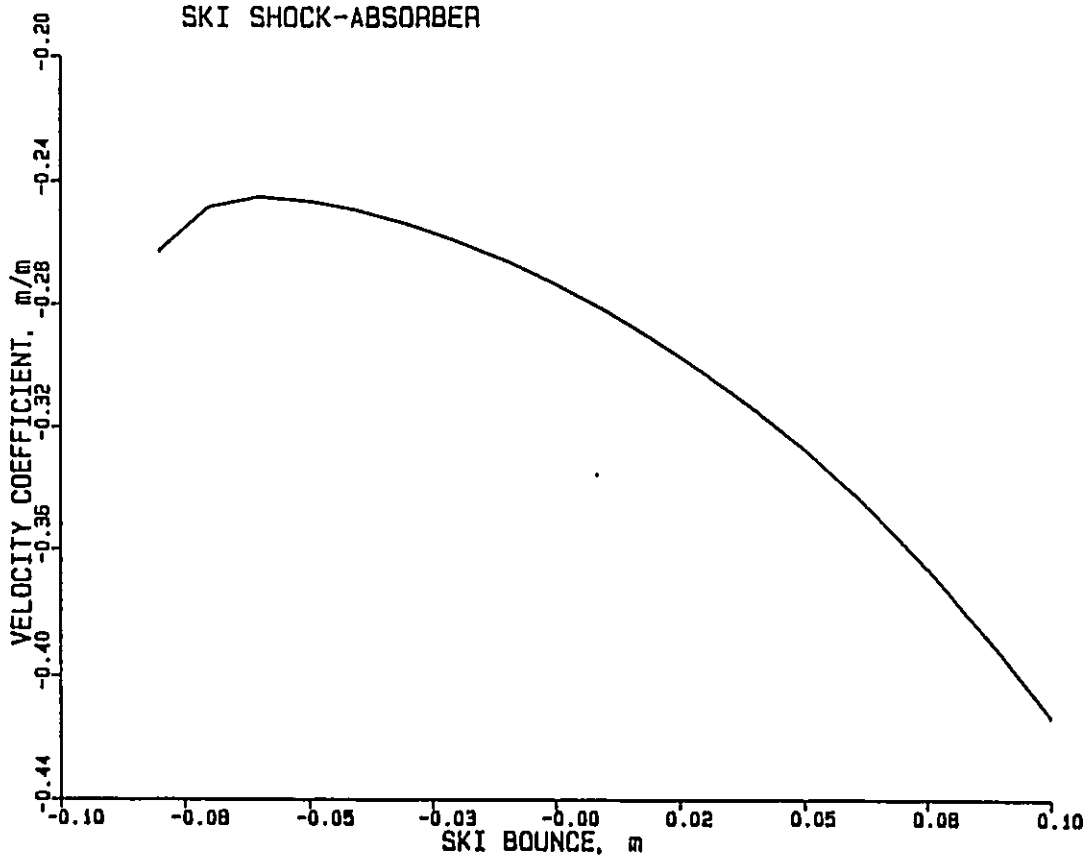

Fig. 6.7: Leverage ratio of shock-absorber deflection vs ski vertical deflection

During dynamic analysis, a second order interpolation or extrapolation is carried out during differential equation solution to find values of these variables at any given position. From these the suspension forces, Q_2 and Q_3 are computed.

6.3.1.3 Chassis and Driver Model

The vehicle chassis and body are assumed to form one rigid body. The dynamic characteristics of this rigid body are its mass, moments of inertia (MOI), and centre of gravity (CG) location. The inertia and CG location parameters are difficult to determine analytically due to the many irregular shapes that make up the vehicle, an experimental procedure was adopted as given in [128]. Using the pendulum method, the unladen vehicle centre of gravity location and moment of inertias were determined about the vehicle pitch, roll, and yaw axes.

The driver is assumed to sit on the vehicle without any relative motion between the two. Using centre of gravity and moment of inertia data given in [129] for human body parts, the driver's CG location and MOI's were computed for a typical riding posture. From this information, the composite vehicle-driver system CG location and MOI's were computed.

6.3.2 Snowmobile Ride Dynamic Model

A two-degree-of-freedom (bounce and pitch) model is used for the

analysis of ride dynamics. Such a model is very widely used for vehicle ride analysis and proven to be adequate in many applications [44-47]. The schematic is shown in Figure 6.8, where the front and rear suspension systems are depicted as generic force-generators. In the front, this force depends on the relative translatory motion between the ski attachment point (ski pivot) and the vehicle, the spring and damping coefficients, and the velocity coefficient relating the shock-absorber motion to the ski pivot vertical motion. In the rear, the track is free to pitch as well as bounce. This causes a vertical force, Q_2, and a torque, Q_3. These depend on the relative track motion, the spring and damping coefficients, and the four velocity coefficients.

6.3.2.1 Equations of Motion

Shock-absorber and spring parameters, as well as the kinematic parameters are determined as described earlier. For dynamic analysis, the vehicle acceleration is determined from Newton-Euler equations, as,

$$m\ddot{x} = Q_1 + Q_2 \tag{6.4}$$

$$I\ddot{\theta} = -Q_1 d_1 + Q_2 d_2 + Q_3 \tag{6.5}$$

where Q_1, Q_2 and Q_3 are functions of the relative deflections q_1, q_2 and q_3, and their velocities, as given in Equations 6.1-3. q_1, q_2 and q_3 are computed assuming small angular motions, θ, for the sprung mass. They are,

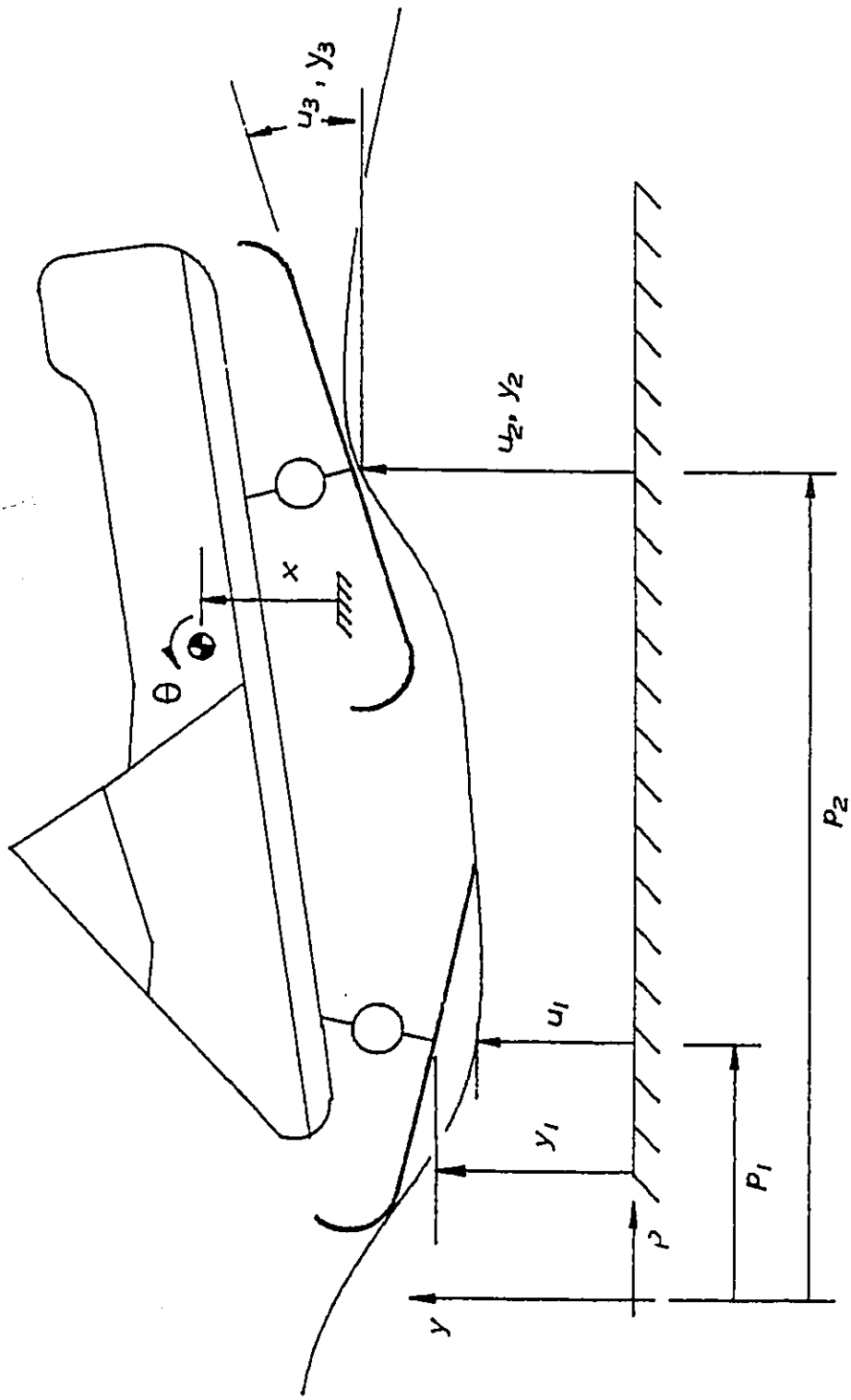

Fig. 6.8: Dynamic model of snowmobile

$$q_1 = y_1 - x + d_1\theta \tag{6.6}$$

$$q_2 = y_2 - x - d_2\theta \tag{6.7}$$

$$q_3 = y_3 - \theta \tag{6.8}$$

In the ride dynamic model of Figure 6.8, u_1 is the elevation of the ski pivot, and u_2 and u_3 are the elevation and rotation of the reference point on the track bottom. As shown in the figure, because of the enveloping action of the ski, the elevation of the snow surface, y_1, and that of the ski pivot, u_1, are not necessarily the same. A similar situation exists for the track as well. For given terrain profiles, we use a terrain pre-processor to pre-compute the values of u_1, u_2 and u_3 as functions of vehicle horizontal position, p.

6.3.2.2 Terrain Pre-Processor

We assume a 'non-deformable' terrain profile, y, expressed as a function of the horizontal distance, p. $y(p)$ is assumed to be a continuous function of p. The ski and track are represented by straight lines with a reference point on it, whose horizontal position is specified. For this point, the terrain pre-processor computes the vertical position, u, and the slope of the ski or track, so that the ski or track is always above the ground and touching it. The computation is carried out using an iterative numerical algorithm. The derivative of u, du/dp is then computed using a 5-point difference formula. The ski and track of the snowmobile pass over the same terrain profile, y, with

a delay depending on vehicle speed. But u_1 and u_2 are not necessarily the same after an axis shift because the ski and track shapes are not the same. The values u_1, u_2 and u_3 are computed by the pre-processor once, and used by the dynamic analysis program repeatedly for various speeds and parameter variations.

The pre-processor is a menu-driven, interactive graphics program. The user can select one of five common transient waveforms as the terrain profile, and specify its parameters. Figure 6.9 shows the menu of profiles from the program. The user also interactively specifies the parameters describing the ski or track shape and the location of a reference point on it whose motion is to be determined. The program then displays the position of the ski or track as it moves over the profile. This tabulated position information can then be written into a file to be used during dynamic simulation. Figure 6.10 shows positions of the ski at fixed p-intervals as it goes over a half-sine profile. In Figure 6.11 we see the actual path traversed by the ski pivot. This clearly shows how the enveloping action of the ski affects the input motion.

6.3.3 Dynamic Analysis

Dynamic analysis was carried out using the two-degree-of-freedom model discussed above. The equation generation and numerical solution was accomplished using the graphics-based dynamic analysis program, CAMSYD, described in Chapter 3. The ski and track suspensions were

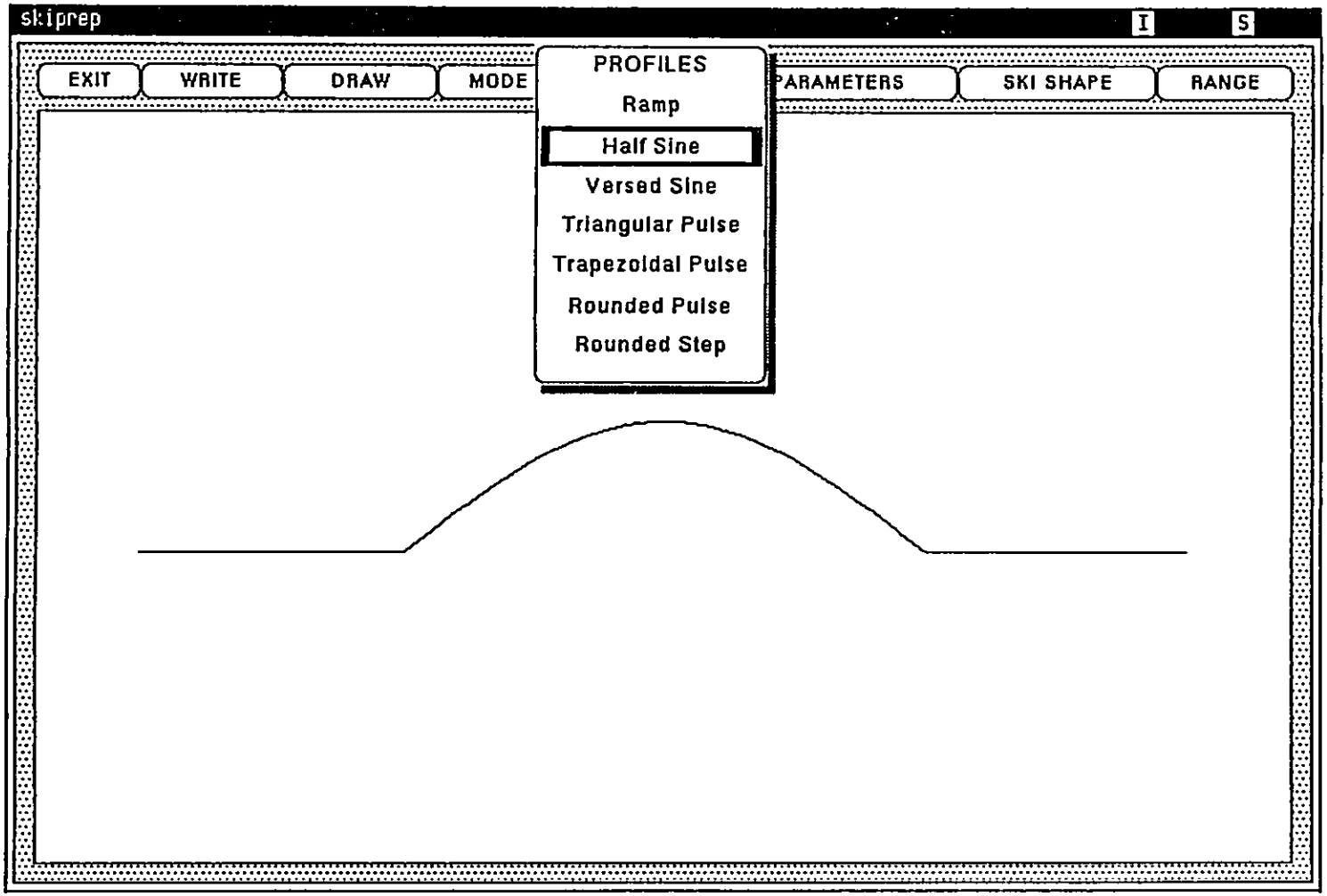

Fig. 6.9: Menu of profiles from terrain pre- processor

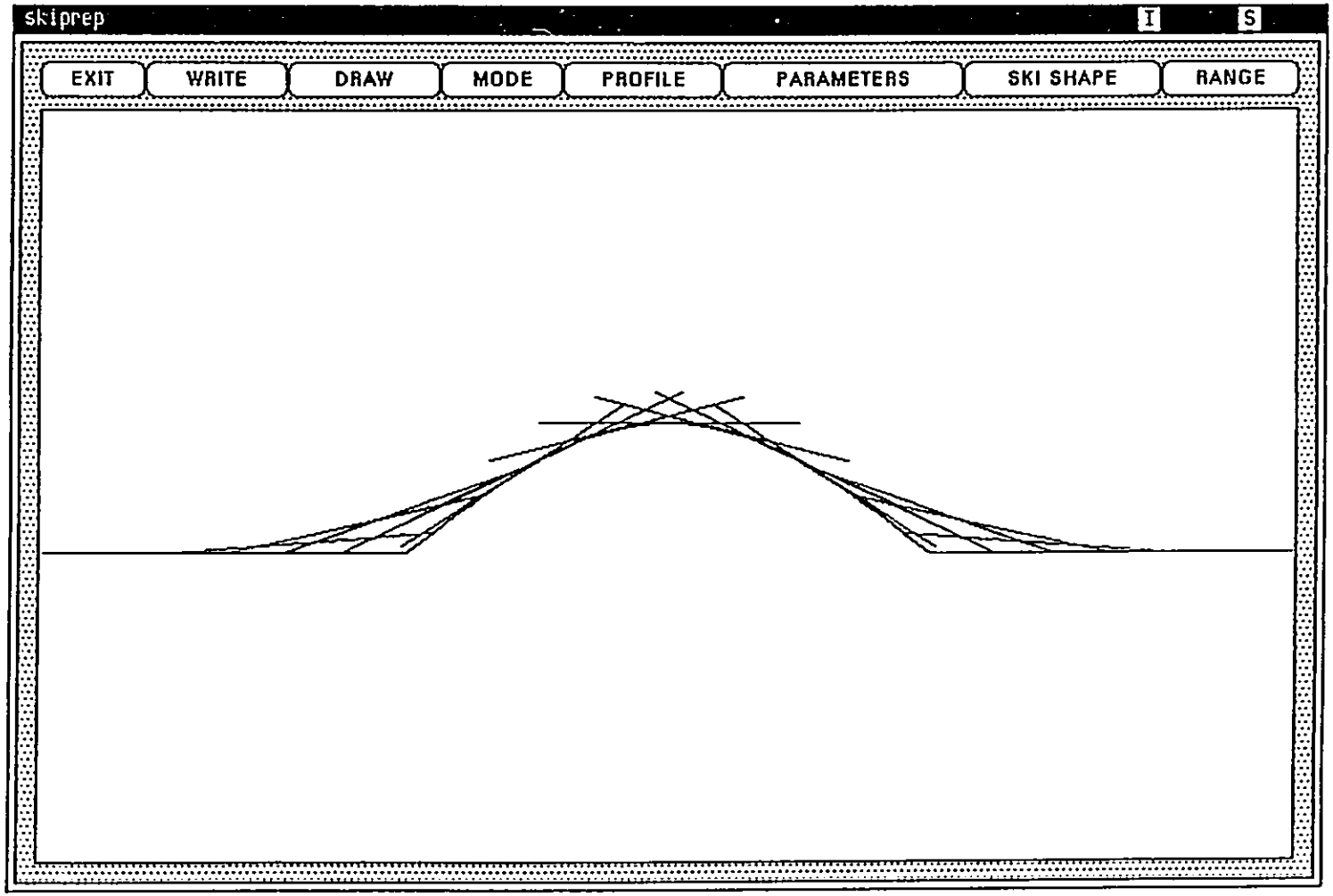

Fig. 6.10: Ski at various positions as it goes over a half-sine profile

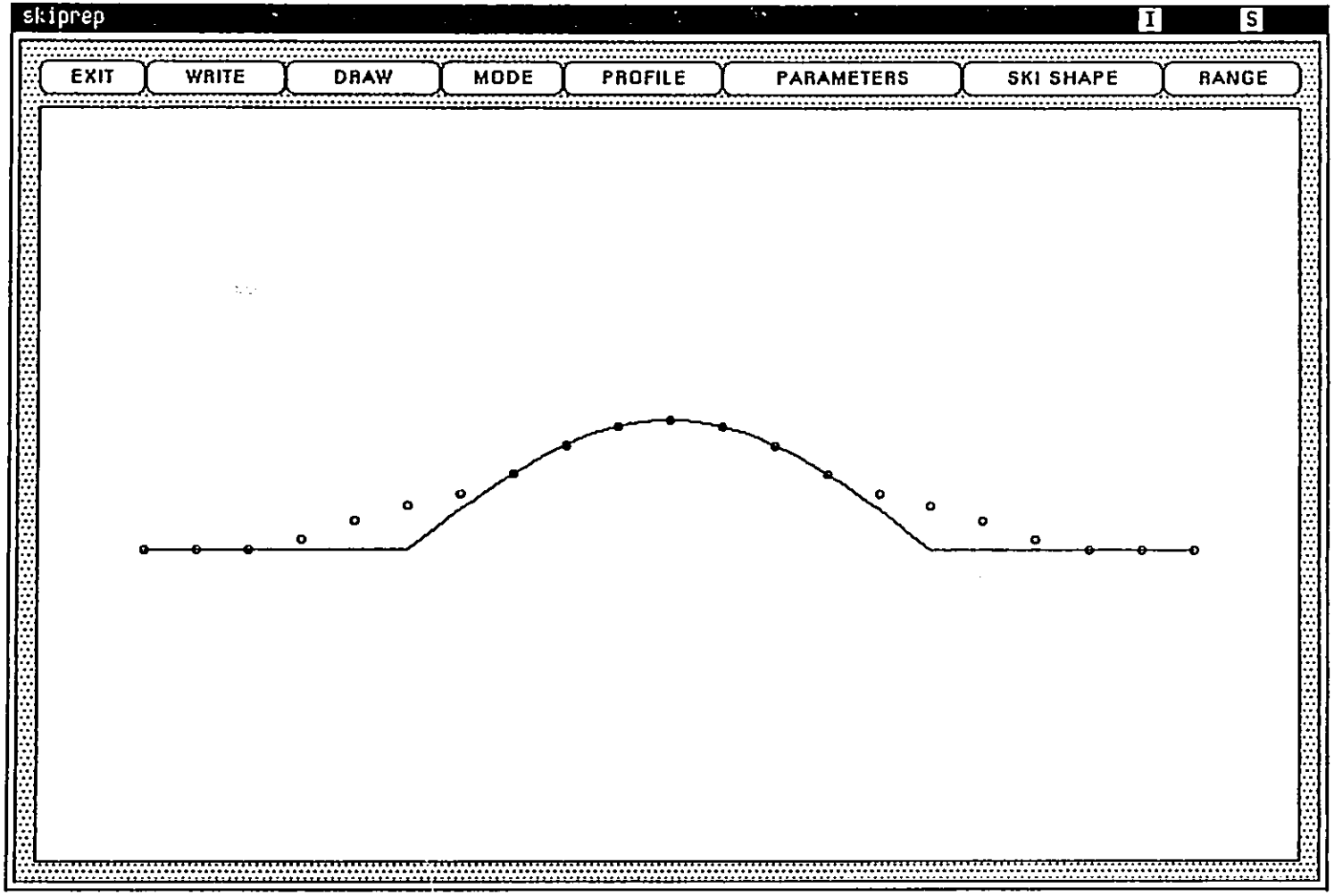

Fig. 6.11: Positions of the ski pivot for the motion shown in Fig.t6.10

modelled in CAMSYD as user-defined elements, and subroutines are appended to the CAMSYD-generated equations of motion to describe the forces generated in these suspension units. The numerical values for suspension parameters as well as the motion of the ski and track appear as tabulated data from the respective pre-processors. The dynamic analysis program makes interpolation techniques to determine their values when the integration time does not fall on the grid points. Since the simulation program does not solve for the kinematics of the suspension linkages and motion of the ski and track, it is very efficient and fast. This means that a variety of dynamic analyses can be carried out in a short time to understand the behaviour of the dynamic system.

A versed sine 'bump' of 20 cm height and 2 meter length was used as the obstacle over which the vehicle was simulated to travel at various speeds. Figure 6.12 shows the profile. Low speeds are used since the profile is quite severe. Numerical simulation was carried out in CAMSYD using a variable step, variable order Adam's method with error control. Simulation results are presented along with test results in the following Section.

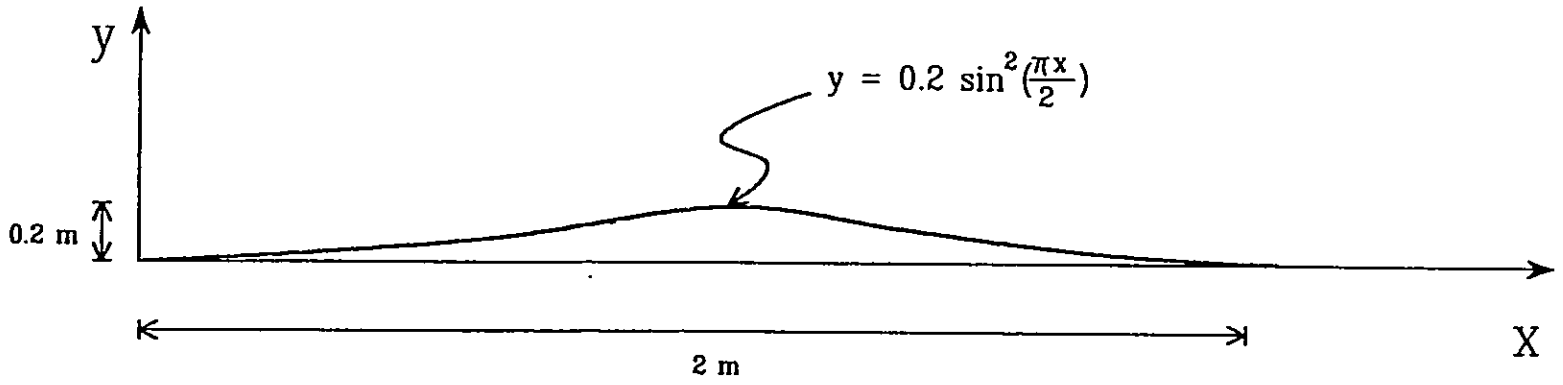

Fig. 6.12: Profile of 'bump'

6.4 FIELD TESTING AND VALIDATION OF SIMULATION RESULTS

6.4.1 Description of Test Setup and Procedure

Testing was carried out to measure the dynamic response of a Formula Mach 1 snowmobile as it went over a 'bump' at various speeds. The bump was made of wood and was rigidly mounted on a smooth snow-covered terrain. Data acquisition was performed as described in [130]. The snowmobile was instrumented to measure accelerations and displacements at various locations. Figure 6.13 shows these locations. The measurements are:

C1: Linear displacement between a point on the tunnel and a point on the rail at the rear.

C2: Linear displacement between a point on the tunnel and a point on the rail at the front.

C3: Linear displacement across the ski shock-absorber.

P4: Angular rotation of the ski with respect to the ski-leg.

A5: Acceleration of the rear of the rail perpendicular to the track.

A6: Acceleration of the front of the rail perpendicular to the track.

A7: Acceleration of the rear of the tunnel perpendicular to the plane of the tunnel.

A8: Acceleration of the front of the tunnel perpendicular to the plane of the tunnel.

A9: Acceleration of the ski-leg along the direction of its length.

A10: Acceleration of the front end of the chassis.

In addition to these signals, the vehicle speed was also recorded.

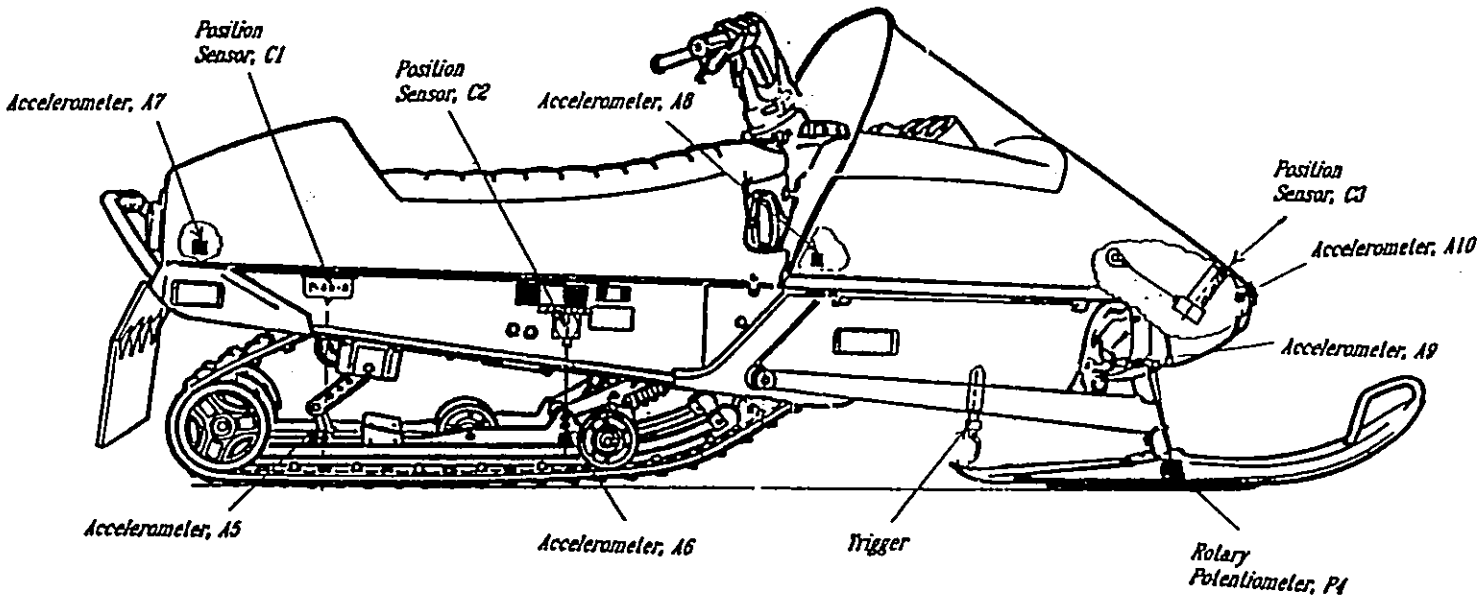

Fig. 6.13: Locations of measuring instruments

Signals were calibrated in engineering units as follows: acceleration - *g*'s; displacements - *mm*; rotation - *degrees*; and speed - *km/hr*. Data was acquired and recorded using a six-channel portable digital acquisition system by Somat™. A trigger signal was used to enable all measurements to be aligned along the time axis. At each test run one channel was used for the trigger signal, another one for the speed and the other four were used for four of the ten measurements listed above. All channels of data were acquired at a rate of 1000 samples per second. A total of five combinations of measurements were carried out at each speed. At each speed the test was repeated four times. Out of the four, the worst one was rejected based on how steady the vehicle speed was maintained. The three sets of data for each run were transferred to an IBM PC™-compatible microcomputer as ASCII files.

We now give some of the 'raw' data signals to show the quality of signals acquired. Figure 6.14 shows a sample of vehicle speed recorded at a nominal speed of 10 km/hr. It shows a variation of approximately ±20%. There is a consistent tendency for the speed to drop as the vehicle encounters the bump. This drop in speed is even more prominent at higher nominal speeds. For a given speed the signals are fairly similar with a maximum variation of 15% for the example shown.

Figure 6.15 shows displacement measurement, C1, at 10 km/hr. This signal is typical of all the displacement measurements. A very high frequency noise is superimposed on the low frequency signal. The amplitude of the noise is typically 20% of the signal.

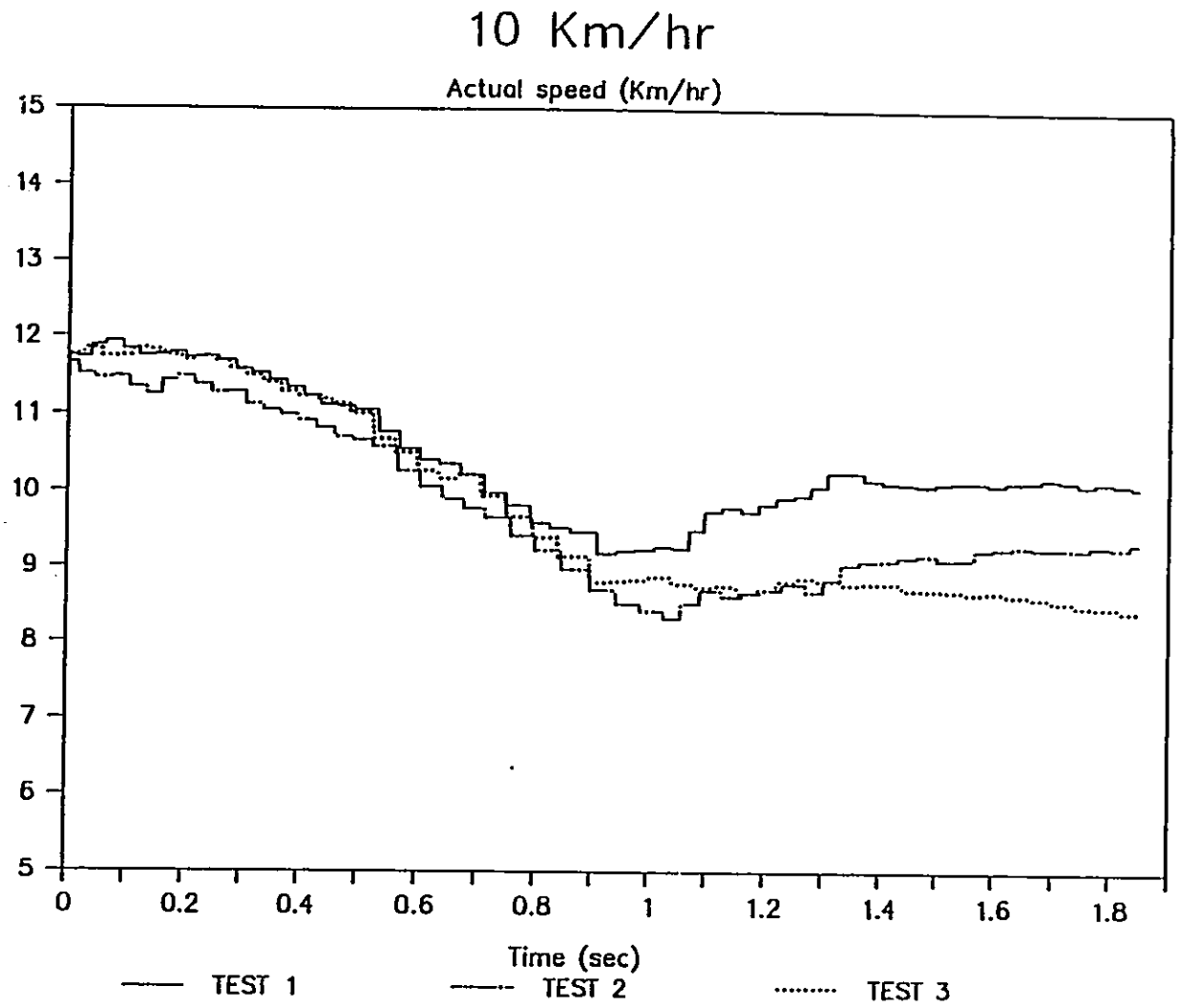

Fig. 6.14: A sample of vehicle speed

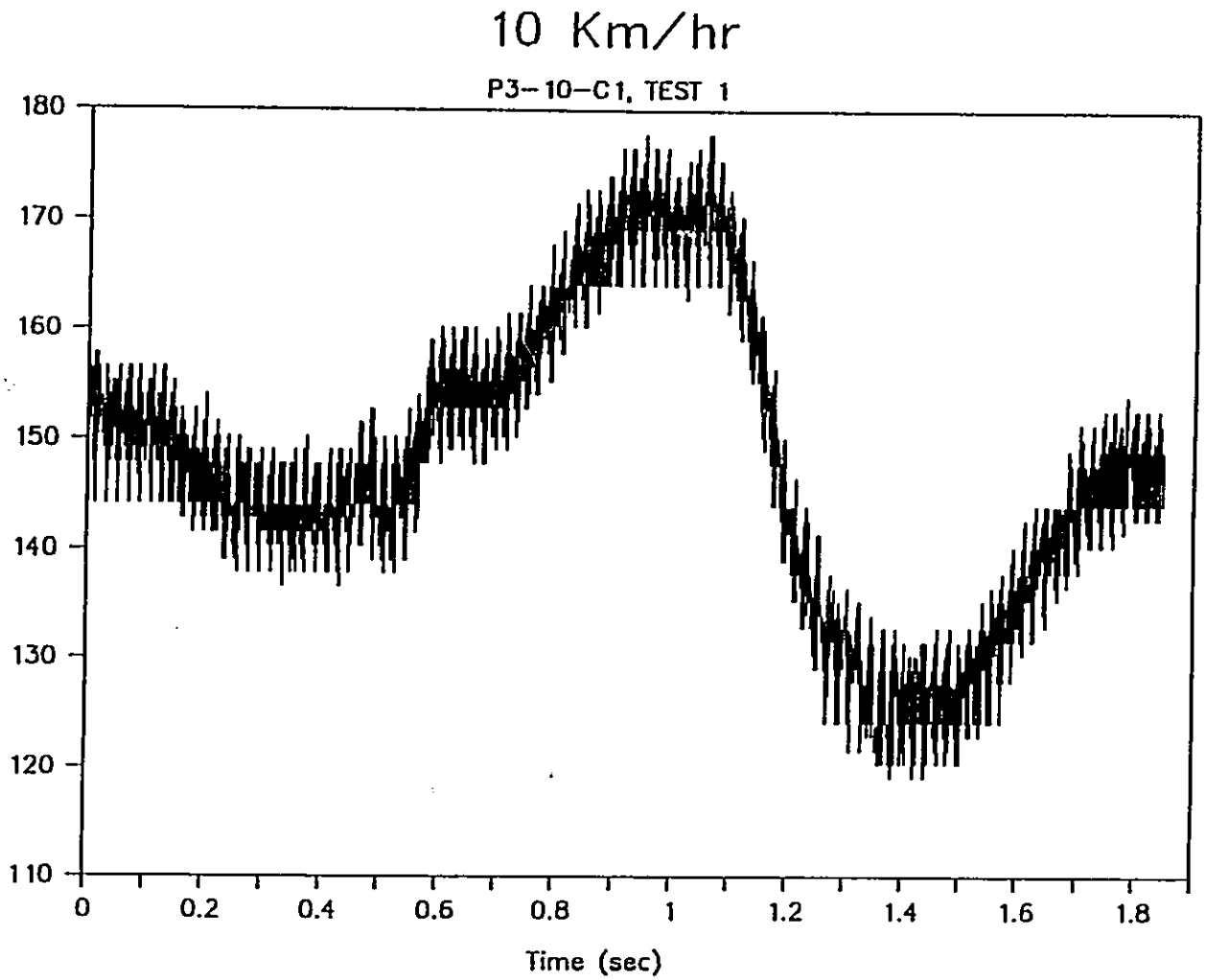

Fig. 6.15: Displacement measurement, C1, at 10 km/hr

Figure 6.16 shows a typical acceleration signal, A7, measured at 10 km/hr vehicle speed. The *Y*-axis is marked in *g*'s and shows very high magnitude peaks of 10*g* acceleration. This is however not experienced by the driver. These high frequency components can also be treated as noise, and may be attributed to the vibration of the structure on which the accelerometer was mounted, and the vibrations due to engine, clutch, and track motion. However, the high amplitude of the noise casts some doubts as to the integrity of the hidden low frequency signal.

6.4.2 Signal Processing

The computer aided dynamic analysis software is intended for the ride analysis of the vehicle-driver system modelled as a rigid body mounted on front and rear suspensions. It is known that this system would undergo vibrations at low frequencies. The high frequency components measured are therefore to be treated as noise, and must be filtered before a meaningful comparison with analysis can be attempted. In this Section we describe how this signal processing was carried out and present some typical results.

Since the data was available on a computer in digital form, it was logical to apply digital filtering by software. Two cascaded first-order low-pass filters were employed, as shown below.

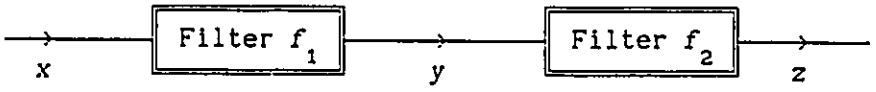

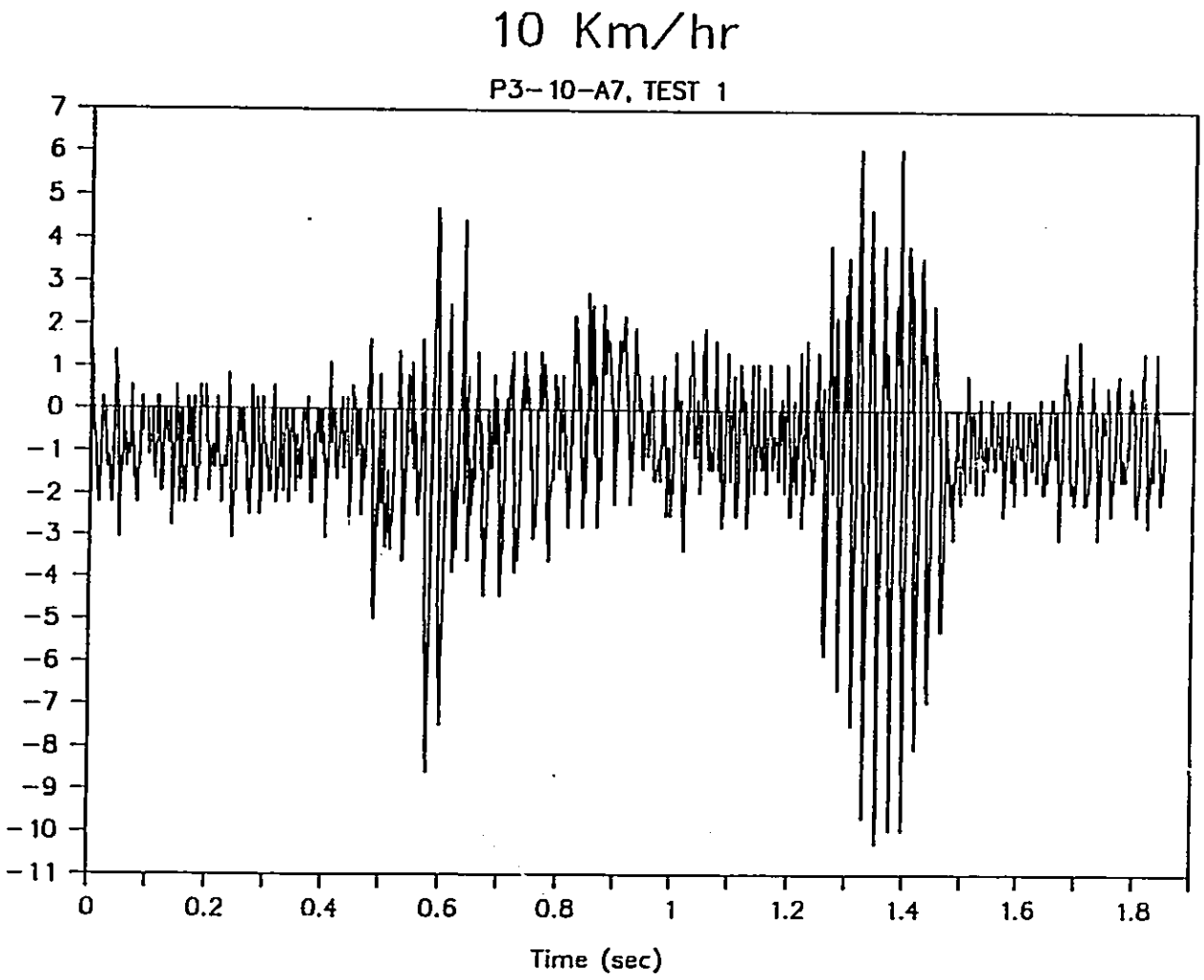

Fig. 6.16: Acceleration signal, A7, measured at 10 km/hr

Here f_1 and f_2 are the *cut-off* frequencies (in Hz) of each of the low-pass filters, x is the unfiltered signal, and z is the final, filtered signal. If T is the sampling period, $\alpha_1 = [1-\exp(-Tf_1)]$ and $\alpha_2 = [1-\exp(-Tf_2)]$ are the constants of the filters, and i is the sampling instant, we can write,

$$y_{i+1} = (1-\alpha_1)y_i + \alpha_1 x_i \tag{6.9}$$

and

$$z_{i+1} = (1-\alpha_2)z_i + \alpha_2 y_i \tag{6.10}$$

We selected the cut-off frequencies, f_1 and f_2, to be 40 Hz and 20 Hz respectively. Filters inevitably distort the low frequency signals even as they suppress the high frequency noise. We have tried other combinations of cut-off frequencies, and visually inspected the results by superimposing filtered and raw data. The above choice of frequencies seemed to give satisfactory results. In some instances it was noted that the peak values of filtered signals are up to 10% lower than they ought to be.

Figure 6.17 shows the filtered displacement signal, C1, for three runs at 10 km/hr speed. The raw data corresponding to "Test 1" was shown earlier in Figure 6.15. It is seen that the filtering has effectively eliminated the noise without causing much distortion. Once

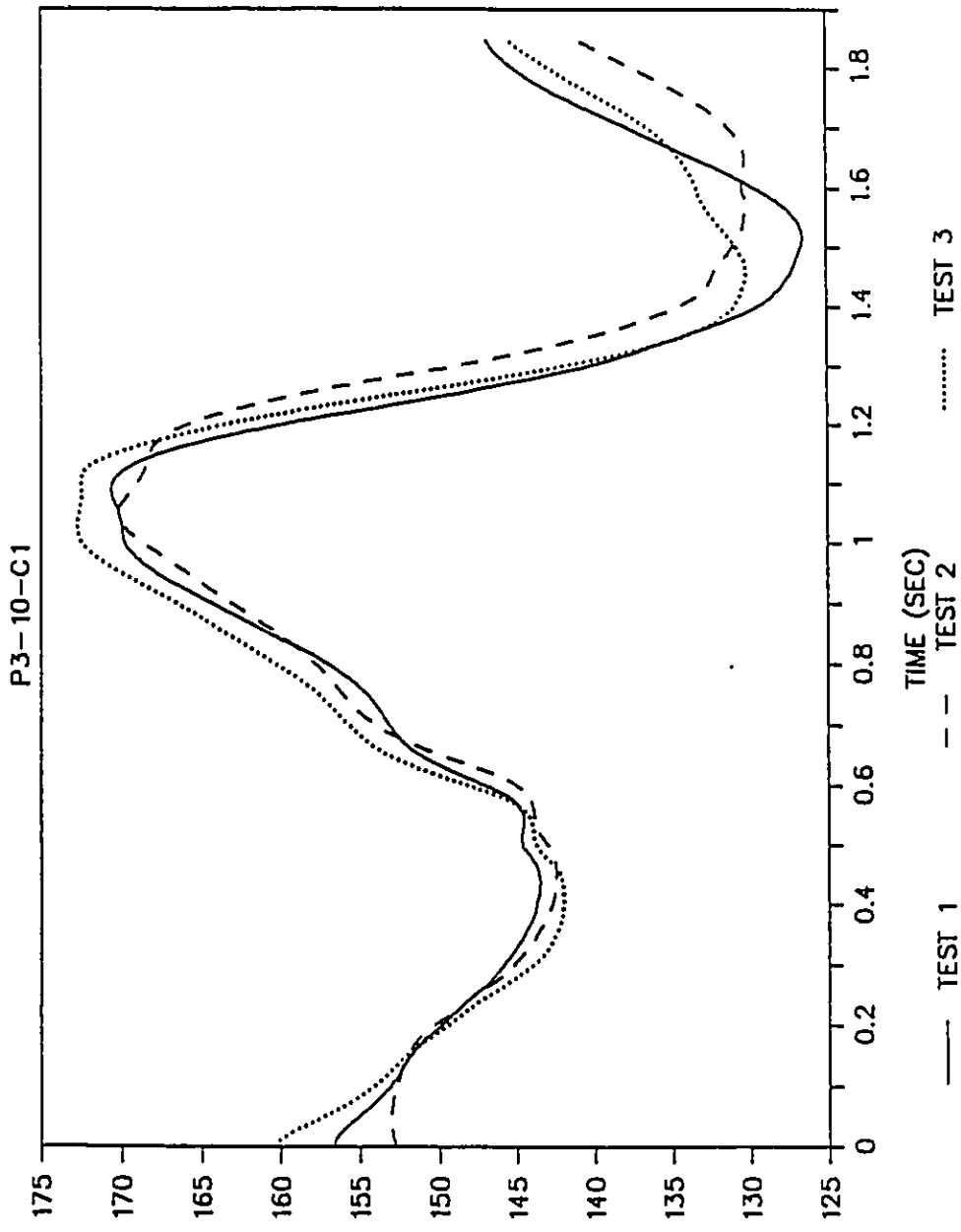

Fig. 6.17: Filtered displacement signal, C1, for three test runs

the noise is filtered, we can attempt meaningful comparison between the test results. It is seen that the data from all three runs are fairly similar, with a maximum deviation of approximately 6%.

Figure 6.18 shows the filtered acceleration signal, A7. The raw data corresponding to "Test 1" was shown earlier in Figure 6.16. It is clear from comparing these two plots that the 'true' signal is really hidden in the raw data. The results are less dramatic for higher vehicle speeds as the magnitude of ride response is higher. A more curious feature we notice is that the different test runs have a significant amount of zero offset. This behaviour is barely discernible in the raw data because of the widely different magnitudes. While the filtered signals have a typical peak-to-peak magnitude of 1.8 *g*, the raw data has 16 *g*. Clearly the signal that shows acceleration to be always below zero is not correct. However, except for the offset, all the signal do look similar and therefore cannot be dismissed.

It is possible that the accelerometer has sustained some impact damage causing the offset. Or it may be that the instrumentation or calibration had a flaw. Had there been a reference signal measured on a stationary vehicle available, it could have been used to correct the error. Since this is not the case we must deal with the situation so that we can make the best of what data we have. A solution that seemed very reasonable is to shift each signal in the Y axis so that its *mean* is zero. This in effect ensures that the velocity associated with the acceleration signal is zero at the end of the recorded data. This is

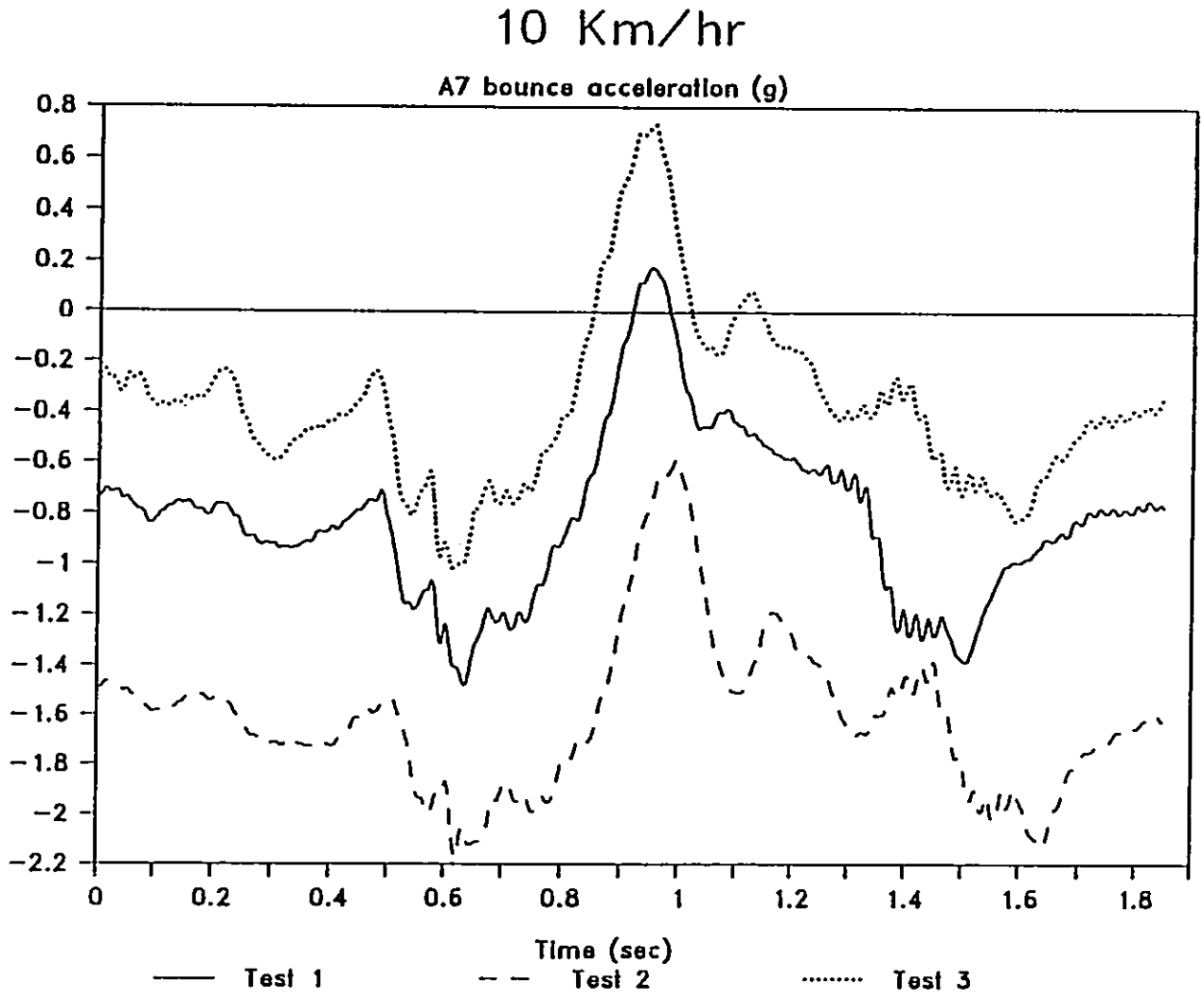

Fig. 6.18: Filtered acceleration signal, A7, for three test runs

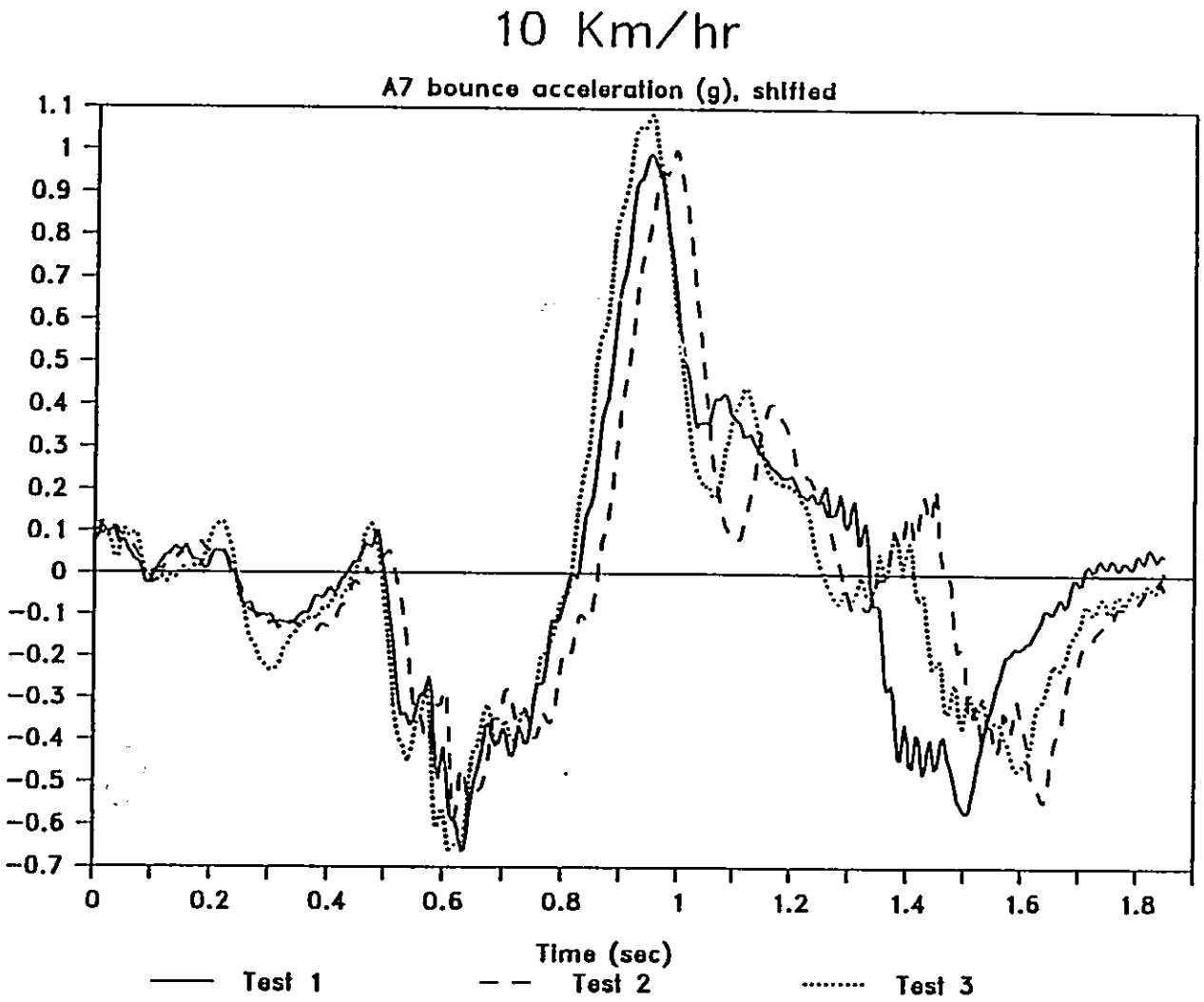

Fig. 6.19: Zero-shifted acceleration signal, A7, for three test runs

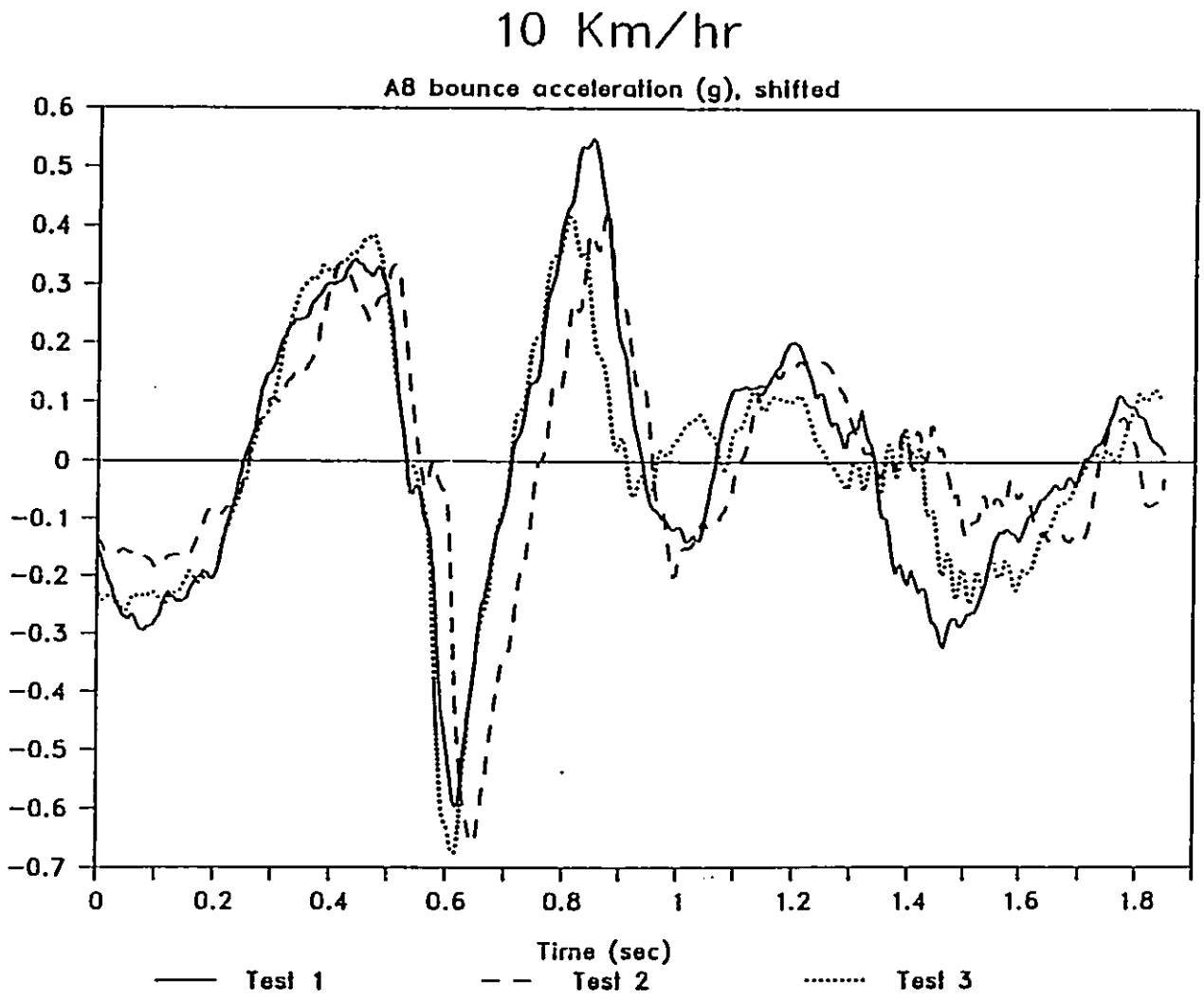

Fig. 6.20: Zero-shifted acceleration signal, A8, for three test runs

strictly true only when the vehicle has come to a rest. However, for lack of a better solution, we use this method. This zero-shifting was carried out after filtering and was applied to all acceleration signals. Figure 6.19 shows the signal, A7, after zero-shifting. Similarly, Figure 6.20 shows the signal, A8.

6.4.3 Comparison of Simulation and Test Data

Among the 32 response quantities available from the dynamic analysis program, the only one directly measured in the test was the deflection of the ski shock-absorber, C3. However, there is sufficient amount of information available so that any of the others can be easily computed. We have decided to carry out the validation of the software by using the data C1, C2, C3, A7 and A8.

As we said earlier, C3 is available directly from simulation. With regard to C1 and C2, the corresponding quantities from simulation are the relative bounce q_2 and the relative pitch q_3 between the track and the tunnel. Quantities corresponding to acceleration signals on the vehicle body, A7 and A8, are the bounce and pitch accelerations of the vehicle-driver system CG, $\ddot{z}$ and $\ddot{\theta}$, respectively. One can use C1 and C2 to compute q_2 and q_3, or conversely, use q_2 and q_3 to compute C1 and C2. Similarly A7 and A8 can be used to compute $\ddot{z}$ and $\ddot{\theta}$, and vice versa. We have chosen to compute C1, C2, A7, and A8 from simulation results and compare each with the test results. The analysis results are presented for the vehicle traversing the bump at constant forward speeds. The

plots that follow show two curves from test and one from analysis. The test data represent the maximum and minimum values from among the three runs. Ideally, the analysis results must be bounded by these curves.

From the location of the various measurements, we can write, for example,

$$C1 = q_2 - 0.226\, q_3 \tag{6.11}$$

$$C2 = q_2 + 0.284\, q_3 \tag{6.12}$$

$$A7 = -\ddot{z} - 1.053\, \ddot{\theta} \tag{6.13}$$

and

$$A8 = -\ddot{z} + 0.112\, \ddot{\theta} \tag{6.14}$$

The assumptions implicit in these equations are that A7 and A8 are measured in the vertical direction (A7 and A8 are measured positive down, while $\ddot{z}$ is positive up) in the inertial frame, which implies that the vehicle pitch angle is "small" ($\cos(\theta)\cong 1$), and that the relative rotation between the track and tunnel is small ($\cos(q_3)\cong 1$). Other assumptions are that the tunnel and the rail are rigid, and the horizontal movement of the rail relative to the tunnel is small. These are reasonably valid assumptions under the circumstances.

The deflection measurements, C1, C2, and C3 do not have a zero starting value. This magnitude is rather arbitrary depending on the mounting locations of the transducers. Therefore, for a valid

comparison with analysis, these curves are offset by a constant so that they all start at zero. The analysis results are also suitably adjusted so that at the static position, C3, q_2 and q_3 are zero.

6.4.3.1 Some Additional Notes on Computer Simulation

With respect to the comparison between computer simulation and test data, certain details of the modelling must be made clearer. The mathematical model used in dynamic simulation is based on the following assumptions:

Mass: The vehicle and the driver are considered to constitute *one* inertia-invariant rigid body. The equations of motion are written for the bounce (vertical) and pitch (rotational) motions of this body. This model neglects the compliance of the seat and the possible movements of the driver (voluntary or involuntary). The model assumes zero or constant velocity in the longitudinal direction. Possible variations in speed will cause longitudinal accelerations which will be coupled to the bounce and pitch degrees of freedom.

Suspension Systems: The suspension systems are modelled as *massless* links, springs and dampers coupling the suspended mass to the ground profile. The nonlinear effect of large deflections in the links are taken into account. However, the limits on these motions due to bump-stops and limit on shock extension etc. are not included. The springs are modelled with linear stiffness. The nonlinearity in

stiffness due to the air-spring effect of air in dampers is not included, due to lack of real data in this regard. Similarly the stiffness of rubber bump-stops was also not included for the same reason. These effects could easily have been incorporated in the model had they been available. Dampers are modelled as bilinear elements, with one coefficient of damping in compression and another in extension. These were determined from test data supplied by Bombardier. Peak forces and velocities in compression and extension for sinusoidal stroking were used. This is a gross approximation in reality. Moreover, it is known that damping can vary as much as 50% from one damper to another. However, for lack of better data, we have used the present model. Again, it is easy to incorporate detailed models of the damping mechanism when desired.

Terrain Vehicle Interaction Model: It is clear that a 'point-contact' model will not be appropriate for our application. The enveloping action of the rigid ski and track is taken into account by using the program SKIPREP, to determine an 'equivalent' profile that would be applicable at the ski pivot and at a reference point on the track/rail. SKIPREP determines the path that will be followed by these points and the angle assumed by the ski and the track, provided the ski and the track are always in contact with the ground. They are both modelled as straight lines, ignoring their smoothly curved profiles at the leading edges. This approximation makes a ground obstacle seem more severe than what it is in reality.

6.4.3.2 Vehicle Speed of 10 Km/hr

Figure 6.21 shows the actual vehicle forward speed for the test runs. As we noted earlier, the speed drops as the profile is encountered. Figure 6.22 shows the deflection of the ski suspension shock-absorber. The shock compresses as the ski ascends the bump and starts to extend as it descends it. It continues to extend as the track goes up the bump and subsequently compresses. Both analysis and test data exhibit the same trends, but the peak magnitudes obtained in simulation are larger than those from testing. The simulation response is more oscillatory than the test data curves, implying that the damping values are probably underestimated. The same reason could also explain the higher peaks. The simulation does not take into account bump-stops and other limits on shock-absorber travel. Therefore, the excess deflections would have been limited in reality. Despite all these the analysis and test results are satisfactorily close.

Figure 6.23 shows the comparison of simulation and test results for relative deflection between the rail and the tunnel, C1, measured at the rear of the vehicle. It is seen that the curves match very well both at the beginning and at the end of the run. When the ski goes over the bump and later as the front of the track hits the bump, the rear of the track compresses. The magnitude of this part of the signal is very close to the test results. During the subsequent extension, the simulation results indicate higher peaks than test results. This is because the dynamic analysis program considers that the track is always completely

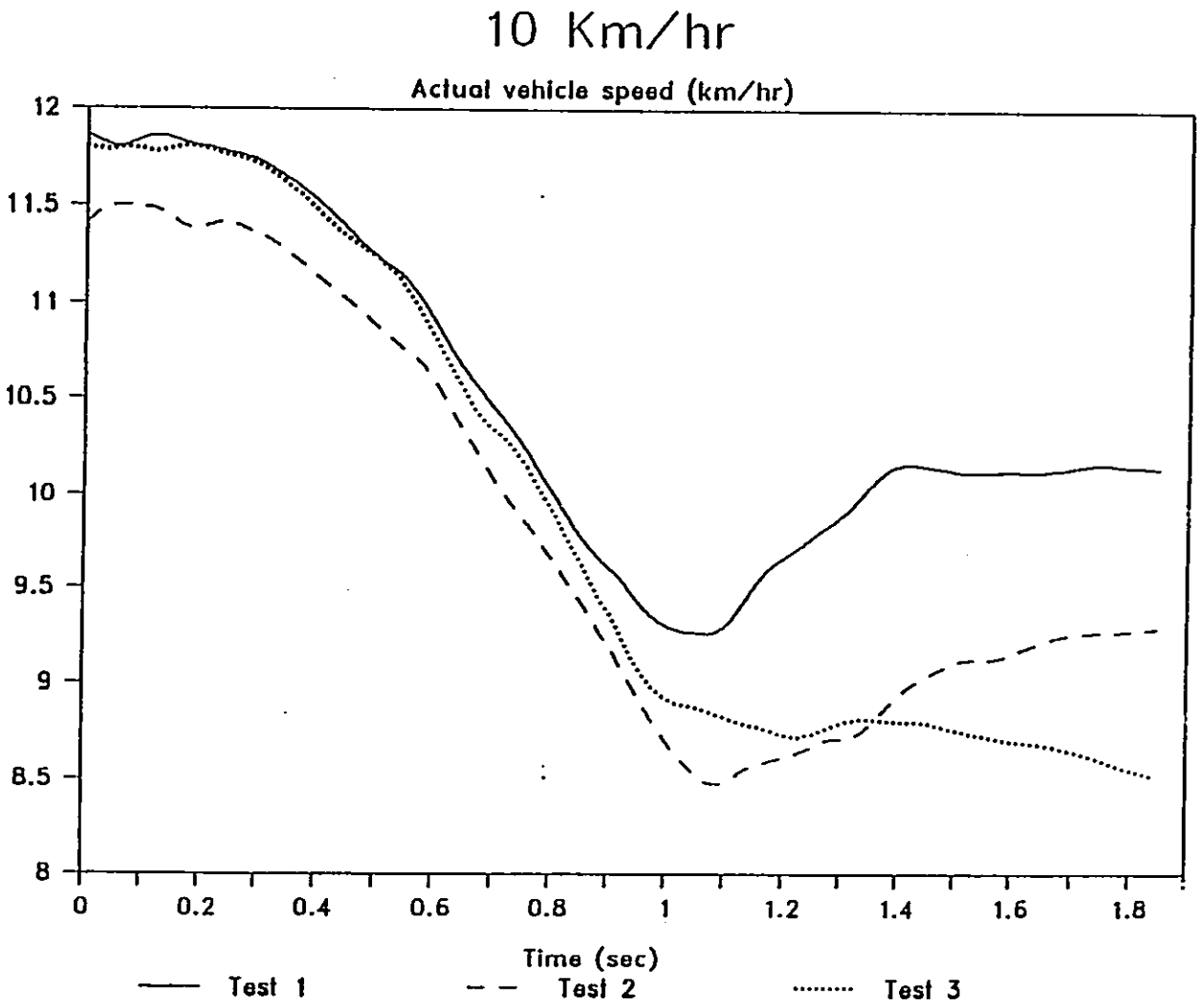

Fig. 6.21: Actual vehicle speed at 10 km/hr

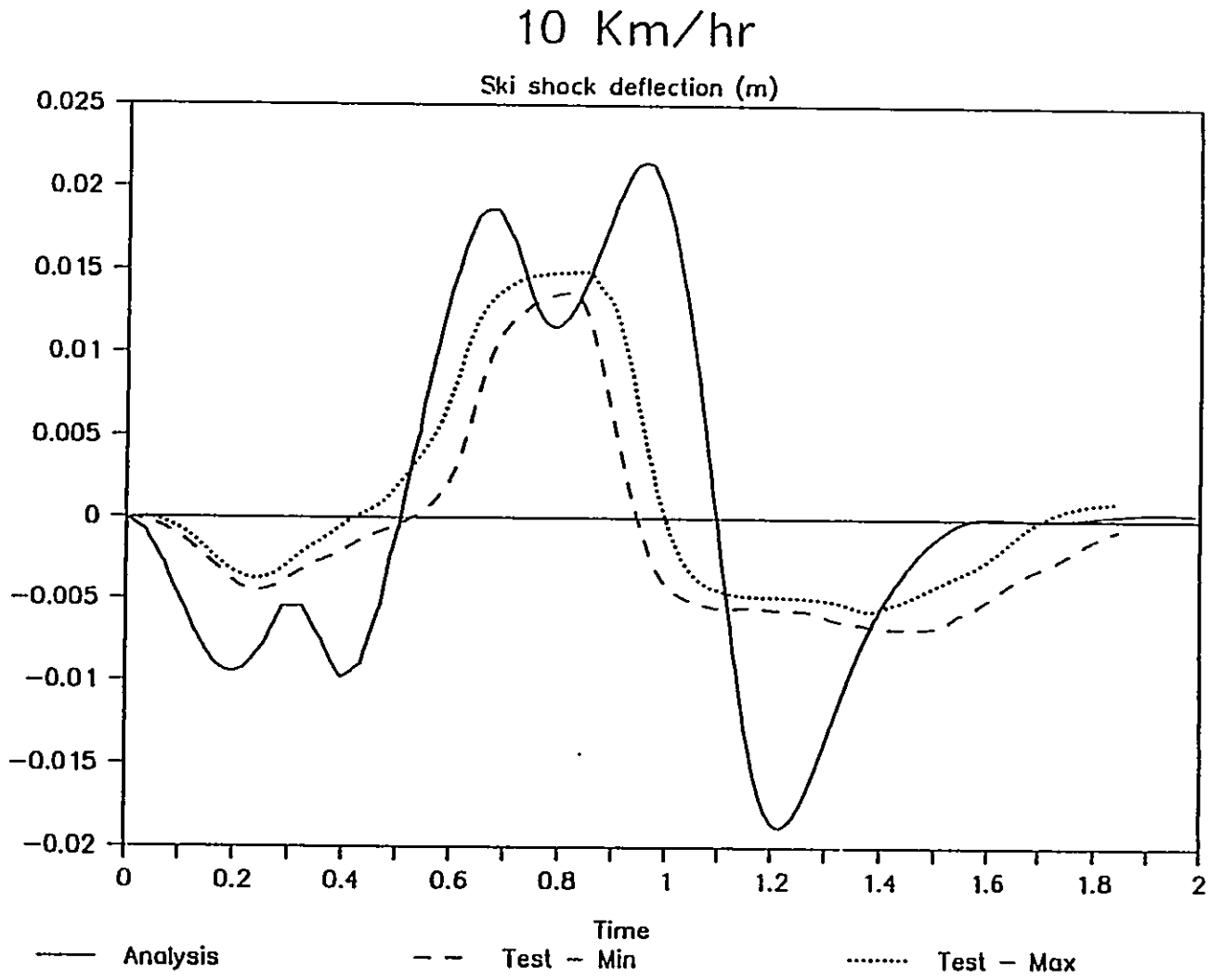

Fig. 6.22: Ski shock-absorber deflection, C3, at 10 km/hr

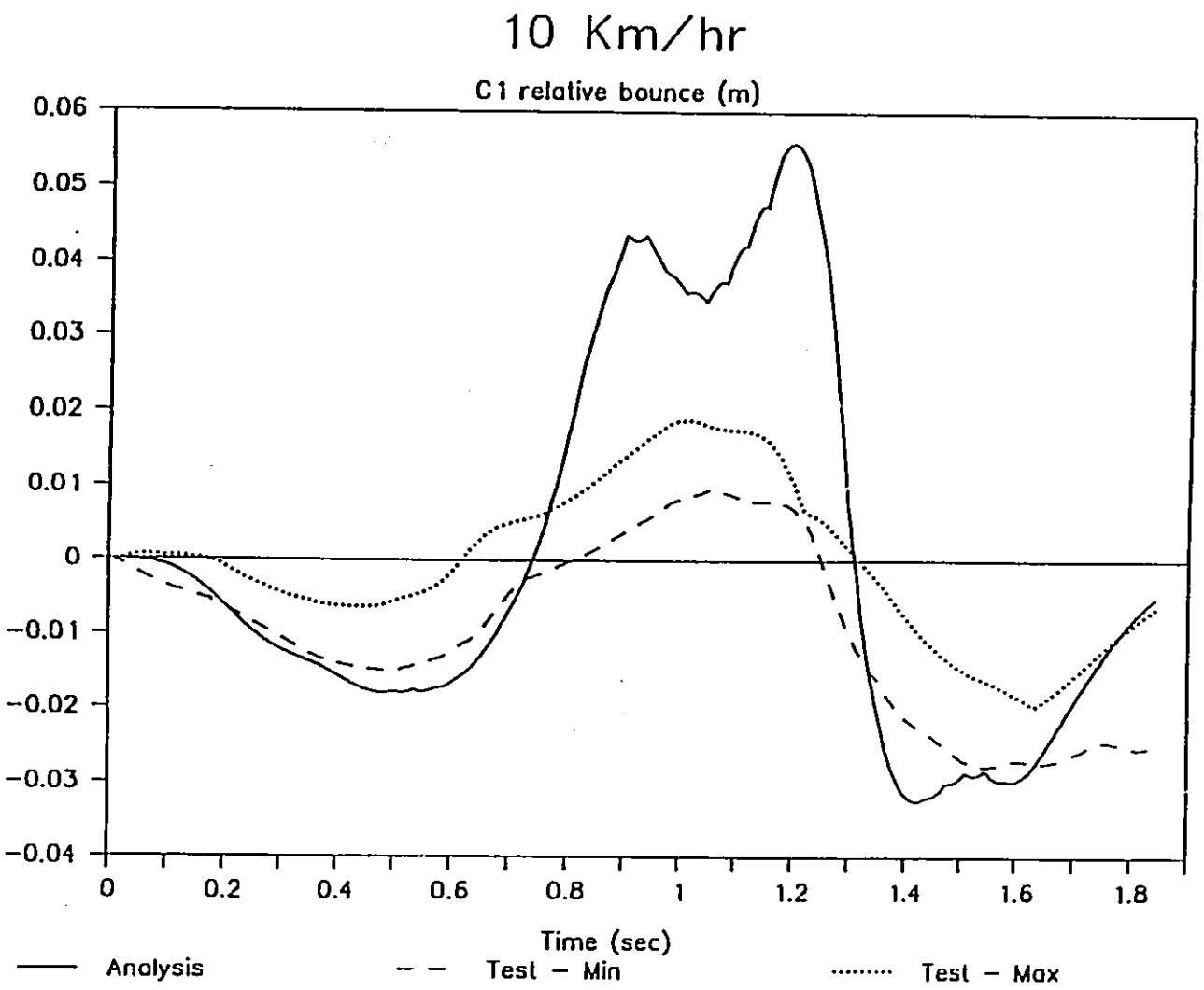

Fig. 6.23: Rail relative deflection, C1, at 10 km/hr

in contact with the profile. However, as the front of the track is toward the top of the bump, the rail must rotate to keep the track in contact with the profile. The program assumes that this is possible. However, due to the constant length of the track, the rail is restricted from extending this far in the rear. As the rail goes down the bump, the rear compresses once again, and during this stage, the theory and experiment give very close results.

Figure 6.24 shows the response at the front of the rail, C2. The curves all show the same basic behaviour, however, there is discrepancy at the peaks. The same explanation that was offered for C1 also applies here. As the ski hits the bump, the entire vehicle is elevated at the front and the track which is still over level ground must lift slightly off the ground. However, the program is not expected to take this into account, and therefore predicts higher values of deflection at the front than what is actually experienced. Similarly as the front of the track encounters the bump, the front compresses more than what was measured. This is due to the presumed rotation of the track as explained above and also because the shock bump-stops are not included in the model. When the centre of the track has just cleared the apex of the bump, the rail must rotate to keep the track in contact with the profile. However, this may not occur because of the length limitation of the track. Therefore, the simulation results vary from the test results. As the rear end of the track is going down the bump, the computer results match the test results very closely.

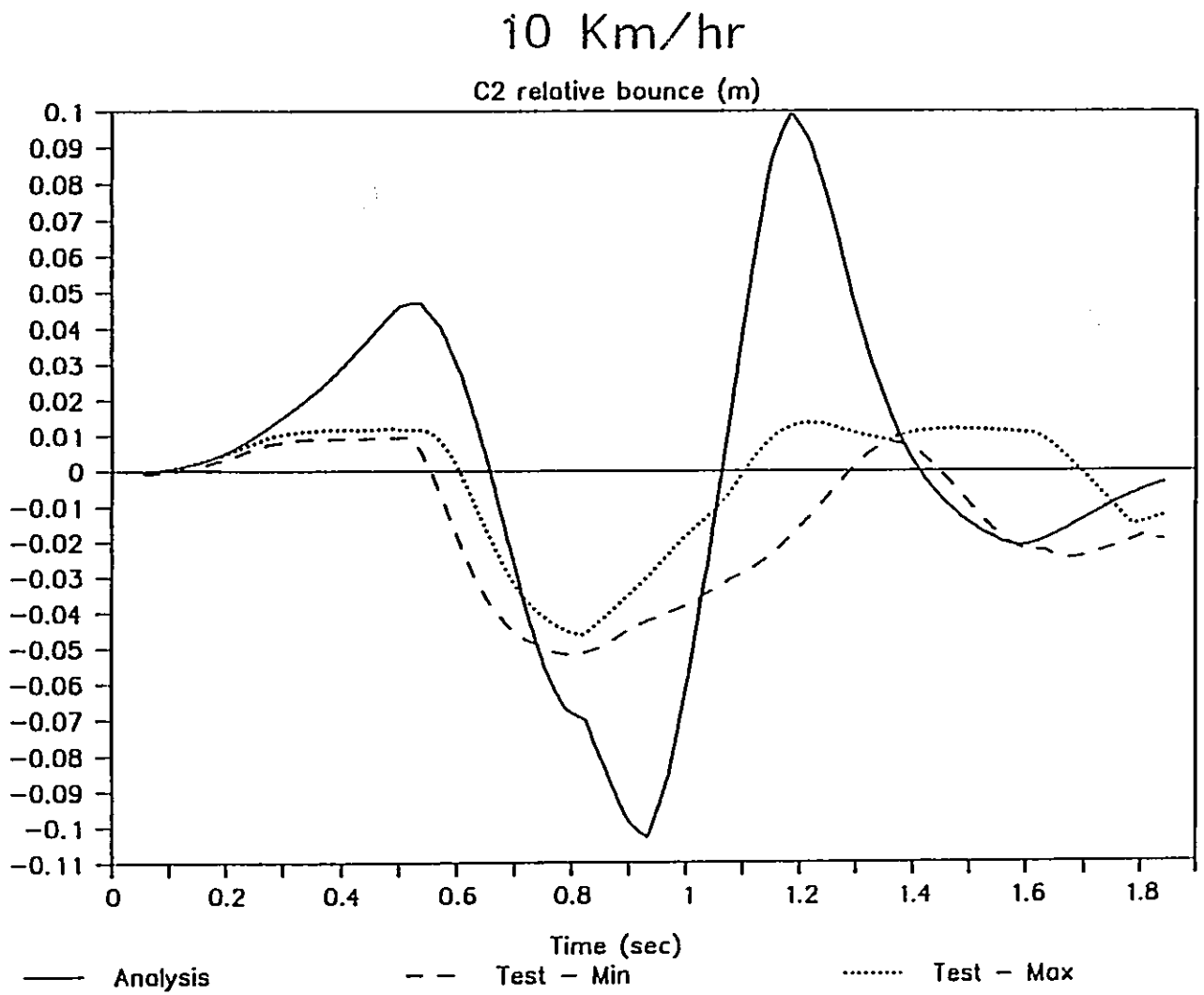

Fig. 6.24: Rail Relative deflection, C2, at 10 km/hr

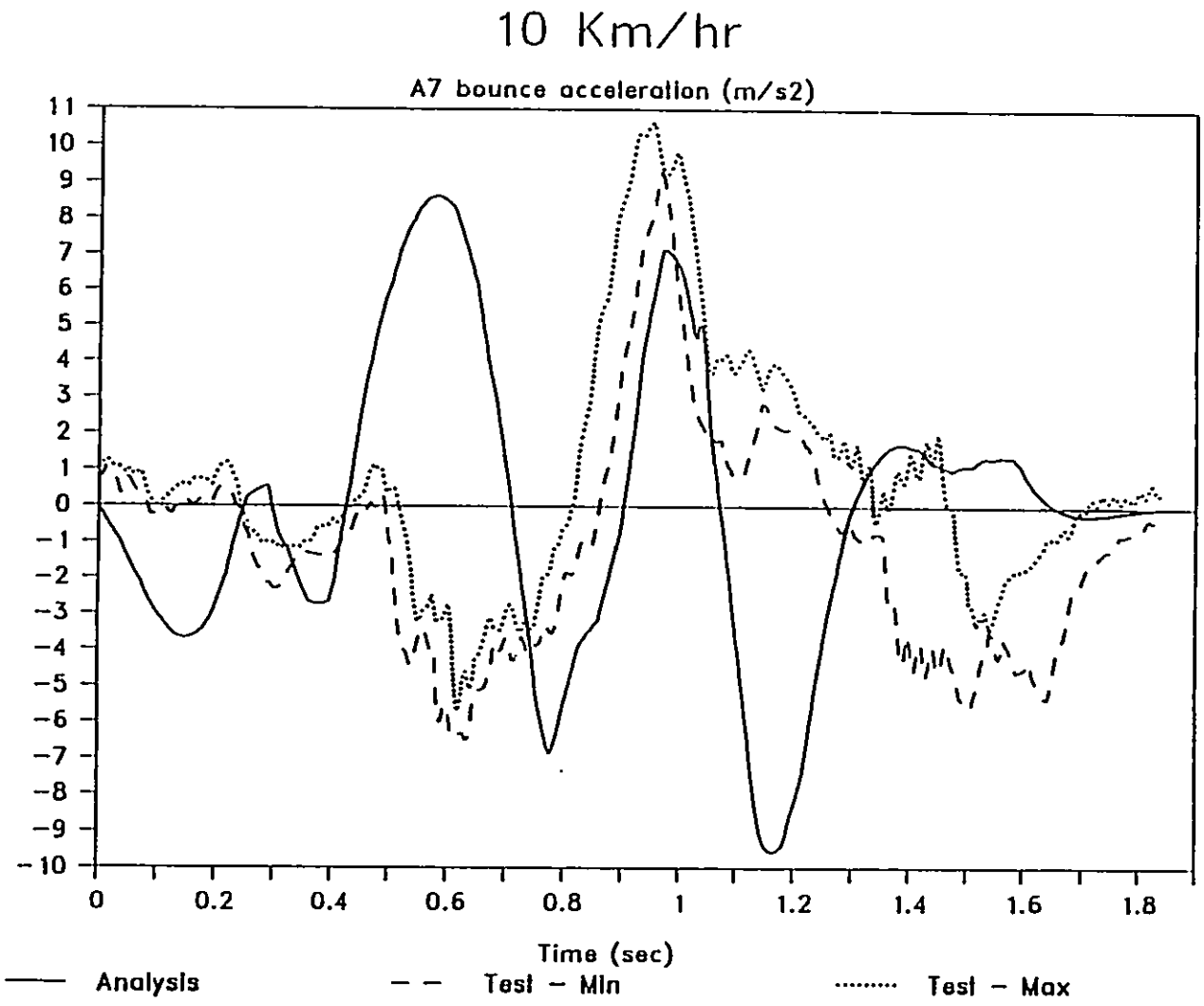

Fig. 6.25: Acceleration signal, A7, at 10 km/hr

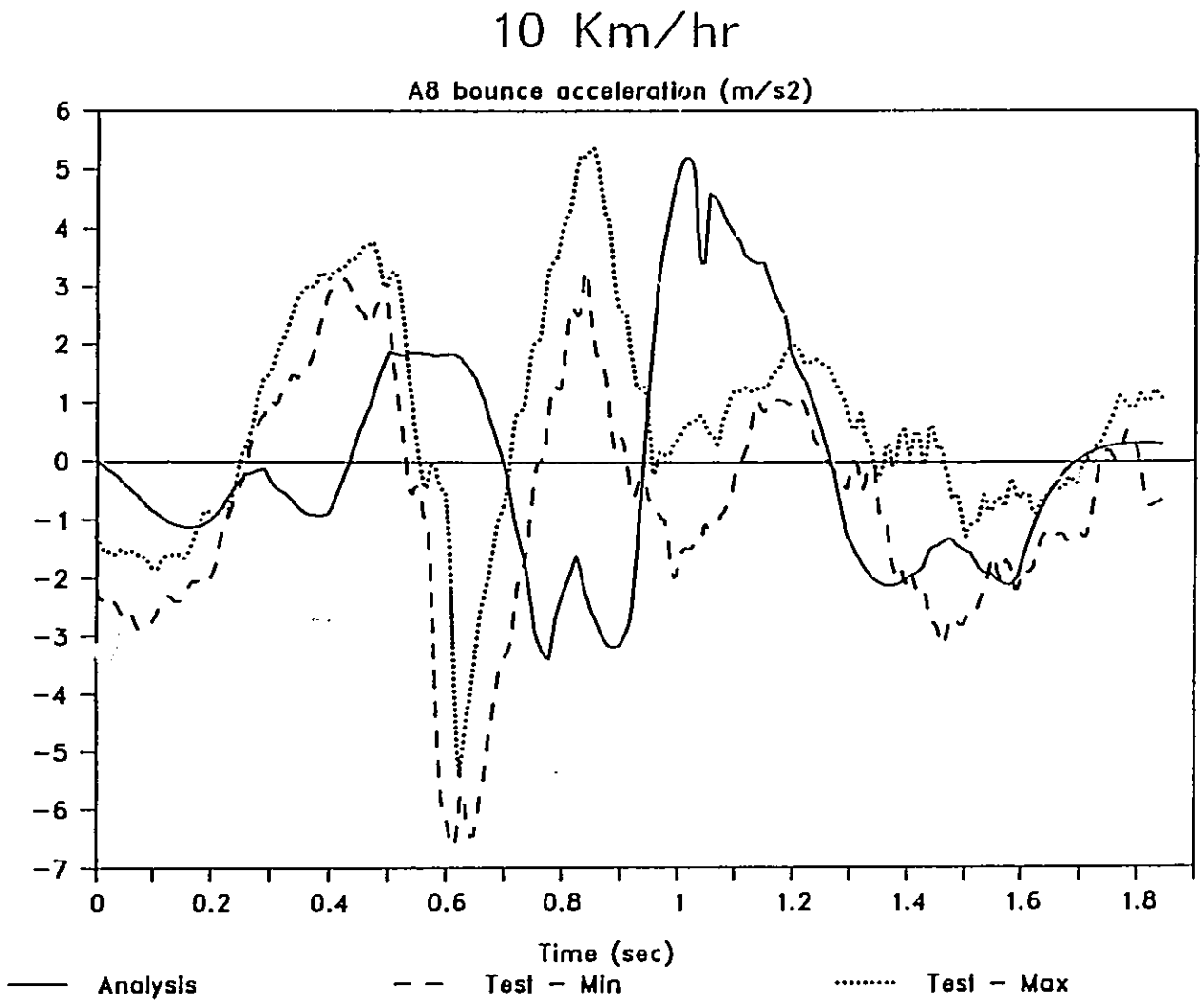

Fig. 6.26: Acceleration signal, A8, at 10 km/hr

Figure 6.25 shows the vertical acceleration on the tunnel, A7, measured almost at the very back end of the snowmobile. The test and analysis give very close peak values, as well as the same type of oscillations. However, there is some discrepancy regarding the location of the peaks on the time axis. These can be attributed to the difference in suspension forces due to the discrepancy in their deflections as seen earlier.

Figure 6.26 shows the vertical acceleration, A8, measured at the front end of the tunnel. This point is almost at the middle of the snowmobile, and is only 112 mm ahead of the system CG. The test and analysis results match very closely in peak values and the type of oscillation, except that the first negative peak is less than what was measured, and that there is a time shift as noted for A7.

6.4.3.3 Vehicle Speed of 20 Km/hr

Figure 6.27 shows the speed variation for the field test. It is steady at 19 km/hr as the ski goes over the bump. Then it drops suddenly to around 17 km/hr. The simulation considered a constant speed of 20 km/hr and therefore represents a more severe condition. This discrepancy is reflected in the results.

Figures 6.28 through 32 show the same five quantities discussed above, plotted for a nominal speed of 20 km/hr. The results are very similar to what we saw for the case of 10 km/hr tests. In comparing the

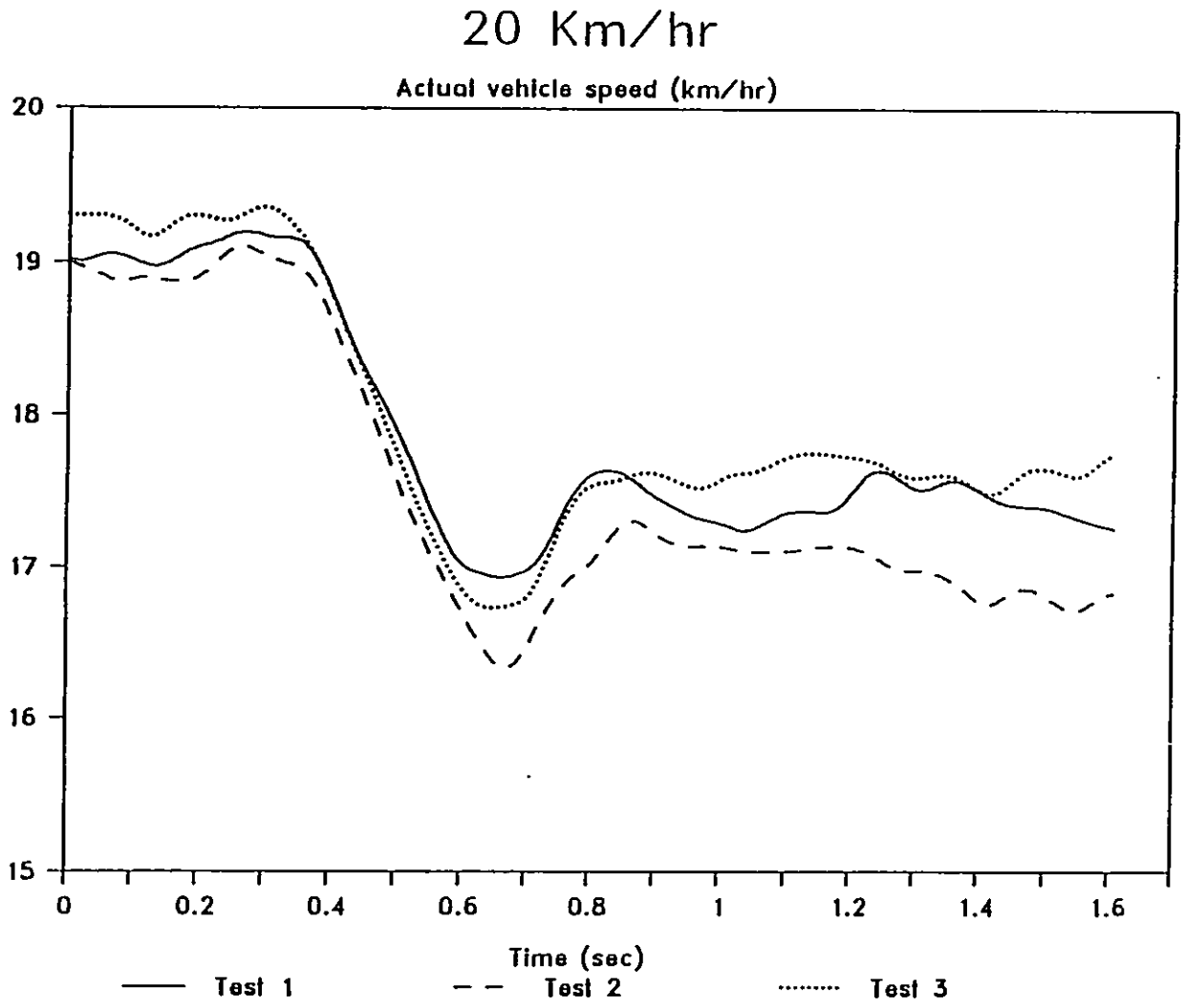

Fig. 6.27: Actual vehicle speed at 20 km/hr

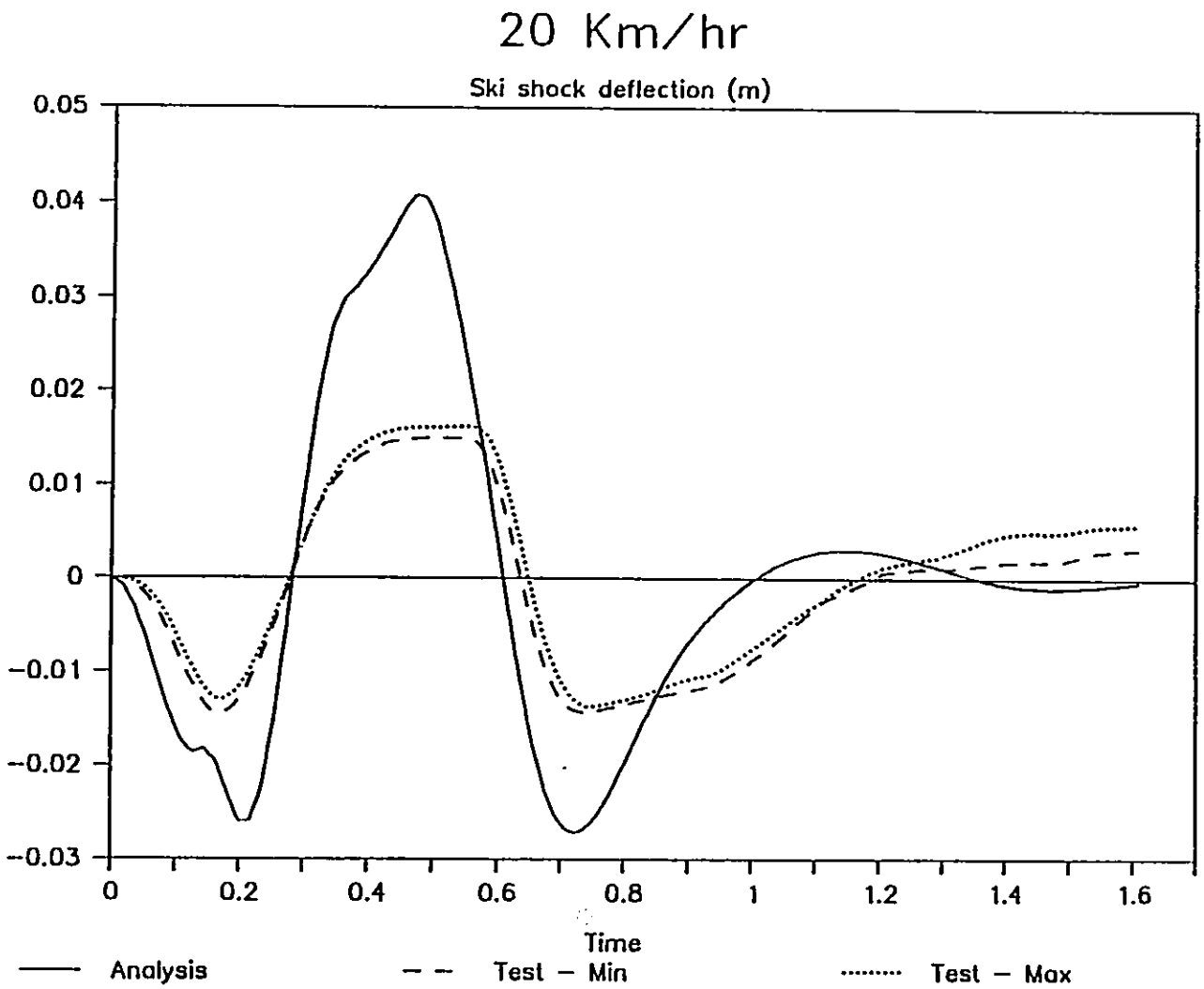

Fig. 6.28: Ski shock-absorber deflection, C3, at 20 km/hr

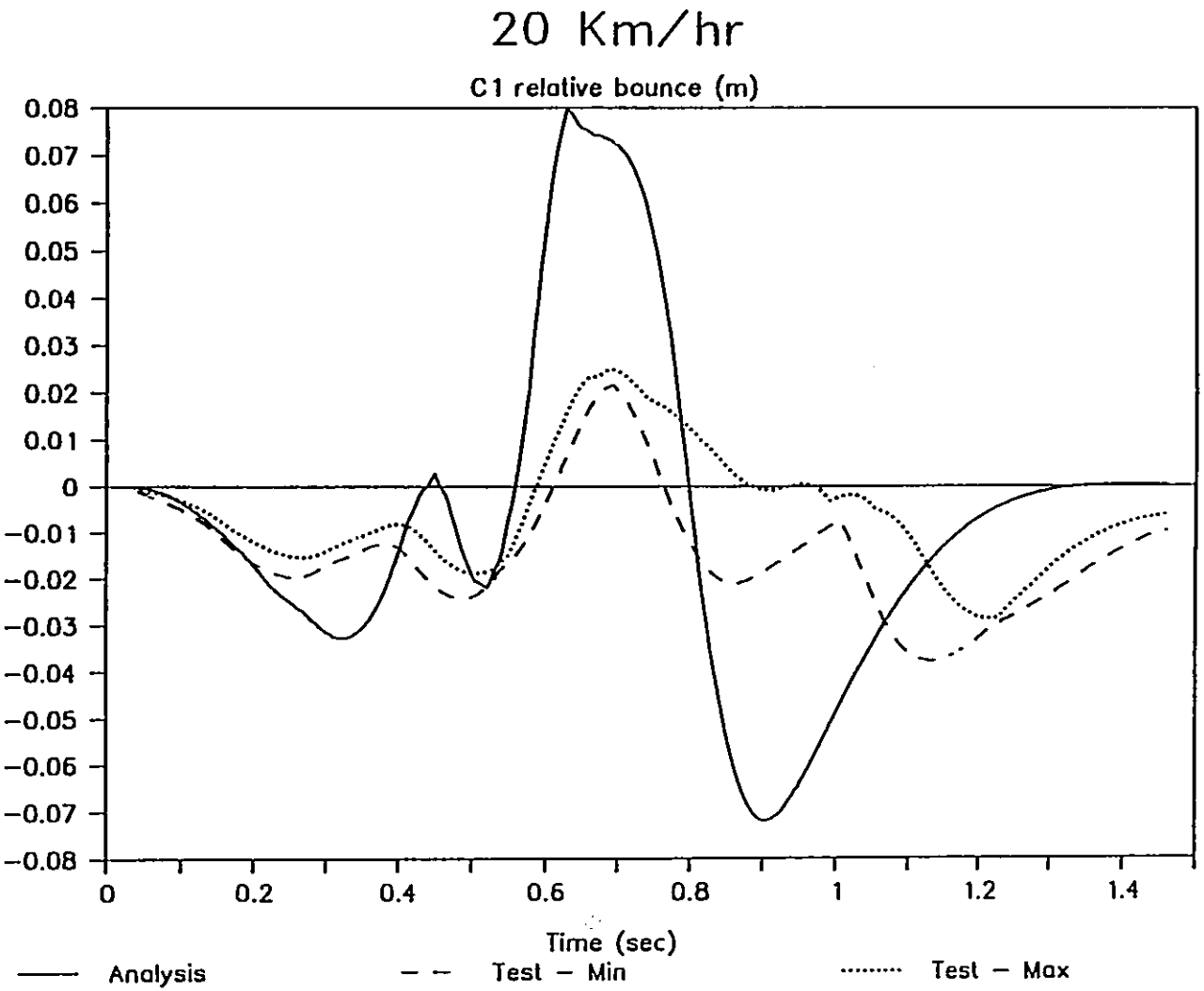

Fig. 6.29: Rail relative deflection, C1, at 20 km/hr

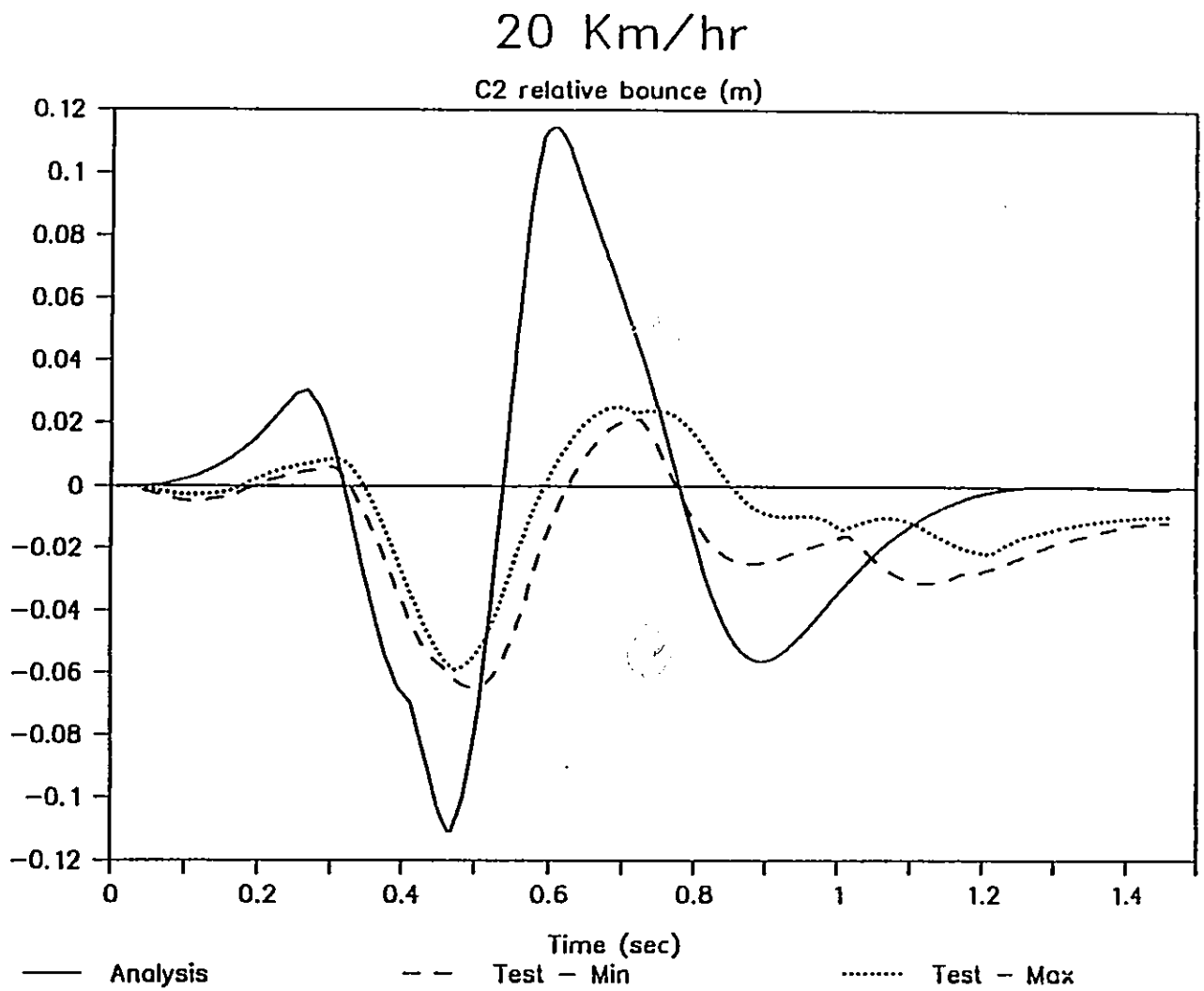

Fig. 6.30: Rail Relative deflection, C2, at 20 km/hr

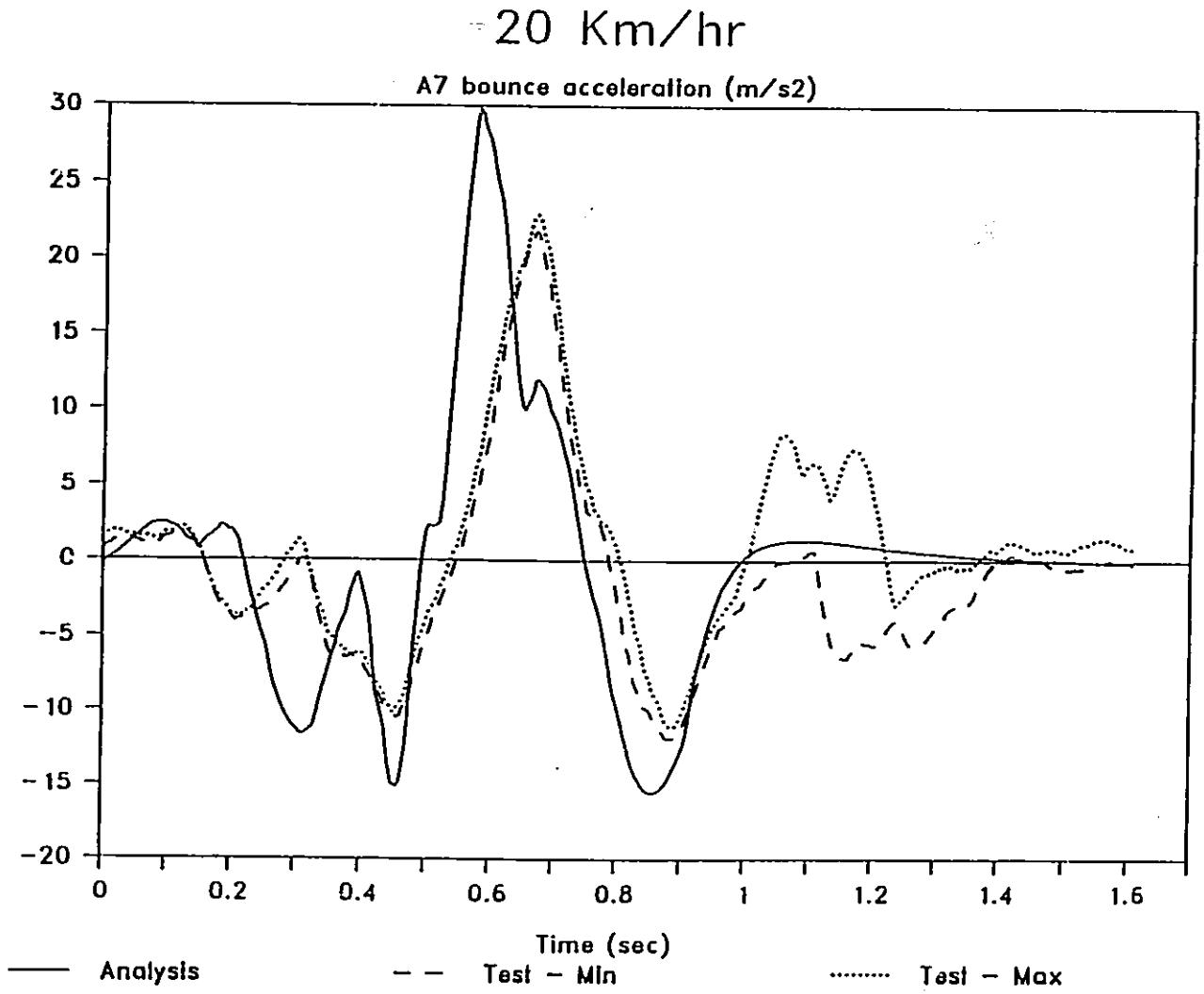

Fig. 6.31: Acceleration signal, A7, at 20 km/hr

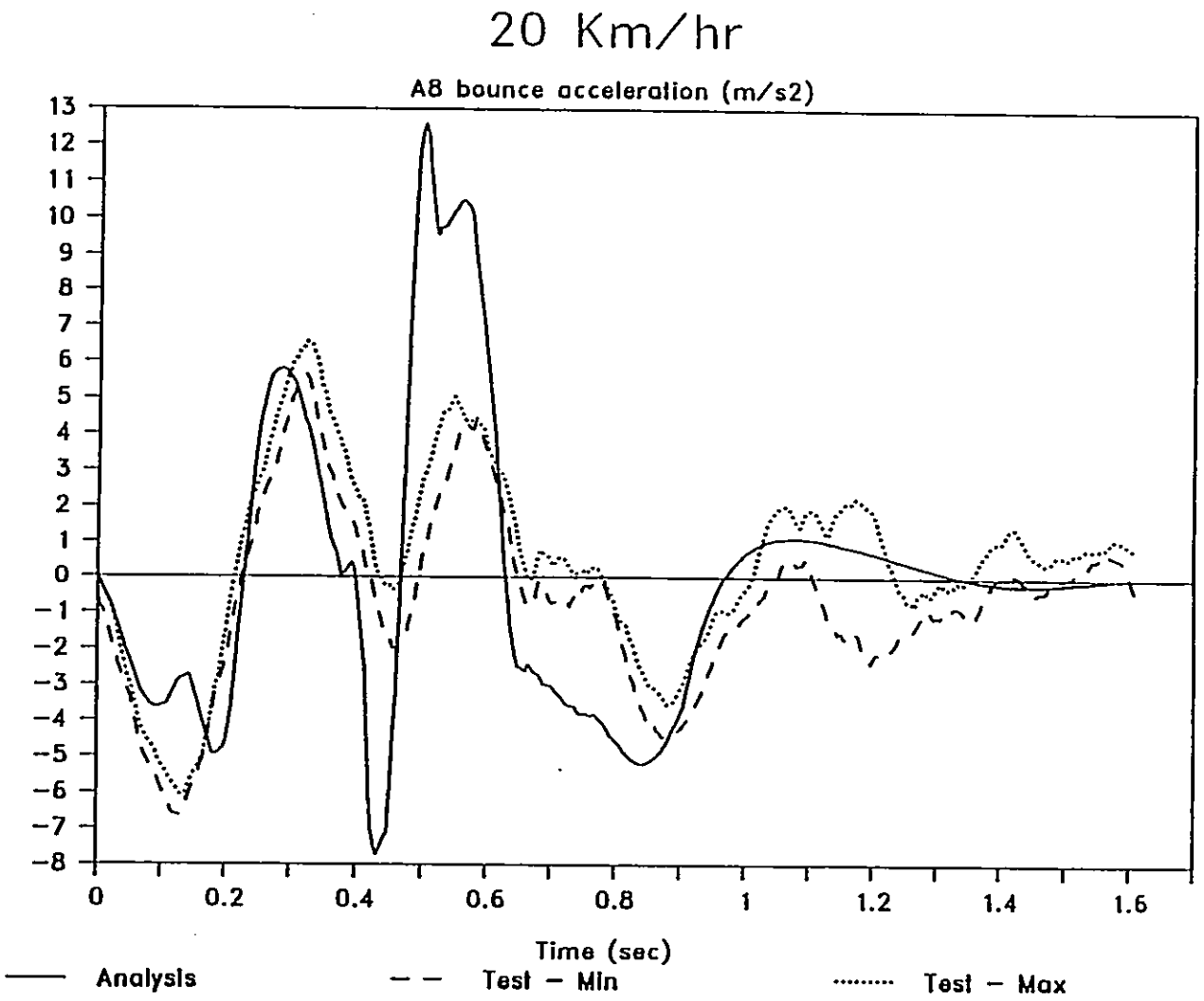

Fig. 6.32: Acceleration signal, A8, at 20 km/hr

deflections C3, C1, and C2, we find that the simulation results show peaks which are higher than the test results. Moreover this variation is more than what was observed in the case of the 10 km/hr run. The reason may be that the simulation ground profile is more severe than the real one, as pointed out earlier. The acceleration signal, A7, shows good correlation. There is a good correlation for A8 also, except that the simulation peaks are larger. From all the five figures we see that the simulation indicates the vehicle moving on level ground for time greater than 0.8 seconds. During this time, the ski and track are in constant contact with the flat ground, and the vehicle response is only due to the residual forces in the suspension. However, the test results indicate that the vehicle is still experiencing terrain inputs. This is due to the fact that the vehicle speed drops as the bump is encountered, and the whole vehicle clears it only at a later time.

6.4.3.4 Vehicle Speed of 30 Km/hr

Figure 6.33 shows the vehicle speed variation at a nominal speed of 30 km/hr. The actual speed averages about 27 km/hr. Figures 6.34 through 38 show the five measurements and analysis results plotted for the three test runs and for simulation at 30 km/hr. The results show very similar qualitative behaviour. However, it is clear that analysis results occur at a shorter time scale than experimental results. Furthermore the analysis data show generally higher peaks than test results. The main reason for this discrepancy is the same as what we discussed for the 20 km/hr case, but now the effects are more

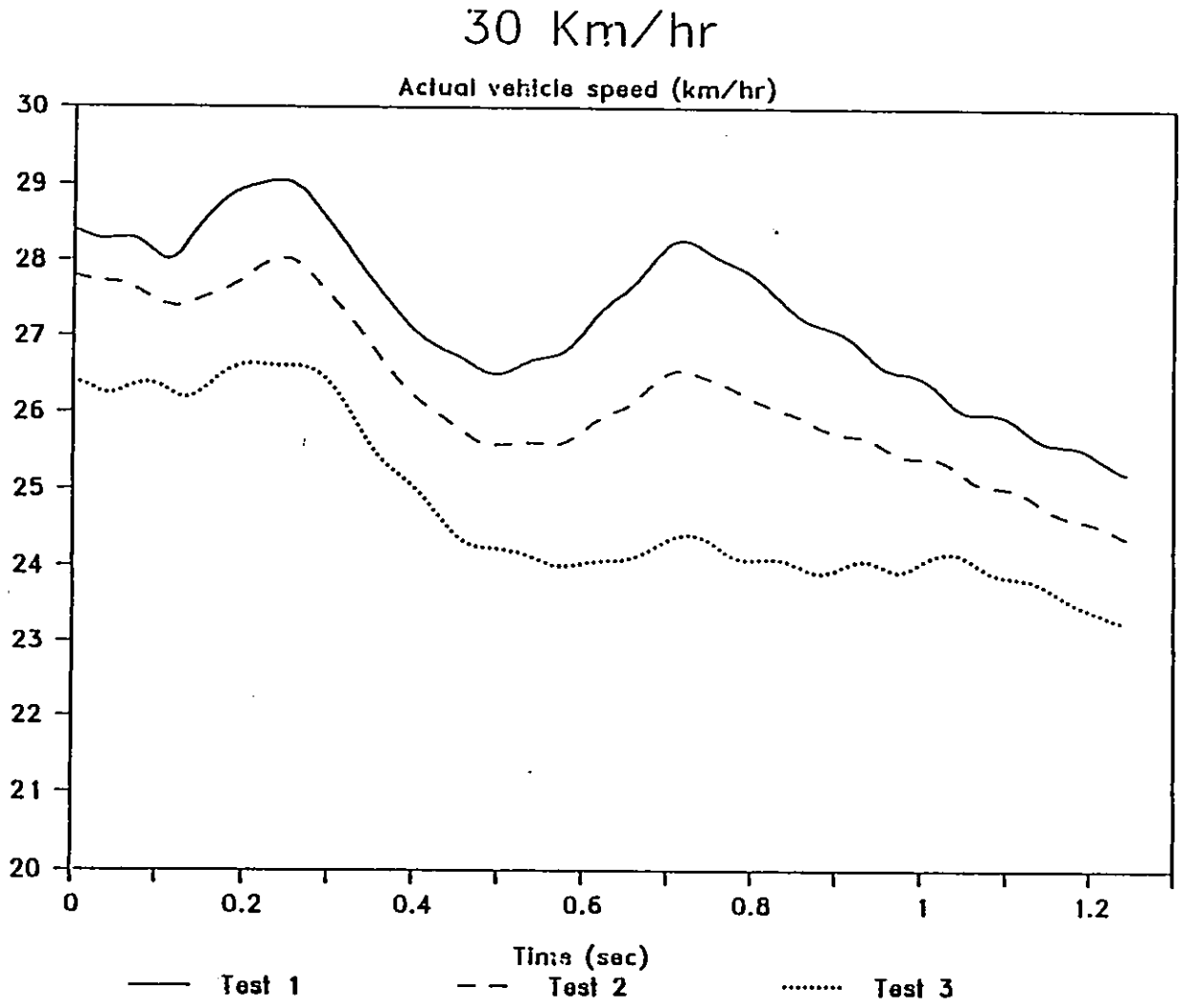

Fig. 6.33: Actual vehicle speed at 30 km/hr

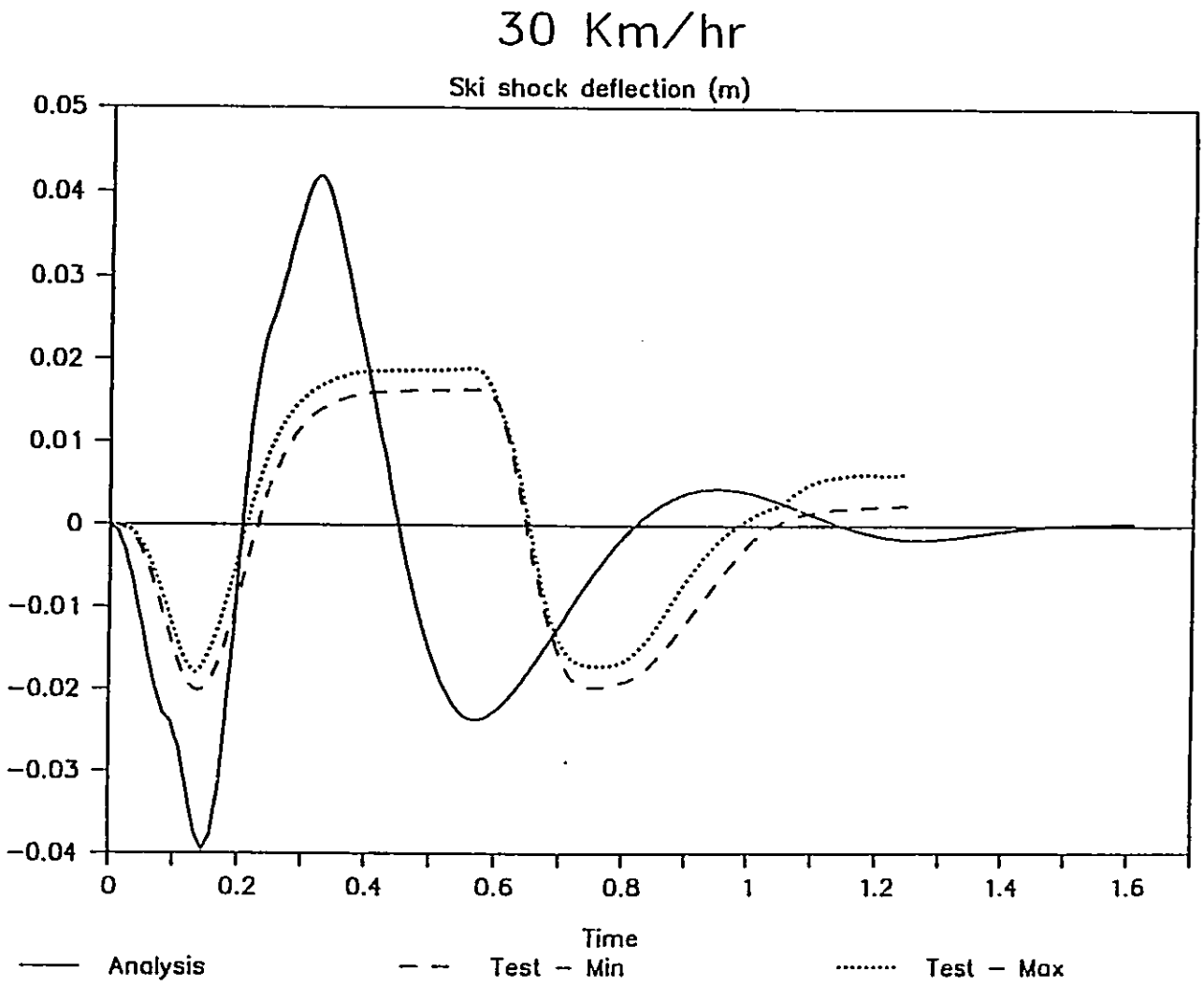

Fig. 6.34: Ski shock-absorber deflection, C3, at 30 km/hr

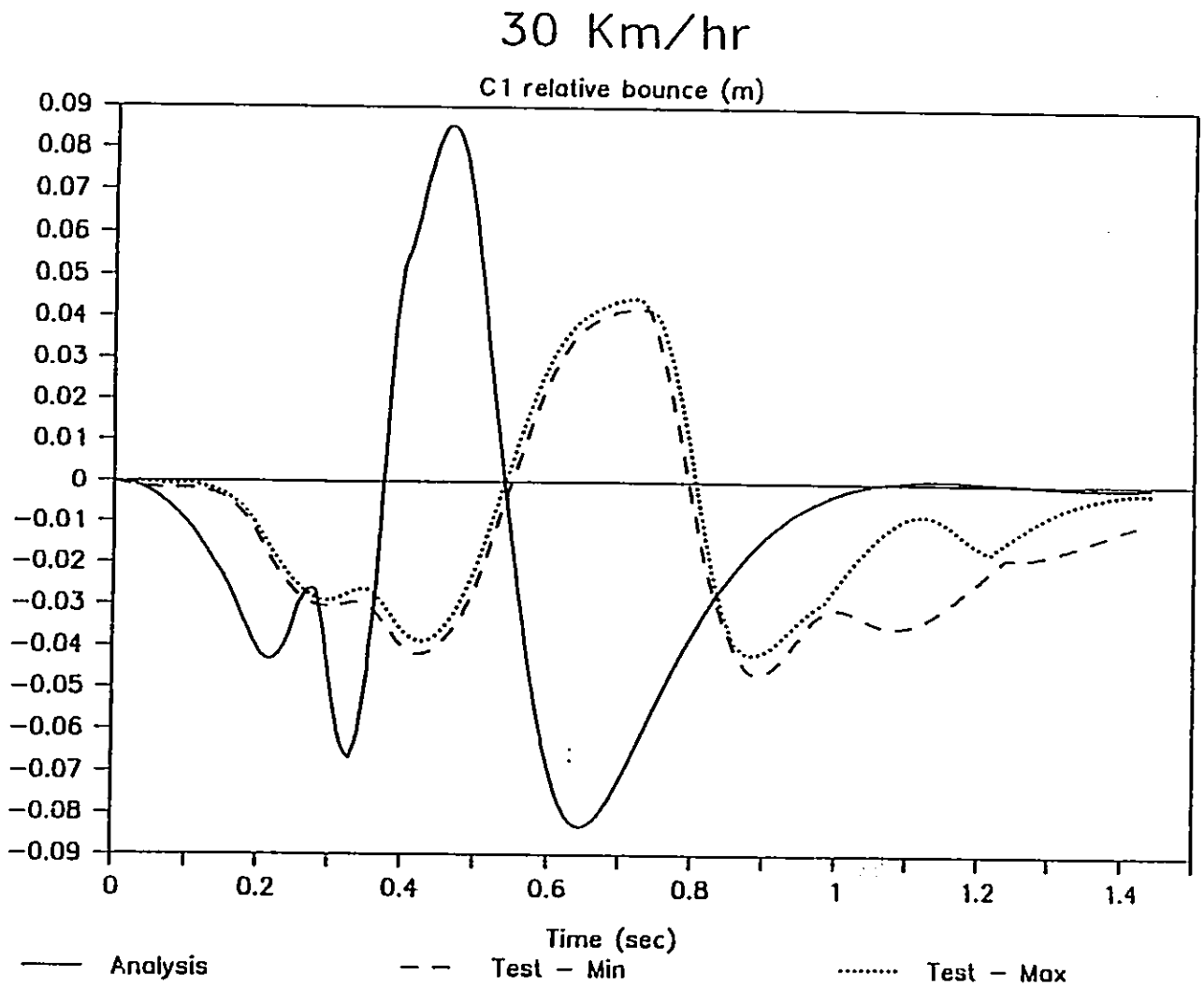

Fig. 6.35: Rail relative deflection, C1, at 30 km/hr

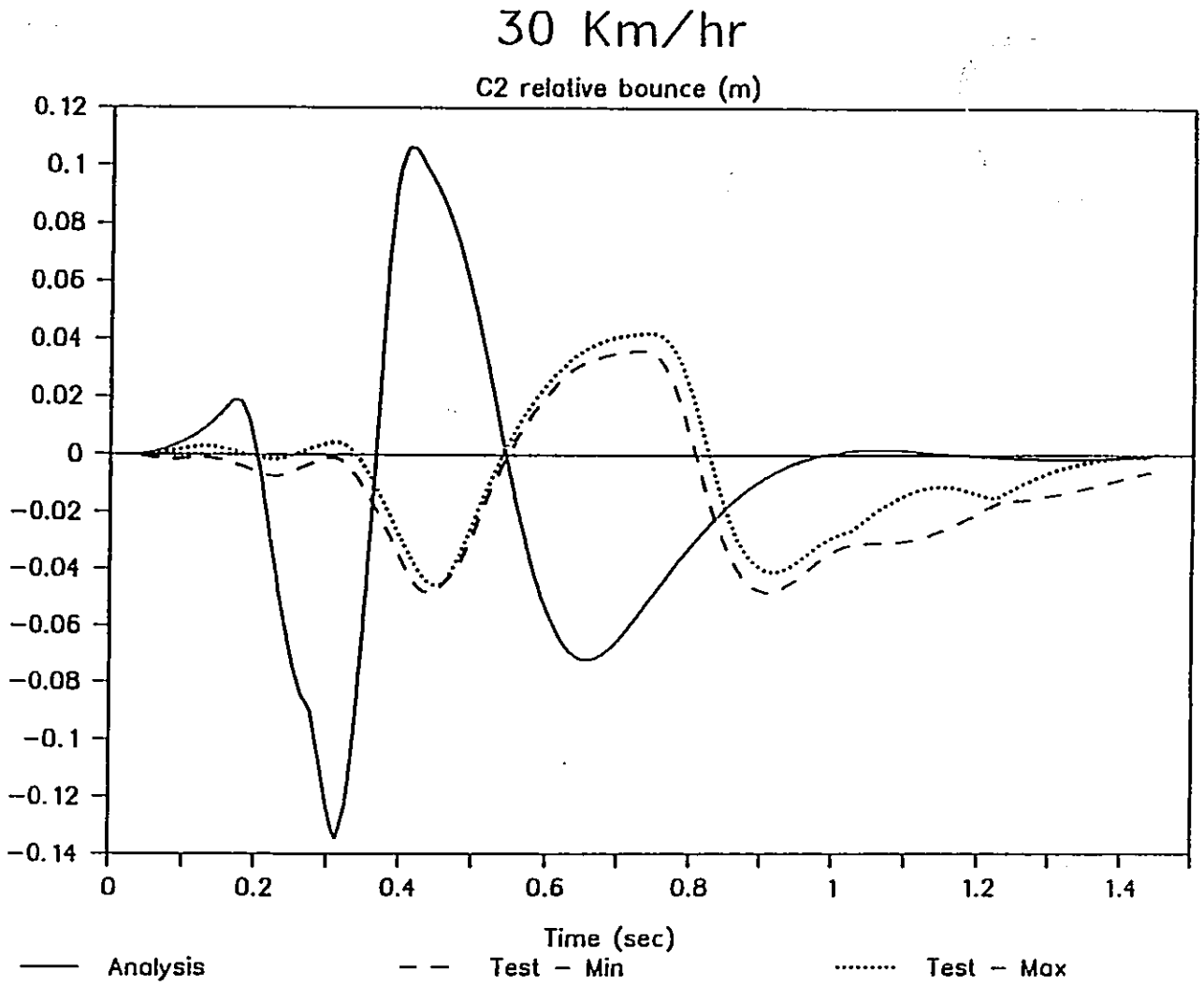

Fig. 6.36: Rail Relative deflection, C2, at 30 km/hr

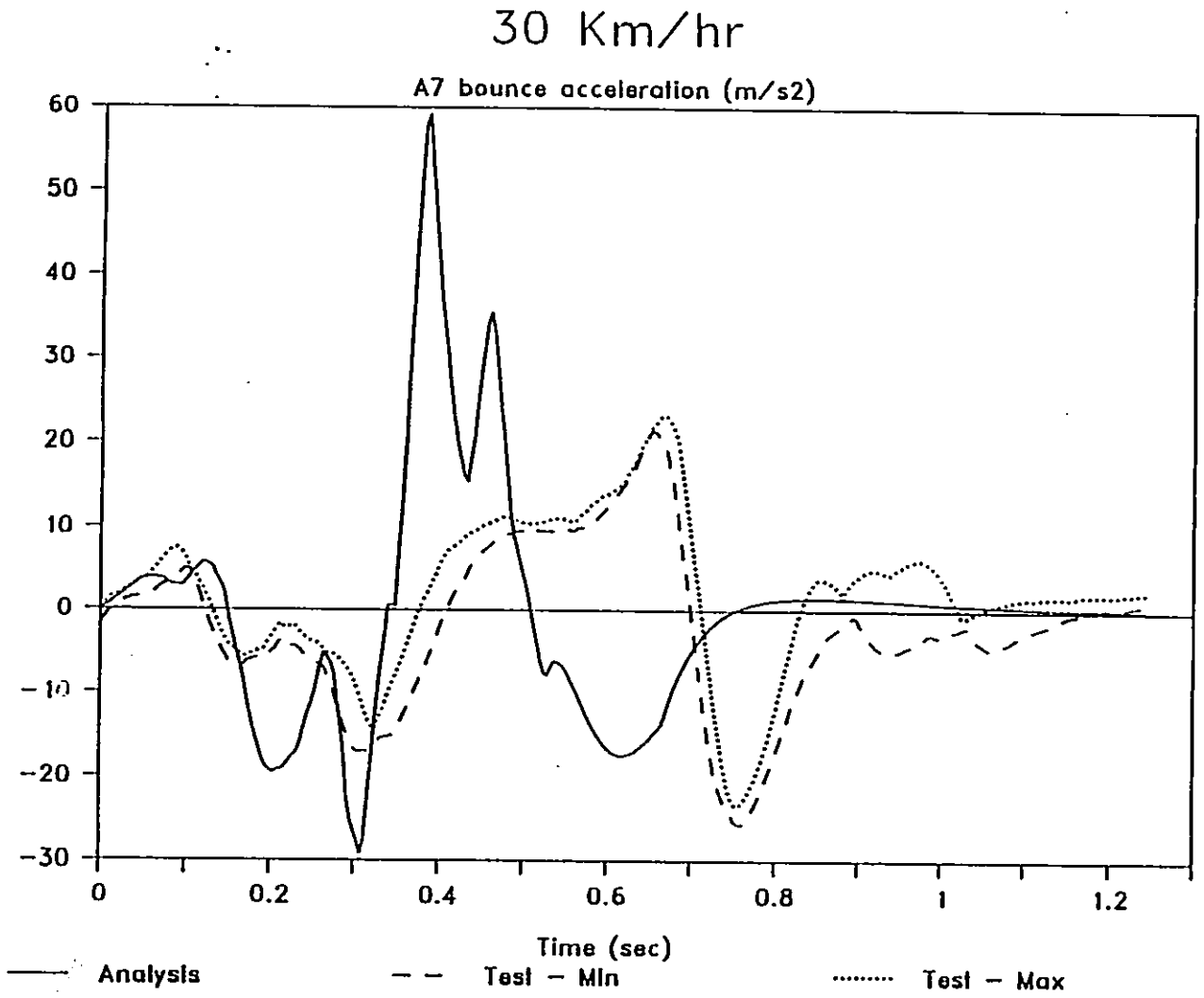

Fig. 6.37: Acceleration signal, A7, at 30 km/hr

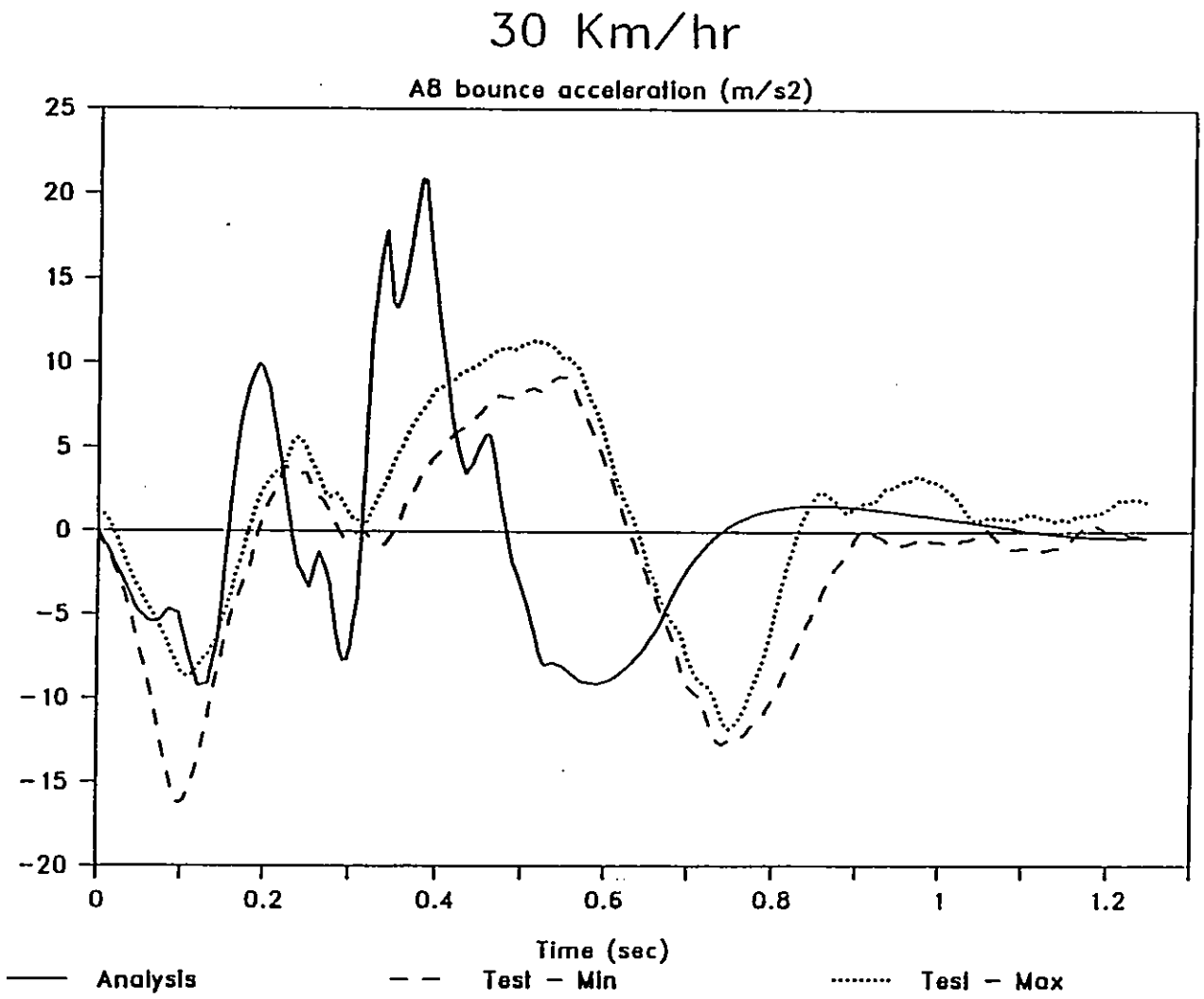

Fig. 6.38: Acceleration signal, A8, at 30 km/hr

pronounced. At a constant 30 km/hr forward speed, the vehicle must completely clear the bump in 0.53 seconds, as indicated from simulation results. However, test results indicate that there is terrain induced inputs even up to 0.8 seconds. There are two possible reasons for this - drop in speed, and the vehicle flying off the top of the bump and impacting the ground one or more times. The drop in speed effectively reduces the severity of the terrain. For these reasons the simulation results are generally higher in magnitude and shorter in duration than test results.

6.5 SUMMARY

In this Chapter we have presented a computer-aided analysis methodology for the ride dynamics of a snowmobile. The approach allows the modelling analysis and design of various subsystems in a modular fashion. For example, the kinematic analysis program determines precisely and completely, the information required for a separate dynamic analysis. The terrain pre-processor computes the trajectory of the ski and track over any specified profile. The vehicle ride dynamic model is built with bounce and pitch degrees of freedom. Computer analysis is performed to simulate the vehicle traversing a bump at 3 speeds. The simulation results are compared with data acquired from field testing.

The overall evaluation of the test and analysis results is that

they exhibit a very good level of correlation. If one takes into account the effect of speed drop in testing, the analysis and test results show excellent *qualitative* correlation. The displacements in suspension units obtained from simulation are generally higher than what were recorded on the field test. The reason for this is quite clear - the mathematical model assumes that the skis and track are in contact with ground profile at all times, and the limits of travel on the suspension units are not taken into account. When a suspension unit reaches its limit of travel in extension, in reality, the unit will lose contact with the ground. This is not a desirable behaviour, because of the consequent loss of traction and loss of control. Therefore, the simulation program helps the designer to know how much suspension travel must be available under various circumstances so that this situation can be avoided.

There is a very good correlation for acceleration peak values, especially at low speeds, between testing and simulation. Barring measurement and recording errors, a factor responsible for the discrepancies may be the bending vibrations of the tunnel structure on which the accelerometer was mounted. The tunnel is made of aluminum sheet and could presumably vibrate at frequencies close the ones we are measuring. Some other effects which may have affected the results are the driver interaction, and the effect of seat stiffness. The seat, made of foam rubber, is mounted directly on the tunnel, and the effect of seat-driver dynamics would be directly felt on the tunnel.

There are several other points of uncertainties both in the mathematical model and its numerical parameters as well as the test data. For example, the mass, moment of inertia, and CG location of the vehicle-driver system is only approximately known; damping coefficients are assumed to be constant; acceleration test data has a very high noise to signal ratio; etc.. Despite all these difficulties, we have been able to get a satisfactory correlation between theory and experiment. Therefore, it is concluded that the modelling, analysis, and interpretation of simulation results are reasonably valid.

Chapter 7

CONCLUSIONS AND RECOMMENDATIONS FOR FUTURE WORK

7.1 HIGHLIGHTS OF THE PRESENT WORK

As set out in Chapter 1, the overall objectives of this research program have been (1) to create an analytical formulation that is suitable for digital computer implementation which allows the engineer to input data that defines a mechanical system of interest (especially vehicle systems) and automatically generates the governing equations; (2) to develop and implement numerical algorithms that automatically solve the equations for dynamic response of the system, and provide computer graphic output of the results to the designer or analyst; (3) to develop new techniques for the analysis and design of suspension linkages; (4) to implement these in a general purpose program; and (5) to use these techniques and software for the analysis of suspension systems for a snowmobile.

These objectives have been accomplished as presented in the preceding chapters. In the present chapter, we point out some highlights of the work and summarize the main findings. We also present some recommendations for future work based on the present research.

A notable aspect of the research presented in this thesis is that the subject matter is very general. This is in contrast to most others, where problems pertaining to *specific* systems are studied in detail. Our aim has been to formulate *general* methods for modelling and analyzing vehicle multi-body systems, which lead to computerized solution. *General purpose* computer programs have been developed which relieve the engineer of a lot of routine manual calculations and programming when studying a wide class of systems. Our overall aim has been to develop *tools* which may be applied in a variety of problems, and we have illustrated their use through many examples.

General multi-body dynamic formalisms and computer programs are of course not new ideas, and have been pursued by many researchers. What is new is the approach we have taken to model vehicle systems, realizing their particular nature, in contrast to a general mechanism model approach. The mechanism approach models the vehicle and the interacting environment as a spatial mechanism. This leads to a very complex and expensive-to-build model which has two main drawbacks - inability to be used in all but transient response simulations, and voluminous output which are hard to interpret in terms of basic system properties. Using the methods and software we have developed, the vehicle system dynamicist can easily model systems in a conventional manner in terms of the schematic representations of various subsystems.

These methods and software are based on a dichotomy apparent in the dynamics of vehicle multi-body systems – the large relative deflections

in the suspension linkages of small masses, and the small relative deflections in the sprung bodies of large masses. The suspension links may contain closed-loop kinematic chains, whereas the sprung masses may only have open kinematic chains. We do not model the vehicle system as large-deflection mechanism as in ADAMS and DADS, or as a small-deflection-only system as in MEDYNA. Large-deflection analysis of the suspension mechanisms is performed separately and prior to the small-deflection-only analysis of the total vehicle system.

Kinematic analysis techniques for suspension linkages have been presented in detail. Suspension force generation characteristics are presented in terms of the generalized coordinates that define its degrees of freedom, using the method of velocity coefficients. The kinematic modelling and analysis extracts only these geometric characteristics so that damping and stiffness parameters can still be varied at will during the dynamic analysis stage. Sensitivity analysis of velocity coefficients and deflections are also presented so that suspension linkages may be designed to give required force-deflection characteristics.

In the course of suspension kinematic analysis, we have examined the concept of roll centres, which is very popular among racing car suspension designers. We have exposed some conflicts in the existing definitions of roll centre. Using the method of velocity coefficients we have presented a general analytical method for determining roll centre location and roll stiffness. The older method uses graphical

constructions and is applicable only to one-degree-of-freedom systems.

Two new software packages which embody the methods and philosophy advanced in thesis have also been developed and presented. These packages are distinguished by the fact that they are based on a schematic, sketch-pad approach to modelling. Using a minimum amount of data the user can interactively build a system model in a schematic form. The system equations are automatically derived in symbolic form and solved for a variety of options common to vehicle system analysis.

We have also formulated suspension and ride dynamics models of a snowmobile. Analyses were carried out using the general purpose software developed. Ride analysis of modern racing snowmobiles have not been presented elsewhere in literature. The analysis results compare favorably with results obtained from field testing.

7.2 GENERAL CONCLUSIONS

We have shown that a large class of mechanical systems, especially vehicle systems, can be modelled as free multi-body systems or constrained multi-body systems in tree configuration. If the internal forces in force-generating elements are proportional or proportional-differential forces, the system equations can be derived in closed form with a minimal set of variables. Each body may be modelled with only the necessary number of Lagrangian coordinates representing

its degrees of freedom. Thus, one may have one-degree-of-freedom bodies, two-degree-of-freedom bodies, or six-degree-of-freedom bodies. Equations are derived in an inertial frame which may move at a constant velocity with respect to the ground-fixed frame, so that large reference-frame motion of vehicles can be accommodated without numerical difficulties.

We have demonstrated that the velocity coefficient method can be employed to model linkage suspensions as equivalent two-port force generators, still maintaining their nonlinearities due to large deflections. This modelling approach affords the engineer a better understanding of the problems, thereby leading to better and faster solutions. The procedure can be used to determine both handling and ride characteristics of a linkage suspension. For ride the suspension system is modelled to determine its vertical force deflection characteristics in terms of velocity coefficients. For handling analysis, the method yields variations of all kinematic parameters, as well as, the location of roll centre and roll stiffness. We have discussed and clarified several confusing points with regard to the concept of roll centre, and presented a new definition as well as a convenient way of computation based on velocity coefficients.

7.3 RECOMMENDATIONS FOR FUTURE WORK

Future work which may be based on the present foundation falls into

two categories, namely, analytical development, and software development. Recommendations for analytical work may be summarized as follows:

1. Include friction-stiction effects in force elements. In the present formulation friction forces can be accounted for as long as motion exists. When the amount of friction is such that a joint is locked-up (stiction), the force-element acts as a rigid link, creating additional kinematic constraints. A formalism based on maximal set of equations and a constraint addition-deletion strategy is implemented in the 2D version of DADS [131]. Since friction or stiction in suspension elements will not cause closed kinematic loops of sprung bodies in most vehicle system models, a constraint addition-deletion strategy can also be implemented based on the formalism presented in this thesis.

2. In constraint addition-deletion occurring due to stiction mentioned above, we are dealing with systems that change their topologies during motion. Another phenomenon that causes the same effect is wheel-hop. In vehicle systems wheels may occasionally lose contact with the ground. The constraint due to contact is really a non-holonomic constraint. However, the assumption of holonomy is generally valid as long as contact exists. When a wheel is no longer in contact it not constrained by the ground profile and a different set equations of motion might apply. The formalism, as well as, the computer code may be enhanced to take this into

account.

3. In the dynamic analysis of vehicle systems we have modelled sprung masses as rigid bodies. The flexibilities of these bodies may have significant effect on the overall dynamics when large wheel spans or small structural stiffnesses are present. The formalism may be extended to include the flexibility and mass distribution effects [132].

4. The definition of roll centre, and a method for determination of its location and roll stiffness has been presented for a planar system. In the 3-dimensional case we have a roll axis, instead of a roll point. The theory developed in Chapter 4 can easily be extended to this case also.

5. Another extension of the present work is the use of expert systems or artificial intelligence techniques in building vehicle system models. As we mentioned earlier, modelling is a very intuitive process, since no one can say there is one and only one model which should be used to study a particular problem. Simpler models may not exhibit all the necessary characteristics of a system which are being investigated, and more complex models are expensive to build and hard to interpret. With help of a model knowledge base, an expert system may guide the analyst in the modelling process. Viable applications of expert systems in mechanical system modelling and analysis are not reported in numbers, although these

are certainly growing [133].

6. Active and semi-active controls are gaining prominence in suspension systems. This brings electronic sensing, and electrical, pneumatic or hydraulic control as integral parts of a suspension systems in addition to springs, dampers and linkages we have considered. A modelling formalism which is touted to be able to handle such a multi-domain systems is the bond-graph method [134]. However, at present the formalism is not well developed to handle kinematic constraints. Future developments in this area will definitely be of use to vehicle dynamics.

The software packages that have been developed can certainly be extended through the implementation of analytical developments mentioned above. Besides them, there are a number of other recommendations for software development work, which may be summarized as follows:

1. Extend CAMSYD to full 2D. Presently the component menu contains only one and two degree-of-freedom masses. Addition of a three degree-of-freedom rigid body will give a full planar capability to CAMSYD.

2. Extend CAMSYD to 3D. The theoretical basis for equation derivation will be the same. However, the main difficulty will be in designing an easy-to-use graphics based 3D sketch-pad as the

pre-processor. Linkage suspension subsystems will be represented as equivalent force generators using a 3D version of GENKAD.

3. Include sensitivity analysis option in CAMSYD for frequency domain computations. These will include eigenvalue and eigenvector sensitivities to design, as well as, sensitivities of frequency response functions. The theory for these already exists [135] and are increasingly being used for vehicle system design [136].

4. Implementation of a full optimization scheme is a logical next step after sensitivity analysis. Instead of using a general nonlinear programming approach, one can make use of the state-space description of system equations, both in kinematics and dynamics, and use state-space methods of optimal design as detailed in the text book by Haug and Arora [110].

5. Another improvement in software implementation would be to integrate GENKAD and CAMSYD into a single software package with the same graphical interface and syntax. One could then build and alter detailed kinematic models of suspension linkages while building the overall lumped parameter dynamic model.

REFERENCES

1. Korn, A., and Wait, J.V., *Digital Continuous System Simulation*, Prentice Hall, Englewood Cliffs, New Jersey, 1978.

2. Haug, E.J., "Elements and Methods of Computational Dynamics", in Ref. [3], pp. 3-38, 1984.

3. Haug, E. J., ed., *Computer Aided Analysis and Optimization of Mechanical System Dynamics*, NATO ASI Series, Springer-Verlag, Heidelberg, FRG, 1984.

4. Magnus, K., ed., *Dynamics of Multibody Systems*, Proceedings of the IUTAM Symposium, Munich, 1977, Springer-Verlag, Berlin, FRG, 1978.

5. Schiehlen, W.O., ed., *Proceedings of the IUTAM/IFToMM Symposium on Dynamics of Multibody Systems*, September 15-21, 1985, Udine, Italy, Springer-Verlag, Hiedelberg, 1986.

6. Pater, A.D., and Pacejka, H.B., ed., *3rd Seminar on Advanced Vehicle System Dynamics*, Proceedings of the third ICTS Seminar, Amalfi, Italy, 1986, Swets & Zeitlinger, Lisse, 1987.

7. Kortüm, W., and Schiehlen, W., "General Purpose Vehicle System Dynamics Software Based on Multibody Formalisms", *Vehicle System Dynamics*, Vol. 14, Nos. 4-6, pp. 229-263, 1985.

8. Wittenberg, J., "Dynamics of Multibody Systems", *Proceedings of the XVth IUTAM/ICTAM Congress*, Toronto, Ontario, pp. 197-207, 1980.

9. Paul, B., "Analytical Dynamics of Mechanisms - A Computer Oriented Overview", *Mechanism and Machine Theory*, Vol 10, pp. 481-507, 1975.

10. Paul, B., "Computer Oriented Analytical Dynamics of Machinery", in Ref. [4], pp. 41-87.

11. Wittenberg, J., *Dynamics of Rigid Bodies*, Teubner, Stuttgart, FRG, 1977.

12. Wittenberg, J., "Analytical Methods in Mechanical System Dynamics", in Ref. [4], pp. 89-127.

13. Hargreaves, B., "GMR DYANA: The Computing System and its Applications", *General Motors Engineering Journal*, 8(1), pp. 7-13, 1961.

14. Lewis, C.R., "GMR DYANA: Extending the Computing System to Solve more Complex Problems", *General Motors Engineering Journal*, 8(1), pp. 14-18, 1961.

15. Ferrer, D.R., "Computer-Aided Analysis of Dynamic Behaviour of Lumped Parameter Mechanical Structures Using Electrical Network

Techniques", in *Engineering Software*, Adey, R.A., ed., Pentech Press, London, England, 1980.

16. Andrews, G.C., and Kesavan, H.K., "The Vector-Network Model: A New Approach to Vector Dynamics", *Mechanism and Machine Theory*, Vol 10, pp. 57-75, 1975.

17. Andrews, G.C., and Kesavan, H.K., "Simulation of Multibody Systems Using the Vector-Network Model", in Ref. [4], pp. 1-13, 1978.

18. Richard, M.J., Anderson, R.J. , "Dynamic Simulation of Three-Dimensional Rigid Body Systems Using the Vector-Network Method", *Mathematics and Computers in Simulation* , 26, pp. 289-296 1984.

19. Li., T-W., and Andrews, C.C., "Application of Vector-Network Method to Constrained Mechanical Systems", *ASME Journal of Mechanisms, Transmissions and Automation in Design*, 1987.

20. Ormrod, M.K., and Andrews, G.C., "ADVENT: A Simulation Program for Constrained Kinematic and Dynamic Systems", *ASME paper no. 86-DET-97*, Presented at the Design Engineering Technical Conference, Columbus, OH, 1986.

21. Chou, J.C.K., Kesavan, H.K., Singhal, K., "Dynamics of 3-D Isolated Rigid-Body Systems: Graph-Theoretic Models", *Mechanism and Machine Theory*, 21 (3), pp. 261-272, 1986

22. Chou, J.C.K., Singhal, K., Kesavan, H.K., "Multi-Body Systems with Open Chains: Graph Theoretic Models", *Mechanism and Machine Theory*, 21 (3), pp. 273-284, 1986.

23. Andrews, G.C., Richard, M.J., Anderson, R.J., "A General Vector-Network Formulation for Dynamic Systems with Kinematic Constraints", *Mechanism and Machine Theory*, 23 (3), pp. 243-256, 1988.

24. Richard, M.J., "Dynamic Simulation of Multibody Mechanical Systems Using the Vector-Network Model", *Transactions of the Canadian Society of Mechanical Engineers*, 12(1), pp. 21-30, 1988.

25. Nikravesh, P. E., "Some Methods for Dynamic Analysis of Constrained Mechanical Systems: A Survey", in Ref. [3], pp. 351-368, 1984.

26. Gear, C.W., "Differential Algebraic Equations", in Ref. [3], pp. 323-334, 1984.

27. Chace, M.A., and Bayazitoglu, "Development and Application of a Generalized d'Alembert Force for Multifreedom Mechanical Systems", *ASME Journal of Engineering. for Industry* 93, pp. 317-327, 1971.

28. Chace, M.A., "DAMN - A Prototype Program for the Dynamic Analysis of Mechanical Networks", *Proceedings of the SHARE/ACM/IEEE 7th*

Design Automation Workshop, 1970.

29. Chace, M.A., "DAMN - A Digital Computer Program for the Dynamic Analysis of Generalized Mechanical Systems", *Transactions of the SAE*, Paper No. 710244, 1971.

30. Chace, M.A., and Angell, J.C., "Interactive Simulation of Machinery with Friction and Impact Using DRAM", *Transactions of the SAE*, Paper No. 770050, 1977.

31. Orlandea, N., Chace, M. A., and Calahan, D. A., "A Sparsity Oriented Approach to the Dynamic Analysis and Design of Mechanical Systems-- Parts I and II", *ASME Journal of Engineering for Industry*, Series B, Vol. 99, pp. 733-779, 780-784, 1977.

32. Chace, M. A., "Methods and Experience in Computer Aided Design of Large-Displacement Mechanical Systems", in Ref. [3], pp. 233-255.

33. Haug, E. J, Wehage, R. A., and Barman, N. C., "Dynamic Analysis and Design of Constrained Mechanical Systems", *ASME Journal of Mechanical Design*, Vol. 104, pp. 778-784, 1982.

34. Wehage, R.A., and Haug, E.J., "Generalized Coordinate Partitioning for Dimension Reduction in Analysis of Constrained Dynamic Systems", *ASME Journal of Mechanical Design*, 104(1), pp. 247-255, 1982.

35. Gear, C.W., "Differential - Algebraic Equations", in Ref. [3], pp. 323-334, 1984.

36. Mani, N.K., Haug, E.J., and Atkinson, K.E., "Application of Singular Value Decomposition for Analysis of Mechanical System Dynamics", *ASME Journal of Mechanisms Transmissions and Automation in Design*, 107(1), pp. 82-87, 1985.

37. Kim, S.S., and Vanderploeg, M.J., "QR Decomposition for State Space Representation of Constrained Mechanical Dynamic Systems", *ASME Journal of Mechanisms Transmissions and Automation in Design*, 108(2), pp. 183-188, 1986.

38. Seth, P. N., and Uicker, J. J., Jr., "IMP (Integrated Mechanism Program), A Computer Aided Design Analysis System for Mechanisms and Linkages", *ASME Journal of Engineering for Industry*, Vol. 94, pp. 454-464, 1972.

39. *I-DEAS Level 4, User Guide*, Structural Dynamics Research Corporation, Milford, OH, 1988.

40. Duffek, W., Kortüm, W., and Wallrapp, O., "A General Purpose Program for the Simulation of Vehicle-Guideway Interaction", in *Dynamics Dynamics of Vehicles on Roads and on Tracks*, Slibar, A., and Springer, H., eds., (Proc. 5th VSD - 2nd IUTAM Symposium, Vienna, Austria), Swets & Zeitlinger, Amsterdam, pp. 105-126, 1977.

41. Wallrapp, O., "MEDYNA, An Interactive Analysis and Design Program for Flexible Multibody Vehicle Systems", in Ref. [6], pp. 166-188, 1987.

42. Schiehlen, W.O., Kreuzer, E.J., "Symbolic Computerized Derivation of Equations of Motion", in Ref. [4], pp. 290- 305, 1977.

43. Panel Discussion on "User Experience in Applying Kinematic Synthesis and Dynamic Analysis Software Packages", 1986 ASME Mechanisms Conference, October 5-8, Columbus, Ohio.

44. Smith, C. C., "Literature Review - Automobile Ride Quality", *Shock and Vibration Digest* Vol. 12, No. 4, pp. 15-20, April 1980.

45. Morman, K. N., and Giannopoulos, F., "Recent advances in Analytical and Computational Aspects of Active and Passive Vehicle Suspensions", in: *Computational Methods in Ground Transportation Vehicles*, M. M. Kamal, and J. A. Wolf Jr., Eds., ASME AMD Vol. 50, American Society of Mechanical Engineers, New York, 1983.

46. Crolla, D. A., Horton, D. N. L., and Dale, A. K., "Off-Road Vehicle Ride Vibration", in: *Vehicle Noise and Vibration*, I Mech E Conference Publication 1984-5, Institution of Mechanical Engineers, London, England, pp. 55-64, 1984.

47. Bernard, J., Vanderploeg, M., and Shannon, J., "Recent Developments in Vehicle Dynamics", *Shock and Vibration Digest,* 19(4), pp. 10-16, 1987.

48. Alanoly, J., and Sankar, S., "A New Concept in Semi-Active Vibration Isolation", *ASME Journal of Mechanisms, Transmissions, and Automation in Design*, 109(2), pp. 224-247, June 1987.

49. Alanoly, J., and Sankar, S., "Semi-Active Force Generators for Shock Isolation", *Journal of Sound and Vibration,* 126(1), pp. 145-156, October 1988.

50. Chalasani, R.M., "Ride Performance of Active Suspension Systems - Part I: Simplified Analysis Based on Quarter-Car Model", and Part II: Comprehensive Analysis Based on a Full-Car Model", *Symposium on Simulation and Control of Ground Vehicles and Transportation Systems*, ASME AMD-Vol. 80, Segel, L. et al., ed., (The Winter Annual Meeting of ASME, Anaheim, California, 1986), ASME, New York, NY, pp. 187-234, 1986.

51. Bahnholzer, D., "The Design of the Running Gear of Light Passenger Cars for comfort and Safety", *International Journal of Vehicle Design*, 7 (5/6), pp 129-146, 1986.

52. Ellis, J.R., *Vehicle Dynamics*, Business Books Ltd., London, UK, 1969.

53. Hales, F.D., "A Theoretical Analysis of the Lateral Properties of Suspension Systems", *Proc. Instn. Mech. Engrs.*, 179 (Pt 2A), pp 73-97, 1964-65.

54. Butler, D.M., and Ellis, J.R., "Analysis and Measurement of the Relative Movements Between the Road Wheels of a Vehicle and the Road Surface", *Proc. Instn. Mech. Engrs.*, 186 (Pt 2A), pp 793-906, 1972.

55. Cronin, D. L., "McPherson Strut Kinematics", *Mechanism and Machine Theory*, 16, pp. 631-642, 1981.

56. Dorgham, M. A., and Ellis J. R., "Digital Simulation of the Kinematic and Dynamic Behaviour of Road Vehicle Suspensions: Part 1 - Planar Suspensions", *ASME paper no. 74-DET-17*, 1974.

57. Majcher, J.S., Michaelson, R.D., Solomon, A.R., Subhedar, J.W., "Analysis of Vehicle Suspensions with Static and Dynamic Computer Simulations", *Transactions of the SAE*, Paper No. 760183, 85, pp. 843-856, 1976.

58. Morman, K.N., "Non-Linear Model Formulation for Static and Dynamic Analysis of Front Suspensions", SAE Paper No. 770052, International Automotive Engineering Congress and Exposition, Detroit, Michigan, February 1976.

59. Reddy, P. J., Nagaraj, P. T., and Ramamurti, V., "Analysis of a Semi-Levered Suspension Landing Gear with Some Parametric Study", *ASME Journal of Dynamic Systems, Measurement, and Control*, 106, pp. 218-224, September 1984.

60. Nalecz, A.G. "Investigation into the Effects of Suspension Design on the Stability of Light VEhicles", Paper No. 870497, *Transactions of the SAE*, 96(1), 1987.

61. Nalecz, A.G, and Bindemann, A.C., "Investigation into the Stability of Four Wheel Steering Vehicles", *International Journal of Vehicle Design*, 9(2), pp. 159-178, 1988.

62. Nalecz, A.G, and Bindemann, A.C., "Analysis of the Dynamic Response of Four Wheel Steering Vehicles at High Speed", *International Journal of Vehicle Design*, 9(2), pp. 179-202, 1988.

63. Speckhart, F.H., "A Computer Simulation for Three-Dimensional Vehicle Dynamics", *SAE Paper No. 730526*, Society of Automotive Engineers, Warrendale, PA, 1973.

64. Belingardi, G., et al., "On the Influence of Suspension Mechanism on the Dynamic Behaviour of a F.1 Racing Car", *Proceedings of the 7th IFToMM World Congress*, pp. 455-458, Sevilla, Spain, September 1987.

65. Smith, C., *Tune to Win*, Aero Publishers, Fallbrook, California,

1978.

66. Bastow, D, *Car Suspension and Handling*, Pentech Press, London, England, 1987.

67. George, G.R., and Sadler, J.P., "Kinetostatic Analysis and Optimization of Beam Axle Vehicle Suspension Geometries", *Proc. ASME Winter Annual Meeting*, ASME DE-Vol 11, pp. 27-34, 1987.

68. vanValkenburgh, P., *Race Car Engineering and Mechanics*, (Published by the Author), Seal Beach CA, 1986.

69. Dixon, J.C., "The Roll-Centre Concept in Vehicle Handling Dynamics", *Proceedings of the Institution of Mechanical Engineers*, Vol. 201, No. D1, pp. 69-78, 1987.

70. Howell, L. J., "Power Spectral Density Analysis of Vehicle Vibration Using the NASTRAN Computer Program", *Transactions of the SAE*, SAE paper no. 740328, pp. 1415-1424, 1974.

71. Duncan, A. E., "Application of Modal Modeling and Mount System Optimization to Light Duty Truck Ride Analysis", *Transactions of the SAE* SAE paper no. 811313, pp. 113-128, 1981.

72. Giannopoulos, F., and Rao, A. K., "Dynamic Loads on Suspension Components Using Mechanisms Programs", *SAE paper no. 811307*, 1981.

73. Rai, N.S., Solomon, A.R., and Angell, J.C., "Computer Simulation of Suspension Abuse Tests Using ADAMS", *SAE Paper No. 820079*, Society of Automotive Engineers, Warrendale, PA, 1982.

74. Orlandea, N.V., "ADAMS Theory and Application", in Ref. [6], pp. 121-166, 1987.

75. Orlandea, N., and Chace, M.A., "Simulation of a Vehicle Suspension with the ADAMS Computer Program", *SAE Paper No. 770053*, Society of Automotive Engineers, Warrendale PA, 1977.

76. Antoun, R.J., Hackert, P.B., O'Leary, M.C., and Sitchin, A.,"Vehicle Handling Dynamic Simulation - Model Development, Correlation, and Application Using ADAMS", *SAE Paper No. 860574*, Society of Automotive Engineers, Warrendale PA, 1986.

77. Hackert, P.B., O'Leary, M.C., and Sitchin, A. "Dynamic Simulation of Light Truck Handling Maneuvers Using ADAMS", *Symposium on Simulation and Control of Ground Vehicles and Transportation Systems*, ASME AMD-Vol. 80, Segel, L. et al., ed., (The Winter Annual Meeting of ASME, Anaheim, California, 1986), ASME, New York, NY, pp. 277-286, 1986.

78. Smith, D.W. et al., "Automated Simulation and Display of Mechanism and Vehicle Dynamics", *Proceedings of ASAE 1982 Summer Meeting*, Madison, Wisconsin, 1982.

79. Weinert, M.S. et al., "Piecing Together the Puzzle: A Look at the Analytical Tools Used in the Design of Off-Highway Equipment", *SAE Paper No. 850789*, Earthmoving Industry Conference, Peoria, Illinois, 1985.

80. Trom,J.D., "Nonlinear Analysis of a Mid-Size Passenger CAr Using a General Purpose Program", Masters Thesis, University of Iowa, 1985.

81. Trom, J.D., Lopez, J.L., and Vanderploeg, M.J., "Modeling of a Mid-Size Passenger Car Using a Multibody Dynamics Program", ASME Journal of *Mechanisms, Transmissions, and Automation in Design*, 104(4), pp. 518-523, 1985.

82. McCullough, M.K., "Terrain - Vehicle system Modelling Using a Multi-Body Dynamics Program", *Journal of Terramechanics*, 23(3), pp. 171-184, 1986.

83. Jaschinski, A., Kortüm, W., and Wallrapp, O. "Simulation of Ground Vehicles with the Multibody Program MEDYNA", *Symposium on Simulation and Control of Ground Vehicles and Transportation Systems*, Segel, L., et al, eds., (ASME Winter Annual Meeting, Anaheim, CA), ASME, New York, pp. 315-341, 1986.

84. Jaschinski, A., "Application of MEDYNA in Vehicle Technology", in Ref. [6], pp. 188-214, 1987.

85. Fuhrer, C., "Algebraic Methods in Vehicle System Analysis", in Ref. [6], pp. 315-328, 1987.

86. Schiehlen, W.O., "Vehicle Dynamics Applications", in Ref. [3], pp. 218-231, 1984.

87. Thomson, B., Rathgeber, H., "Automated Systems Used for Rapid and Flexible Generation of Vehicle Simulation Models Exemplified by a Verified Passenger car and Motorcycle Model", *The Dynamics of Vehicles on Roads and on Tracks*, Hedrick, J.K., ed, Proc. 8th IAVSD Symposium, MIT, MA, Swets & Zeitlinger, Lisse, pp. 645-654, August 1983.

88. Alanoly, J., and Sankar, S., "Computerized Analysis of Mechanical System Dynamics", *Proceedings of the 3rd Canadian Universities Conference on CAD/CAM*, pp. 2-12, University of Ottawa, Ottawa, July 2-3, 1987.

89. Alanoly, J., and Sankar, S., "CAMSYD: A Software for Computerized Analysis of Mechanical System Dynamics", Presented at the *CAD/CAM 87 Conference and Exhibition*, Palais des congres, Montréal, September 22-24, 1987.

90. Alanoly, J., and Sankar, S., "Vibratory System Dynamic Analysis Using a Graphics Based Self-Formulating Program", *Proceedings of the 59th Shock and Vibration Symposium*, pp. 293-301, Albuquerque,

NM, October 18-20, 1988.

91. Sankar, S., Alanoly, J., Germain, D., and Mallette, B., "Snowmobile Suspension System Design Under University-Industry Collaboration", *Proceedings of the SAE-SATL Subzero Engineering Conditions Conference*, pp. 183-191, Ravoniemi, Finland, January 9-11, 1989.

92. Alanoly, J., and Sankar, S., "A General Purpose Formalism for Lumped Parameter Mechanical Systems with Application to Vehicle Dynamics", *Proceedings of the 7th Modal Analysis Conference*, pp. 878-883, Las Vegas, NV, January 2 - February 2, 1989.

93. Sankar, S., Alanoly, J., and Negrin, D., "Vehicle Ride Analysis Using Interactive Graphics", *International Journal of Vehicle Design*, 10(3), pp. 347-367, 1989.

94. Young, S.-S.D., and Shoup, T.E., "The Sensitivity Analysis of Cam Mechanism Dynamics", *ASME Paper No. 80-DET-93*, Design Engineering Technical Conference, Beverly Hills, California, Sept. 28-Oct. 1, 1980.

95. Özgüven, H.N., and Houser, D.R., "Mathematical Models Used in Gear Dynamics- A Review", *Journal of Sound and Vibration*, 121(3), pp. 383-411, 1988.

96. White, R.C., "Car Rocking Simulations of Two 140-Ton Railroad Flatcars", in *Symposium on Simulation and Control of Ground Vehicles and Transportation Systems*, L. Segel, et al, Eds., AMD-Vol. 80, pp. 399-410, American Society of Mechanical Engineers, New York, 1986.

97. ElMadany, M.M., "A Procedure for Optimization of Truck Suspensions", *Vehicle System Dynamics*, 16, pp. 297-312, 1987.

98. Wymore, A.W., *System Engineering Methodology for Inter Disciplinary Teams*, John Wiley & Sons, New York, 1976.

99. Swamy, M.N.S., and Thulasiraman, K., *Graphs, Networks, and Algorithms*", John Wiley & Sons, Toronto, 1976.

100. Nikravesh, P.E., "Application of Animated Graphics in Large Scale Mechanical System Dynamics", in Ref. [3], pp. 369-377, 1985.

101. Matsumoto, N., Suzuki, S., "Graphics for Dynamic Analysis/Synthesis of Vibration Systems with Arbitrary Degrees-of-Freedom (DAVIS)", *Computers & Graphics*, 6(4), pp. 159-169 1982.

102. Maruyama, K., and Fujita, T., "Automatic Generation of Equations of Motion from Graphic Input of Vibration Model", *JSME International Journal*, Series III, 31(2), pp. 400-408, 1988.

103. Thatch, B.R., Myklebust, A., "A PHIGS-Based Graphics Input Interface for Mechanism Design", *Proceedings of 1987 ASME Design*

Automation Conference, Boston, MA, ASME DE-Vol. 10-1, pp. 379-389, September 1987.

104. Barris, W.C., and Riley, D.R., "The Impact of Workstation Technology on Mechanism Synthesis Strategy", *ASME Paper No. 86-DET-150*, Design Engineering Technical Conference, Columbus, OH, October 5-8, 1986.

105. Müller P.C., and Schiehlen, W.O., *Linear Vibrations*, Martinus Nijhoff Publishers, Dordrecht, The Netherlands, 1985.

106. ElMadany, M.M., "Random Response of Articulated Road Vehicles", Ph.D. Thesis, McMaster University, Hamilton, Ontario, Canada, 1979.

107. *Vehicle Dynamics Terminology*, SAE Publication J670e, Society of Automotive Engineers, 1976.

108. Paul, B., *Kinematics and Dynamics of Planar Machinery*, Prentice-Hall, Englewood Cliffs, NJ, 1979.

109. Benedict, C.E., "Dynamic Response Analysis of Quasi-Rigid Mechanical Systems Using Kinematic Influence Coefficients", *Journal of Mechanisms* 6(4), pp. 383-403, 1971.

110. Haug, E.J., and Arora, J.S., *Applied Optimal Design*, Wiley Interscience, New York, NY, 1979.

111. Rankers, H., "Synthesis of Mechanisms", in Ref. [3], pp. 421-498, 1984.

112. Olson, D.G., Erdman, A.G., and Riley, D.R., "A Systematic Procedure for Type Synthesis for Mechanisms with Literature Review", *Mechanism and Machine Theory*, 20(4), pp. 285-295, 1985.

113. Pennestri, E., and Strozzieri, A., "Optimal Design and Dynamic Simulation of a Motorcycle with Linkage Suspension", *International Journal of Vehicle Design*, 9(3), pp. 339-350, 1980.

114. Norton, R., "Four-Bar and Five-Bar Linkage Analysis Programs for the Apple Computer", *Mechanism and Machine Theory*, 20(4), pp. 313-320, 1985.

115. Freudenstein, F., and Beig, H.S.M., "On a Computationally Efficient Microcomputer Kinematic Analysis of the Basic Linkage Mechanisms", *Mechanism and Machine Theory*, 21(6), pp. 467-472, 1986.

116. Radcliffe, C.W., "MECHAN: An Interactive Program for Dynamic Analysis of Multi-loop Planar Mechanisms", *Proceedings of the 7th IFToMM World Congress*, pp. 541-544, Sevilla, Spain, September 1987

117. Llorens, A., Martell, J., "CINPLA: A Program for the Kinematic Analysis of Planar Mechanisms The Theory of Machines and Mechanisms", *Proceedings of the 7th IFToMM World Congress*,

pp. 111-114, Sevilla, Spain, September 1987.

118. Fabrikant, V.I., and Sankar, T.S., "CAD of Planar Mechanisms", *Proceedings of the 7th IFToMM World Congress*, pp. 945-948, Sevilla, Spain, September 1987.

119. Suh, C.H., and Radcliffe, C.W., *Kinematics and Linkage Design*, John Wiley and Sons, New York, 1978.

120. Koeppel, W., "Computer Modelling - State-of-the-Art Report", *Journal of Terramechanics*, 22(1), pp. 27-36, 1985.

121. Wong, J.Y., "A Comprehensive Computer Simulation Model for the Off-Road Performance of Tracked Vehicles", *Proceedings of 1986 ASME Winter Annual Meeting*, AMD-Vol. 80, American Society of Mechanical Engineers, New York, 1986.

122. Newman, J.A., and Beale, D.J., "Snowmobile Suspension System- A High-Speed Motion Picture Study", *SAE Paper No. 710667*, Society of Automotive Engineers, Warrendale, PA, 1971.

123. Newman, J.A., Cheng, S., and Suri, V.K., "A Hybrid Computer Simulation of the Recreational Snowmobile", *SAE Paper No. 720261*, Society of Automotive Engineers, Warrendale, PA, 1972.

124. Hollnager, H.E., "Snowmobile Ski Suspensions", *SAE Paper No. 740677*, Society of Automotive Engineers, Warrendale, PA, 1974.

125. Kho, J.H., and Newman, J.A., "Braking Characteristics of the Recreational Snowmobile", *SAE Paper No. 730783*, Society of Automotive Engineers, Warrendale, PA, 1973.

126. Smith, C.O., "Dare You Ride Your Snowmobile ?", *ASME Paper No. 77-RC-13*, American Society of Mechanical Engineers, New York, 1977.

127. Holecek, D.F., ed., *Proceedings of the 1973 Snowmobile and Off th Road Vehicle Research Symposium*, September 1973, Michigan State University, MI.

128. Newhouse, T.C., and Pavelic, V., "Determination of Moment-of-Inertia by Experimental Methods", *ASME Paper No. 75-DE-29*, Design Engineering Technical Conference, New York, April 21-24, 1975.

129. Huston, R.L., and Passerello, C.E., "The Mechanics of Human Body Motion", in *Human Body Dynamics: Impact, Occupational, and Athletic Sports*, D.N. Ghista, ed., Clarendon Press, Oxford, 1982.

130. Boulanger, D., "Data Acquisition from the Field, with Somat Acquisitor", DB-89-404, Bombardier Inc., February 28, 1989.

131. Wu., S.C., Yang, S.M., and Haug, E.J., "Dynamics of Mechanical Systems with Coulomb Friction, Stiction, Impact and Constraint

Addition-Deletion – I: Theory", "II: Planar Systems", and "III: Spatial Systems", *Mechanism and Machine Theory*, 21(5), pp. 401-425. 1986.

132. Shabana, A.A., "Automated Analysis of Constrained Systems of Rigid and Flexible Bodies", *ASME Journal of Vibration, Acoustics, Stress and Reliability in Design*, 107, pp. 431-439, October 1985.

133. Kota, S., Erdman, A.G., and Riley, D.R., "Development of Knowledge Base for Designing Linkage-Type Dwell Mechanisms: Part 1 - Theory", and "Part 2 - Application", *ASME Journal of Mechanisms, Transmissions, and Automation in Design*, 109(3), pp. 308-321, September 1987.

134. Pacejka, H.B., "Bond Graphs in Vehicle Dynamics", in Ref. [6], pp. 263-287, 1987.

135. Frank, P.M., *Introduction to System Sensitivity Theory*, Academic Press, New York, NY, 1978.

136. Sharp, R.S., and Brooks, P.C., "Application of Eigenvalue Sensitivity Theory to the Improvement of the Design of a Linear Dynamic System", *Journal of Sound and Vibration*, 114(1), pp. 19-32, 1987.

APPENDIX A

Equations of Motion for a Tractor-Semitrailer Model

```
      SUBROUTINE INIT(IUN, IER)
C.
C     INITIALIZES THE COMMON BLOCKS /PAR/ AND /MAS/
C
      REAL MASS( 7), SPAR(11), DIST( 5)
      REAL MIN1(3,3), MATR(3,3)
      COMMON /PAR/ MASS, SPAR, DIST
      COMMON /MAS/ MIN1
C
C     READ IN IN DATA
C
      READ(IUN,*) (MASS(I),I=1,  7)
      READ(IUN,*) (SPAR(I),I=1, 11)
      READ(IUN,*) (DIST(I),I=1,  5)
C
C     MASS MATRIX FOR TREE 1
C
      MATR( 1, 1) = MASS(1)+MASS(3)
      MATR( 1, 2) = DIST(1)*MASS(3)
      MATR( 1, 3) = -DIST(4)*MASS(3)
      MATR( 2, 2) = DIST(1)*MASS(3)*DIST(1)+MASS(2)
      MATR( 2, 3) = -DIST(1)*MASS(3)*DIST(4)
      MATR( 3, 3) = DIST(4)*MASS(3)*DIST(4)+MASS(4)
      MATR( 2, 1) = MATR( 1, 2)
      MATR( 3, 1) = MATR( 1, 3)
      MATR( 3, 2) = MATR( 2, 3)
C
C     INVERT THE MASS MATRIX
C
      DET = MATR(1,1)*(MATR(2,2)*MATR(3,3)-MATR(2,3)**2) -
     $      MATR(1,2)*(MATR(1,2)*MATR(3,3)-MATR(1,3)*MATR(2,3)) +
     $      MATR(1,3)*(MATR(1,2)*MATR(2,3)-MATR(1,3)*MATR(2,2))

C
      IF(DET.EQ.0.0)THEN
        IER = 2
        RETURN
      ENDIF
C
      MIN1(1,1) = (MATR(2,2)*MATR(3,3)-MATR(2,3)**2)/DET
      MIN1(1,2) = (MATR(1,3)*MATR(2,3)-MATR(1,2)*MATR(3,3))/DET
      MIN1(1,3) = (MATR(1,2)*MATR(2,3)-MATR(1,3)*MATR(2,2))/DET
      MIN1(2,2) = (MATR(1,1)*MATR(3,3)-MATR(1,3)**2)/DET
      MIN1(2,3) = (MATR(1,3)*MATR(1,2)-MATR(1,1)*MATR(2,3))/DET
      MIN1(3,3) = (MATR(1,1)*MATR(2,2)-MATR(1,2)**2)/DET
      MIN1(2,1) = MIN1(1,2)
      MIN1(3,1) = MIN1(1,3)
      MIN1(3,2) = MIN1(2,3)

C
      RETURN
      END
```

```
      SUBROUTINE DIFFUN (NDE, T, X, XDOT)
C
C     SYSTEM EQUATIONS IN STATE SPACE FORM
C
      REAL X(12), XDOT(12), FEL( 7), FTR( 3)
      REAL MASS( 7), SPAR(11), DIST( 5)
      REAL MIN1(3,3)
      COMMON /PAR/ MASS, SPAR, DIST
      COMMON /MAS/ MIN1
C
C     COMPUTE ELEMENTAL FORCES, FEL
C
      CALL ELFORCS(T, X, FEL)
C
C     SYSTEM EQUATIONS OF MOTION IN STATE SPACE FORM
C     XDOT(.) = F(X,T)
C
      DO 10 I=1,  6
        XDOT(I) = X(I +  6)
 10   CONTINUE
C
C
C     TREE 1
C
      FTR( 1) = -FEL(2)-FEL(3)-FEL(4)
      FTR( 2) = -DIST(1)*FEL(4)-FEL(2)*DIST(2)-FEL(3)*DIST(3)-FEL(1)
      FTR( 3) = DIST(4)*FEL(4)-FEL(4)*DIST(5)+FEL(1)
C
      XDOT( 7) = MIN1(1,1)*FTR(1)+MIN1(1,2)*FTR(2)+MIN1(1,3)*FTR(3)
      XDOT( 8) = MIN1(2,1)*FTR(1)+MIN1(2,2)*FTR(2)+MIN1(2,3)*FTR(3)
      XDOT( 9) = MIN1(3,1)*FTR(1)+MIN1(3,2)*FTR(2)+MIN1(3,3)*FTR(3)
C
C     ISOLATED BODIES
C
      XDOT(10) = (FEL(2)-FEL(5))/MASS(5)
      XDOT(11) = (FEL(4)-FEL(7))/MASS(6)
      XDOT(12) = (FEL(3)-FEL(6))/MASS(7)
C
      RETURN
      END
```

```
      SUBROUTINE ELFORCS(T, X, FEL)
      REAL X(12), FEL( 7), RV(11)
      REAL MASS( 7), SPAR(11), DIST( 5)
      COMMON /PAR/ MASS, SPAR, DIST
C
C     GET MOTION ACROSS EACH ELEMENT, RV(.)
C
      CALL ELEMOT(T, X, RV)
C
C     COMPUTE ELEMENTAL FORCES, FEL(.)
C
      FEL( 1) = FORCE07(RV( 1), SPAR( 1))
      FEL( 2) = FORCE04(RV( 3), SPAR( 3))
      FEL( 3) = FORCE04(RV( 5), SPAR( 5))
      FEL( 4) = FORCE04(RV( 7), SPAR( 7))
      FEL( 5) = FORCE01(RV( 9), SPAR( 9))
      FEL( 6) = FORCE01(RV(10), SPAR(10))
      FEL( 7) = FORCE01(RV(11), SPAR(11))
C
      RETURN
      END
```

```
      SUBROUTINE ELEMOT(T, X, RV)
C
C     COMPUTE THE REQUIRED MOTION VARIABLES FOR EACH ELEMENT
C
      REAL X(12), RV(11), XX(14)
      REAL MASS( 7), SPAR(11), DIST( 5)
      COMMON /PAR/ MASS, SPAR, DIST
C
C     GET MOTION OF EACH BODY, XX(.), USING X(.)
C
      CALL BODYMOT(X, XX)
      CALL BODYMOT(X( 7), XX( 8))
C
C     COMPUTE MOTION ACROSS EACH ELEMENT
C
      RV( 1) = XX(2)-XX(4)
      RV( 2) = XX(9)-XX(11)
      RV( 3) = XX(1)+XX(2)*DIST(2)-XX(5)
      RV( 4) = XX(8)+XX(9)*DIST(2)-XX(12)
      RV( 5) = XX(1)+XX(2)*DIST(3)-XX(7)
      RV( 6) = XX(8)+XX(9)*DIST(3)-XX(14)
      RV( 7) = XX(3)+XX(4)*DIST(5)-XX(6)
      RV( 8) = XX(10)+XX(11)*DIST(5)-XX(13)
      RV( 9) = XX(5)-Y(10,T)
      RV(10) = XX(7)-Y(12,T)
      RV(11) = XX(6)-Y(14,T)
C
      RETURN
      END
C-----------------------------------------------------------------------
      SUBROUTINE BODYMOT(X, XX)
C
C     MOTION OF EACH BODY USING THE STATE VECTOR
C
      REAL X( 6), XX( 7)
      REAL MASS( 7), SPAR(11), DIST( 5)
      COMMON /PAR/ MASS, SPAR, DIST
C
      XX( 1) = X(1)
      XX( 2) = X(2)
      XX( 3) = X(1)+X(2)*DIST(1)-X(3)*DIST(4)
      XX( 4) = X(3)
C
      XX( 5) = X(4)
      XX( 6) = X(5)
      XX( 7) = X(6)
C
      RETURN
      END
```